## 1.1 Zeolites –An Introduction

Zeolites are crystalline aluminosilicates, either of natural or synthetic origin with highly ordered structures (1-8). They consist of $SiO_4$ and $AlO_4^-$ tetrahedra, which are interlinked through shared oxygen atoms to give a three dimensional network. They consist of channels and in some cases cavities. The interior of these channels contain adsorbed water molecules and exchanged alkali metal ions, the latter can be exchanged with other metal cations. These cations compensate for the excess negative charge in the framework resulting from the substitution of aluminum in the lattice. The interior of the pore system, with its atomic-scale dimensions, is the active surface of the zeolites. The inner pore structure depends on the zeolite type, composition, and the cations. Thus, zeolites are represented by the general formula:

$$\mathbf{M_{y/n}[(SiO_2)_x (AlO_2)_y].zH_2O}$$

where **M** is the charge compensating cation with the valency **n** (Figure 1.1). M represents the exchangeable cation (eg. alkali or alkaline earth metals or an organic cations). The ratio x/y can have the value 1 to α. According to Lowenstein's rule no two aluminum tetrahedra can exist adjacent to one another. The Si/Al molar ratio corresponds to the acid sites in the zeolites. **z** represents the number of water molecules, which can be reversibly adsorbed in the pores, while **y** represents the exchange capacity. Zeolites are also popularly known as ***'molecular sieve**s'* due to their ability to differentiate between molecules of different shapes and size. Zeolites have found widespread application as adsorbents, ion exchange materials, detergent builders and catalysts, especially in petroleum refining, petrochemicals, and as fluidized catalytic cracking catalysts (FCC) (7). Furthermore, zeolite functionality has also been compared with catalytic antibodies (9) and metalloenzymes (10). The characteristic features of zeolites, which make them effective catalysts are:

- High surface area and adsorption properties.
- Active acid sites; to use as solid acid.
- Shape selectivity (due to uniform pores and channels),
- Easy regeneration

- High thermal stability.
- Eco friendliness.

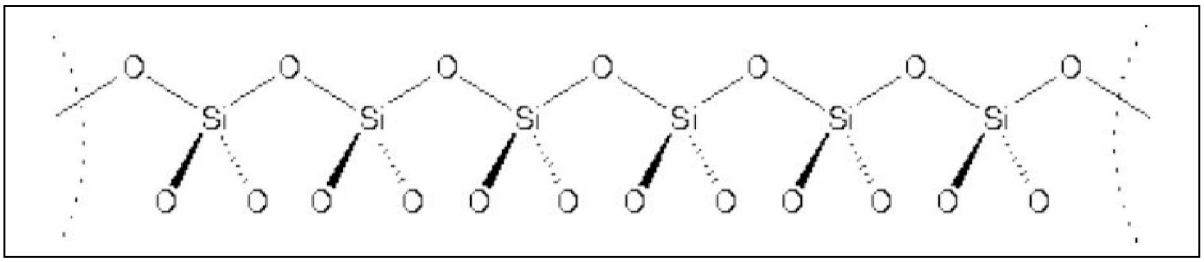


**a**

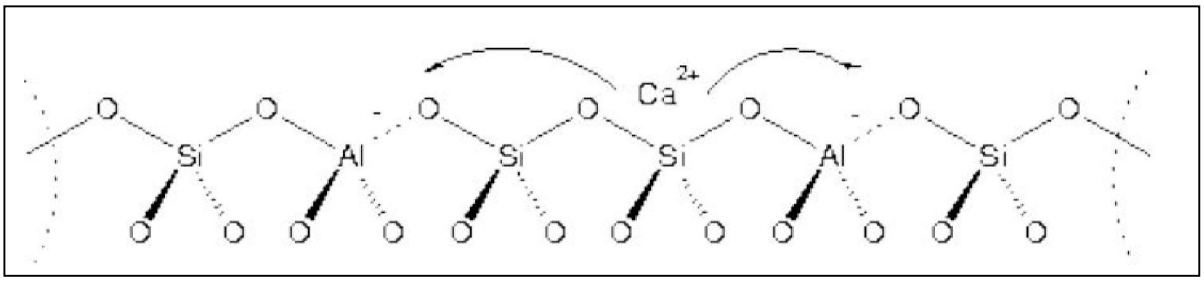


**b**

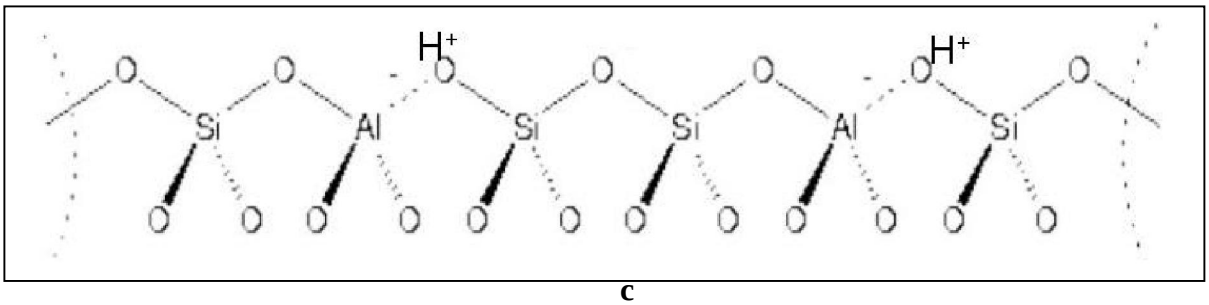


**c**

**Figure 1.1 a) $SiO_4$ connectivity in silicon rich zeolite b) Exchangeable cation positions in zeolites and c) Protonated form of zeolites**

### 1.1.1 Historical background

Axel Fr. Cronstedt (11) (1756), a Swedish mineralogist, observed that certain rock minerals, when heated sufficiently, appeared as were boiling. He named them ***'zeolite**s'* **(zeo** means to boil and **lithos** means stone). Damour (12) observed that zeolites could be reversibly dehydrated without changes in the structure or morphology. The role of water as a mineralizing agent, aided by alkaline conditions, drew the attention of mineralogists towards hydrothermal reaction conditions for the synthesis. The first claim, to have synthesized a zeolite named levynite, was made by St. Claire Deville and Thompson in 1862 (13, 14). In 1962, the commercialization of natural zeolites namely chabazite, erionite, mordenite and clinoptillotite started for a number of applications (15). McBain introduced the term ***molecular sieve*** to describe a class of materials that exhibited selective adsorption properties (16). Molecular sieves separate components of a mixture on the basis of molecular size and shape differences. However, Barrer (17) was the first to demonstrate the molecular sieve behavior of zeolites and their potential in separation techniques (Fig. 1.2). Since 1940, systematic studies on zeolites were undertaken. ZK-5 (18-20) was the first known synthetic zeolite (no natural counterpart) crystallized under hydrothermal conditions. Hydrogen forms of zeolites were also made for the first time in the year 1949, by heating ammonium-exchanged forms of mordenite (21). Special features of molecular sieves and zeolites are given below.

| Molecular Sieve | Zeolite |
|---|---|
| Ø It covers all the porous materials that can separate molecules by their size.<br><br>Ø AlPO's and their metal analogs, TS-1, VS-1 and all the metallosilicates etc. | Ø A particular class of molecular sieves containing $SiO_4$ and $AlO_4^-$.<br><br>Ø ZSM-5, X, Y, beta, L, Ferrierite, Mordenite etc. |

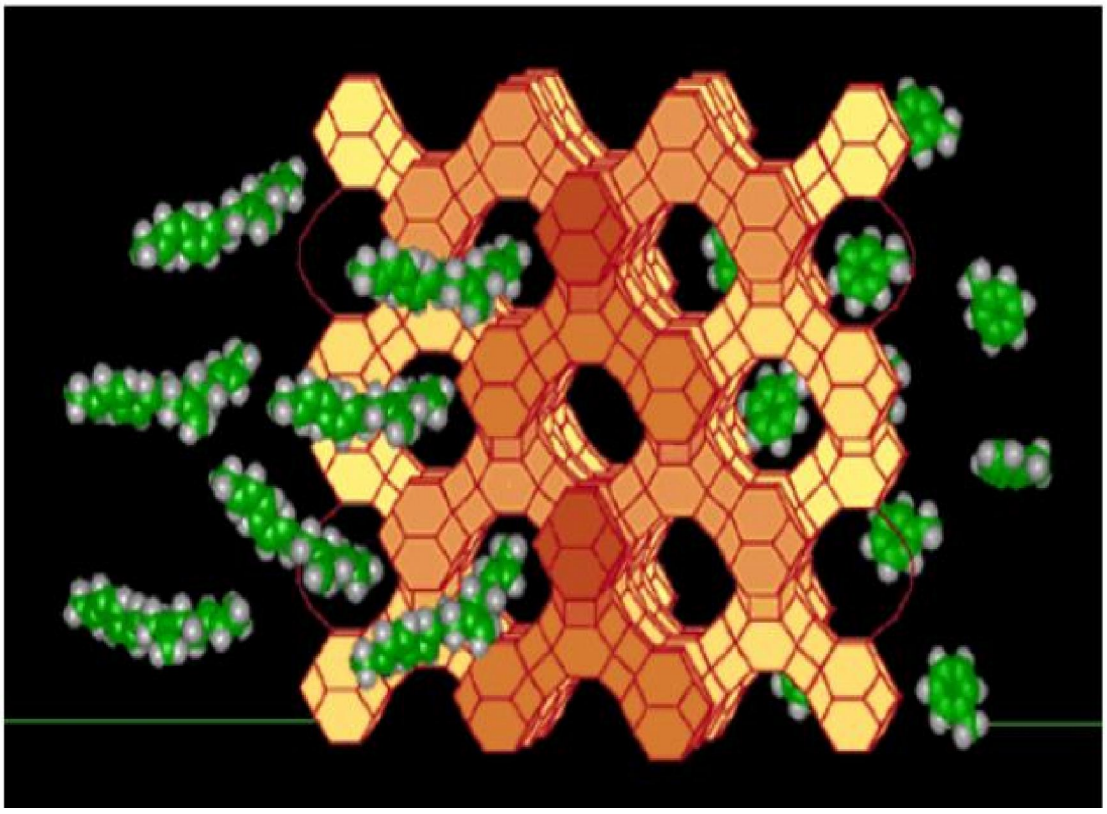

**Fig. 1.2: 3D Structure of Molecular Sieve**

### 1.1.2 Nomenclature

**Table 1.1 : Structural Codes of Zeolites**

| Structural codes | Zeolites |
|---|---|
| FAU | Faujasite, X and Y |
| MFI | Mobil Five : ZSM-5 |
| MEL | Mobil Eleven : ZSM-11 |
| MOR | Mordenite |
| FER | Ferrierite, ZSM-35, ZSM-21 |

Although, there is no systematic nomenclature for molecular sieve materials, the structure commission of International Zeolite Association and IUPAC has assigned structural codes to synthetic and natural zeolites (22, 23). Designations consisting of three capital letters have been used to identify structure types (Table 1.1). The codes for zeolite identification have generally been derived from the names of the type of species, and do not include numbers and characters other than Roman letters. Structure type codes are independent of

chemical composition, distribution of various possible T atoms, (e.g. $Si^{4+}$, $Al^{3+}$, $P^{5+}$, $Ti^{4+}$, etc.), cell dimensions or crystal symmetry.

### 1.1.3 Classification

Zeolites have also been classified in accordance with the morphology (24) (Table 1.2), crystal structure (1, 3, 25), chemical composition (26) (Table 1.3) and effective pore diameter (27, 28) (Table 1.4). Smith (29), Fischer (30) and Breck (31) have

**Table 1.2 : Classification of zeolites on the basis of morphology**

| | |
|---|---|
| The tetrahedra are linked more numerous in one crystallographic direction. | **Fibrous** |
| Zeolites have structural linkages more numerous in one plane and are characterized by a platy cleavage. | **Lamellar** (openframework materials) |

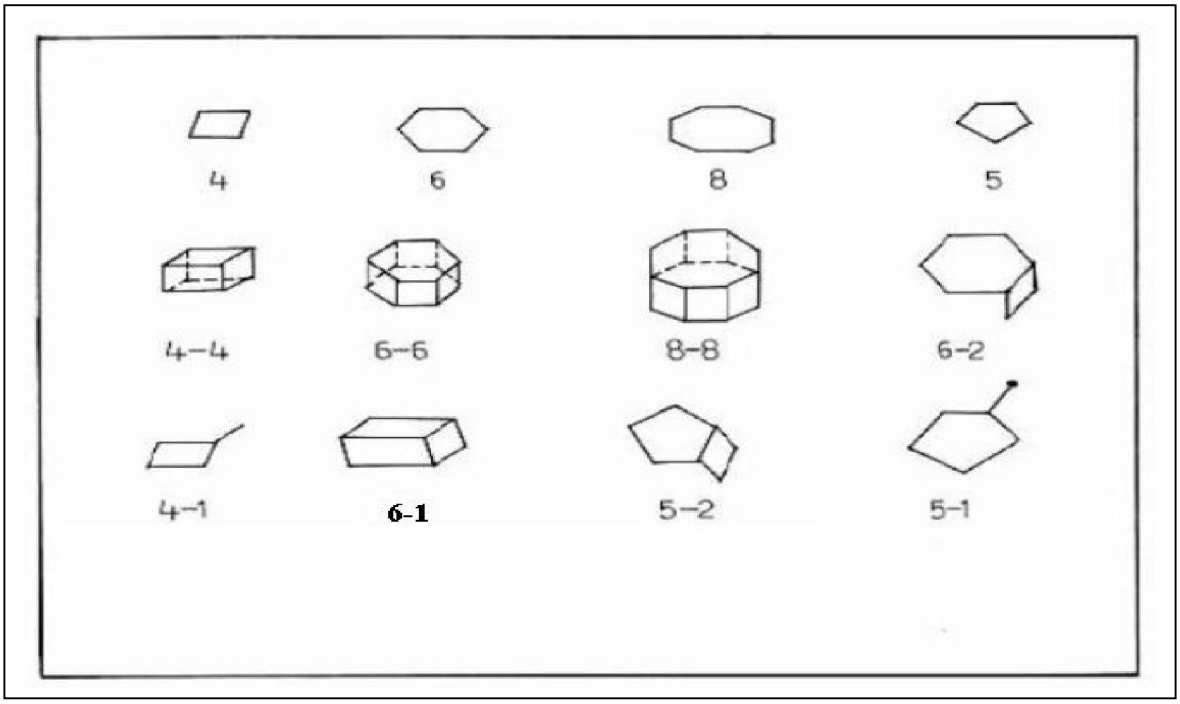


**Figure 1.3: Secondary Building units**

classified zeolites on the basis of differences in the secondary building units (SBU). SBU (Fig.1.3) are the aluminosilicate oligomers having chain, ring and cage like structures which are basic building units of zeolite framework structure. Flanigen (26) has also classified zeolites according to their chemical composition as shown below and some of their salient features are described.

**Table 1.3: Classification of zeolites on the basis of chemical composition.**

| | **Si/Al ratio** | **Names of Zeolites** |
|---|---|---|
| Low silica zeolites | Si/Al = 1- 1.5 | A, X, sodalite, etc |
| Intermediate silica zeolites | Si/Al = 2.0 - 5.0 | erionite, chabazite, mordenite, X, Y, L,W, etc. |
| High silica zeolites | Si/Al = 5 – 500 | MFI, FER, BEA, etc. |
| Pure silica zeolites | Si/Al = ∝ (only silicates) | Si-MFI (silicalite-1), Si-MEL (silicalite -2), Si-TON, Si-MTW, Si-ZSM-48, Si-NCL-1, Si-FER, Si-UTD-1, etc. |

- The thermal stability increases from low silica zeolites to high silica zeolites.
- The high silica zeolites are hydrophobic in nature while low silica zeolites are more hydrophilic.
- The acidity tends to increase in strength with increase in Si/Al ratio.
- The cation concentration and ion exchange capacity (which is directly proportional to the aluminum content) decreases with the increase in Si/Al ratio.
- Low silica zeolites are formed predominantly with 4-, 6- and 8- rings of tetrahedra while in case of intermediate silica zeolites there is an onset of 5- rings and in case of high silica zeolite 5-ring tetrahedra predominate in the structure.

Zeolites are also classified according to their effective pore diameter, which is dependent on the number of tetrahedra present in the ring aperture, which circumscribe the pore. Barrer (27) has classified zeolites into five groups. Sand (28) has further modified the classification into three groups, as shown in Table 1.4. In 1988, Davies et al. discovered a

very large pore aluminophosphate molecular sieve VPI-5 containing 18 membered ring pore openings (32). Recently, an extra large pore gallophosphate molecular sieve containing 20 membered ring pore opening called cloverite has been synthesized (33). A 14- membered ring structure called UTD-1 has also been reported (34).

**Table 1.4: Classification of zeolites on the basis of the effective pore diameter**

| **Small pore (8 MR)** | **Medium pore (10 MR)** | **Large pore (12 MR)** |
|---|---|---|
| MTN | Ferrierite (FER) | cancrinite |
| NU-1 | ZSM-5 (MFI) | Linde X,Y, L. |
| chabazite | ZSM-11(MEL) | mazzite |
| clinoptillolite | EU-1 (ZSM-50) | mordenite |
| erionite | Stilbite | offretite |
| ZK-5 | ZSM-23 | ZSM-12 (MTW) |
| Linde A | theta-1 (ZSM-22) | omega |
| Rho | ZSM-48 (EU-2) | Beta (BEA) |

MR- membered ring

## 1.2 Special Features of Zeolites

### 1.2.1 Active Sites: Acidity

Each zeolite type can be easily obtained over a wide range of compositions directly by synthesis and/or after various post synthesis treatments. Moreover, various compounds can be introduced or even synthesized within the zeolite pores (ship in a bottle synthesis). This explains why zeolites can be used in acid, base, acid-base, redox and bifunctional catalysts, larger proportion being however in acid and bifunctional catalysis. Most of the hydrocarbon reactions as well as many transformations of functionalised compounds are catalysed by protonic sites (35). In zeolites, they are associated with bridging hydroxyl groups attached to framework oxygens linking tetrahedral Si and Al atoms: (Al (OH) Si). **The maximum number of protonic sites is equal to the number of framework aluminium atoms,** the actual number being smaller due to limitations in cation exchange, dehydroxylation and dealumination during activation at high temperatures. The number

(and density) of protonic sites can therefore be adjusted either during synthesis or during post synthesis treatments of the zeolite: dealumination, ion-exchange, etc. However, as aluminium atoms cannot be adjacent (Lowenstein's rule), the maximum number of protonic sites is obtained for a framework Si/Al ratio of 1 (8.3 mmol $H^+$ $g^{-1}$ zeolite). Moreover, no pure protonic zeolite is stable with this low framework Si/Al ratio, hence this maximum number can never be achieved. In order to design zeolite catalysts, the parameters controlling the other features of the protonic sites and particularly their acid strength (Figure 1.4) have also been assessed. A first feature of zeolite is their **stronger acidity compared to amorphous aluminosilicates.** This is for instance evidenced by the higher heats of adsorption of nitrogen bases. To explain this stronger acidity, Mortier (36) proposed the existence of an enhanced donor-acceptor interaction in zeolites.

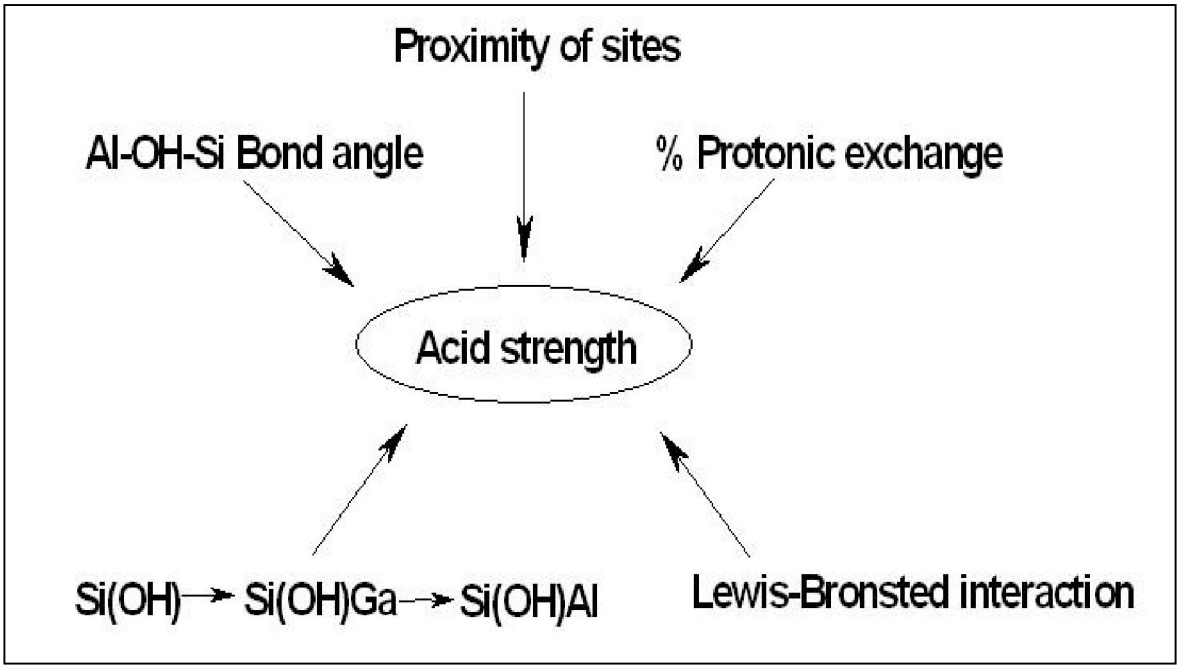


**Figure 1.4: Parameters determining the acid strength of the zeolite protonic sites**

Indeed, NMR data indicates that the OH groups of amorphous aluminosilicates are primarily terminal whereas those of zeolites are primarily bridging, the interaction of oxygen with Al weakening the OH bond and increasing the acid strength (37).

A relation exists between the T-O-T **bond angles and the acid strength of the associated proton in the zeolites** (37). The greater the angle, the stronger the acid sites. Thus, the protonic sites of HMOR (bond angle range between 143-180$^{o}$) and HMFI (133-177$^{o}$) are stronger than those of HFAU (138-147$^{o}$). This explains why HMOR is active and HFAU is not active for n-butane or n-hexane isomerisations at 473-523 K, as the two reactions require very strong acidity. Again, the protonic sites of the zeolites are influenced by the basicity of the reactants and the temperature will also play a role.

The synthesis of **metallosilicates** containing trivalent elements in the framework other than Al (like B, Ga, In, Fe) is of interest in moderating the acid strength. The ranking in acid strength drawn from theoretical calculations is in relatively good agreement with acidity measurements (38). Thus, according to IR spectroscopy (wavenumber of the OH groups) and ammonia TPD over MFI samples, the acid strength is in the following order:

$$B(OH)Si < In(OH)Si << Fe(OH)Si < Ga(OH)Si < Al(OH)Si$$

Theoretical and experimental studies of the effect of **framework Si/Al ratio** on the acidity led to the conclusion that the strength of the protonic sites of zeolites is influenced by the presence of neighbours (37, 38). Each framework Al atom has 4 Si atoms (Lowenstein's rule) in the first surrounding layer (nearest neighbours) and, depending on the zeolite topology, 9-12 Al or Si atoms are in the second layer (Next- Nearest-Neighbours or NNN). According to the NNN concept, the acid strength of a protonic site depends on the number of Al atoms in the NNN position (39); the strength is maximum at 0 Al as NNN and minimum at full occupancy of the NNN sites with Al. Using statistical calculations, Wachter (40) determined that the Si/Al value for which all the Al atoms were isolated was 7. Barthomeuf (41) improved this idea by using topological densities to include the effects of layers 1 to 5 surrounding the Al atom. The values of Si/Al for which **the protonic sites are isolated, hence have the maximum strength,** were calculated for 33 different zeolites and found between 5.8 (FAU) and 10.5 (Bikitaite-BIK).

### 1.2.2 Shape selectivity

The term shape selective catalysis was coined 40 years ago by Weisz and Frilette to describe the unexpected catalytic behaviour of an LTA zeolite exchanged with $Ca^{2+}$ (CaA). They found that at 533 K, CaA dehydrated 60% of 1-butanol but did not convert isobutanol. CaA also cracked n-hexane (but not 3-methylhexane) exclusively into linear products (42). These results suggested that reactions occurred inside the pores of CaA (0.5nm pore openings) making it impossible for the branched molecules to enter or exit these pores. The first shape selective catalytic process Selectoforming, was based on this simple and elegant concept of shape selectivity by sieving (43). Table 1.5 shows the significant highlights of the history of shape selective catalysis.

**Table 1.5: History of shape selective catalysis**

| | |
|---|---|
| 1925 | First molecular sieve effect (adsorption on Chabazite, Weigel, Steinhoff) |
| 1932 | " Molecular sieve "; porous material that acts as sieve on a molecular scale (Mac Bain) |
| 1960 | Shape selective catalysis through molecular sieving (Weisz-Frilette) |
| 1966 | Shape selective catalysis in Encyclopedia of Chemistry ( Reynolds Publ. Co) |
| 1968 | First commercial process, selectoforming (natural erionite, Weisz and Chen) |
| 1967 | Synthesis of ZSM-5<br>→ Many shape selective commercial processes: methanol to gasoline; dewaxing, xylene isomerisation etc. |
| 1968 | Transition state selectivity (Csicsery) |
| 1970 | Concentration Effect (Venuto, Rabo, Poutsma etc.) |
| 1984 | Nest effect → confinement effect (Derouane, 1986) |
| 1991 | Pore mouth catalysis (Martens et.al.) |
| 1995 | Key-lock mechanism (Martens et.al.) |

#### 1.2.2.1 Size exclusion

Separation among molecules of different sizes and shapes can be achieved by the proper choice of the zeolites. The effective pore size of the zeolite can be further modified by the choice of cations associated with zeolites. Catalytically, molecular shape selectivity by size exclusion can be achieved either through reactant selectivity or product selectivity. Many manifestations and applications of shape selective catalysis involve acid catalysed reactions such as isomerisation, cracking, dehydration etc. In these reactions, shape selectivity reverses the usual order of relative carbocation reaction rates. Acid catalysed reactivities of primary, secondary and tertiary carbocations differ. Tertiary carbon atoms form carbocations easily; and therefore they react much easier than the secondary carbon atoms. Primary carbon atoms do not from carbocations under ordinary conditions and therefore do not react. Only secondary carbocations can form from normal paraffins, whereas tertiary carbocations can be generated on singly branched isoparaffins. Therefore, in most cases isoparaffins crack and isomerise much faster than normal paraffins. This order is reversed in most shape selective acid catalysis; that is the normal paraffins react faster than branched ones, which sometimes do not react at all. This is the essence of many applications of shape selective acid catalysis. **Reactant shape selectivity** occurs when the feed stock contains two sizes of molecules, one of which is too large to pass through the channel system of the zeolite (Figure 1.5). Examples of reactant selectivity are alcohol dehydration (Table 1.6), cracking and hydrogenation. Over non-shape-selective catalysts, such as Ca-X, secondary alcohols dehydrate much easier, and therefore they require much lower temperature than primary alcohols. Over the shape selective Ca-A catalyst secondary alcohols do not react at all. The dehydration rate of the branched primary alcohol, isobutanol is also very low (44, 45). Table 1.7 compares cracking conversions of 3-methylpentane and normal hexane. Both hydrocarbons react over silica-alumina but only normal hexane can react over the shape selective Ca-A. The iso/normal product ratios of the product butanes and pentanes show **product shape selectivity**. These ratios are high over silica-alumina: 1.4 for the butanes and over 10 for the pentanes. Isobutane and isopentane are practically absent in the product over Ca-A because even if formed

internally, they would not be able to diffuse out (45). Linear olefins are hydrogenated about two orders of magnitude faster than branched ones over Pt-ZSM-5 (Table 1.8) (46).

**Table 1.6: Dehydration of alcohols (Reactant and Product selectivity) (45)**

| Reactant alcohol | Reaction Temp (K) | Conversion wt % | |
|---|---|---|---|
| | | Ca-A | Ca-X |
| Normal Butanol | 533 | 60 | 64 |
| Secondary butanol | 403 | 0 | 82 |
| Isobutanol | 533 | <2 | 85 |

**Table 1.7: Reactant and product selectivity; cracking of $C_6$ at 500 $^{O}$C (45)**

| Catalyst | Cracking conv. % | Cracking conv. % | | |
|---|---|---|---|---|
| | 3-Methylpentane | n-Hexane | $iC_4/nC_4$ | $iC_5/nC_5$ |
| Silica-alumina | 28 | 12 | 1.4 | 10 |
| Linde Ca-A | <1 | 9.2 | <0.05 | <0.05 |

**Table 1.8: Reactant selectivity; olefin hydrogenation (46)**

| Substrate | Temp. (K) | $Pt\text{-}Al_2O_3$ | Pt-ZSM-5 |
|---|---|---|---|
| | | Conversion % | Conversion % |
| Normal hexane | 548 | 27 | 90 |
| 4,4- Dimethylhex-1-ene | 548 | 35 | <1 |
| Styrene | 673 | 57 | 50 |
| 2-Methylstyrene | 673 | 58 | <2 |

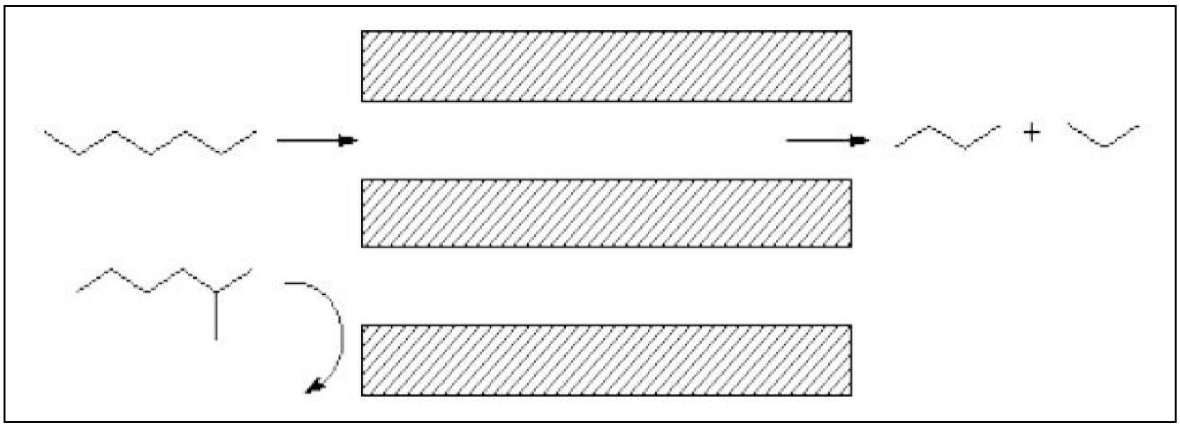

**Figure 1.5: Reactant shape selectivity**

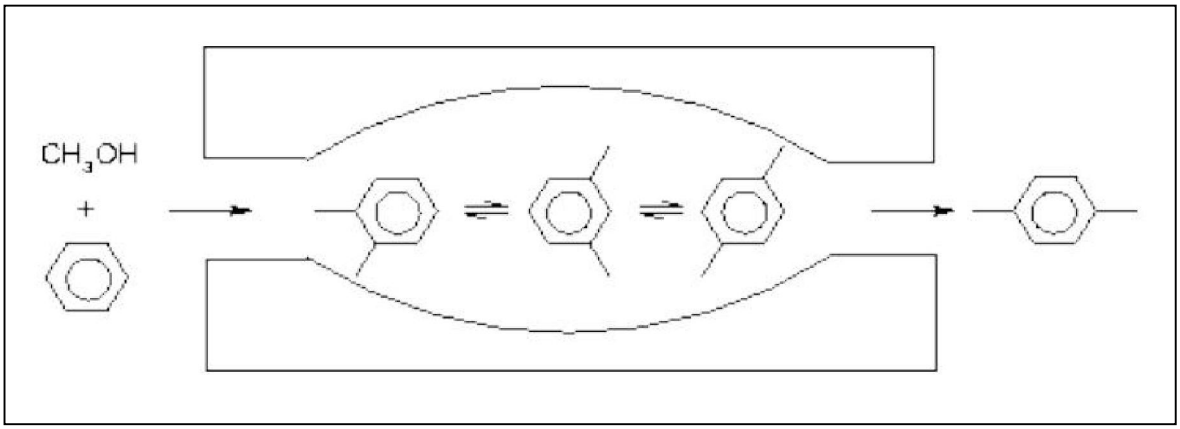


**Figure 1.6: Product shape selectivity**

Product shape selectivity plays a key role in various processes developed by Mobil for the selective synthesis of para-dialkylbenzenes (47), selective toluene disproportionation (STDP), toluene alkylation by methanol (TAM) or by ethylene (PET) etc. In all these processes, the bulkier ortho and meta isomers are also formed in the pores, but their exit is hampered by their slow diffusion; this selective removal of a product (para isomer) allows the bulkier isomers (ortho and meta) to be isomerised into less bulky species (para). Above thermodynamic yields are thus possible by the simple application of Le Chatelier's principle (Figure 1.6). Thus, the diffusion coefficient of para-xylene in ZSM-5 zeolite modified by coking at high temperatures in toluene disproportionation is of several orders of magnitude higher than those of ortho- and meta-xylene. It should be emphasized that in

the case of dialkyl-benzene synthesis, the situation is ideal. Indeed, the ortho- and meta-isomers trapped in the pores transform rapidly into the para- isomer. In other reactions, the molecules trapped in the pores transform only very slowly into desorbable molecules, their accumulation and their transformation into larger molecules ('coke') lead to a fast deactivation of the zeolite catalyst.

Venuto et.al. (48) proposed that coke formation in a Y zeolite at a high temperature was an example of reverse shape selectivity; the bulky molecules formed in the supercages (1.3 nm) cannot escape, the pore apertures (0.7 nm) being too narrow. This reverse shape selectivity, related to molecular sieving, has, of course, a negative effect; coke molecules limiting or inhibiting the access of reactant molecules to the active sites hence causing catalyst deactivation.

As stated above, shape selectivity due to molecular sieving depends on the relative rates of diffusion and reaction, hence on the respective sizes and shapes of molecules and pores and on the characteristics of the active sites (e.g. concentration, nature and strength of acid sites). Obviously, the diffusion rate, hence the selectivity also depends on the length of the diffusion path (i.e. on the size of the zeolite crystallites). The selectivity of the zeolite catalyst can be optimized by an adequate choice of operating conditions (temperature especially has a large effect on the reaction rates) and by adjusting the zeolite characteristics. For instance, in the toluene disproportionation process the selectivity to p-xylene of the MFI zeolite is significantly increased by deposition of silica, magnesia, coke etc, on the outer surface which limit the desorption of ortho- and meta- isomers (49). However, this positive effect is also partly due to the selective deactivation of the (non selective) external surface sites.

#### 1.2.2.2 Restricted Transition state-type selectivity

This type of selectivity was proposed first by Csicsery (50) to explain the absence of 1,3,5-trialkylbenzenes in the disprportionation products of dialkyl benzenes over H-mordenite catalysts, although these trialkybenzenes could diffuse in the zeolite channels. In restricted transition state-type selectivity certain reactions are prevented because the transition state is too large for the space available inside the molecular sieve. However, neither reactants

nor potential products are hindered from diffusing through the pores; only the formation of the transition state is inhibited. Acid catalysed transalkylation of diethylbenzenes provides an example (51). In this reaction one of the alkyl groups is transferred from one molecule to another. The reaction is bimolecular and it involves a diphenylmethane-type transition state. Products are monoalkylbenzene and various trialkylbenzene isomers. At equilibrium symmetrical 1,3,5- trialkylbenzenes are the main components of the isomer mixtures. For example, at 578 K the equilibrium mixture of methyl diethylbenzenes contains 46.8% 1-methyl-3, 5-diethylbenzene (52). Over HY zeolite and amorphous silica-alumina symmetrical trialkylbenzenes are formed together with the other isomers. Relative concentrations are close to equilibrium. Over H-mordenite, however, the symmetrical trialkybenzene is almost absent from the reaction product (Table 1.9) (53, 54). One can distinguish experimentally between restricted transition state selectivity and reactant (and product) shape selectivity by particle size effects. In general, observed rates depend on intrinsic (uninhibited) rate constants. If mass transfer is limiting, then the diffusivities of the reactant (or product) molecules depend on catalyst particle size. Reactant and product selectivities are mass transfer limited and therefore affected by crystallite size, whereas restricted transition state shape selectivity is not (55). Intrinsic cracking rates of monomethyl paraffins over ZSM-5 are affected by steric constraints on their transition states.

**Table1.9: Restricted transition state selectivity; the transalkylation of methylethylbenzenes**

| **Catalyst** | **HMOR** | **HY** | **Silica-alumina** | **Thermodynamic equlibrium** |
|---|---|---|---|---|
| Temperature K | 477 | 477 | 588 | 588 |
| 1,3-Dimethyl-5-ethylbenzene % of total $C_{10}$ | 0.4 | 31.3 | 30.6 | 46.8 |
| 1-methyl-3,5-diethylbenzene % of total $C_{11}$ | 0.2 | 16.1 | 19.6 | 33.7 |

### *Advantages of restricted transition state shape selectivity*

One of the most important advantages of ZSM-5 over other crystalline and amorphous catalysts is low coking rate. Because coking is low in ZSM-5, it is deactivated much slower than other zeolites. This longer life made the commercialization of a number of processes (56-61) using this zeolite. Coking is less severe in ZSM-5 than in most other catalysts because the pores lack enough space for the polymerisation of coke precursors. In ZSM-5 coke is deposited on the outer surface of crystals; whereas in large-pore zeolites, such as mordenite or offrerite, most of the coke is formed within the pores (56). Activity is barely affected in the first case but decreases rapidly in the second.

#### 1.2.2.3 Molecular traffic control

A number of zeolites, including ZSM-5, ferrierite, clinoptilolite, offrerite, and mordenite, have intersecting channels of differing size. Since the smaller channels are accessible only to smaller molecules while the larger channels are accessible to both smaller and larger molecules, a new type of shape selectivity can be envisaged. This concept was first proposed by Derouane, who termed it as the molecular traffic control (62). Derouane used this concept to explain the unusual absence of counterdiffusional effects in the ZSM-5 catalysed conversion of simple molecules such as methanol. According to the concept of traffic control, the smaller molecules enter the sinusoidal channels, while the larger molecules exit from the elliptical channels. The significance of this effect was tested by comparing the catalytic properties of ZSM-5 with ZSM-11, the later having intersecting straight channels of the same size (63). But for such reactions as the conversion of methanol to hydrocarbons and the alkylation of toluene to methanol, their results show no major differences in the catalytic activity and stability of these two zeolites other than minor differences in product distribution, which thus largely negated the presence of this effect. However, it is an interesting concept, which should operate in any zeolite containing two intersecting channels of different channel sizes, since the smaller channels are accessible only to smaller molecules while the larger channels are accessible to both smaller and larger molecules. For example synthetic offretite, which has intersecting 12-ring and 8-ring channels, showed some interesting catalytic properties in the cracking of

paraffins (64). It was found to be more selective to the cracking of n-paraffins than a 10-ring zeolite and also to yield lower molecular weight cracked products (Table 1.10). It was speculated that this is because of the blockage of the 12-ring channels by a small amount of stacking faults, which reduce the accessibility of the larger branched paraffins and the availability of all the 8-ring channels to n-paraffins and other smaller molecules.

**Table 1.10: Distribution of cracked products from catalytic dewaxing**

| | $CH_4$ | $C_2$ | $C_3$ | n-$C_4$ | i- $C_4$ | n-$C_5$ | i-$C_5$ | $C_6$ | $C_7^+$ |
|---|---|---|---|---|---|---|---|---|---|
| **TMA-offretite** | 1 | 3 | 23 | 27 | 12 | 26 | 5 | 3 | 0 |
| **ZSM-5** | 1 | 1 | 8 | 11 | 11 | 21 | 18 | 20 | 10 |

### 1.2.2.4 Configurational Diffusion

Configurational diffusion (65) occurs in situations where the pore structural dimensions of the catalyst approach those of molecules. In this diffusion regime, even a subtle change in the dimensions of the molecule can result in a large change in its diffusivity. For example, the diffusivity of trans-butene-2 is at least 200 times that of cis-butene-2 in zeolite Ca-A even though these two molecules differ in size by only about 0.2 ´ (66). Thus the rate of hydrogenation (Table 1.11) of trans-butene-2 over Pt/zeolite-A can be much faster than that of cis-butene-2.

**Table 1.11: Hydrogenation of a mixture of trans- and cis- butene-2**

| | Initial Composition | | Final composition | | | Converison Є, wt % | | $k_{trans}^{a} / k_{cis}$ |
|---|---|---|---|---|---|---|---|---|
| Temp K | trans | cis | trans | cis | n-butane | trans | cis | |
| 393 | 78.7 | 21.3 | 37.2 | 17.0 | 45.9 | 52.9 | 10.8 | 3.3 |
| 376 | 78.7 | 21.3 | 57.3 | 19.8 | 22.9 | 27.2 | 7.1 | 4.3 |
| 371 | 78.7 | 21.3 | 69.4 | 20.9 | 9.7 | 11.8 | 1.8 | 7.0 |

**a** $k_{trans} / k_{cis} = \ln (1- Є_{cis}) / \ln (1- Є_{trans})$

### 1.2.2.5 Confinement effect

The idea of confinement encompasses various interacting effects of the host on the guest molecules, including chemisorption, physisorption and molecular orientation within the zeolite. This conformational relation between the reactant and the framework is proposed (67, 68) to play an important role in the diffusion of the guest molecule in the zeolite and the reactivity of the guest molecule. An example of such an effect is the high selectivity for dehydrocyclization of hexane over Pt-BaKL zeolite (69).

### 1.2.2.6 Shape selectivity related to molecular concentration in zeolite micropores

The interactions between organic molecules and the pore walls of similar size are very strong (Type I adsorption isotherms) and zeolites may be considered as solid solvents (70, 71, 72). The reactant concentration in zeolite micropores is therefore considerably higher than in the gas phase with a significant positive effect on the reaction rates. This effect is all the more pronounced as the reaction order is greater, favouring the bimolecular over the monomolecular reactions.

The concentration of reactant molecules in the zeolite micropores is largely responsible for the observation that zeolite activities are much higher than that of more conventional catalysts (70, 73, 74). In the case of catalytic cracking (FCC), where REHY zeolites were found to be 10 to 10,000 times more active than amorphous silica-alumina depending on the hydrocarbon reactant. Moreover, the selectivity was completely different, the gasoline fraction in the cracked product being richer in aromatics and alkanes (at the expense of naphthenes and alkenes) on zeolites than on silica-alumina. This drastic change in selectivity is due to different ratios between the rates of hydrogen transfer (bimolecular reaction) and cracking (monomolecular reaction), on zeolites compared to silica alumina (73). The effect is dramatic as far as the gasoline yield is concerned: paraffins and aromatics being more ‘ refractory’ towards cracking, the ‘zeolitic’ gasoline is less prone to secondary cracking and yields (but not octane) are much higher on zeolites than on amorphous silica-aluminas. The use of zeolites has spread so rapidly in FCC for this very reason. In other cases however, the high concentration of some reactants leads to undesired side reactions. In the alkylation of isobutene with butanes, zeolites are very efficient

catalysts but lack stability because olefins are more strongly adsorbed than the paraffin and in a matter of minutes, their oligomerisation takes over the alkylation reaction and deactivates the catalyst by pore blocking.

#### 1.2.2.7 The cage or window effect

This effect was proposed by Gorring (75) to explain the non-linear effect of chain length observed in hydrocracking of various n-alkanes over T zeolite, chabazite (CHA) and erionite (ERI). Thus, when a n-$C_{22}$ alkane is cracked over erionite, there are two maxima in the size distribution of the product molecules at carbon numbers of 4 and 11 and a minimum at carbon number of 8. The diffusitivies of n-alkanes also change in a similar periodic manner by over two orders of magnitude between the minimum at 8 and the maxima. This shows that for diffusion, and hence for shape selective effects, not only the size but also the structure of the reactant and product molecules need to be considered.

#### 1.2.2.8 Pore mouth catalysis

The possibility of selective reactions on the external surface of zeolites, more exactly at the pore mouth, was recently addresses by Martens at.al (76, 77) to explain the unusual selectivity of several intermediate pore size zeolites and especially of ZSM-22 (TON) in the aromatisation of long chain n-alkanes. Over PtHZSM-22, this isomerisation is very selective towards monobranched isomers even though they cannot desorb form the narrow channels of this monodimensional zeolite. Pore mouth catalysis could also be responsible for the selective isomerisation of n-butene into isobutene observed over aged HFER samples. However in this case carbonaceous compounds trapped in the pores in the vicinity of the external surface were proposed to be the active species (78). Furthermore, the second branching of n-alkanes over PtHZSM-22 was shown to occur only in positions determined by the distance between pore apertures at the surface of the zeolite crystallites. This type of selectivity was considered to be due to a key-lock catalysis (77) i.e. similar to what occurs in enzymatic catalysis. This concept of zeolites as enzyme mimics was used by Derouane and Vanderveken (79) to explain the selective aromatisation of n-hexane on Pt/LTL zeolite. Catalysts confinement effects combined with the unique pore structure of

LTL zeolite must be responsible for the rapid and selective conversion of n-hexane to benzene.

## 1.3 Modifications

The use of zeolites can further be enhanced by altering various properties. Zeolites can be modified either by isomorphous substitution, cation exchange, metal loading dealumination or silylation.

### 1.3.1 Isomorphous substitution

Modification of zeolites by isomorphous substitution induces variation in acidic properties and unit cell volume, which may lead to interesting catalytic properties. Goldsmith (80) was the very first to report isomorphous substitution of $Si^{4+}$ by $Ge^{4+}$ in the lattice. This was followed by isomorphous substitution of $Si^{4+}$ or $Al^{3+}$ by elements such as B (81-85), Fe (82, 83), Ga (82, 84), Ti (86), V (87), etc. It has been well established (88) that isomorphous substitution of Si and Al by P, Ge, B, Ga and Al modify the acid strength and catalytic properties of various zeolites. This was followed by synthesis of a number of new aluminophosphate molecular sieves containing $Al^{3+}$ and $P^{5+}$ in lattice. Further, the isomorphous substitution of $Co^{2+}$, $Fe^{3+}$, $Mg^{2+}$, $Zn^{2+}$, $Be^{2+}$, $B^{3+}$, $Ga^{3+}$, $Cr^{3+}$, $Ti^{4+}$, $Si^{4+}$ and $Mo^{3+}$ in AlPO structure is also well established (88, 89). Barrer (90) classified four types of substitution in zeolites namely, (i) cation exchange, (ii) framework substitution, (iii) isomorphous substitution of isotopes and (iv) substitution of intracrystalline salts and molecular water. Isomorphous substitution can be achieved by direct hydrothermal synthesis or by post synthesis methods. Using characterization techniques such as XRD, IR, MASNMR, ESR, UV-vis, XPS and by catalytic test reactions, the tetrahedral occupancy of the substituted metal cation can be verified.

### 1.3.2 Cation exchange

The ion exchange capacity of a zeolite is dependent upon the amount of aluminum present in the framework of zeolite. Majority of the zeolites synthesized are in their cationic forms, wherein, positively charged cations neutralize the charge created by the aluminum

tetrahedra in the framework. These extra framework cations are exchangeable and the degree of cation exchange depends on

- The type of cation being exchanged, its size as well as its charge.
- The nature, size and strength of any cation coordination complex.
- The temperature of the ion-exchange treatment.
- The thermal treatment of the parent zeolite before and after exchange.
- The structural properties of the zeolites and its silica to alumina ratio.
- The location of the cations in the zeolite structure.
- The concentration of the cation exchange solution
- The prior treatment of the zeolite.

### 1.3.3 Silylation

Reacting the outside surface of the zeolite crystallites with reactive silicon or other reactive materials can reduce diffusivities within the zeolites. The silane reagent should be larger than the pore entrance so that it does not affect internal pore diameters or acid sites. A frequently used silane reagent is tetraethyl orthosilicate (TEOS). As the silane reacts with surface hydroxyls it forms a surface layer which extends over part of each pore entrance. The surface silane group is converted to the oxide or hydroxide after hydration or oxidation.

## 1.4 Physico-Chemical Characterization of zeolites

X-ray powder diffraction and adsorption measurements are very important techniques employed in the zeolite characterization. Infrared spectroscopy, Uv-vis spectroscopy, nuclear magnetic resonance spectroscopy and electron spin resonance spectroscopy have also been applied to obtain structural information about zeolites.

### 1.4.1 X-ray diffraction

Among the various spectroscopic techniques employed for structural evaluation of zeolites, x-ray diffraction is one of the most important and useful technique to identify zeolite

structure (91), to determine phase purity, percent crystallinity, unit cell parameters and crystallite size. It further helps in understanding the kinetics of crystallization. As the powder pattern is the finger print of the individual zeolite structure, phase purity and percent crystallinity of the synthesized zeolite can be arrived at by comparing with the standard pattern for the zeolite under investigation. Isomorphous substitution of a heteroatom in zeolitic framework results in changes in the unit cell parameters and unit cell volume. This is one way of confirming isomorphous substitution (92).

### 1.4.2 Infrared spectroscopy

For a long time, IR spectroscopy has been mainly used to characterize zeolites and zeolite/adsorbate systems. IR studies on zeolites and zeolite/adsorbate systems reported in the literature before 1975 have been extensively reviewed by Ward (93) and in 1992, a very concise overview has been published by Foerster (94).

The main areas of application of IR spectroscopy are

(a) Investigation of framework properties

(b) Study of adsorption or catalysis sites of the zeolite

(c) Characterization of zeolite/adsorbate systems

(d) Measurements related to the motion of guest molecules in the pores and cavities of the zeolites.

#### 1.4.2.1 Study of Framework vibrations of zeolites

Flanigen et al. (95) studied the relationship between IR spectral features of zeolites and structural properties. The bands observed in mid infrared were classified into two main categories, viz. bands due to internal vibrations of the $TO_4$ tetrahedra (T= Si or Al) and external vibrations of tetrahedral linkages e.g., in double rings (as in A-, X-, Y- type) or pore openings (e.g., as in mordenite). Assignment of various zeolite lattice vibrations are listed in Table 1.12.

**Table 1.12 Assignments of zeolite lattice vibrations**

| | |
|---|---|
| **Internal tetrahedra** | |
| Asymmetric stretch | 1250 - 950 $cm^{-1}$ |
| Symmetric stretch | 720 -650 $cm^{-1}$ |
| T— O bend | 420 - 500 $cm^{-1}$ |
| **External linkages** | |
| Double ring | 650 - 500 $cm^{-1}$ |
| Pore opening | 300 - 420 $cm^{-1}$ |
| Symmetric stretch | 750 - 820 $cm^{-1}$ |
| Asymmetric stretch | 300 - 420 $cm^{-1}$ |

### 1.4.2.2 Investigation of acidity and basicity in zeolites using IR spectroscopy

Acid sites, such as acidic -OH groups (Brönsted acid centers), true Lewis sites (aluminium-containing extra-framework species) and cations as well as basic sites (such as basic oxygen atoms or alkaline metal clusters) are encountered in zeolites and are of paramount importance in acid-base catalysis of zeolites. Employing IR spectroscopy, only the Brönsted acid sites may be investigated with and without probe molecules, whereas acidic Lewis sites, cations and basic sites can be identified and quantitatively determined only with the help of probe molecules. Probe molecules frequently that are employed for acidity determination are pyridine, substituted pyridines, ammonia, amines, carbon monoxide, methane, hydrogen and fluoro-/chloroethane and ethane for acidic centers and carbon dioxide or pyrrole for basic sites. A detailed description about determination of zeolite acidity is given in section 1.4.6.

### 1.4.3 Thermal Analysis

Generally zeolites are thermally stable, but heating at elevated temperatures may lead to structure breakdown and therefore decrease in crystallinity. Thermo analytical data obtained from TGA, DTA and DTG studies are useful in evaluating the thermal properties of zeolites (96). The shape and splitting of the endotherms (low temperature) helps to

identify the location of water molecules and also helps in studying kinetics of dehydration of water molecules. Zeolites are known to possess high thermal stability, which increases with silica to alumina ratio (97, 98). Ferrierite zeolite is found to be stable up to 1273 K.

### 1.4.4 Sorption and Diffusion properties

As zeolites are microporous with channels and cavities they are able to selectively sorb certain molecules. Generally in zeolites, intracrystalline surface area is higher and constitutes to about 97% of the total surface area. Damour (1846) demonstrated that water could be reversibly removed from a zeolite without altering its structure. Subsequently a number of reports appeared on sorption of gases and vapors on dehydrated zeolites (99, 100). Furthermore, Barrer and his co-workers studied sorption of various gases and vapors on natural as well as synthetic zeolites (101, 102). The selective adsorption of molecules depends on molecular size of adsorbate, polarizability and polarity of the adsorbate, organophilicity and hydrophilicity of the host zeolite structure, degree of unsaturation of organic adsorbate and polarizing power of the host cation. Sorption studies on zeolites can provide information about their void volumes, pore size, percentage crystallinity, surface area, acidity, diffusion properties and pore blockage, if any. Low temperature (77 K) nitrogen sorption isotherms help in determining pore volume, pore size distribution as well as the surface area of zeolite under study (103, 104). Adsorption and diffusion properties of zeolite play an important role on the rate of chemical reaction at the active sites. Barrer et al. (105) studied in detail the diffusion process in zeolites. Diffusion in zeolites has been categorized as configurational, Knudsen and bulk diffusion.

### 1.4.5 Scanning Electron Microscopy

The crystal morphology of zeolite samples is investigated using scanning electron microscopy (SEM JEOL, JSM-5200). Cathode rays are bombarded on the sample and the scattered secondary electrons are used to obtain an image. A thin layer (~ 0.1 mm) of the sample is mounted on a carrier made from alumina that was coated with a film of gold to prevent surface charging and to protect the zeolite material from thermal damage by the electron beam. The major advantage of the SEM is that bulk samples can be studied by this technique.

### 1.4.6 Determination of zeolite acidity

The acidity of zeolites is mainly due to the presence of Brönsted acid sites. But, some Lewis acid sites may be present especially when zeolites are treated at high temperature. The measurement of the number, type and strength of acid sites provides the key experimental data regarding zeolite acidity. For a complete characterization of zeolite acidity, it is, therefore, necessary to determine number and strength of both types of acid sites. Several methods have been developed for this purpose, most important among them are

(i) Titration methods
(ii) Adsorption and desorption of bases
(iii) IR spectroscopy of –OH groups
(iv) IR spectroscopy of adsorbed species
(v) NMR spectroscopy of –OH groups
(vi) NMR spectroscopy of adsorbed species

#### 1.4.6.1 Desorption of bases: Temperature programmed desorption

When an acid is neutralized by reaction with a base the heat of neutralization is evolved. The higher the heat of neutralization, stronger is the acid strength and so it can be used to characterize acid-strength. This principle can be used to characterize the acid sites present on a zeolite sample. Temperature programmed desorption (TPD) of probe molecules like ammonia and pyridine is a popular method for the determination of acidity of solid catalysts as well as acid strength because it is an easy and reproducible method. Ammonia is used frequently as a probe molecule because of its small molecular size, stability and strong basic strength (106). The acidity measurements have been carried out by ammonia TPD method. First the zeolite is contacted with a base ($NH_3$ or pyridine) to neutralize the acidic sites present. Then the temperature is raised at a constant rate and the amount of desorbed base is monitored and recorded. As a result, a desorption spectrum is obtained. In short, TPD consists of heating a sample at a constant rate and measuring the quantity of material desorbed at each temperature. TPD data provide a partially averaged value for acid strength. It is a simple and rapid method to characterize zeolite acidity. Numerous

theoretical and experimental studies have been devoted to the adsorption of $NH_3$ (107-120). $NH_3$-TPD is one of the most often used methods (110-119). In principle, both the concentration of sites having similar acid strength and the average heat of adsorption or activation energy of $NH_3$ desorption can be determined using the TPD method. Often the temperature of maximum desorption rate, i.e., the temperature of a TPD peak ($T_{max}$), is used as a rough measure of the acid strength of the sorption sites. Among the limitations of this method is that it can distinguish sites by sorption strength only, but not Lewis and Bronsted type sites. Moreover, desorption may proceed simultaneously from sites of different types resulting in composite curve consisting of overlapping TPD peaks. In a TPD spectrum, generally two peaks are observed, one at low temperature (LT) corresponding to $NH_3$ desorbing from the weaker acidic sites (also observed for nonacidic silicates) and another one at higher temperature (HT) corresponding with the stronger acidic sites. The area under these peaks gives information about the amount of these strong acid sites whereas the peak-maximum-temperature ($T_{max}$) gives information about its acid-strength.

### 1.4.6.2 IR spectra of OH groups

Hardly any property of a solid acid catalyst has been studied so frequently as the nature and concentration of the functional (hydroxyl) groups (121-124). The origin of these hydroxyl groups may be (i) the relaxation of the terminating lattice by dissociative sorption of water or (ii) the balancing of charges arising from substitution of lattice cations with cations of different valency. A more direct study of the Brönsted acidic –OH groups in zeolites is possible by IR-spectroscopy. The weaker the O-H bond, the lower the stretching frequency and the higher the acid-strength. General IR spectrum of a zeolite shows three peaks in the O-H stretching region. The peak at 3720-3740 $cm^{-1}$ is assigned to the non-acidic silanol groups that are present on the outer surface of the zeolite crystals and at structural defects. The peaks between at 3640 and 3540 $cm^{-1}$ correspond to -OH groups that have weaker O-H bond strength and hence more acidic character. From these bands the one at 3640 $cm^{-1}$ disappears after adsorption of pyridine and so this band is assigned to the accessible acidic –OH groups. This method only gives qualitative information on the number of acid sites.

#### 1.4.6.3 IR spectroscopy of adsorbed bases

Instead of looking at the acidic –OH groups, it is also possible to study the IR absorption of bases that are reacted with the acid sites of the zeolite. Frequently, the reaction with pyridine is used for this purpose. Pyridine can react with Brönsted (B) acid sites as well as with the Lewis (L) acid sites of a zeolite. The reaction of the Brönsted acid sites results in the formation of pyridinium ion while the pyridine molecule is coordinatively bound to the Lewis acid sites. Both the pyridinium ion and the coordinatively bound pyridine have characteristic IR absorption bands. The intensity of these bands corresponds to the number of these sites; however, it is impossible to obtain information on the acid strength. The presence of the absorption bands only shows that acid-sites are present with an acid-strength large enough to react with the basic probe molecule pyridine. FTIR analysis of adsorbed pyridine allows a clear distinction between Brönsted and Lewis acid sites, the absorption bands appearing at 1545 and 1455 $cm^{-1}$ in the IR spectra is assigned to adsorbed pyridinium ions and pyridine coordinated to Lewis acid sites, respectively (125-127).

## 1.5 Catalysis over Zeolites

Zeolites offer advantages over conventional catalysts in acid, acid-base, oxidation and reduction reactions. The major properties such as well defined structure, uniform pores, high thermal stability, high surface area, easy regeneration, well defined micro-pore system etc. make zeolites unique heterogeneous catalysts.

### 1.5.1 Acidic reactions

The catalytic sites for acid catalyzed reactions in aluminosilicate zeolites are mainly the Brönsted acid centers associated with protons. The as-synthesized form of zeolite can be converted into catalytically active protonic form (H form) by a number of techniques. The first and the simplest one being ion exchange of cations by protons using a dilute acid. However, presence of acid may lead to dealumination and result in the structural collapse, hence the above method is not practiced for all zeolites. The second method involves the replacement of cations (e.g. Na) by ammonium ions, using a solution containing ammonium salts followed by thermal decomposition of ammonium form to produce protonic form of the zeolite. The strength and the concentration of the acid sites can also be

modified by isomorphous substitution of trivalent Al and tetravalent Si by other metal ions. All the alkylation (128-132), disproportionation and isomerization (133-136) reactions carried out on zeolites are due to acidity present in the zeolite. Zeolites are used as solid acids in many conventional acid catalysed reactions where hazardous and corrosive chemicals like mineral acids, $AlCl_3$ are utilized as catalysts. Aromatics have a wide variety of applications in the petrochemical and chemical industries. They are an important raw material for many intermediates of commodity petrochemicals and valuable fine chemicals, such as monomers for polyesters, engineering plastics, intermediates for detergents, pharmaceuticals, agricultural-products and explosives (137). Among them, benzene, toluene and xylenes (BTX) are the three basic materials for most of chemical intermediates (138). Dialkylbenzenes, a subcategory of aromatics, include xylenes, diethylbenzene (DEB) and dipropylbenzene (DPB), all of which may be derivable to valuable performance chemicals. For example, xylenes are the key raw materials for polyesters, plasticizers and engineering plastics (139), p-DEB is a high-valued desorbent used in p-xylene adsorptive separation process (140), whereas increasing applications of diisopropylbenzene (DIPB) have been found, ranging from photo-developers, anti-oxidants to engineering plastics (141). Process development in aromatic interconversion is therefore an important research task with great industrial demand. There are many driving forces for the development of new processes. In addition to the economically relevant variables such as market demand, feedstock availability and operating cost, legislative aspects such as environmental laws and new reformulated gasoline specifications etc., also come into play. In response to the worldwide environmental awareness, there are active programs to search for clean processes. Solid acid catalysts have long been demonstrated as the key to the success of the historical efforts. Tanabe et al. (142) comprehensively discussed acid catalyst properties in their well-known review on solid acids and bases. Aromatics alkylation was one typical example of the use of solid acid catalysts in the development of environmentally sound processes. Zeolites were used to replace the traditional Friedel-Craft's catalysts, making the process cleaner, less corrosive and more economically competitive. By using Friedel-Craft's catalysts, solid and liquid wastes in the ethylbenzene (EB) production of 390 000 tons/year were 500 and 800 tons/year, respectively. By using

ZSM-5 catalyst, the wastes were significantly reduced to 35 and 264 tons/year respectively (143).

#### 1.5.1.1 Alkylation reactions

Generally, alkylation reactions can be catalysed by strong liquid acids such as sulphuric or hydrofluoric acid. However, these are hazardous chemicals and their employment, thus, entails serious problems. The serious disadvantage of Friedel-Crafts alkylation is the contamination of the alkyl aromatic products with chlorinated compounds. Moreover, the use of $AlCl_3$ is not friendly to the environment from two points of view, namely operation of the unit and disposal of the spent catalyst. Alkylation of benzene requires medium-strength acidity and, as monoalkyl benzenes are more reactive compared to benzene, they are readily alkylated to dialkyl benzenes in a subsequent step. Their transalkylation with benzene to monoalkylbenzenes requires stronger acidity compared to that required for the formation of monoalkyl benzenes. In addition to the alkylation reactions, dimerisation or oligomerisation of olefins can take place as well in parallel. To suppress the formation of dimers or oligomers, an excess of benzene is used. The higher the reactivity of olefin (increasing with increasing length of the olefin chain), the higher the benzene-to-olefin ratio should be. This value is typically 4 for benzene/ethylene and 4-10 for benzene/propylene, depending on the catalyst used. Dimers or oligomers, which are formed from olefins, further alkylate benzene or monoalkylbenzenes easily, and finally, with the participation of hydrogen transfer reactions, they yield high-molecular weight product, coke, that leads to catalyst deactivation. Some of the alkylation processes that have been thoroughly investigated are benzene alkylation with ethylene and propylene, toluene alkylation with methanol, ethylene/ ethanol and propylene/ propanol, ethylbenzene alkylation with ethanol/ ethylene etc (144-152).

#### 1.5.1.2 Disproportionation reactions

Disproportionation and transalkylation are the two major practical processes for the interconversion of aromatics, especially for the production of dialkylbenzenes. They are coined as “alkyl group transfer reactions”, which deal mainly with the alkyl group transfer among different aromatic rings. Such processes are commonly used in the conversion of

toluene into benzene and xylenes. Moreover, disproportionation of EB and isopropylbenzene (IPB) yields diethylbenzene (DEB) and dipropylbenzene (DPB), respectively. Improving and finding cost effective disproportionation and transalkylation catalytic processes are interesting and challenging tasks in industrial research. Several newly developed novel processes produced dialkylbenzenes which are particularly rich in para isomers compared to their thermodynamic equilibrium compositions, for example, MSTDP$^{SM}$, MTPX$^{SM}$ and PX-Plus$^{SM}$ for p-xylene production (153-156) and TSMC's (Taiwan Styrene Monomer) selective PDEB process for p-DEB production (157). In addition, several new emerging heavy aromatics conversion processes with maximum approach to thermodynamic equilibrium xylene yield have also been developed, namely Tatoray$^{SM}$ (158-160) and TransPlus$^{SM}$ (161-164). Disproportionation and transalkylation are both acid catalyzed reactions. In the early days, liquid Friedel-Crafts (165) and HF-$BF_3$ systems (166) were commonly used. Then, the metal oxide catalysts, such as CoO-$MoO_3$ on aluminosilicate /alumina (167) and noble metal or rare earth on alumina were developed and used (168). In modern technology, zeolite catalyst systems, for example zeolite Y, mordenite, ZSM-5 and other large-pore zeolites, are predominant (169). Transalkylation processes are normally catalyzed by large pore zeolites which can also be used for toluene disproportionation. The latter, however, is mostly catalyzed by 10-membered oxygen ring zeolites having medium-pore size such as ZSM-5 zeolite. DEB can also be produced by the EB disproportionation reaction. A variety of different zeolitic catalysts, such as ZSM-5, mordenite, faujasite and zeolite Beta, etc. have been studied (170-172). Compared to other monoalkylbenzene processes, EB disproportionation has a much more stable activity (172). Most catalysts show acceptable stability in EB disproportionation. The products obtained in the disproportionation reaction normally give the thermodynamic equilibrium composition that requires energy intensive separation process for p-DEB recovery. Thus, the technical challenge in producing p-DEB by EB disproportionation is technology development to enhance para selectivity. In line with the developments in para selective processes, discussed earlier, many earlier approaches are applied for p-DEB process development.

## 1.6 Scope of the thesis

In this thesis we, report para-selective preparation of various aromatic compounds, p-diethylbenzene, p-xylene, p-tertiary butyltoluene and p-cumylphenol on modified catalysts and characterization of these catalytic materials by x-ray diffraction (XRD), surface area by nitrogen sorption, scanning electron microscopy (SEM), temperature programmed desorption (TPD) of ammonia and FTIR of adsorbed base. The thesis is divided in to six chapters.

Chapter 1 is a general introduction to zeolites, their classification, catalytic activity and their shape selective aspects. A brief summary of various modification methods involved in preparing selective catalysts is also described. Some of the reported literature pertaining to the reactions that are described in the succeeding chapters has also been cited. In the end, the aim and objectives of the present work has been described.

Chapter 2 deals with the selective preparation of p-dialkylbenzenes on isomorphously substituted MFI type zeolites. A small account of importance of isomorphous substitution is described as an introduction. The various synthesis procedures used for the preparation of Al, Ga, Fe, B substituted MFI zeolites have been described. Some of the physical and chemical methods like XRD, framework IR and TPD of ammonia that are applied to characterize the as synthesized zeolites by the above methods have been discussed. The catalytic activity of the above zeolites has been evaluated for the alkylation of ethylbenzene with ethanol for the synthesis of diethylbenzene. Further, the zeolites were silylated through liquid phase silylation of tetraethyl orthosilicate for attaining high selectivity of p-diethylbenzene. The same catalysts were also used for the synthesis of p-xylene by methylation of toluene. The variation in the activity of these zeolites with silylation, correlated through TPD of ammonia has been described.

Chapter 3 deals with the synthesis of p-dialkyl benzenes on Al-MFI zeolite by alkylation and disproportionation reactions. A comparison of the catalytic activity and selectivity has been made for the pure powdered samples and extrudated (with $Al_2O_3$) forms of the

zeolites. Silylation with TEOS has been carried out for improving the para-selectivity. Mixed $C_8$ alkyl aromatic isomer feeds, containing various isomers of xylenes, in addition to EB, have been used to study the influence of xylenes on the selectivity of p-DEB. Reaction with these feeds has an added advantage as reaction of EB (alkylation or disproportionation) is carried out directly using $C_8$ aromatics cut which is obtained from xylene isomer unit, that has high concentration of EB after removal of xylenes. It is essential to reduce the excess ethylbenzene from these feeds to mix them back into xylene isomerisation loop. The time on stream stability of the modified zeolites for conversion of these streams is also given in this chapter.

In chapter 4, studies on the synthesis of p-tert-butyltoluene over large pore zeolites Y, MCM-22, ZSM-12 and beta have been presented. Efforts have been made to correlate the activity and selectivity with the structure of various zeolites and also to get high selectivity by variation of parameters like silica to alumina ratio, temperature, space velocity, toluene to tert-butyl alcohol mole ratio have been described.

In chapter 5, synthesis of 4-cumylphenol (4-CP or PCP), which is an industrially important chemical intermediate, has been described on various large pore zeolites like Y, beta and mordenite. 4-cumylphenol is synthesized by the reaction of phenol with alpha-methylstyrene (AMS). This chapter also describes some studies that are carried out on dimerisation of alpha-methylstyrene, which is a competing reaction in this system. The effect of various parameters like temperature, $SiO_2/Al_2O_3$ ratio and mole ratio of phenol to AMS has been given. Effect of various concentrations of cumene as diluent/solvent which helped to maximize the selectivity of 4-CP is also reported.

Chapter 6 highlights the salient features of the work presented in this thesis. A brief summary of all the chapters has also been presented.

## 1.7 References


1 Barrer, R. M., Hydrothermal Chemistry of Zeolites academic press, New York (1982).

2 Barrer, R. M., J. Chem. Soc.(1961) 971.

3 Breck, D.W., Zeolites Molecular Sieves., Wiley, New York (1974).

4 Chen, N. Y., Kaedly, W. W. and Dwyer, F .G., J. Am. Chem. Soc. 101 (1979) 6783.

5 Liebau, F., Zeolites 3 (1983) 191.

6 Szostak, R., Molecular Sieves: Principles of Synthesis and Identification, Van Nostrand Reinhold, New York (1989).

7 Rees, L. V. C. Nature 296 (1992) 492.

8 McBain, J. W., The Sorption of gases and vapours by solids, Ritledge and Sons, London, (1932) Ch. 1.

9 Szhultz, P. G., Angew Chem. Int. Ed. Engl. 28 (1989) 1283.

10 Davis, M.E. , Acc. Chem. Res. 26 (1993) 111.

11 Cronstedt, A. F., Kongl Vetenskaps Acad. Handl. Stockholm 17 (1756) 120.

12 Damour, A., Ann. Mines 17 (1840) 191.

13 Deville, St. Claire, Compt. Rend. 54 (1862) 324.

14 Thomson, H. S., J. Roy. Agric. Soc. 11 (1862) 68.

15 Breck, D. W., Molecular Sieves Zeolites, Adv. Chem. Ser. (American Chemical Society, Washington DC) 101 (1971) 251.

16 McBain, J. W., The Sorption of gases and vapors by solids, Pub. Rutledge and Sons London (1932) Ch. 5.

17 Barrer, R. M. Proc. Roy. Soc. (London) 162 A (1938) 393, Trans. Far. Soc. 40 (1944) 559.

18 Barrer, R. M. J. Chem. Soc. (1984) 127.

19 Barrer, R. M. and Marcilly, C., J. Chem. Soc. A (1970) 2735.

20 Barrer, R. M. and Robinson, D. J., Zeit. Krist, 135 (1972) 374.

21 Barrer, R.M., Nature 164 (1949) 112.

22 Barrer, R. M. Pure and Appl. Chem., 51 (1979) 1091.

23 Meier, W. M. and Olson, D. H., Atlas of Zeolite Structure Types, Butterworths (1987).

24 Bragg, W. L, The Atomic Struc. of Miner. Cornell University Press, Ithaca, New York (1937).

25 Meier, W. M., Molecular Sieves Soc. of Chem. Ind. London (1968) 10.

26 Flanigen, E. M., In Proceedings of the fifth Interanational Conference of Zeolites, (L.V.C Rees Eds.) Naples, Italy, June 2-6, (1980) 760.

27 Barrer, R. M., Molecular Sieves Soc. of chem. Ind. London (1968) 10.
28 Sand, L. B. Econ. Geol. (1967) 161.
29 Smith, J. V., Mineral Soc. Amer. Spec. paper 1 (1963).
30 Fischer, K. F., Meier, W. M. Fortschi Mineral 42 (1965) 50.
31 Breck, D. W. Molecular Sieves Zeolites, Adv. Chem. Ser., Amer. Chem. Soc., Washington DC, 101 (1971) 1.
32 Davis, M. E., Saldarriaga, C., Montes, C., Graces, J. and Crowder, C., Nature 331 (1988) 968.
33 Estemann, M., McCusker, L. B., Baelocher, C., Merrouche, A. and Kessler, H., Nature 352 (1991) 320.
34 Freyharett, C. C., Tsapatsis, M., Lobo, R. F. Balkus Jr., K. J. and Davis, M. E., Nature 381 (1998) 295.
35 Zeolites for cleaner technologies. Guisnet, M., and Edimbourg in Supported Catalysts and their Applications, Ed. Sherrington D. C. and Kybett A. P., (The Royal Society of Chemistry, Cambridge, 2001) 55.
36 Mortier W. J., Proceeding 6$^{th}$ Int. Zeolite Conference, Ed. Olson D. and Bisio A., (Buttersworth, Guildford, 1984) 734.
37 Rabo, J. and Gajda, G. J., in Guidelines for Mastering the Properties of Molecular Sieves, Ed. Barthomeuf D. et al., 221 (NATO ASI Series B: Physics, Plenum Press, New York, 1990) 273.
38 Martens, J. A., Souverijns W., van Rhyn W. and Jacobs, P. A., in Handbook of heterogenous catalysis, Ed. G. Ertl et.al., 1 (Wiley, 1997) 324.
39 Pines, l. A., maher, P. J., Wachter W. A., J. Catal. 85. (1984) 466.
40 Wachter W. A., Proceeding 6$^{th}$ Int. Zeolite Conference, Ed. Olson D. and Bisio A., (Buttersworth, Guildford, 1984) 141.
41 Barthomeuf, D., Materials Chemistry and Physics 17 (1987) 49.
42 Weisz, P. B., Frilette V. J., Maatman, R. W. and Mower E. B., J. Catal. 1 (1962) 307.
43 Chen, N. Y., Mazuik J., Schwartz A. B. and Werisz P. B., Oil and Gas J. 66 (1968) 154.
44 Weisz, P. B. and Frilette, V. J., J. Phys. Chem.. 64 (1960) 382.
45 Weisz, P. B., Frilette, V. J., Maatman, R. W., and Mower, E. B., J. Catal. 1 (1962) 307.
46 Dessau, R. M., J. Catal. 77, (1982) 304.
47 Chen, N. Y., Garwood, W. E., Dwyer, F. G., eds., Shape Selective Catalysis in Industrial Applications , Chemical Industries, 36 (1989)
48 Venuto, P .B. and Hamilton, L. A., Ind. Eng. Chem. Prod. Res. Develop. 6 (1967) 190.

49 Olson, D. H., and Haag, W. O., ACS Symposium Series 248 (1984) 275.

50 Csicsery S. M., J. Catal. 23 (1971) 124.

51 Csicsery, S. M., J. Org. Chem. 34, (1969) 3338-3342.

52 Csicsery, S. M., J. Chem. Eng. Data, 12, (1967) 118-122.

53 Csicsery, S. M., J. Catal. 19 (1970) 394-397.

54 Csicsery, S. M., J. Catal. 23 (1971) 124-130 same as 34 in zeolites for clean technology

55 Haag,W. O., Lago, R. M., and Weisz, P. B., Faraday General Discussion No. 1982, 72, 317. Selectivity in Heterogenous Catalysis, September 14-16, 1981, University of Nottingham, England.

56 Dejaifve, P., Auroux, A., Gravelle, P. C., Vedrine, J. C., Gabelica, Z., and Derouane, E. G., J. Catal. 70 (1981) 123.

57 Rollmann, L. D., J. Catal. 47 (1977) 113.

58 Walsh, D. E., and Rollmann, L. D., J. Catal. 49 (1977) 369.

59 Rollmann, L. D. and Walsh, D. E., J. Catal. 56 (1979) 139.

60 Walsh, D. E., and Rollmann, L. D., J. Catal. 56, (1979) 195.

61 Rollmann, L. D. and Walsh, D. E., Progress in Catalyst Deactivetion, p. 81, Figueiredo J. L. Ed. Martinus Nijhoff, The Hague, Boston, London, (1982).

62 Derouane, E. G., and Gabelica, Z., J. Catal. 132 (1980) 269.

63 Derouane, E. G., Dejaifve, P., and Gabelica, Z., Chem.Soc. Faraday Disc. 72 (1981) 331

64 Chen, N. Y., Schlenker, J. L., Garwood, W. E. and Kokotialo,G. T., J. Catal .86, (1984) 24.

65 Weisz, P. B., Chemtech 3, (1973) 498.

66 Chen, N. Y. and Weisz, P. B.; Chem. Eng. Prog. Symp. Ser. 73 (1967) 86.

67 Derouane, E. G., Andre, J. M., and Lucas, A. A., J. Catal. 110, (1988a) 58.

68 Nagy,J. B., Fernandez, Z., Gabelica, Z., Laurent, E., and Malijean, Appl. Catal. 40, (1988b) L1.

69 Derouane, E. G. and Vanderveken, D., Appl. Catal. 45, (1988) L15.

70 Rabo, J. and Gajda, G. J., in Guidelines for Mastering the Properties of Molecular Sieves, Ed. Barthomeuf D. et al., 221 (NATO ASI Series B: Physics, Plenum Press, New York, 1990) 273.

71 Martens, J. A., Souverijns, W., van Rhyn, W. and Jacobs, P. A., in Handbook of heterogenous catalysis, Ed. G. Ertl et.al., 1 (Wiley, 1997) 324.

72 Derouane, E. G., J. Mol. Cat. A: Chemical 134 (1998) 29.

73 Gates, B. C., Katzer, J. R., and Schuit, G. L. A., eds., Chemistry of Catalytic Processes, (Chemical Engineering Series, McGraw Hill Book Company, New York, 1979) Ch.1.

74 Fraissard, J., Stud. Surf. Sci. Catal. 5 (1980) 343.

75 Gorring, R. L., J. Catal. 31 (1973) 13; Gorring, R. L. and Danills, R. H., ACS Symposium Series 248 (1984) 51.

76 Martens, J. A., Parton, R., Uytterhoeven, L., Jacobs, P. A., Froment, G. F., Appl. Catal. 76 (1991) 95.

77 Martens, J. A. et.al., Angew. Chem. 34 (1995) 252.

78 Andy, P. et.al., J. Catal. 173 (1998) 322.

79 Derouane, E. G. and Vanderveken, D.; Appl. Catal. 45, (1988) L15.

80 Goldsmith, T. R., Min. Mag. 29 (1952) 952.

81 Becker, K.; John, H; Steinburg, K; Weber, M. and Nestler,K., Catalysis on Zeolites (Kallo. D and Minachev, Kh. M., Eds.), Akademia Kiado, Budapest (1988) 515.

82 Naccache, C. and Ben Tarrit, Y. Zeolite Science and Technology, Riberio, F. R., Rodrigues, A. E., Rollmann, L. D. and Naccache, E. Eds.) Martinus Nijhoff, The Haque (1984) 373.

83 Kotasthane, A. N.; Shiralkar, V. P.; Hegde, S. G. and Kulkarni, S. B., Zeolites 6 (1986) 233.

84 Rao, G. N.; Shiralkar, V. P.; Kotasthane, A. N. and Ratnasamy, P. Molecular Sieves; Synthesis of Microporous Materials, Vol 1, Ed. M. L. Occelli and H. E. Robson, Van Nostrand Reinhold-New York.

85 Minachev, Kh. M, Khariamov, V. V. and Garanin, V. I. Catalysis on Zeolites (Kallo. D and Minachev, Kh. M., Eds.), Akademia Kiado, Budapest (1988) 489.

86 Pergo, G., Bellusi, G., Corono, C., Taramasso, M. and Buonomo, F., Stud. Surf. Sci. Catal. 28 (1986) 129.

87 Kornatowki, J. Sychev, M., Goncharuk, V. and Bauer, W-H. Stud. Surf. Sci. Catal. 65 (1991) 581.

88 Tielen, M., Geelen, M., Jacobs, P. A. J. Catal. 91 (2) (1985) 352.

89 Ward, J. W. Zeolite Chemistry and Catalysis, [C. Rabo, J.A. Eds.], ACS mongraph. Chp. 2 171 (1976) 118.

90 Barrer, R. M., Bayhans, J. W. Bultitude, F. W. and Meier, W. M., J. Chem. Soc. (1995) 195.

91 Von Ballmoos R. Collection of Simulated XRD Powder Patterns for Zeolites, Butterworths London (1984).

92 Meyer, B. L., Ely S. R., Kutz, N. A., Kuduk and Bossche, E. V., J. Catal. 91 (1985)

352.

93 Ward, J. W. in Zeolite Chemsitry and Catalysis. Rabob, J. A. (ed) Am. Chem. Soc, Mon 171, Washington, DC, (1976) p 118.

94 Foerster, H., in Spectroscopic And Computational Studes of Supramolecular Systems, Davies, J. E., (ed) Kluver Academic Publishers, dordrecht, The Netherlands, (1992) p 29.

95 Flanigen, E. M., Szymanski, H. A., Khatami. H., Adv. Chem. Ser., 101 (1971) 201.

96 Barrer, R. M. and Langley, D. A., J. Chem. Soc. (1958) 3804, 3811, 3817.

97 Rabo, J.A., Zeolite Chemistry and Catalysis, Eds. Beringer, F. M., Am. Chem. Soc. Washington D.C. (1976) pg 285.

98 Bremer, H., Marke, W., Schodel, R. and Vogt, F., Adv. Chem. Ser. 121 (1973) 249.

99 Friedel, G., Bull. Soc. Fr. Mineral Crystallogr. 19 [14] (1986) 96.

100 Rabinowitch, R. and Wood, W. C., Trans. Faraday Soc. 32 (1936) 947.

101 Barrer, R. M., Proc. Roy. Soc. A 167 (1938) 39Z.

102 Barrer, R. M., Quart. Rev., London, (1949) 3239.

103 Hong -Xin. Li., Martens, J. A., Jacobs, P. A., Innovation in Zeolite Material Sci., Gribit, P. J. (Eds.) (1985) 75.

104 Tapp, N. J., Milestone, N. B., Bibby, D. M., Ibid pg 393.

105 Barrer, R. M., Adv. Chem. Ser. 102 (1971) 41.

106 Satsuma, A., Kamiya, Y., Westi. Y., Hattori, T., Appl. Catal. A, 194 (2000) 253.

107 Lok, B. M., Marcus, B. K., Angell, C. L., Zeolites, 6(3), (1986) 185.

108 Sawa, M., Niwa, M., Murakami, Y., Zeolites, 10(4), (1990) 307.

109 Valyon J., Gy. Onyestyak,. Rees, L. V. C., Langmuir, 16 (2000) 1331.

110 Martin, A., Wolf, U., Berndt, H., Lucke, B., Zeolites, 13 (1993) 309.

111 Sato, H., Catal. Rev. –Sci. Eng., 39 (1997) 395.

112 Hidalgo, C. V., Itoh, H., Hattori, T., Niwa, M., Murakami, Y., J. Catal., 85 (1984) 362.

113 Topsoe, N.-Y., Pedersen, K., Derouane, E. G., J. Catal., 70 (1981) 41.

114 Meshram, N. R., Hegde, S. G., Kulkarni, S. B. Zeolites, 6 (1986) 434.

115 Woolery, G. L. Kuehl, G. H. Timken, H. C. Chester, A. W. Vartuli, J. C. Zeolites, 19 (1997) 288.

116 Karge, H.G., Stud. Surf. Sci. Catal., 65 (1991) 133.

117 Karge, H. G., Dondur, V., J. Phys. Chem., 94 (1990) 765.

118 Froni, L., Vatti, F. P., Ortoleva, E.,Micropor. Mater., 3 (1995) 367.

119 Bagnasco, G. J. Catal., 159 (1996) 249.

120 Alberti,A., Zeolites, 19 (1997) 411.

121 Ward, J. W., J. Catal., 18 (1970) 348.
122 Jacobs, P. A., Catal. Rev. –Sci. Eng., 24 (1982) 415.
123 Fritz, P. O., Lunsford, J. .H. , J. Catal., 118 (1989) 85.
124 Datka, J., Boczar, M., and Gil, B., Langmuir, 9 (1993) 2496.
125 Barzetti, T., Selli, E., Moscotti, D., Forni, L., J. Chem. Soc., Faraday Trans., 92 (1996) 1401.
126 Hughes, T. R., White, H.M. J., Phys. Chem., 71 (1967) 2192.
127 Emeis, C. A., J. Catal., 141 (1993) 347.
128 Pradhan A. R. and Rao B. S., J. Catal., 132 (1991) 79.
129 Witcherlova B. and Jiri Ccjka., J. Catal., 146 (1994) 523.
130 Siddhesh Shevade, Ahedi R. K., Kotasthane A. N.and Rao B. S., Recent Trende in Catalysis, (Eds.) Murugesan et.al., Narosa Publishig House, (1999) 383.
131 Becker, K. A., Karge H. G. and Streubel W. D., J. Catal., 28 (1973) 403
132 Barrer, R. M., Bultitude, F. W. and Sutherland, J. W., Trans Faraday Soc., 53 (1957) 1111.
133 Martens, J. A., Perez Pariente, J., Sastre. E., Corma A., Jacobs P.A.; Appl. Catal.; 45 (1988) 85.
134 Csicsery S. M., J. Catal.; 108 (1987) 433.
135 Kim, M. H., Chen C. Y., Devis, M. E., ACS Symp. Ser. , 517 (1993) 222.
136 Weitkamp J., Newber N., Stud.Surf. Sci. Catal., 60 (1991) 291.
137 Hatch, L. F., Mater, S., Hydrocarbon Process. 58 (1) (1979) 189.
138 Wittcoff, H. A., The Chemical Industry: Technology and Concepts, Chem Systems Inc., in: Union Chem. Lab., Ind. Tech. Res. Inst., Hsinchu, Taiwan, 12-13 March, 1992.
139 Jeanneret, J. J., Low, C. D., Zukauskas, V. Hydrocarbon Process. 6 (1994) 43.
140 Swift, J. D., Moser, M. D., 20th Dewitt Petrochemical Review, 21-23 March(1995).
141 Colvin, H. A., Muse, J., CHEMTECH 16 (1986) 500.
142 Tanabe, K., Solid Acids and Bases, Academic Press, NewYork, (1970).
143 Wood, A., Chem. Week 17 (1994) 34.
144 Frank, H. G., stadelhofer, J.W., Industrial Aromatic Chemistry, Springer: Berlin, (1988) 486 pp.
145 Friedel, C., Crafts, J. M., Compt. Rend. (1877), 84, 1450.
146 Meima, G. R. CATTECH 3 (1998) 5.
147 Chen, N. Y., J. Catal. 114 (1988) 17.
148 Chen, N.Y., Kaeding, W. W., Dwyer, F. G., J. Am. Chem. Soc. 101 (1979) 6783.

149 Young, L. B., Butter, S. A., Kaeding, W. W., J. Catal. 76 (1982) 418.
150 Kaeding, W. W.,Young, L. B., Chu, C. C., J. Catal. 89 (1984) 267.
151 Medina-Valtierra, J., Zaldivar, O., Sanchez, M. A., Montoya, J. .A., Navarrte, J., delos reyes, J. A., Appl. Catal. A 166 (1998) 387.
152 Cejka, J., Krejci, A., Zilkova, N., Dedecek, J., Hanika, J., Micropor. Mesopor. Mater. 499 (2001) 44-45.
153 Gorra, F., Breckenridge, L. L., Guy, W. M., Sailor, R. A., Oil Gas J. 12 (1992) 60.
154 Lesnoy, H. G. , Hydroc. Asia, Nov/Dec (1993) 16.
155 Europ. Chem. News, 11 (1995) 24.
156 Johnson, J. A., Roeseler, C. A., Stoodt, T. J., 22nd Annual DeWitt Petrochemical Review, Houston, TX, 18-20 March (1997)
157 Wang, I., Ay, C. L., Lee, B. J., Chen, M. H., Proceedings of the Ninth International Congress on Catalysis, Calgary, (1988) p.324.
158 Ponder, T., Hydroc. Process. (1979) 141.
159 D'auria, J. H., Stoodt, T. J., Hart's fuel technology and management, (1997) 35.
160 Mowry, J. R., Meyers, R. A., (Ed.), Handbook of Petroleum Refining Processes, Section 10-10, McGraw-Hill, New York, (1986)
161 Tsai, T. C., Huang, D. S., Lin, C. M., Chiu, C. T. , Kao, J. W., Ku, C. S., Tsai, K. Y., Beech, J., Kinn, T., Mizrahi, S., Rouleau, N. ,Sapre, A., Wang, H. J., 2nd Joint China/US Chemical Engineering Conference, Beijing, 19-22 May (1997)
162 Farnos, L., BTX Intermediates and Derivatives Conference, Singapore, 19-20 June (1997)
163 Beech, J., Cinimi, R., Rouleau, N., Tsai, T. C. ,The Aromatics, V51 (1999), to be published.
164 Mobil TransPlus Process Brochure, Mobil TechnologyCompany.
165 Belenkil, M. S. , Pavlov, G. P., Ulitskaya, N. V., SO Patent 192 190 (1964).
166 Lien, A.P., McCaulay, D. A., J. Am. Chem. Soc. 75 (1953) 2107.
167 Petrochemical Handbook, Hydro. Process. 56(11) (1977) 132.
168 Wells, G. M., Handbook of Petrochemicals and Processes, Gower Press, Vermont, (1991)
169 Haag, W. O., Chen, N. Y., Hegedus, L. L., (Ed.), Catalyst Design, Progress and Prospectives, Wiley, New York, (1987) 193.
170 Wang, I., Tsai, T. C., Aye, C. L., Stud. Surf. Sci. Catal. V75 (1993) 1673.
171 Karge, H. G., Ladebeck J., Sarbak, Z., Hatada, K., Zeolites 2 (1982) 94.
172 Tsai, T. C., Ph.D. Dissertation, National Tsing Hua University, Hsinchu, Taiwan, (1991)

## 2.1 Introduction

### 2.1.1 Importance of isomorphous substitution

Zeolites are used as catalysts with a wide range of applications due to their Bronsted acidity and shape-selectivity (1,2). The acid sites are mostly bridging hydroxyls, that arise when trications replace Si in their framework. In the past there were many efforts for the synthesis, characterization and application of the isomorphously substituted zeolites with elements other than Si and Al, such as B, Ga, Fe, Ti, Zn etc. (3-7). Incorporation of heteroatoms can change the acidity and pore structure of zeolites and the modified zeolites have altered catalytic activity, selectivity and stability. This offers the potential to design zeolites for novel applications. For e.g. Fe-MFI is an active catalyst for the oxidation of methane to methanol (8) and benzene to phenol (9). Ga-MFI shows high selectivity for alkane aromatisation (10). TS-1 is well known for its excellent performance in oxidation reactions (11). There were many reports (12-16) dealing with the structure and acidity of zeolites and the isomorphously substituted zeolites containing different framework atoms. Chu et al. (15) used infrared (IR) spectroscopy and temperature-programmed desorption (TPD) of $NH_3$ to study the acidity of several isomorphously substituted M-MFI zeolites with their acid strength increasing in the order Si-(OH) < B-(OH)–Si << Fe-(OH)–Si < Ga-(OH)–Si < Al-(OH)–Si. The acidity and reactivity of zeolites have been predicted by ab initio and DFT quantum mechanical methods (17-30). Chatterjee et al. (22) reported DFT calculations on isomorphously substituted MFI clusters of B, Al, Ga and Fe, and the relative acidity derived from proton affinities agree well with the experimental results. Yuan et al. (31) have reported cluster model and DFT calculations on the strength of the Bronsted acid sites in the isomorphously substituted MFI by Al, B, Ga and Fe. On the basis of the calculated proton affinities (PA), the natural charge on the proton and the $NH_3$ adsorption energy as the measure of the Bronsted acidity, they have shown that the acid strength follows the order, B-(OH)–Si << Fe-(OH)–Si < Ga-(OH)–Si < Al-(OH)–Si. $NH_3$ adsorption results showed that $NH_3$ is protonated ($NH_4^+$) in contact with Al- and Ga-MFI, while it is only physisorbed on Fe- and B-MFI. It was found that there are two N-H-----O

hydrogen bonds in the Al-and Ga-MFI, while only single hydrogen bond in reversed pattern (N----------H-O) for Fe- and B-MFI.

Though there is a difference in the ionic radii of $Al^{3+}$ (0.53 nm) and $Ga^{3+}$ (0.61nm), the gallium substitution in place of aluminum is possible. The gallium analogs of many zeolites (32-34) including faujasite (32, 35, 36), ZSM-5 (37) have been reported. As gallium zeolite is moderately acidic than aluminum it will have milder acidity for acid catalysed reactions (38). In the synthesis of the gallosilicate, the interaction between gallium ions and the silicate gel appears to be similar to the aluminum ion interactions with the gel (39). In aqueous solution, however, the free gallate ions are more stable than aluminates (40). Under the alkaline conditions used in zeolite synthesis, sodium gallate in solution is found to be extremely stable. Thus, a true solution of gallic acid can be formed, which is not true for the aluminate acid, as it forms dimeric and polymeric species in solution (41). The presence of monomeric gallate ions in solution thus should not impede gallium's ability to be incorporated into a crystallizing silicate structure, as dissolution of a secondary gallium oxide (hydroxide) phase does not occur. Irreversible formation of metal oxide (hydroxide) species, prohibiting incorporation into a silicate framework, occurs for other elements that form amphoteric hydroxides such as the transition metals, iron and chromium, but this is not a factor in the gallosilicate system.

The ionic radii of $Si^{4+}$, $Al^{3+}$ and $Fe^{3+}$ are 0.039, 0.057 and 0.067 nm, respectively. In addition, $Fe^{3+}$ can also undergo change in the oxidation state thereby leading to a lowering of the stability of the crystal structure. The possibility that $Fe^{3+}$ ions can occupy tetrahedral framework positions in zeolite was established long ago. In 1972, McNicol and Pott (42) showed unambiguously that iron impurities in faujasite zeolites can occupy substitutional lattice positions. From EPR studies of the $Fe^{3+}$ impurities in $NH_4^+$ faujasite, Derouane et.al (43) showed that iron can be simultaneously present in three forms; $Fe^{3+}$ species in the aluminosilicate framework, $Fe^{3+}$ ions acting as counterions and $Fe_3O_4$ or any other $Fe^{3+}$ compound with strong exchange spin-spin interactions, precipitated on the zeolite. Marosi et al. (44, 45), Dwyer (46) and Kouwenhoven and Stork (47) were among the earliest to claim the synthesis of ferrisilicate analogs of the high silica zeolite (ZSM-5). During the synthesis of ferrisilicate molecular sieves the objective is to incorporate Fe(III) ions in to

the growing lattice framework that is made up of silica tetrahedra. To achieve this objective the reaction leading to the formation of the ferrisilicate complex (reaction 1) has to be enhanced while that leading to the formation of iron hydroxides (reaction 2) has to be suppressed. This can be accomplished by complexing the iron with silica at low pH using an aluminium-free source of Si and choosing the raw material and reaction conditions to maximize the concentration of monomeric/short chain silicate species. As seen earlier, above pH=4, insoluble iron hydroxide species are formed. It is not easy to incorporate these polymeric species of iron in to a growing silicate network. Hence, the monomeric/short chain silicate species is usually added to an acidic solution (pH below 4) containing the $Fe^{3+}$ ions to form the ferrisilicate complexes. Once all the Fe is complexed with the silicates to form the ferrisilicates, the pH of the reaction mixture can be safely increased to values needed for the synthesis of zeolitic structure without the precipitation of the rust red iron hydroxides. The organic base is added after the formation of the ferrisilicate gel. After adjusting the pH to the desired value, the amorphous gel is converted

$$Fe^{3+} + Si(OH)_4 \rightleftharpoons FeH_nSiO_4^{(n-1)+} + (4-n)H^+ \qquad (1)$$

$$Fe^{3+} + H_2O \rightleftharpoons Fe(OH)^{2+} + H^+ \qquad (2)$$

into the crystalline structure in an autoclave at elevated temperatures and autothermal pressure.

The synthesis of boron-containing ZSM-5 was reported by Taramasso et al. (48) in 1980. Since then, there have been reports supporting the fact that the boron is incorporated in the framework using MAS $^{11}B$ nmr (49-52) and IR studies (51-54), X-ray studies (55-56) and cation exchange capacity measurements (57). There are also patents (58-59) describing their application in new catalytic processes. Many authors have shown (53, 54, 60, 61, 62) that B-MFI had an attenuated acidity compared to Al-MFI due to the absence of strong acid sites from $NH_3$ TPD studies. The weak acidity of B-MFI compared to A1-MFI has also been confirmed by the diminished activity of B-MFI for acid catalyzed reactions (57, 63, 64). However, the decreased acidity is also shown to be an advantage, since B-MFI retains its catalytic activity for the reactions such as disproportionation of ethylbenzene

(63) and methanol to olefin conversions (64-65) longer than does the more acidic Al-MFI catalyst. The weakly acidic boron pentasil zeolite has been shown to be useful for the synthesis of enol ethers from acetals (66). This catalyst is superior to the conventional supported catalysts such as phosphates, sulfates, or carbonates in terms of lifetime and selectivity. The presence of boron is also reported (55, 56) to distort the framework and cause a decrease in the unit cell volume. As a consequence, synthesis of olefins from methanol has a different selectivity over B-MFI catalysts (64, 67-69) Hoelderich (70) has shown that B-MFI is more selective (although less active) in the conversion of 2-phenylpropanol to 1-phenylpropan-2-one than is Fe-MFI.

### 2.1.2 Modification by silylation: Chemical Liquid Depostion (CLD)

Pore size modification of zeolites is a very promising way to produce catalysts that have a range of industrial applications in fine chemical and petrochemical products etc. The crystallographic changes brought out by thermal treatment, internal and external structural modification by implantation of additional atoms/groups, or external surface modification of the zeolite crystal (coating process) can produce important changes in the molecular sieving behaviour of zeolites (71). It can be used for external surface modifications, to design a catalyst to be more shape selective towards certain reactions (73). The technique to alter the internal pore system of a zeolite can be divided in to two main classes: (i) transient and (ii) permanent modifications, the former can be performed by adsorption of polar molecules, such as water, amines (74) and coke. The later include the introduction of bulky compounds inside the porous structure of a zeolite, which is commonly performed by ion exchange (75), silylation and disilylation, boronation, impregnation with organic and inorganic phosphorus compounds, and the treatment with metal halides or organo metallic compounds. Both the transient and the permanent modification influences the accessibility and geometrical neighbourhood of the active sites, as well as the acidic properties of these sites. Many of these methods also induce changes at the external surface of the zeolite particle. Although the external surface of the zeolite crystal should account for only a very little percentage of the total area, the role of catalytic sites on the external crystallite surface cannot be neglected in some applications (76, 77). Some gain in

selectivity can be obtained by the inactivitation of these surface sites, which do not possess shape selective properties. However, the distinction between surface inactivation and pore size reduction is unclear, since in many cases, both come in to effect simultaneously. The internal implantation of polar groups by chemisorption of small inorganic molecules such as silane ($SiH_4$), disilanes ($Si_2H_6$) and boranes ($B_2H_6$), which are very reactive towards the hydroxyl groups of the zeolites, can lead to changes in the pore dimensions and the electrical field within the zeolite crystal channels (72, 78-83). The effect of reducing the pore size using this technique has been analysed mainly for the processes involving adsorption and separation of gaseous mixtures (84, 85), but it shows a great potential for shape selective catalysis (82). The extent of modification can be controlled by the operating conditions namely pressure of the modifying agent and temperature (81-83). Concomitant modification of the external surface can occur for certain ranges of experimental conditions (83).

Several authors have reported modification using halides. Treatment with $SiCl_4$ to stabilize and dealuminate Y zeolite is a common practice; however similar procedures when applied to small pore zeolites, led to surface or internal deposition. Hidalgo et al. (86) have examined the modification of mordenite with $SiCl_4$, $GeCl_4$, $TiCl_4$ and $SnCl_4$ and found metal chloride deposits, either in the channels or near the channel entrance depending on the reactivity, molecular size of the halide and experimental conditions. Methanol conversion on these modified mordenites showed changes in selectivity and activity. Guisnet (87) et al. found significant changes in the selectivity for aromatics production, during the propane aromatisation on H-ZSM-5 catalysts that are deposited with zinc by reaction with zinc chloride.

Depending on the size of the zeolite pores and the molecular size and reactivity of the modifying agent, it is possible to passivate the external surface and simultaneously control the size of pore opening, without affecting the internal pore structure and acidity. The methods that are used most commonly consists of chemical vapor deposition (CVD) of silicon compounds, impregnated with organic solutions of silicone polymers, and also by coking of the surface. The alkoxides react with terminal silanol groups and on their decomposition they cover the zeolite crystal surface. Deposition of silica or germanium

oxides occurs on the external surface as a thin layer, which narrows the pore openings of zeolite and simultaneously deactivates acid sites on the external surface, without changing the internal properties of the zeolite. Similar results of silicon alkoxides, $Si(OCH_3)_4$, $Si(OC_2H_5)_4$ and $Ge(OCH_3)_4$, have also been proposed by Niwa et al. (88-94), and confirmed by TPD (88, 89). This method has been applied to H-mordenite (88-91) and H-ZSM-5 (90-93) and their shape selectivity have improved in hydrocracking of paraffins, cracking of octane isomers, methanol conversion, alkylation of toluene with methanol and toluene disproportionation. Recently Hibino et al. (94) found that the silicon concentration required for the inactivation of the external surface of mordenites and ZSM-5, does not depend on the Si/Al ratio. This technique has attracted much attention from various researchers who have been using $Si(OC_2H_5)_4$ to improve the catalytic stability of zeolite for cumene disprportionation (95), or to enhance shape selectivity of ZSM-48 in xylene isomerisation (96)

Other methods reported in the literature to passivate the external surface include the work of Kaeding et al. (97), using carbonate polymers to deactivate the external surface of MFI, impregnation of MFI with dimethylsilicone polymer (98), to enhance para selectivity during toluene disproportionation albeit with a decrease of catalytic activity, Recently, the replacement of acidic protons on the external surface by lithium ions from a lithium complex with a crown ether (dicyclo-18-crown-6) is reported (99). The deposition of bulky organo metallic complexes such as $Mbu_4$, $MPh_4$, (M=Sn, Ge), $ZrNp_4$ and $MgNp_2$, on the external surface of mordenite, followed by calcination, produces, an improvement of the catalytic behaviour of mordenite-based catalysts during the isomerization of $C_8$ aromatics (100).

If the operating conditions are carefully selected, it is possible to use conventional internal modifiers to perform external modifications selectively. This is true in the case of treatment with $SiCl_4$ or $SiF_6(NH_4)_2$, which are commonly used to dealuminate large pore zeolites, but due to its high reactivity, it is not possible to control the deposition so that it occurs mainly on the surface of the crystals. The treatment of $SiCl_4$ studied by Namba (101) and Anderson et al. (102) produced materials that were surface enriched in silicon. Also, ZSM-5 treated with $SiF_6(NH_4)_2$, has silicon enriched surfaces showing a decrease in

disproportionation activity during m-xylene isomerization (103). The effects of surface passivation have also been observed in the increased concentration of p-hydroxy acetonephenone, during phenol acylation over MFI (104).

External modification using disilane can also occur when high reaction temperatures are used. Increasing the chemisorption temperature, increases the reactivity between disilane molecules and the structural OH groups under these conditions, hence disilane molecules immediately react with OH groups on the external surface and at the pore entrances. These chemisorbed molecules prevent the other disilane molecules from diffusing into the internal pore system (82, 83). Therefore the modification at higher temperature produce a substrate with smaller pore size and without much loss in the internal volume, which can be advantageous for some catalytic applications. For small pore zeolites, such as HRHO zeolite, it was possible to deactivate external acid sites with trimethyl phosphite without affecting pore size, or the internal acid sites, improving the selectivity for the synthesis of methylamines from methanol and ammonia (105). The CVD technique has its own drawbacks, e.g., scaling up the process is difficult, and it is only useful for modifying the H-form of the zeolite because the amount of $SiO_2$ deposited on the Na-form or other cation –form zeolites is very limited (106-108). Thus, chemical liquid deposition (CLD) has been developed to overcome these shortcomings. The control of size of the pore-opening of NaY zeolite has already been achieved successfully in solution by using silicon alkoxide as the deposition agent (109-110). Also the temperatures required for the CVD technique are much less than that required for CLD.

The present work is to explore the possibility of using silicon alkoxides as the deposition agent for CLD of ZSM-5 zeolites and their use in the selective synthesis of p-dialkylbenzenes (p-DAB).

## 2.2 Experimental

### 2.2.1 Synthesis of Al-, Ga-, Fe- and B-MFI zeolites

***Synthesis of Al-MFI*:** Al-MFI was synthesized by the procedure of Argauer and Landolt (111). Two solutions A and B were prepared in the following way. Solution A was prepared by dissolving appropriate amounts of aluminium sulphate ($18H_2O$) and $H_2SO_4$ in distilled water. Required amount of TPABr was added to a solution of sodium silicate (60

% $SiO_2$) to yield solution B. The reactive gel composition was obtained by the slow addition of solution A to solution B with vigorous stirring. The pH of the gel was adjusted to 10.0 by using 1:1 $H_2SO_4$. After stirring to get a homogenous mixture the gel was autoclaved at 453K for 24 hrs under autogenous condition. The crystalline product was filtered, washed, dried at 393K for 12hrs and calcined at 823 K in air to decompose the organic template.

***Synthesis of Ga-MFI:*** Required solution of $Ga(NO_3)_3.6H_2O$ and $H_2SO_4$ in water was added to sodium silicate (60% $SiO_2$) in water. To the resulting gel, a solution of tetrapropyl ammonium bromide in water was added. After stirring for one hour the mixture was placed in an autoclave and heated under autogenous conditions for 3 days at 443 K.

***Synthesis of Fe-MFI:*** Fe-MFI was synthesized according to the procedure by Ratnasamy et al. (112). A solution of TEOS (Aldrich) in absolute ethanol was added very slowly to a solution of Fe $(NO_3)_3$. $9H_2O$ in $H_2O$. The pale lemon coloured liquid mixture was stirred for about 1h before adding it to a solution of TPAOH (Aldrich, 20 wt%) in $H_2O$. During the addition of TPAOH a white gel was formed which finally redissolved to give a clean liquid (pH=11). The later was filled in a stainless steel autoclave and the crystallization was carried out at 443 K for 3 days. The crystalline product was white in colour.

***Synthesis of B-MFI:*** B-MFI was synthesized by using silica sol as the silica source and $B(OH)_3$ as the source of boron in the presence of sodium hydroxide. TPABr was used as the template. The procedure followed is similar to the one used for Al-MFI.

After the decomposition of organic template all the samples were converted to H-form by exchanging thrice with 1 M ammonium nitrate, followed by calcinations at 773 K that yielded the H-form of the zeolite.

### 2.2.2 Zeolite modification

The CLD of TEOS was performed on some of the zeolite samples. Before silylation the zeolite was activated at 823 K for 6 hours. The zeolite was reacted with a mixture (2 ml per gram of zeolite) of 20% TEOS + 35% MeOH + 45% toluene in a round-bottom flask at 355 K. The reaction mixture was cooled after 12 hours, dried at 393 K for 4 hours and

calcined at 823 K for 12 hours to remove all the organics. The whole process was repeated for the second time.

### 2.2.3 Evaluation of catalytic activity

Catalytic studies were carried out at atmospheric pressure, in a fixed bed, down flow, integral silica reactor (Fig. 2.1). Prior to the reaction the catalyst was calcined at 823 K for 3-6 hours. About 1.5 g. of catalyst (10-20 mesh) was placed at the center of the silica reactor supported by porcelain beads, that was placed vertically in a two zone furnace (Geomechanique, France). Liquid reactants were fed with a high-pressure syringe pump (ISCO 500D). The reaction products were condensed using a cold water condenser and samples were collected at various intervals. These product samples were analysed using gas chromatography (HP 6890) equipped with FID and capillary column (BP-1, 50m x 0.32 μm) for EB alkylation. The toluene methylation products were analysed using Shimadzu 15 A equipped with 4 m long packed column with 5% Bentone + 5% DIDP on Chromosorb

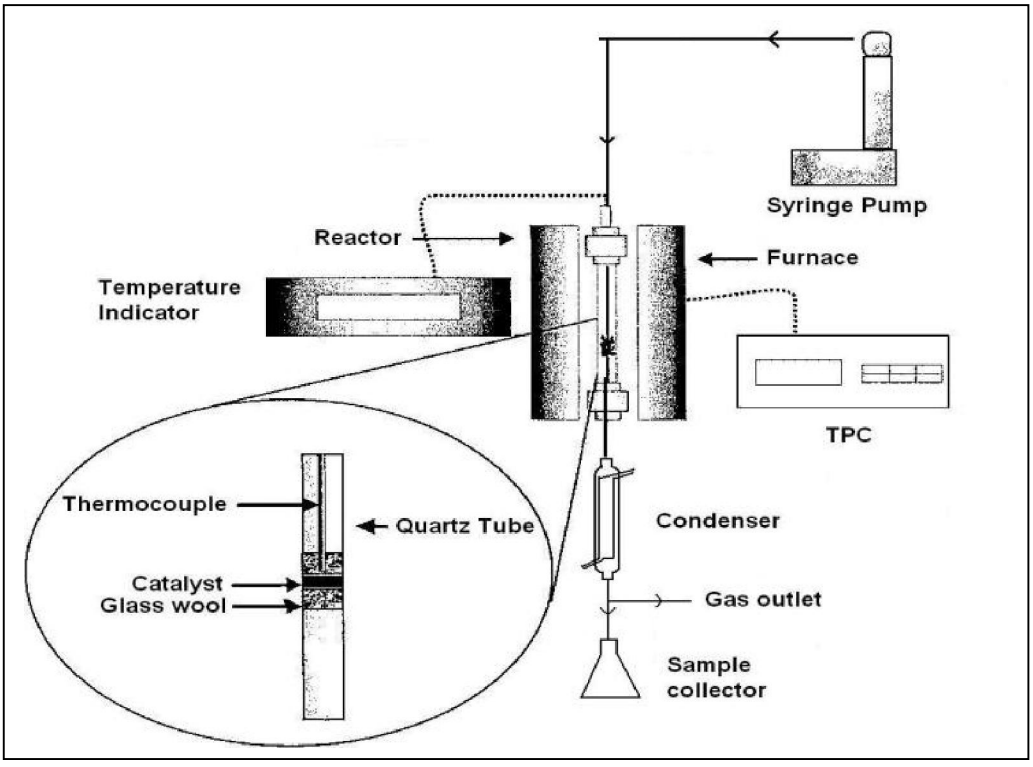


**Fig. 2.1: Fixed bed down flow reactor**

### 2.2.4 Catalyst characterization

The zeolites were characterized by XRD, $N_2$ sorption, TPD of ammonia and SEM. For TPD studies, the catalyst was activated in helium flow for 2 hours at 823 K. The furnace was cooled to 353 K before the adsorption of ammonia. Ammonia (10% in helium) flow (10ml/min) was maintained for 30 minutes and then the sample tube was flushed with helium for 1 hr. The desorption experiments were carried out in the temperature range 373 K to 873 K at a heating rate of 10 K/min.

## 2.3 Results and Discussion

### 2.3.1 Catalyst Characterisation

Various Physico-Chemical techniques were used to characterize the modified and unmodified zeolite catalysts.

#### 2.3.1.1 X-ray Diffraction

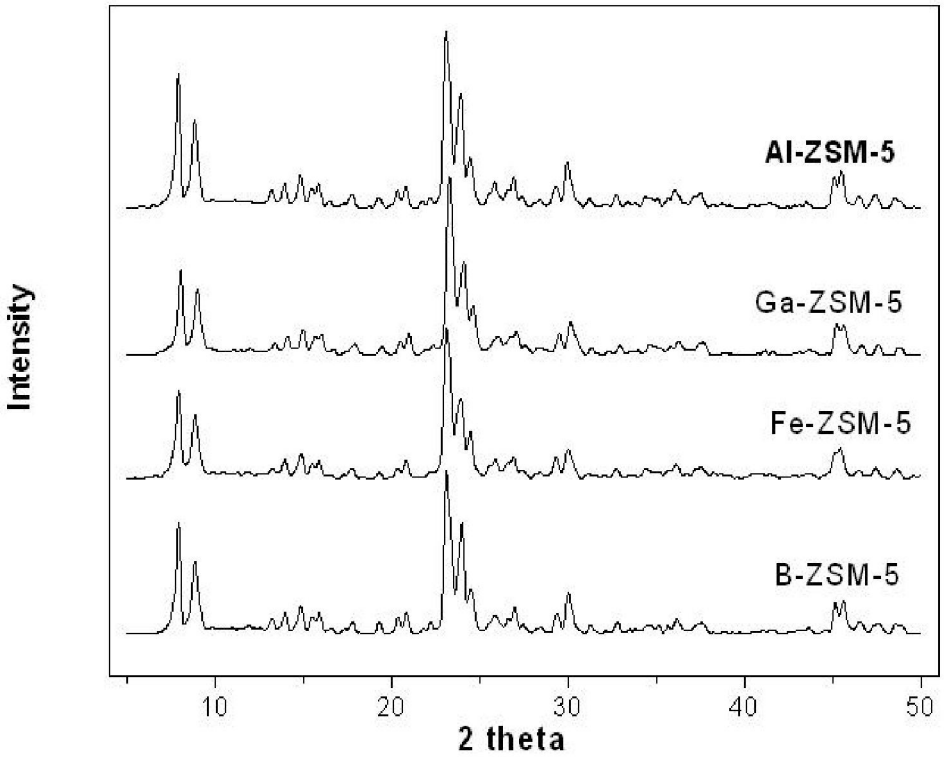


**Fig. 2.2: XRD patterns of isomorphously substituted samples**

All the MFI zeolites with Al, Ga, Fe and B substituted in their framework were subjected to X-ray diffraction. The diffractograms shown in Fig. 2.2 are for the calcined samples. It can be seen that the prepared samples were indeed MFI type structures of high purity. The d-values were in good agreement with those reported (113). The as-synthesised samples (not shown) have the most intense peak at $2\theta=23.2^{o}$, and the peaks at $8.05^{o}$ and $8.95^{o}$ were relatively weak. The intensity of the later two peaks was enhanced after removal of the TPA from the intra-crystalline voids.

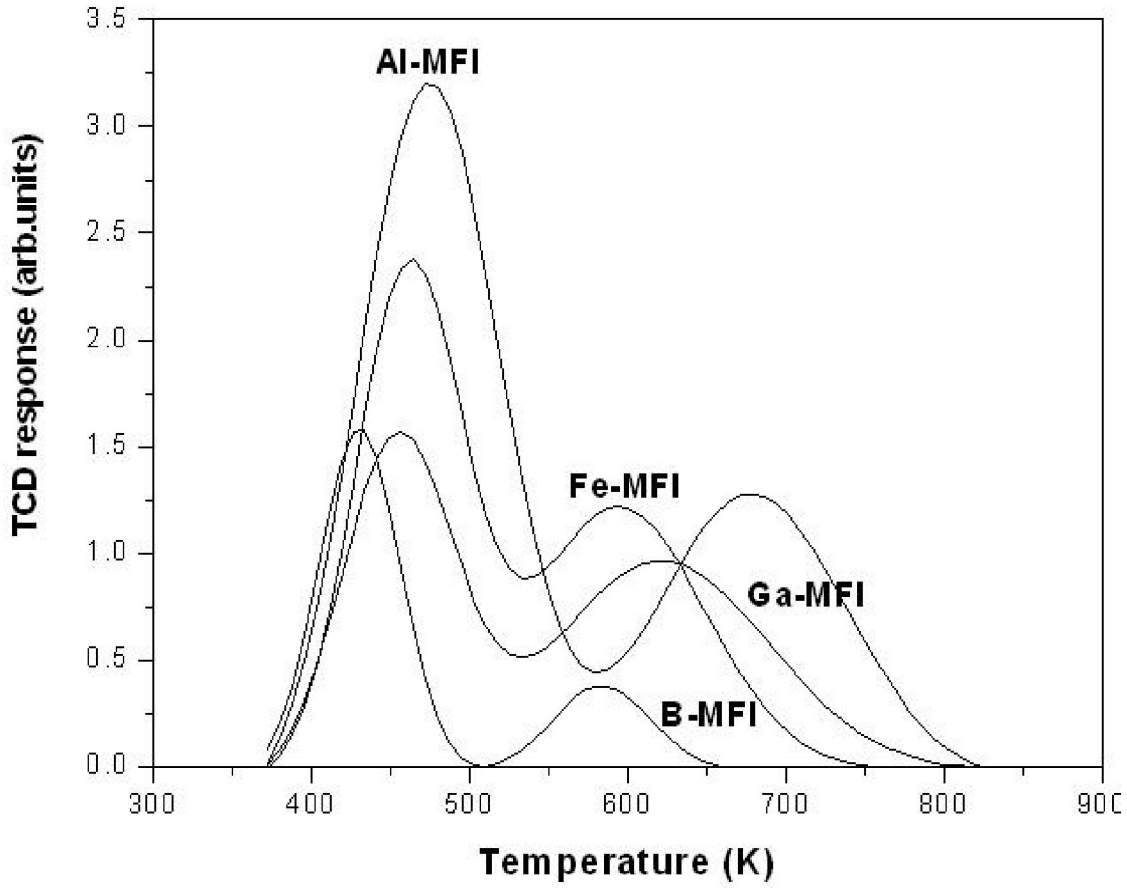


**Fig. 2.3: Ammonia TPD plots of metal substituted MFI zeolites**

### 2.3.1.2 TPD of Ammonia

Fig. 2.3 depicts the TPD of ammonia plots of the samples, all samples show two desorption peaks. Usually, the low temperature peak is attributed to ammonia desorbed

from weakly acidic Lewis sites (non-framework M (III) species, tri-coordinated Me in the framework and $NH_3$ associated with SiOH groups which are surface silanols), whereas the high temperature peak is assigned to desorption from strong Bronsted acid sites (114, 115), the sites that take part in the catalytic reaction. The effect of metal substitution is clearly visible. Temperature-programmed desorption (TPD) of $NH_3$ shows that the acid strength increases in the order B-(OH)-Si < Fe-(OH)-Si < Ga-(OH)-Si < Al-(OH)-Si. The temperature maximum of the high temperature TPD peak shifts to lower temperatures with decreased acidity viz. Al > Ga > Fe > B (Table 2.1).

**Table 2.1 Physico-chemical properties of isomorphously substituted zeolites**

| **Catalyst** | **$SiO_2/Me_2O_3$** | **$T_{max}$ (K)** | | **Total acidity (mmoles)** | |
|---|---|---|---|---|---|
| | | **LT** | **HT** | **weak** | **strong** |
| **Al-MFI** | 100 | 475 | 677 | 0.41 | 0.23 |
| **Ga-MFI** | 124 | 455 | 621 | 0.13 | 0.15 |
| **Fe-MFI** | 114 | 461 | 593 | 0.17 | 0.14 |
| **B-MFI** | 79 | 430 | 583 | 0.10 | 0.03 |
| **Ga-MFI-CLD1** | 3.5 % $SiO_2$ | 445 | 614 | 0.058 | 0.072 |
| **Ga-MFI-CLD2** | 7.0 % $SiO_2$ | 441 | 615 | 0.042 | 0.038 |

The effect of silynation with TEOS on H-Ga-ZSM-5 is shown in the Fig. 2.4. It is seen that there is decrease in the acidity of the parent zeolite with successive silylation cycles. There is a decrease in the areas of the high as well as low temperature peaks.

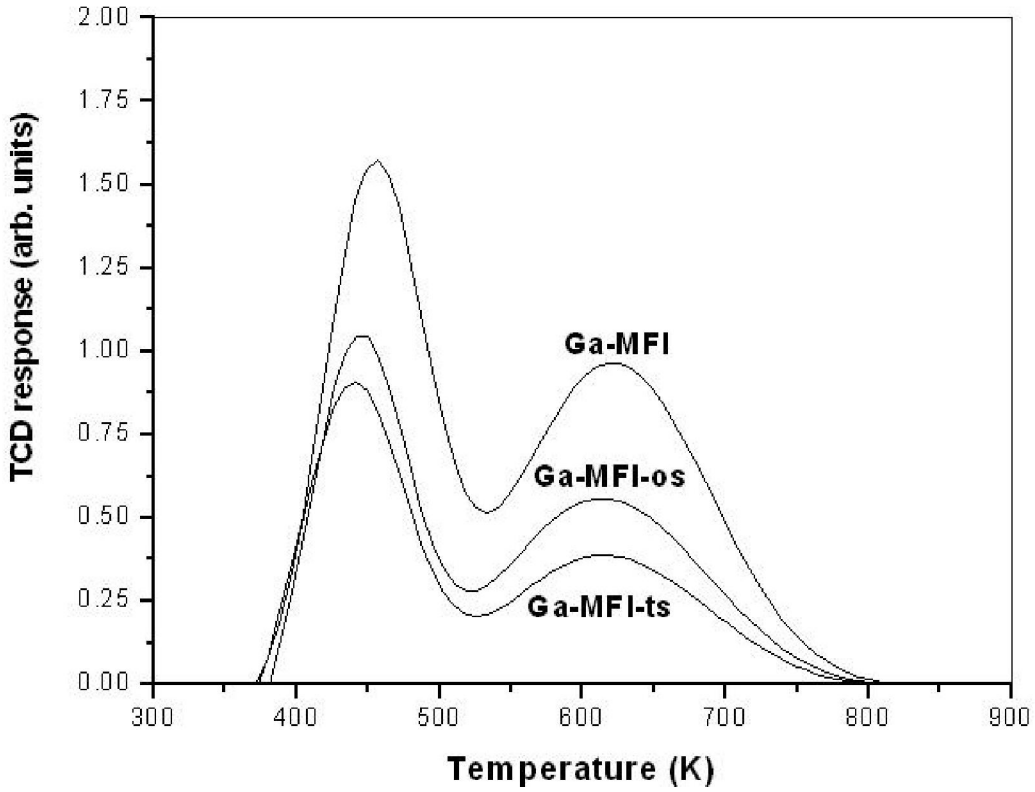


**Fig. 2.4: Comparison of the TPD ammonia plots of modified and unmodified Ga-MFI zeolites**

### 2.3.1.3 Framework IR spectroscopy

The framework FTIR spectra (400-1300 $cm^{-1}$) shown in Figure 2.5 is typically used for characterization of aluminosilicates. Similar to aluminosilicates the gallo-, ferri- and boro-silicates also exhibit distinct absorption bands at 1230, 1098, 793, 610, 548, and 468 $cm^{-1}$. Flanigen etal. (116) assigned the frequencies 1230, 1098 and 793 $cm^{-1}$ to internal asymmetric stretching, external asymmetric stretching and external symmetric stretching, respectively. Further the double rings and TO bending vibration of $TO_4$ tetrahedra (T= Al, Ga, Fe, B) exhibit absorption band at 548 $cm^{-1}$ and 468 $cm^{-1}$ respectively. The presence of band around 610 $cm^{-1}$ is probably due to external links of 5-membered rings. MFI-type zeolites exhibit bands around 590-620 $cm^{-1}$ and are usually assigned to external links of complex 5-membered rings (117).

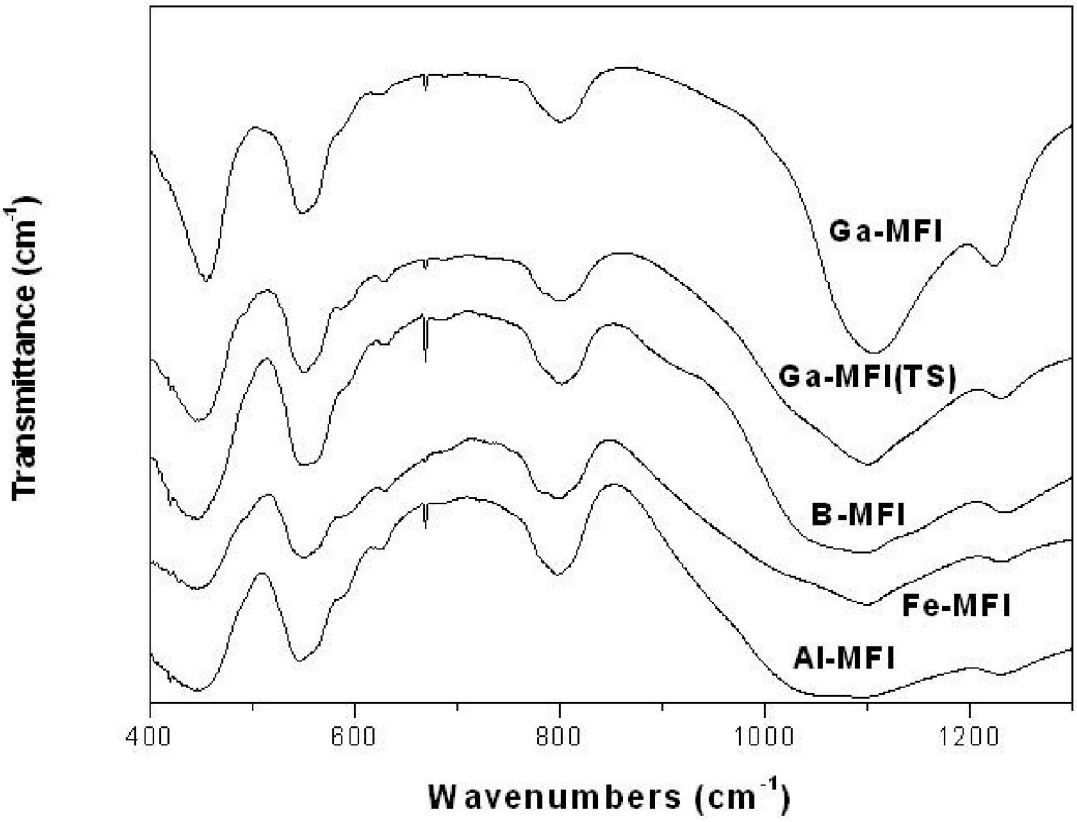


**Fig. 2.5: FTIR spectra of modified and unmodified Me-MFI zeolites**

### 2.3.1.4 Scanning Electron Microscopy (SEM)

The crystal morphology and size of the Al and Ga substituted MFI samples are shown in Fig. 2.6. The crystals of Al-MFI are in 3-4 μm range while that of Ga-MFI are small spherical particles of 1μm. In literature it is given that smaller crystal sizes lead to higher catalytic activity in case of alkylation reactions. Even though the particle size of Ga-MFI is smaller than that of Al-MFI, the activity of Ga-MFI for EB alkylation is lower. This also shows that gallium substituted samples have lower acidity.

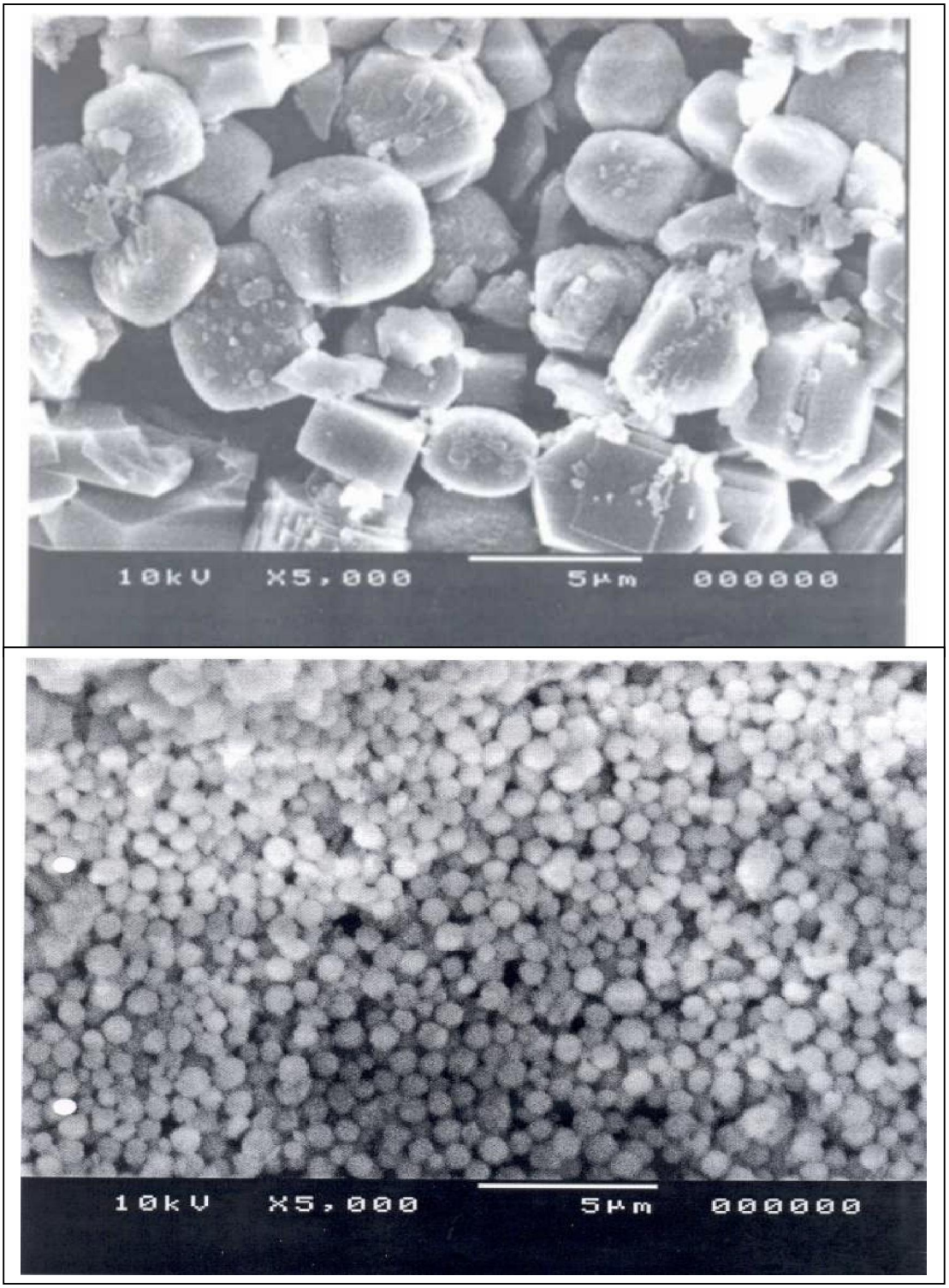


**Fig. 2.6: SEM pictures of Al-ZSM-5 (upper) and Ga-ZSM-5 (lower) samples**

### 2.3.2 Catalytic activity

#### 2.3.2.1 Ethylation of Ethylbenzene for preparation of p-DEB

The ethylation of ethylbenzene with ethanol is an electrophilic substitution reaction on the aromatic ring. The ring is activated at the ortho and the para-positions as a result of ethyl group in EB, by inductive and mesomeric effects. However rapid secondary isomerisation reactions usually generate equilibrium mixtures of all three isomers. The meta isomer, which is the major component in the product mixture is formed by isomerisation on external surface (non shape selective), though the amount formed through direct ethylation on these catalysts is negligible. For mechanistic reasons as mentioned, by far the most important route is isomerisation.

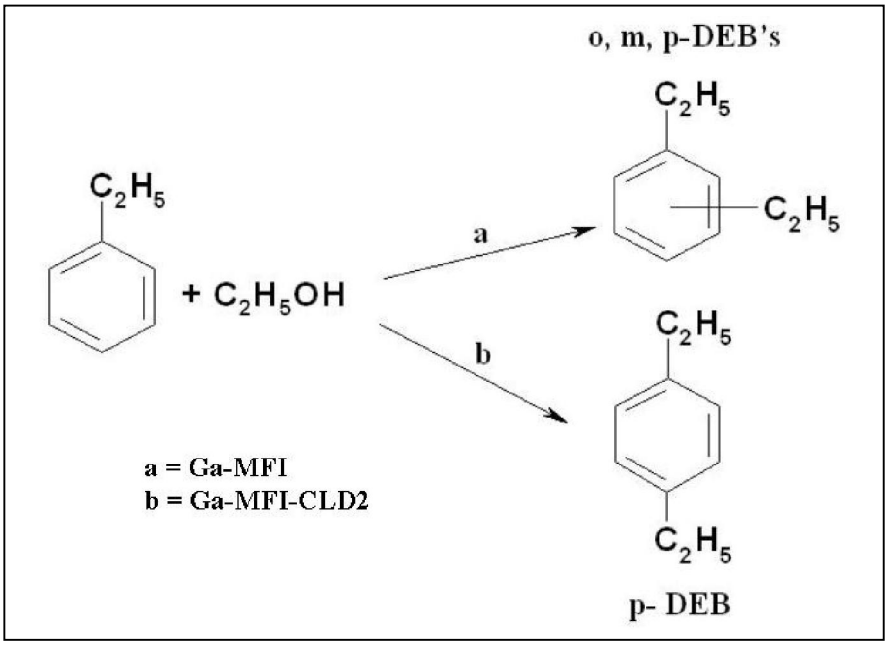


**Fig. 2.7: Scheme for EB alkylation on modified and unmodified zeolites**

#### *Effect of isomorphous substitution on ethylation of EB*

The catalytic activity of isomorphously substituted MFI (T= Al, Ga, Fe, B) zeolites has been compared for ethylation of ethylbenzene (Table 2.2) under identical reaction conditions and the results are summarized below. A look at the table shows that the activity of zeolites for EB alkylation exhibits a decreasing trend in the order Al-MFI > Ga-

MFI > Fe-MFI > B-MFI, the most active being Al-MFI. However there were many side reactions that took place on Al-MFI. High dealkylation activity resulted in the production of benzene. The B/DEB mole ratio, which is another indicator of dealkylation was very high on Al-MFI as compared to that of other metallosilicate zeolites. The DEB selectivity was high on gallium substituted zeolite because of its medium strength acidity. Ferri and boro-silicates showed higher DEB selectivity than Ga-MFI but their catalytic activity was vey low as compared to that of Ga-MFI. Hence Ga-MFI was used for further studies.

**Table 2.2 Ethylation of EB on various Isomorphously substituted MFI zeolites**

| Product Comp. (Wt%) | Al-MFI | Ga-MFI | Fe-MFI | B-MFI |
|---|---|---|---|---|
| **NA** | 1.8 | 0.5 | 0 | 0 |
| **Benzene** | 16.2 | 7.8 | 1.1 | 1.4 |
| **Toluene** | 3.3 | 0.9 | 0 | 0.8 |
| **EB** | 49.6 | 61.0 | 86.8 | 85.0 |
| **Xylenes** | 1.0 | 0.3 | 0.1 | 0.1 |
| **$C_9$ aromatics** | 3.6 | 1.5 | 0 | 0.2 |
| **p-DEB** | 7.6 | 10.4 | 4.1 | 6.0 |
| **m-DEB** | 14.8 | 16.9 | 7.9 | 5.9 |
| **o-DEB** | 0.2 | 0.1 | 0 | 0 |
| **HB** | 2.0 | 0.7 | 0 | 0.5 |
| **EB conv.** | 49.5 | 38.5 | 13.2 | 14.9 |
| **B/DEB (moles)** | 1.3 | 0.5 | 0.2 | 0.2 |
| **p-DEB Sel.** | 33.7 | 37.9 | 34.5 | 50.4 |
| **DEB Sel** | 46.3 | 70.9 | 91.4 | 79.4 |

Temp.623 K, WHSV=$2h^{-1}$, EB:EtOH= 4:1

NA-non aromatics

### *Effect of modification of Ga-MFI on ethylation of EB*

Table 2.3 shows the comparison of the modified and unmodified Ga-MFI catalysts in EB ethylation activity and p-DEB selectivity. After the first cycle of silylation there is a steep increase in the p-DEB selectivity (73.7 %) with concomitant decrease in the EB conversion. On second silylation the p-DEB selectivity further increases to 99 %, with a

further drop in conversion of EB. The DEB selectivity also increases on modified catalysts. There is a decrease in the B/DEB ratio with silylation. This indicates that the dealkylation activity is low on silylated catalyst.

**Table 2.3 Effect of modification of Ga-MFI zeolites on EB ethylation**

| **Product Comp (Wt%)** | **Ga-MFI** | **Ga-MFI CLD-1** | **Ga-MFI CLD-2** |
|---|---|---|---|
| **NA** | 0.5 | 0 | 0.3 |
| **Benzene** | 7.8 | 1.9 | 0.9 |
| **Toluene** | 0.9 | 0.4 | 0.7 |
| **EB** | 61.0 | 77.6 | 87.0 |
| **Xylenes** | 0.3 | 0.2 | 0.3 |
| **$C_9$ aromatics** | 1.5 | 0.3 | 0.8 |
| **p-DEB** | 10.4 | 14.3 | 9.7 |
| **m-DEB** | 16.9 | 5.1 | 0.1 |
| **o-DEB** | 0.1 | 0 | 0 |
| **HB** | 0.7 | 0.1 | 0.2 |
| **EB conv.** | 38.5 | 21.9 | 12.7 |
| **B/DEB (moles)** | 0.5 | 0.2 | 0.2 |
| **p-DEB Sel.** | 37.9 | 73.7 | 99.0 |
| **DEB Sel** | 70.9 | 73.4 | 76.8 |

Temp.623 K, WHSV=$2h^{-1}$, EB:EtOH= 4:1

CLD-Chemical liquid deposition

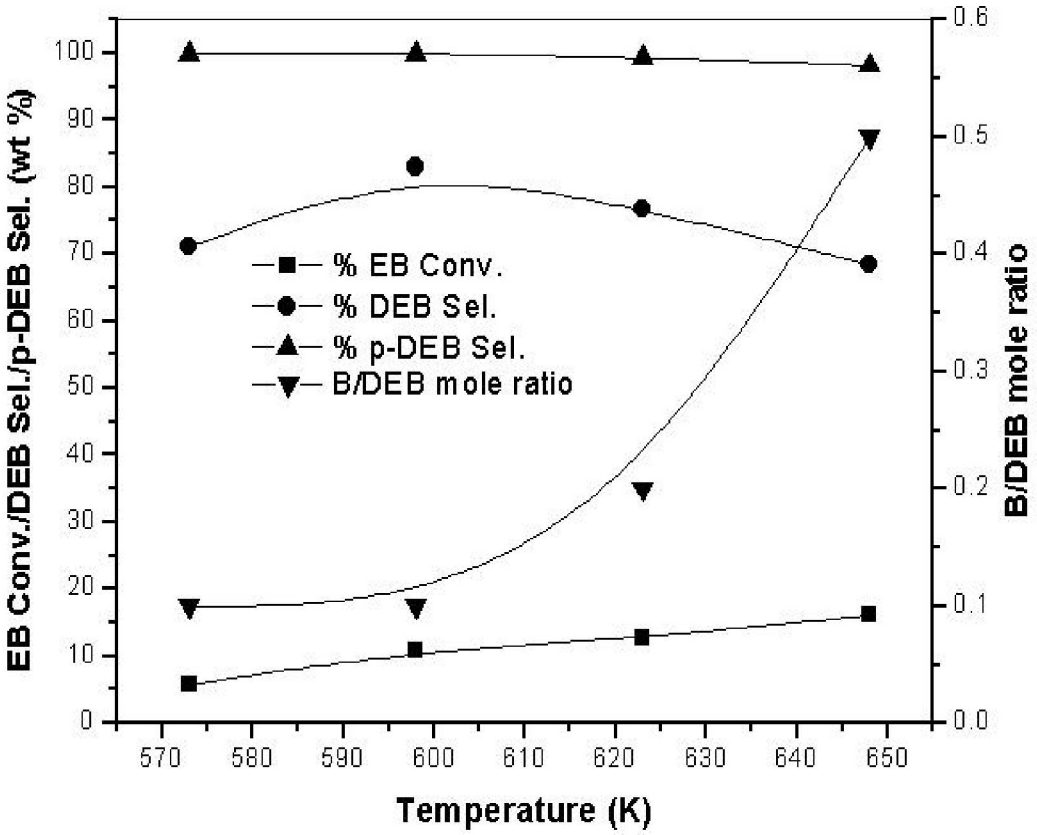


**Fig. 2.8: Effect of temperature over Ga-MFI CLD-2 zeolite during EB ethylation**

WHSV=2$h^{-1}$, EB:EtOH= 4:1

### *Effect of Temperature*

The effect of temperature over Ga-ZSM-5 CLD-2 zeolite on EB ethylation is shown in Fig. 2.8. During EB alkylation with EtOH, alcohol dehydration activity is low at lower temperature. As the temperature is increased the alcohol conversion increases to maximum, hence the conversion of EB and other side products also increase. But further increase in temperature leads to ethylbenzene dealkylation to benzene and ethylene, B/DEB ratio has also increased and selective conversion of ethylbenzene to diethylbenzene is lowered. The p-DEB selectivity remains more or less same.

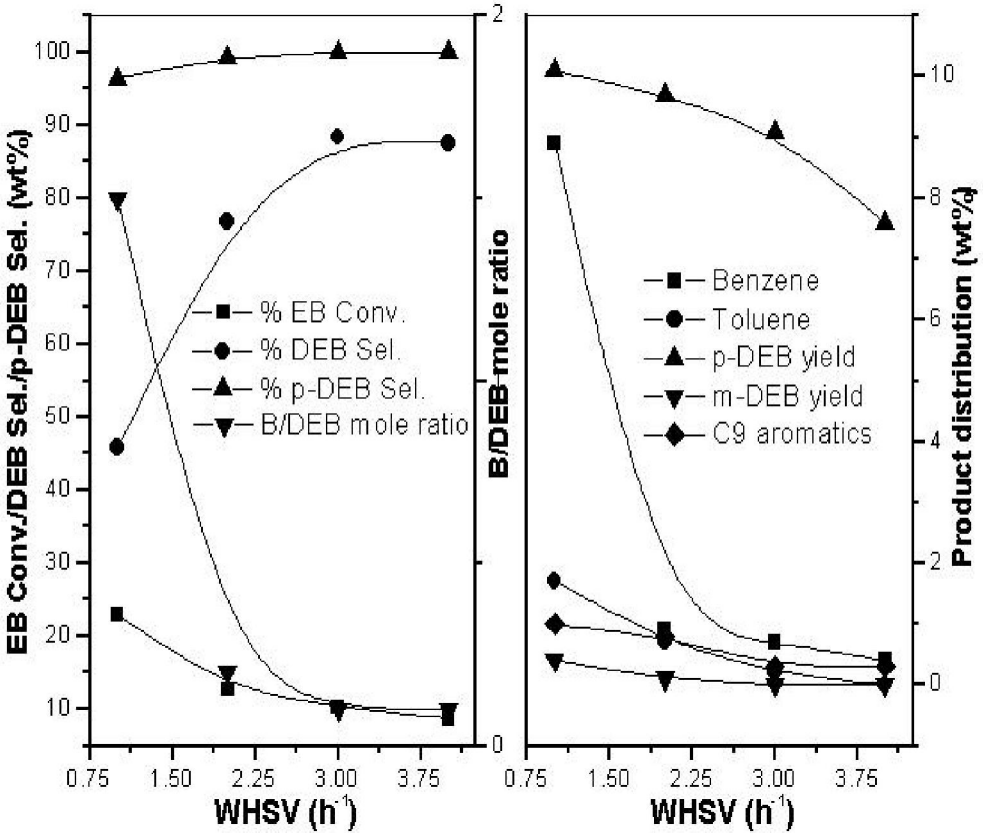


**Fig. 2.9: Effect of space velocity on Ga-MFI CLD-2 catalyst during EB ethylation**

Temp.623 K, EB: EtOH= 4:1

### *Effect of Space velocity*

Fig. 2.9 shows the effect of space velocity on Ga-MFI CLD-2 zeolites for EB ethylation The EB conversion has decreased at higher space velocities, whereas para selectivity is increased simultaneously. This also confirms that para is the primary product. At higher space velocity, the secondary isomerization as well as dealkylation is suppressed and also there is a drop in the level of impurities. At lower space velocities, diethylbenzene yield is higher and the EB conversion also increases. In case of ethylbenzene alkylation at lower space velocity, substantial dealkylation activity was observed and side product formation is clearly seen. At higher space velocities, drop in alkylation selectivity and also drop in dealkylation is observed.

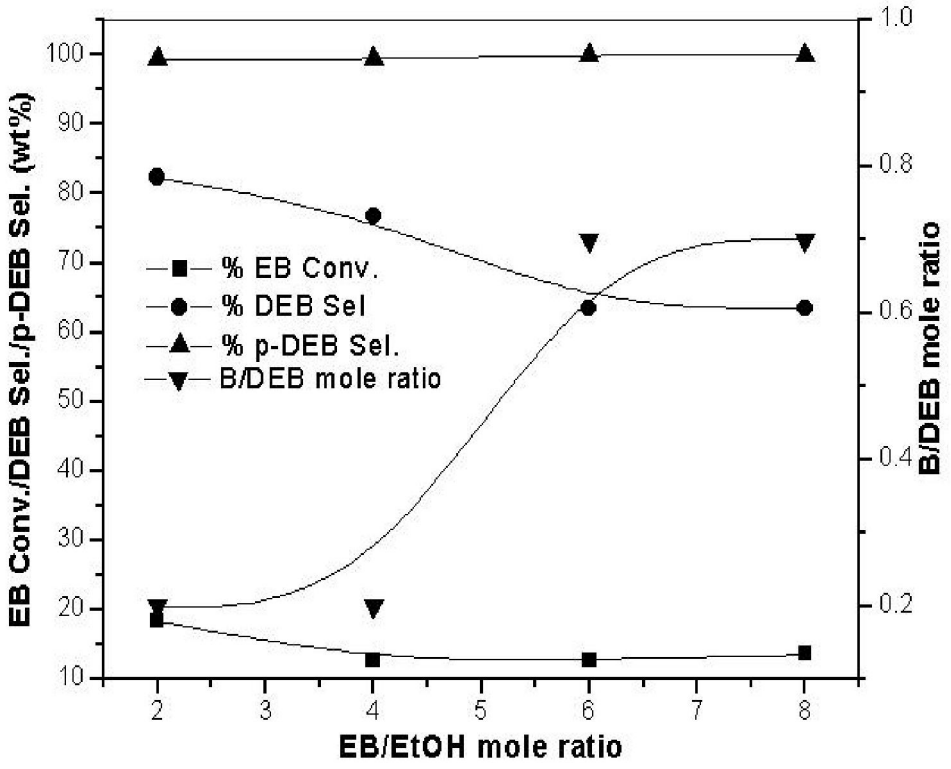


**Fig. 2.10: Effect of EB/EtOH mole ratio on EB ethylation over Ga-MFI CLD-2 zeolite**

Temp.623 K, WHSV=2$h^{-1}$

### *Effect of mole ratio*

Fig. 2.10 shows the effect of EB/EtOH mole ratio on Ga-MFI CLD-2 zeolites for EB ethylation. At low mole ratios of EB/EtOH, ethylbenzene conversion was higher because of higher content of alkylating agent. The concentration of unwanted products like xylenes, $C_9$ aromatics and high boilers are less as the EB/EtOH ratio increases. The differences in the product pattern are observed only till EB to ethanol molar ratio of 5-6, after which the conversion reaches a steady state value. The p-DEB selectivity is always > 99 %, while DEB selectivity drops with less EtOH content in the feed. The results show that EB/EtOH ratios between 4-6 appear to be optimum. Though higher EB/EtOH ratios appear to be better for reasonable conversion of EB and p-DEB selectivity, valuable EB is dealkylated under these conditions.

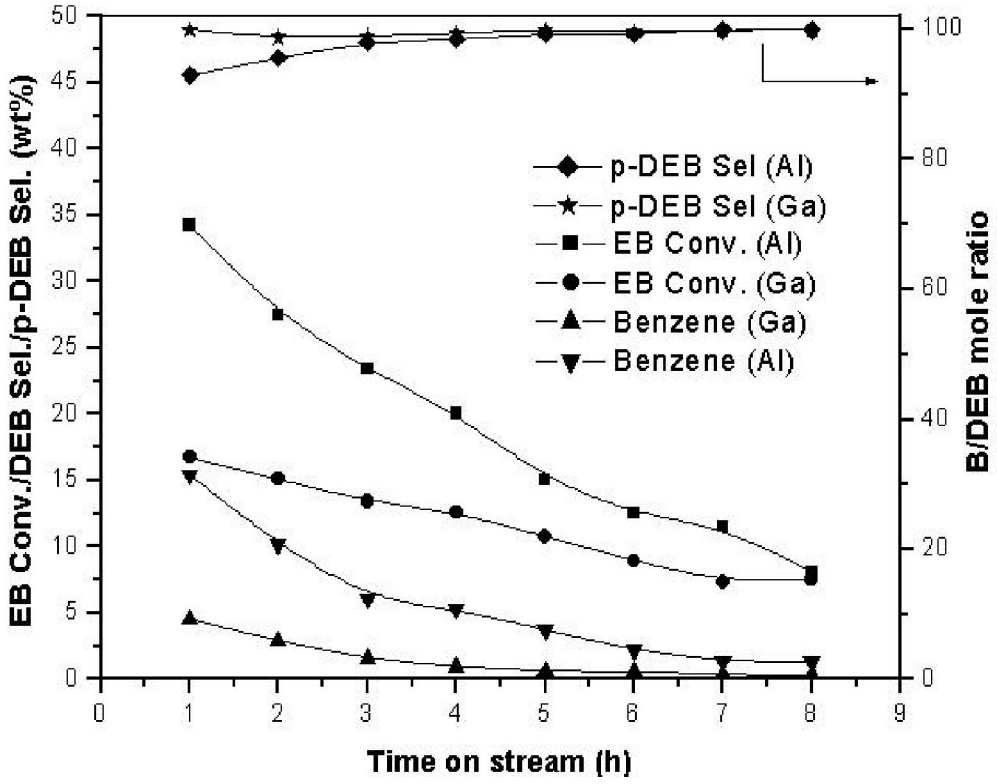


**Fig. 2.11: Comparison of the effect of time on stream on EB ethylation reaction over twice silylated (CLD2) Al and Ga forms of MFI zeolites**

Temp.623 K, WHSV=2$h^{-1}$, EB/EtOH=4:1

**Effect of time on stream on EB ethylation**

Comparison of the influence of time on stream on EB ethylation reaction over Al and Ga forms of ZSM-5 zeolites is shown in Figure 2.11. It is observed that in the initial stages of the reaction EB conversion is very high in case of Al-MFI zeolite while it rapidly drops with TOS. This is because the dealkylation activity is very high on Al-MFI zeolite in the initial stages of the reaction, which is reflected in the yield of benzene. The rapid drop in the activity on Al-MFI is because of the formation of coke due to oligomerisation of ethylene formed by EB dealkylation. With time, the yield of benzene continuously decreases. In case of Ga-MFI zeolite, the conversion is much lower than that of Al-MFI and its rate of deactivation is slower than that of Al-MFI zeolite. The p-DEB selectivity is

lower in the initial stages on the Al-MFI zeolite, but with time both show similar selectivity for p-DEB.

### 2.3.2.2 Toluene methylation

The shape-selective properties of high-silica MFI type zeolites have been intensively studied in recent years (118, 119). Using these types of zeolites as catalysts aromatics are formed during the conversion of methanol (120), olefins (121, 122) and alkanes (123). Special attention has been paid to selective para-xylene production by toluene disproportionation, alkylation with methanol or isomerization of the xylenes (124, 125, 126). Several factors may influence the para-xylene selectivity on pentasils, viz. diffusional effects (127), temperature, the nature of the feed (119), the degree of conversion, the composition of the catalyst and its crystal dimensions and the acidity. The selective production of para-xylene by toluene methylation is favoured by the orientation of the methyl group. However, the Bronsted acid sites of the zeolite also catalyse the isomerization of the xylenes simultaneously. As a result, the composition of the xylene fraction usually corresponds to the thermodynamic equilibrium between the three isomers (128).

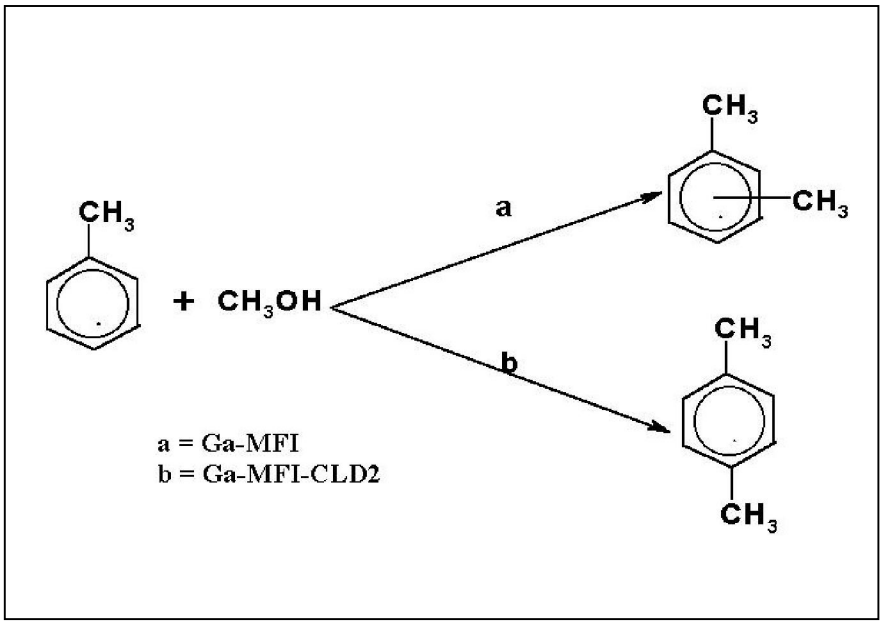


**Fig. 2.12: Scheme for toluene methylation on unmodified and modified zeolites**

In recent literature, shape-selective zeolite catalysts have been used to produce xylenes with para selectivity above 50% (129-131). p-Xylene selectivity was enhanced by impregnation with phosphorus and boron compounds and by coating the catalyst surface with polymers. A plausible explanation is that the pores of the MFI zeolite are approximately 6 $A^o$ in diameter, which permit the rapid diffusion of toluene and para xylene with molecular diameters of 6.3 Å, but severely retard the diffusion of ortho- and meta-xylenes with molecular diameters of 6.9 Å (133, 134). This diffusion takes place in the "configurational" region (132). Hence even if primary products of alkylation or disproportionation were near equilibrium the rapid diffusion of para-xylene through the pores would shift the product selectivity.

**Table 2.4 Comparison of Al-MFI and Ga-MFI for Toluene methylation activity**

| **Product comp. (Wt%)** | **Al-MFI** | **Ga-MFI** |
|---|---|---|
| **NA** | 0.7 | 0.3 |
| **Benzene** | 2.4 | 0.3 |
| **Toluene** | 69.9 | 75.6 |
| **EB** | 0.3 | 0.3 |
| **p-Xylene** | 5.0 | 5.2 |
| **m-Xylene** | 10.8 | 8.0 |
| **o-Xylene** | 4.6 | 3.4 |
| **p-ET** | 1.4 | 1.7 |
| **m-ET** | 2.2 | 2.7 |
| **TMB** | 2.6 | 2.5 |
| **% Toluene Conv** | 29.3 | 24.1 |
| **% Xyl. Sel.** | 69.4 | 68.7 |
| **B/Xy (moles)** | 0.2 | 0.02 |
| **% p-Xylene Sel.** | 24.7 | 31.2 |
| Temp 673 K, WHSV=4$h^{-1}$, Tol : MeOH=2:1 | | |

### *Comparison of Al-MFI and Ga-MFI in toluene methylation*

In case of toluene methylation, Al-MFI shows higher toluene conversion than Ga-MFI, but the difference is not much. This may be due to the higher acidity required for toluene

methylation than that for EB ethylation. However, the dealkylation activity is higher on Al-MFI zeolite. This can be seen from the concentration of benzene (Table 2.4). The concentration of ethyltoluenes is higher on Ga-MFI, than on Al-MFI zeolite. This is due to the dealkylation of ethyltoluenes on Al-MFI zeolite due to its higher strength of acidic sites.

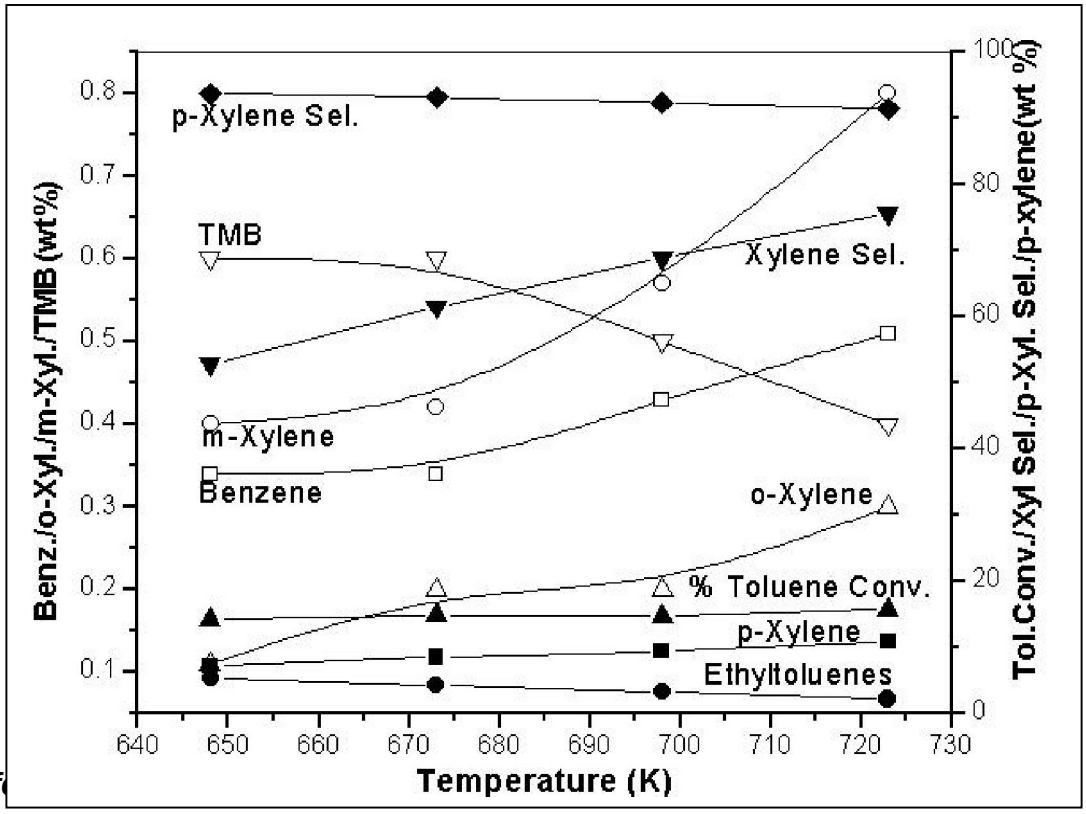


***Eff***

During toluene alkylation with methanol (Fig. 2.13), the toluene conversion increases with temperature. At lower temperature, though the conversion is low para-isomer selectivity is high and as the temperature increased a small drop in p-xylene selectivity was noticed. However, the yield of p-xylene as well as total xylene has increased with temperature. The xylene selectivity increases at higher temperatures because of the decrease in the concentration of the ethyltoluene isomers due to cracking and increase in the xylene yield. The ethyltoluenes are formed by the alkylation of toluene with ethylene which is the first intermediate formed in the methanol to gasoline reaction. A small amount of EB is also formed by benzene alkylation with ethylene. This benzene is probably produced due to toluene dealkylation.

**Table 2.5 Effect of space velocity on toluene methylation Ga-MFI CLD-2**

| Product comp. (Wt%) | WHSV ($h^{-1}$) | | |
|---|---|---|---|
| | 2 | 3 | 4 |
| NA | 0.5 | 0.4 | 0.4 |
| Benzene | 0.2 | 0.3 | 0.3 |
| Toluene | 84.5 | 83.6 | 84.7 |
| EB | 0.3 | 0.6 | 0.4 |
| p-Xylene | 9.2 | 9.2 | 8.5 |
| m-Xylene | 0.4 | 0.4 | 0.4 |
| o-Xylene | 0.2 | 0.2 | 0.2 |
| p-ET | 4.1 | 4.5 | 4.2 |
| m-ET | 0.1 | 0.2 | 0.1 |
| TMB | 0.6 | 0.3 | 0.6 |
| % Toluene Conv | 15.1 | 15.6 | 14.9 |
| % Xyl. Sel. | 65.2 | 62.7 | 61.5 |
| B/Xy (moles) | 0.02 | 0.04 | 0.05 |
| % p-Xylene Sel. | 93.9 | 93.9 | 93.2 |

Temp 673 K, Tol:MeOH=2:1

### *Effect of Space Velocity*

During toluene alkylation at lower space velocities (Table 2.5) the xylene selectivity is higher and with increase in space velocity the xylene selectivity marginally decreases, with a simultaneous drop in xylene yield. There is a slight decrease in toluene conversion at higher space velocities. However, not much change in the p-xylene selectivity was observed with variation in space velocity. Marginal changes were observed in case of B/Xy ratio and ethyltoluene contents.

### *Effect of Tol/MeOH mole ratio*

The effect of Tol/MeOH mole ratio on methylation is shown in Fig. 2.14. The conversion of toluene decreases with increasing toluene to methanol mole ratio. This is because the concentration of the alkylating agent is diluted in the feed. In case of xylene selectivity, it has initially increased at higher Tol/MeOH ratio, but subsequently falls with further increase in Tol/MeOH mole ratio. There is a decrease in the concentration of side products

especially $C_9$ aromatics at higher Tol/MeOH ratios. There is a slight enhancement in the p-xylene selectivity at higher toluene mole ratio, whereas there is a decrease in the benzene to xylene ratio as the concentration of toluene in the feed increases.

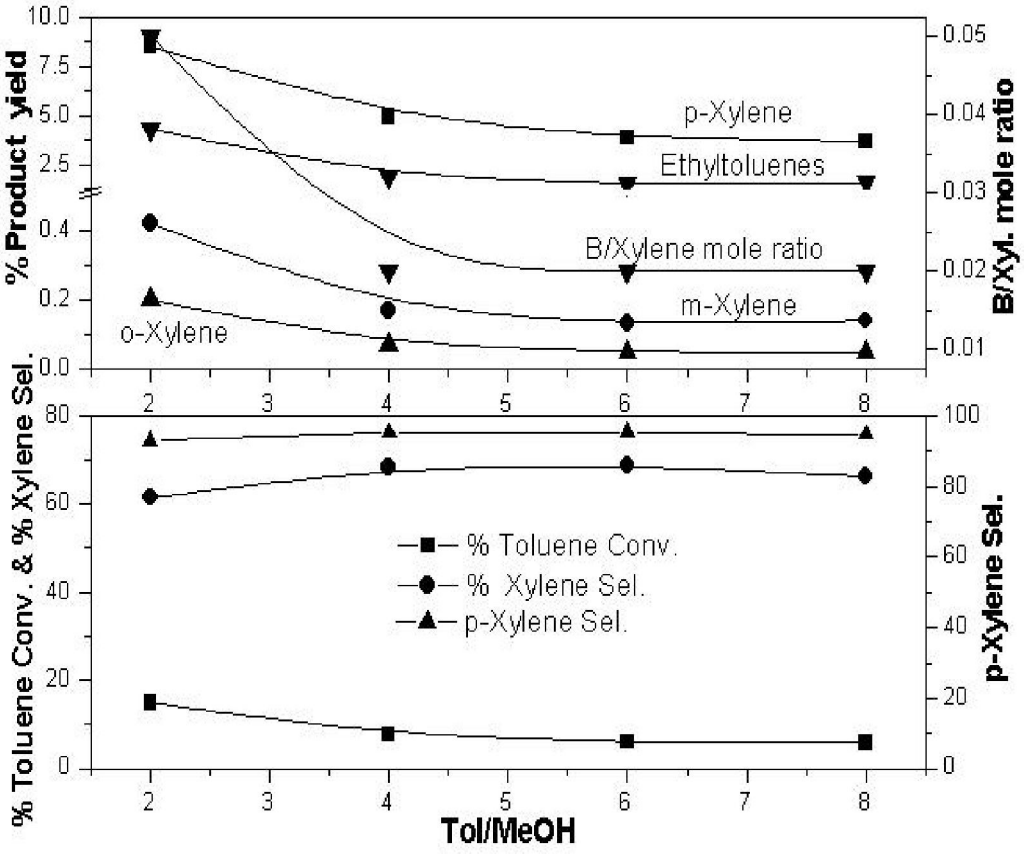


**Figure 2.14: Effect of mole ratio of toluene/MeOH on methylation of toluene over Ga-MFI CLD-2 catalyst**

Temp 673 K, WHSV=4$h^{-1}$

### *Effect of Time on stream on toluene methylation*

Comparison of the influence of time on stream for toluene methylation reaction over Al and Ga forms of MFI zeolites is shown in Figure 2.15. It is observed, that in the initial stages of the reaction the p-xylene selectivity is slightly lower for the aluminium substituted catalyst. But with time both give almost similar selectivity for p-xylene. In case of toluene conversion, the Ga-MFI shows higher conversion than Al-MFI zeolite. The yields of xylene and $C_9$ are higher on Ga-MFI zeolite than on Al-MFI zeolites.

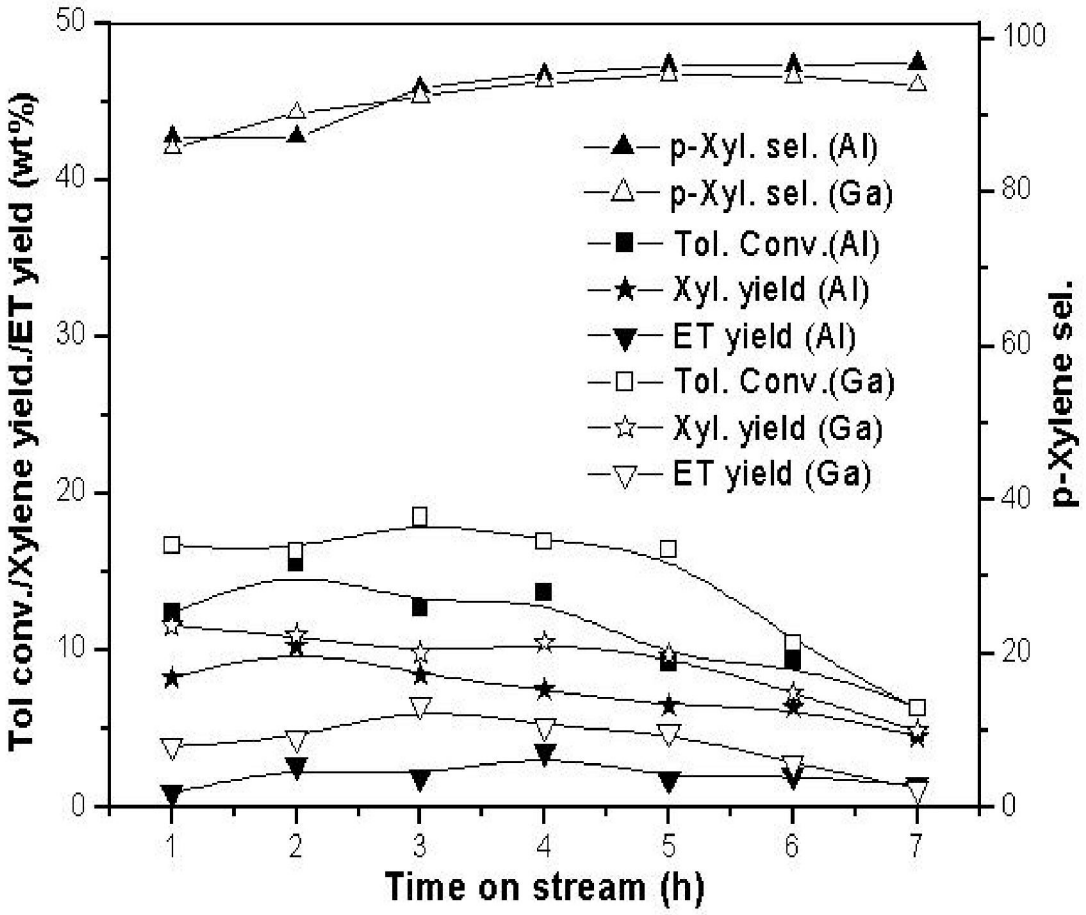


**Fig. 2.15: Comparison of the effect of time on stream for toluene methylation reaction over twice silylated (CLD2) Al and Ga forms of MFI zeolites**

Temp 673 K, WHSV=4$h^{-1}$, Tol:MeOH=2:1

### *Mechanistic aspects of toluene methylation*

According to the infrared adsorption studies, (135, 136) adsorption of methanol on the strongly acidic bridging OH groups of H-ZSM-5, at temperatures up to 473 K and at very low partial pressure of reactants (about 1 Torr), led to the formation of methoxonium ions, while toluene interacted with the OH groups via hydrogen bonding. Ab initio quantum chemical calculations (137) of methanol interaction with zeolites have showed that physically adsorbed methanol is the most stable binding geometry while a methoxonium cation represents a transition state and not a local minimum. Density functional theory

calculations (138) of methanol activation by an acidic proton confirmed the formation of a methoxonium intermediate as a transition state. Moreover, it was proposed that methanol can be adsorbed on the hydroxyl groups in two different orientations. Either it is oriented perpendicular to the zeolite surface (end-on configuration) or the methyl group is directed towards the basic oxygen of the zeolite, parallel to the zeolite surface (side-on configuration). The position of the adsorbed methanol molecule strongly influences its activity in toluene alkylation (139-140). In the co-adsorption of methanol with toluene, regardless of the order of adding the two reactants, the formation of methoxonium ions is very fast and the interaction of toluene with the acid OH groups is thus very limited. A new infrared adsorption band at 3460 $cm^{-1}$ was assigned by Mirth and Lercher (135) to the adsorption complex of toluene with an adsorbed methoxonium ion (Fig.2.16A). According to other interpretations of the infrared spectra of adsorbed methanol over acidic zeolites, methoxy groups can be formed (141-144). It has also been suggested that zeolite methoxy groups can form another adsorption complex with toluene, as shown in Fig 2.16B (145). A similar complex was also proposed for benzene alkylation with methanol over Y zeolites (146). Both interaction complexes can be formed according to the Rideal-Eley mechanism where a toluene molecule interacting with a methoxonium or methoxy group is kept in the zeolite channel system by its strong electrostatic field. The occurrence of methoxonium or methoxy groups bound to the zeolite framework depends strongly on the reaction conditions and the acid strength of the individual zeolite used. Generally, methoxonium ions are converted to methoxy groups at higher reaction temperature and partial pressure of methanol; however, no quantitative data are available in this respect. Despite a large number of papers discussing the mechanism of toluene alkylation with methanol, the real nature of the alkylating species has still not been unambiguously demonstrated. Some authors have concluded that methoxy species alkylates toluene (144, 145, 147, 148) while others favour the methoxonium species (135, 149, 150). There is also no doubt that dimethylether is formed under the conditions of alkylating reactions, (139, 151) and several authors reported dimethylether as the alkylating agent (139, 152). $^{13}C$ MAS NMR studies of toluene alkylation with methanol confirmed that both methanol and dimethylether can alkylate toluene and end-on types of adsorbed species have been

proposed as the precursors of the methanol-dimethyl ether interconversion and toluene alkylation (142).

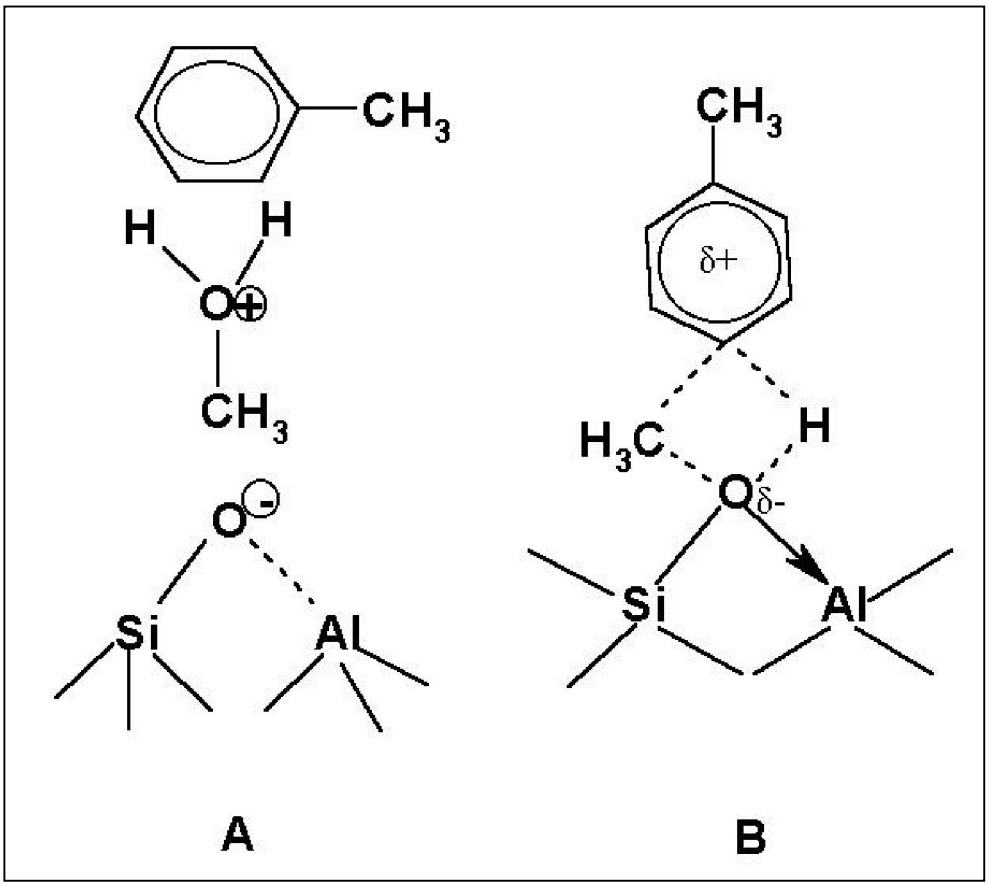


**Fig. 2.16: Proposed intermediates in the toluene methylation reaction**

## 2.4 References

1 Weitkempt, J., Ernst, S., Daums, H., Gallie, E. Chem. Eng. Technol. 58 (1986) 623.

2 Stocker, M. Microporous Mesoporous Mater. 29 (1999) 3.

3 O' Malley, P. J., Dwyer, J. J. Chem. Soc., Chem. Commun. (1987) 72

4 Fricke, R., Kosslick, H., Lischke, G., Richter, M. Chem. Rev. 100 (2000) 2303.
5 Yoshizawa, K., Yumura, T., Shiota, Y., Yamabe, T. Bull. Chem. Soc. Jpn. 73 (2000) 29.
6 Bordiga, S., Coluccia, S., Lamberti, C., Marchese, L., Zecchina, A., Boscherini, F., Buffa, F., Genoni, F., Leofanti, G., Vlaic, G. J.Phys.Chem. 98 (1994) 4125.
7 Dong, M., Wang, J., Sun, Y. Microporous Mesoporous Mater. 43 (2001) 237.
8 Shilov, A. E., Shul¢pin, G. B. Chem. Rev. 97 (1997) 2879.
9 Morrison, R. T.; Boyd, R. N. *Organic Chemistry*, 6th ed.; Prentice Hall: New York, 1992; p 893.
10 Gnep, N. S., Biyemet, J. D., Guisnet, M. D. J. Mol. Catal. 45 (1988) 281.
11 Thangaraj, A., Kumar, R.; Ratansamy, P. Appl. Catal. 57 (1990) L1-L3.
12 Hidalgo, C. V., Itoh, H., Hattori, T., Niwa, M., Murakami, Y. J. Catal. 85 (1984) 362.
13 Topsoe, N.-Y., Pedersen, K., Derouane, R. G. J. Catal. 70 (1981) 41.
14 Hegde, S. G., Abdullah, R. A., Bhat, R. N., Ratnasamy, P. Zeolites 12 (1992) 951.
15 Chu, C. T.-W., Chang, C. D. J. Phys. Chem. 89 (1985) 1569.
16 Ramaswamy, V. Editors: Gupta, N. M.; Chakrabarty, D. K. *Catal. [Pap. Nat. Symp.], 12th* 1996, 95-99. (Meeting Date: Dec 19-22, 1994. Narosa: New Delhi, India.)
17 Greatbanks, S. P., Sherwood, P., Hillier, I. H. J. Phys. Chem. 98 (1994) 8134.
18 Shah, R., Payne, M. C., Lee, M.-H., Gale, J. D. Science 271 (1996) 1395.
19 Gonzales, N. O., Chakraborty, A. K., Bell, A. T. Catal. Lett. 50 (1998) 135.
20 Deka, R. C., Vetrivel, R., Pal, S. J. Phys. Chem. A 103 (1999) 5978.
21 Limtrakul, J.; Khongpracha, P.; Jungsuttiwong, S.; Truong, T. N. J. Mol. Catal. A 153 (2000) 155.
22 Chatterjee, A., Iwasaki, T., Ebina, T., Miyamoto, A. Microporous Mesoporous Mater. 21 (1998) 421.
23 Sierka, M., Sauer, J. Faraday Discuss. 106 (1997) 41.
24 Viswanathan, B., Jayashree, S. Theor. Anal. Chem. 35A (1996) 1034
25 Chatterjee, A., Vetrivel, R. Microporous Mater. 3 (1994) 211.
26 Lewis, D. W., Catlow, C. R. A., Sankar, G., Carr, S. W. J. Phys.Chem. 99 (1995) 2377.
27 Stave, M. S., Nicholas, J. B. J. Phys. Chem. 99 (1995) 15046.
28 Parrillo, D. J., Biaglow, A., Gorte, R. J., White, D. Stud. Surf. Sci.Catal. 84 (1994) 701.

29 Kramer, G. J., van Santen, R. A. J. Am. Chem. Soc. 115 (1993) 2887.
30 Vetrivel, R., Pal, S., Krishnan, S. J. Mol. Catal. 66 (1991) 385.
31 Yuan, S.P., Wang, J.G., Li,Y.W., Jiao, Haijun J. Phys. Chem. A 106 (2002) 8167
32 Goldsmith, J.R. Miner. Mag., 29 (1952) 952.
33 Barrer, R.M., Brynman, J.W., Bultitude, F.W., Meier, W.M., J.Chem. Soc. (1959) 195.
34 Newsam, J.M., Vaughan, D.E.W. "New Developments in Zeolite Science and Technology"; Y.Mizukami at.al. Eds.; Elsevier, Amsterdam, (1986) 457.
35 Selbin, J. Inorg. Nucl. Chem. 20 (1961) 222.
36 Kuhl, J. Inorg. Nucl. Chem.; 33 (1971) 3261.
37 Hayashi; Bull.Chem. Soc. Jpn.; 59 (1985) 52.
38 Shevade, Siddhesh, Ahedi, R.K., Kotasthane, A.N. and Rao, B.S.; "Recent Trend inCatalysis"; Eds. Murugesan et.al.; Narosa Publishig House, India; (1999), 383.
39 Iler, R.K.; "The chemister of Silica"; Wiley, New York; (1979).
40 Ivanov-Emin, B.N., Nisel'son, L.A., Larionova, L.E. Russian J.Inorg.Chem. 7 (1962) 266.
41 Johansson, G. Acta. Chim. Scand.; 14[3] (1960) 771.
42 McNicol, B.D. and Pott, G.T. J.Catal., 25 (1972) 223.
43 Derouane, E.G., Mestsdagh, M. and Vielvoye, L. J.Catal., 33 (1974) 169.
44 Marosi, L., Stabenow J., and Schwarzmann, M., Ger.Pat. 2,831,611.
45 Marosi, L., Stabenow J., and Schwarzmann, M., Ger.Pat. 2,831,630.
46 Dwyer, F. U.S.Pat. 3,941,871.
47 Kouwenhoven H.W., and Stork, W.H. U.S.Pat. 4,208,305.
48 Taramasso, M., Perego, G. and Notari, B., in Proceedings of the 5th International Conference on Zeolites, (Ed. L.V.C. Rees) Heyden, London, 1980, p. 40
49 Gabelica, Z., Debras, G. and Nagy, J.B. Stud. Surf.. Sci. Catal. 19 (1984) 113
50 Gabelica, Z., Nagy, J.B., Bodart, P. and Debras, G. Chem.Lett. (1984) 1059
51 Kessler, H., Chezea~, J.M., Guth, J.L., Strub, H. and Coudurier, G. Zeolites 7 (1987) 360
52 Coudurier, G., Auroux, A., Vedrine, J.C., Farlee, R.D., Abrams, L. and Shannon, R.D.J. Catal. 108 (1987) 1
53 Scholle, K.F.M.G., Kentgens, A.P.M., Veeman, W.S., Frenken, P. and van der Velden, G.P.M.J. Phys. Chem. 88 (1984) 5
54 Chu, C.T.W. and Chang, C.D.J. Phys. Chem. 89 (1985) 1569
55 Meyers, B.L., Ely, S.R., Kutz, N.A., Kaduk, J.A. and van den Bossche, E. J. Catal.

91 (1985) 352

56 Jansen, J.C., Biron, E. and Van Bekkum, H. Stud. Surf. Sci. Catal. (1988) 37, 133

57 Howden, M.G. Zeolites 5 (1985) 334

58 Romano, U., Clerici, M.G., Bellusi, G. and Buonomo, F. Eur. Pat. 203 632 (Dec. 3, 1986) Enichem Sintesi S.p.A 102 (1986) 467

59 Kuehl, H.G. US Pat. 4 661 467 (1987)

60 Ratnasamy, P., Hegde, S.G. and Chandwadkar, A. J. J. Catal. 102(2) (1986) 467.

61 Beyer, H.K. and Borbely, G. Stud. Surf. Sci. Catal. 28 (1986) 867

62 Coudurier, G. and Vedrine, J.C. Stud. Surf. Sci. Catal. 28 (1986) 643

63 Weitkamp, J., Beyer, H.K., Borbely, G., Cortes-Corberan, V. and Ernst, S. Chem. Ing. Tech. 68 (1986) 969

64 Hoelderich, W., Eichhorn, H., Lehnert, R., Marosi, L., Mross, W., Reinke, R., Ruppel, W., and Schlimper, H. in Proceedings of the 6th International Zeolite Conference, Reno (Eds. D. Olson and A. Bisio) Butterworths, London, 1984, p. 545

65 Wendlandt, K.P., Unger, B. and Becker, K. Appl. Catal. 66 (1990) 111

66 Hoelderich, W.F. and Goetz, No DE 37 22 891 (July 10, 1988)

67 Romannikov, V.N., Chumachenko, L.S. and lone, K.G., in Proceedings of the 1st Sov. Indian Semin. Cata/., Catal. Prog. Chem. Eng. 1984, p. 127

68 Ione, K.G., Vostrikova, L.A., Petrova, A.V. and Mastikhin, V.M., in Proceedings of the 8th International Congress onCatalysis, Berlin, Verlag Chemie, Frankfurt, 1984, p. 519

69 Romannikov, V.N., Chumachenko, C.S., Mastikhin, V.Mo and Ione, K.G. React. Kinet. Catal. Lett. 29 (1985) 85

70 Hoelderich, W.F. Pure Appl. Chem. 58 (1986) 1383

71 Argauer,R.J., and Landolt,G.R., US.Patent 3 702 886 (1972).

72 Vansant.E.F., " Pore Size Engineering in zeolites " Eds.John Wiley & sons, New York, (1990).

73 Ramoa Riberio, F. Catal.Lett., 22 (1993) 107.

74 Barrer, R.M., and Rees, L.V.C., Trans faraday Soc., 50 (1954) 852.

75 Breck,D.W., Eversole,D.G., Milton,R.M., Reed, T.B. and Thomas,T.L., J.Am.Chem.Soc., 78 (1956) 5963.

76 Fraenkel ,D., Ind.Eng.Chem.Res., 29 (1990) 1814.

77 Paparatto, Alberti, G, de., leofanti, G. and Padovan, M. Stud. Surf. Sci. Catal., 44 (1989) 255.

78 Barrer, R.M., Jenkins,R.G. and Peeters,G. in katzer, J.R., (Ed) Molecular sieves II, ACS Symp.Ser. 40 (1977) 258.

79 Thijs,A., Peeters,G., Vansant.E.F., Verhaert,I. and Bievre, P.De., J. Chem. Soc., Faraday Trans. I, 79 (1983) 2821.

80 Vansant.E.F. Stud. Surf. Sci. Catal ., 37 (1988) 143.

81 Thijs, A., Peeters,S., Vansant. E. F., Peeters,G. and Verhaert, I., J. Chem. Soc., Faraday Trans. I, 82 (1986) 963.

82 Yan, Y., Verbiest, J., Hulsters, P. De., Vansant. E. F., J. Chem. Soc., Faraday Trans. I, 85 (1989) 3087.

83 Yan, Y., Verbiest, J., Vansant. E. F., J. Philippaerts and Hulsters, P. De., Zeolites, 10 (1990) 137.

84 Jentys, A.A., Rumplmayr, G., and Lercher, J.A., Appl. Catal., 53 (1989) 299.

85 Rumplmayr, G. and Lercher, J.A., Zeolites , 10 (1990) 283.

86 Hidalgo, C.V., Kato, M., Hattori, T., Niwa, M and Murakami,Y., Zeolites , 4 (1984) 175.

87 Guisnet, M., Gnep, N.S., Vasques, H. and Riberio, R. F., Stud. Surf. Sci. Catal., 69 (1991) 321.

88 Niwa, M., Itoh,H., Kato, M., Hattori, T.and Murakami,Y., J. Chem. Soc. Chem. Commun., (1982) 819.

89 Niwa, M., Kawashima, Y. and Murakami, Y., J. Chem. Soc. Faraday.Trans. I. 81 (1985) 2757.

90 Niwa, M., Morimoto, S., Kato, M., Hattori, T. and Murakami,Y., Proc. 8th.In.Congr.Catal. Berlin, Vol.IV,p.701 (1984).

91 Niwa, M., Hidalgo, T., Hattori, T. and Murakami, Y., Stud. Surf. Sci. Catal., 28 (1986) 297.

92 Niwa, M., Hidalgo, T., Hattori, T. and Murakami, Y., J. Phys. Chem. 90 (1986) 6233.

93 Hibino,T., Niwa, M., Murakami,Y, J.Catal., 128 (1991) 551.

94 Hibino,T., Niwa, M., Murakami,Y, Zeolites 13 (1993) 518.

95 Tsai, T., and Wang, I. Appl. Catal., 77 (1991) 209.

96 Ratnasamy,P., and Pokhriyal, S.K., Appl. Catal. 55 (1989) 265.

97 Kaeding, W.W., Chu, C., Young, L.B., Weinstein, B., and Butter, S.A., J. Catal., 67 (1981) 159.

98 Uguina, M.A., Sotelo, J.L., Serrano, D.P., and Grieken, R.Van., Ind. Eng. Chem. Res., 31 (1992) 1875.

99 Parenago,O.O., Lebedeva,O.E., Ivanova, I.I., Vil' yareal, N.E., Latysheva, L.E., Skornikova, S.A., Chenets, V.V. and Lunina, E.V., Kinetic. Katal., 34 (1993) 183.

100 Bennazi,E., tavernier,S.De., Beccat, P., Joly, J.F., Nedez, Ch. Basset, J.M. and Choplin, A., Symposium on Chemical Modified molecular sieves, 206th national meeting, ACS, vol 38, N.3, Chicago.p- 561 (1993)

101 Namba,S., Inaka.A.and Yashima,T., Zeolites, 6 (1986) 107.

102 Anderson, J.R., Chang,Y.F., Hughes, A.E., Catal.Lett. 2 (1989) 279.

103 Silva, J.M., Riberio, M.F., Ramoa Riberio, F., Gnep,N.S., Guienet,M. and Bennazi. E., React.Kinet. Catal.Lett., 1 (1994) 54.

104 Neves, I., Jayat, F., Magnoux, P., Perot,G., Ramoa Riberio, F., Gubelmann, M. and Guisnet,M., J. Chem. Soc. Chem. Commun., 6 (1994) 717.

105 Corbin, D., Keane, M.Jr., Abrams, L., Farlee, R.D., Bierstedt, P.E., and Bien, T., J. Catal., 124 (1990) 268

106 Hibino, T., Niwa, M., Murakami,Y., Appl.Catal. 44 (1988) 95-103.

107 Tang,Y., Lu,L., Gao, Z., Acta Physico-Chim.Sin. 10 (1994) 514-520.

108 Yue,Y., Tang,Y., Gao,Z., Acta Physico-Chim.Sin. 11 (1995) 1-4.

109 Niitsuma, M., Sato, K., Preparation of silylated zeolites. Japan Patent Kokai 1-108113, 1989.

110 Yue,Y., Tang,Y., Kan, Y., Acta Physico-Chim.Sin. 1995c, in press.

111 Argauer, R.J., Landolt, G.R., US. Patent 3 702 886 (1972)

112 Ratnasamy, P., Kumar, R. Catal. Today. 9 (1991) 329

113 Szostak, R., Molecular sieves, Principles of synthesis and identification, Van NostrandRheinhold, New York, (1989) p. 285

114 Alsdorf, E., Feist, M., Fichtner-Schmittler, H., Gross, Th., Jerschkerwitz, H.J., Lohse, U., and Parlitz, B., Adsorp. Sci. Technol., 5 (1988) 127.

115 Parikh, P.A., Subramanyam, N., Bhat, Y.S. and Halgeri, A.B., Catal.Lett., 14 (1992) 107.

116 Flanigen, E.M., Khatami, H., Szymanski, H.A., Advances in chemistry series, 101 (1971) 201.

117 Casci, J.L., Whittam, V.T, and Lowe, B.M., Proc. 6th Int. Conf. On zeolites, Reno, (1983) p. 894

118 Derouane, E.G. Catalysis by Zeolites, B. Imelik et al. (Eds.), Elsevier, Amsterdam, 1980, p.5.

119 Csicsery, S., Zeolites, 4 (1984) 202.

120 Chang, C.D., Catal. Rev. -Sci. Eng., 25 (1983) 1.

121 Dejaifve, P., Vedrine, J.C., Bolis, V. and Derouane, E.G., J. Catal., 63 (1980) 331.
122 Bezuhanova, C., Nenova, Dimitrov, V., Lechert, C. H. and Dimitrov, L., Proc. Vth Intern. Symp. Heterog. Catal., Varna 1983, Part I, 423.
123 Anderson, J.R., Foger, K., Mole, T., Rajadhyaksha R.A., and Sanders, J., J. Catal., 58 (1979) 114.
124 Young, L.B., Butter S.A. and Kaeding, W.W. J. Catal., 76 (1982) 418.
125 Namba, S., Nakanishi S., and Yashima, T., J. Catal., 88 (1984) 505.
126 Nunan, J., Cronin, J. and Cunningham, J., J. Catal., 87 (1984) 75.
127 Wei, J., J. Catal., 76 (1982) 433.
128 Kaeding, W.W., Chu, C., Young, L.B., 67 (1981) 159.
129 Yashima, T., Ahmad, H., Yamazaki, K., Katsuta, M., and Hara, N., J. Ccrtul. 16, 273 and 17, 151 (1970).
130 Yashima, T., J. Catal. 26 (1972) 303.
131 Chen, N. Y., Kaeding, W. W., and Dwyer, F. G., J. Amer. Chem. Sot. 101 (1979) 6783.
132 Weisz, P. B., Chem. Tech. (1973) 498.
133 Kaeding, W. W., Chu, C., Young, L. B., Weinstein, B., and Butter, S. A., J. Curd. 67 (1981) 159.
134 Kaeding, W. W., Chu, C., Young, L. B., and Butter, S. A., J. Curd. 69 (1981) 392.
135 Mirth, G., Lercher, J.A. J.Phys.Chem. 95 (1991) 3736.
136 Mirth, G., Lercher, J.A. J. Catal. 147 (1994) 199.
137 Gale, J.D., Catlow, C.R.A., Carruthers, J.R. Chem.Phys.lett. 216 (1993) 155.
138 Blaszkowski, S.R., van Santen, R.A. J.Phys.Chem. 99 (1995) 11728.
139 Ivanova, I.I., Corma, A. Stud. Surf. Sci. Catal. 97 (1995) 27.
140 Ivanova, I.I., Corma, A. J.Phys.Chem. B. 101 (1997) 547.
141 Salvodor, P., Kladnig, W. J. Chem.Soc., Faraday Trans. I 73 (1977) 1153.
142 Kubelkova, L., Novakova, J., Jiru, P. Stud. Surf. Sci. Catal. 18 (1984) 217.
143 Forrester, T.R., Wong, S.T., Howe, R.F., J. Chem.Soc., Chem. Commun. (1986) 1611.
144 Corma, A., Sastre, G., Viuela, P., Stud. Surf. Sci. Catal. 84 (1994) 2171.
145 Rakoczy, J., Sulikowski, B. Zeolites React. Kinet. Catal. Lett. 36 (1988) 241.
146 Rakoczy, J., Romotowski, T. Zeolites 13 (1993) 256.
147 Bosacek, V. Z.Phys. Chem. 189 (1995) 241.
148 Bosacek, V., Klik, R., Genoni, F., Spano, G., Rivetti, F., Figueras, F., magn. Reson.

Chem. 37 (1999) S135.

149 Mirth, G., Lercher, J.A. J. Catal. 132 (1991) 244.

150 Vinek, H., Derewinski, M., Mirth, G., Lercher, J.A. Appl. Catal. 68 (1991) 277.

151 Philippou, A., Anderson, M. W. J. Am. Chem. Soc. 116 (1994) 5774.

152 Sefcik, M.D. J. Am. Chem. Soc. 101 (1979) 2164.

## 3.1 Introduction

p-Diethylbenzene (p-DEB) is a valuable chemical that has many industrial applications. It is used as an organic solvent, precursor and a crosslinking agent for many resins and speciality chemicals. The DEB is the main raw material for manufacturing divinylbenzene. It is a key intermediate for the preparation of vinyl ethyl and divinyl-benzenes (1). Addition of a small quantity of divinylbenzene to styrene markedly modifies the linear styrene polymers. The crosslinking between styrene and divinylbenzene results in resins with reduced solubility in most of the solvents, increased heat distortion temperatures, increased surface hardness and improved impact and tensile strength. It is also used as an adsorbent in the PAREX process (2, 3) for the separation of para-xylene from xylene isomers. It is difficult to separate DEB isomers by distillation or by cryogenic freezing. p-DEB has a much higher product value (ca. US$ 4000 per metric ton) than p-xylene (ca. US$ 450 per metric ton). It is used as a desorbent in adsorptive separation processes, for example in Parex$^{SM}$ (UOP) and possibly also in Eluxyl$^{SM}$ (IFP) (4, 5, 6). There is a constant demand for the routine make-up requirements of existing operating units, with estimated consumption of 8000 tons/year. In addition, there are requirements for new loads of p-DEB for grass root units, with estimated demand of around 4000 tons/year. Therefore, worldwide annual demand is estimated at 12, 000 tons, accounting for annual sales volume of around US$ 48 million.

## 3.2 Synthesis of p-Diethylbenzene

In the past, p-DEB was mainly recovered from the DEB mixtures that are normally multi alkylation side products of the EB process. Three DEB isomers exist, namely, p-, m- and o-DEB, all of which have very similar physical properties (Table 3.1). For example, the boiling point and melting point of p-DEB and m-DEB only differ by 0.3 K and 11.7 K, respectively. Although it has not been disclosed, it is generally believed that the early p-DEB recovery was mostly done by adsorptive separation. There are several drawbacks for applying adsorptive separation for p-DEB recovery. The technique is highly energy intensive. Moreover, owing to the distribution of EB production, the feed (DEB) has to be

collected from different manufacturers and thus increase the feed collection cost. Furthermore, the separated raffinate (mainly m- and o-DEB isomer mixture) can only be used as fuel oil and the mixed DEB feedstock required to produce one pound of p-DEB is ca. 4 pounds. These three factors, namely, high energy consumption for separation, high feed collection cost and high feedstock requirements are the main reasons that made the p-DEB cost high. Hence, to avoid the above factors it is necessary to synthesize p-DEB selectively (above 95% purity). This chapter deals with the synthesis of p-dialkyl benzenes on Al-MFI zeolite by alkylation and disproportionation reactions. A comparison of the catalytic activity and selectivity has been made for the powdered and extrudated forms of the zeolites. Silylation with TEOS and ion exchange with lanthanum has been carried out for improving the para-selectivity. Mixed $C_8$ alkyl aromatic isomer feeds, containing various isomers of xylenes, in addition to EB, have been used to study the influence of xylenes on the selectivity of p-DEB. Reaction with these feeds has an added advantage as reaction of EB (alkylation or disproportionation) is carried out directly using EB enriched $C_8$ aromatics cut which is obtained from xylene isomer unit, that has high concentration of EB after removal of xylenes. It is essential to reduce the excess ethylbenzene from these feeds to mix them back into xylene isomerisation loop. The time on stream stability of the modified zeolites for conversion of these streams is also given in this chapter.

**Table 3.1 Boiling and Melting points of DEB's**

| **($C_{10}$ aromatics)** | **B.P. (K)** | **M.P. (K)** | **$d^{20}$** |
|---|---|---|---|
| p-Diethylbenzene | 456 | 230.1 | 0.8670 |
| m-Diethylbenzene | 454.1 | 191.8 | 0.8684 |
| o-Diethylbenzene | 456.5 | 241.8 | 0.8839 |

## 3.3 Materials and Experimental Methods

### 3.3.1 Materials and Chemicals

Various chemicals and catalysts were used in this study, details of which are given in Table 3.2. The catalyst modification procedures have also been described in this section.

**Table 3.2 Materials and chemicals used for reactions.**

| Chemical/Catalyst | Trade Name |
|---|---|
| HMFI 40, 100, 250 (powdered form) | NCL catalyst pilot plant |
| HMFI 40, 100 (70% extrudates) | Sud-Chemie, Baroda |
| HMFI 250 (Various binder contents) | Prepared using pseudoboehemite |
| Lanthanum nitrate | Indian Rare Earths Limited |
| Ethylbenzene | S.D. Fine Chemicals |
| Toluene | Qualigens |
| Ethanol | Rectified spirit (93%) wt/wt purity |
| Methanol | Qualigens |
| Mixed $C_8$ Feed | Reliance Industries Ltd., Hazira |
| TEOS | Aldrich Chemicals |

### 3.3.2 Experimental procedures

# Various experimental procedures adopted for preparation of catalysts and their characterization using various Physico-Chemical methods is described below.

#### 3.3.2.1 Preparation of silylated catalysts

Before silylation, the zeolite was activated at 823 K for 6 hours. The zeolite was reacted with a mixture (2ml per gram of zeolite) of 20% TEOS + 35% MeOH + 45% Toluene in a round-bottom flask at 355 K. The reaction mixture was cooled after 12 hours of refluxing, dried at 383 K for 8 hours and calcined at 823 K for 4 hours to remove all the organics. The whole process was repeated second time depending on the required loading.

#### 3.3.2.2 Preparation of lanthanum exchanged catalyst

The silylated extrudates were exchanged with lanthanum using a solution of lanthanum nitrate in water. The mixture was refluxed at 353 K for about 12 hrs after which it was cooled to room temperature, filtered and washed with distilled water, oven dried at 383 K and calcined at 773 K.

#### 3.3.2.3 Preparation of extrudates of Al-MFI

For preparing Al-MFI extrudates, the zeolite and the binder were mixed and grinded in a mortar in required quantities till the mixture became homogenous, fine and smooth powder mixture. This powder was then mulled in to a paste with the help of 5% acetic acid in water and extrudated. The extrudates (1/16") were dried in air for 12 h, subsequently at 383 K for another 12 h and then calcined at 823 K to improve the extrudate crush strength.

#### 3.3.2.4 Evaluation of the catalytic activity

For the catalyst evaluation, a silica reactor was charged with 1.5 grams of catalyst and activated at 823 K in air for 5 hours. The catalyst was placed in the centre of the reactor in between two layers of porcelain beads, the first layer to act as preheater for keeping the reactants and products in vapor state. The reactants were fed accurately through a syringe pump (ISCO 500D). The products, after condensing through a cold water trap were collected in a gas-liquid separator. These product samples were analysed using gas chromatograph (HP 6890) equipped with FID and BP-1 capillary column 50m for EB alkylation. The toluene methylation products were analysed using GC (Shimadzu 15 A) equipped with FID and a 4 m long column packed with 5% Bentone + 5% DIDP on Chromosorb.

### 3.3.3 Catalyst characterisation

The zeolites were characterized using XRD, TPD of ammonia and FTIR of pyridine. For TPD studies, the catalyst was activated in helium flow for 2 hours at 823 K. The furnace was cooled to 353 K for the adsorption of ammonia. Ammonia (10% $NH_3$ in helium) flow (10ml/min) was maintained for 30 minutes and then the tube was flushed with helium for 1 hr. The temperature programmed desorption was carried out from 373 K to 973 K at a rate

of 10 K/min. For infrared spectra of chemisorbed pyridine, self supported thin wafers (5–6 mg $cm^2$) were prepared, evacuated ($10^{-5}$ Torr) at 673K for 12 h and cooled to 373 K. Subsequently, pyridine vapors were introduced into the cell and the sample was equilibrated for 30 min. The spectra were recorded after evacuation of the sample (for 2 h) at various desorption temperatures. All the spectra were recorded using a Nicolet 60 SXB spectrometer with 2 $cm^{-1}$ resolution, averaging over 500 scans.

### 3.4 Results and discussion

#### 3.4.1 Catalyst characterisation

**The results of the various characterization techniques like XRD, TPD of ammonia and FTIR of pyridine used for evaluating the physico-chemical properties of the catalysts are discussed in the following sections.**

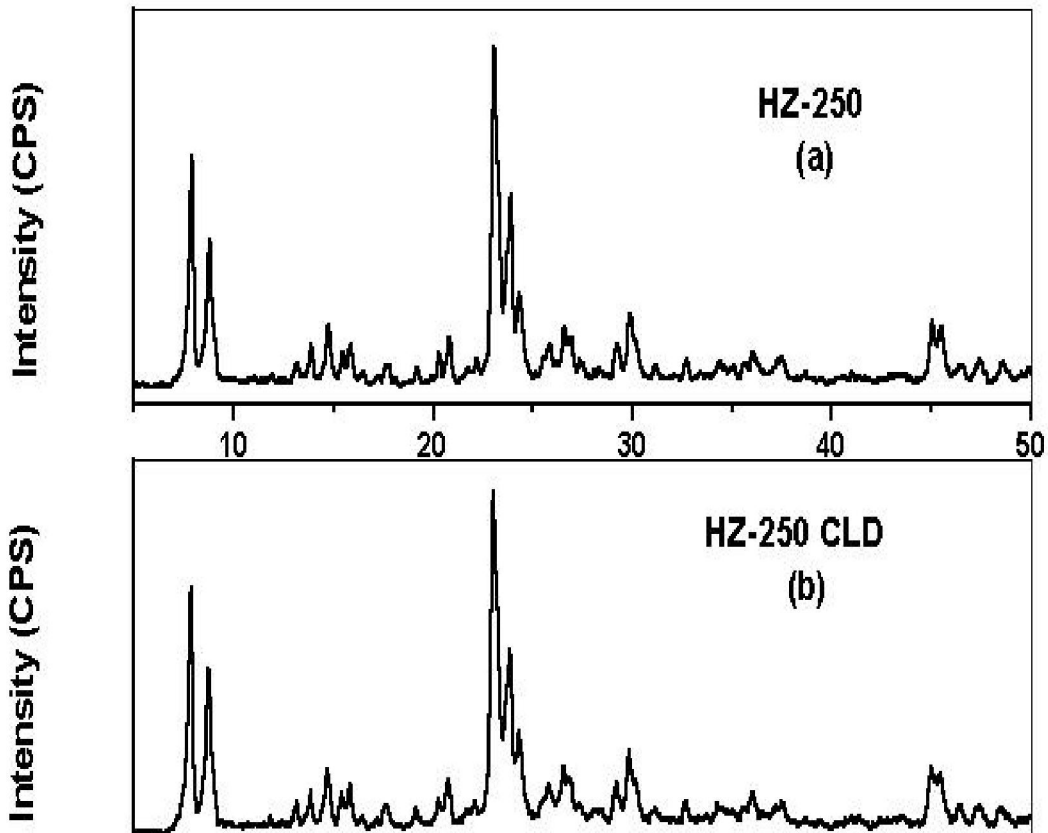

**Figure 3.1: Powder XRD of HZ-250 (a) before and (b) after silylation**

#### 3.4.1.1 X-ray diffraction

**There is no change in the XRD patterns (Fig. 3.1) of the catalyst obtained before and after silylation treatments. This shows that silylation does not cause any changes in the framework of the zeolite. Also, no changes in the relative intensities of the peaks were observed.**

#### 3.4.1.2 Temperature programmed desorption of ammonia

Though infrared spectroscopy of pyridine is an excellent technique for finding Bronsted and Lewis acid site concentrations for a given zeolite, it has certain drawbacks. The most important limitation is the accessibility of all acid sites to this bulky molecule. In addition,

it is difficult to obtain extinction coefficients for quantification. Kojima et al. (7) have observed that pyridine was unable to gain access to all the acid sites located in the pores. Ammonia has a definite advantage in this respect as it can reach all acid sites in the zeolite pores because of its smaller size. Temperature programmed desorption (TPD) of ammonia for various H-MFI zeolites is shown in Figure 3.2. Two desorption peaks were observed, the first, a low temperature (LT) peak and the second, a high temperature (HT) peak. It is clear from the figure that the total acidity of the zeolite decreases with the increase in $SiO_2/Al_2O_3$ ratio, as expected. The LT peak is assigned to interaction of ammonia with surface oxide or hydroxyl groups through non-specific hydrogen bonds (8). The high temperature peak is generally assigned to ammonia adsorbed at strong structural Bronsted and Lewis acid sites that are more important catalytically.

**Table 3.3 Acidity of the catalysts used for the reaction**

| Catalyst | $T_{max}$ (K) | Acidity (mmoles of $NH_3$ desorbed) | |
|---|---|---|---|
| | | weak | strong |
| HZ-40 | 473, 594 | 0.43 | 0.34 |
| HZ-100 | 471, 621 | 0.34 | 0.31 |
| HZ-250 | 459, 601 | 0.18 | 0.29 |
| HZ-250 CLD | 446, 582 | 0.12 | 0.19 |
| HZ-250 CLD-LE | 455, 577 | 0.14 | 0.11 |

The modification of HZ-250 sample by silylation (HZ-250 CLD) and thereafter exchange with lanthanum (HZ-250 CLD-LE) reflects noticeable changes which are depicted in Figure 3.2. There is a further decrease in the acidity of HZ-250 after silylation as seen from Table 3.3 because of the inactivation of the external surface acid sites. Again, further decrease in the acidity, particularly, the sites with higher strength were reduced after lanthanum exchange due to exchange of strong Bronsted acid sites by lanthanum.

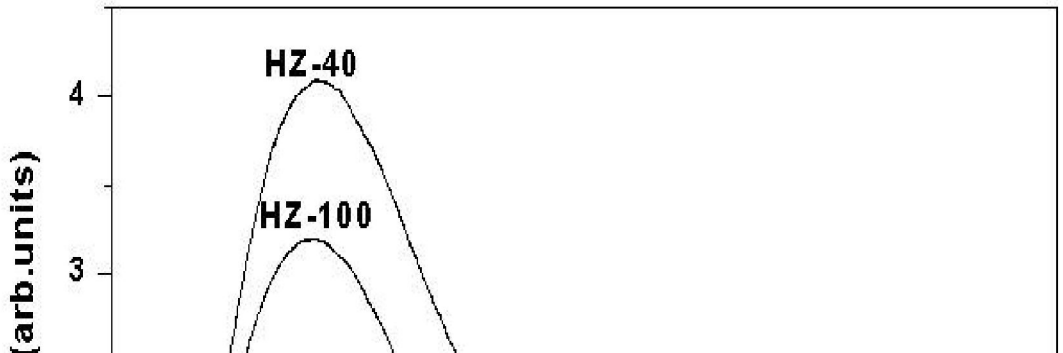

**Figure 3.2: TPD patterns of the catalyst samples**

### 3.4.1.3 FTIR of Pyridine

**Infrared spectroscopy is a powerful technique for studying acidity of zeolites. Infrared spectra of the hydroxyl region (Fig. 3.3 A) of H-MFI after evacuation at 673 K, showed three infrared bands at 3745 $cm^{-1}$, 3670- 3690 $cm^{-1}$ and 3600 $cm^{-1}$. The**

**3600 $cm^{-1}$ band may be assigned to bridging hydroxyl (Si-OH-Al) groups. This is the strongest Bronsted acid site in H-MFI zeolites and has been reported to increase in intensity with aluminium content of the zeolite (9). On the other hand, the 3745 $cm^{-1}$ band is due to the weakest Bronsted acidity assigned to terminal silanols, mostly located on the external surface (10, 12). The intensity of this hydroxyl band has been found to increase with dealumination (11). Jacobs and Ballmoos has attributed this band to poor quality of zeolite and identified it as arising from extra-zeolite material. However, studies of Guanlin Quin et al. (10) revealed that smaller the crystallite of H-MFI more intense was this band. Zeolites synthesized with TPA were found to have a very high**

**concentration of these groups (13), presumably due to the defects generated during the removal of the template (11). Based on these observations, this band may be delinked from the presence of amorphous material in our materials although amorphous silica gives this band. The 3670 $cm^{-1}$ band has been assigned to hydrated silanol groups. This band has not been always noticed by others. Vedrine et al. (9) noticed a shoulder at 3665 $cm^{-1}$, but they did not assign this band. Sayed et al. (12) while reporting this band at 3670 $cm^{-1}$, observed that this becomes weaker at higher activation temperatures and subsequently was overlapped by the 3730-3745 $cm^{-1}$ band. It virtually disappeared on subsequent evacuation at 873 K. We have observed that 3670**

**$cm^{-1}$ band is very broad and after many hours of evacuation decreases in intensity, when a part of water associated with this band is removed. It may be inferred from these observations that this band is due to silanol hydroxyls perturbed by water. The hydroxyl spectra of the silylated catalysts shows two bands, at 3740 $cm^{-1}$ and another centred around 3600 $cm^{-1}$ which is very broad. This is due to hydrogen bonded hydroxyl. The peak position of the later entirely depends upon the amount of hydrogen bonding. Shrinivasan (14) et al. have compared IR spectra of cabo-sil derived from $SiCl_4$, Degussa Aerosil972 obtained from dimethyl dichlorosilane, Stober silica obtained from TEOS and acid washed Davson952 silica gel. They reported that Cabosil and Stober silica**

**show isolated and hydrogen bonded hydroxyls, whereas Degussa and Stober silica only hydrogen bonded silanol groups. Overlayers of silica derived by liquid phase silylation of TEOS on HM-250 sample seems to be identical to that of silica obtained from TEOS.**

Infrared spectra of adsorbed pyridine and the effect of pyridine adsorption on the hydroxyl bands is helpful in characterizing acidity of zeolites. Figure 3.3 (B-F) shows the infrared spectra of the hydroxyl region and the pyridine ring vibration region after pyridine has been desorbed at various temperatures. It is known that the pyridinium ions associated with Bronsted acid sites show three additional vibration frequencies. Of these $N^{+}$-H stretching vibration is not seen due to broadness of the bands. The other two vibrations appear at 1545 and 1490 $cm^{-1}$. Coordinately bound pyridine exhibits infrared bands at 1450 and 1490 $cm^{-1}$.We have observed three bands due to chemisorbed pyridine at 1450 –1455 $cm^{-1}$, 1490 and 1545-1547 $cm^{-1}$ with the simultaneous disappearance of hydroxyl bands. The band near 1450 $cm^{-1}$ is due to pyridine at Lewis site and the one at 1545 $cm^{-1}$ is due to pyridine at Bronsted site. The variation in relative B/L ratio with increasing evacuation temperature is given in Table 3.4. For all $SiO_2/Al_2O_3$ratios, B/L ratio increased with the evacuation temperature. This shows that the intensity of the infrared band at 1450 $cm^{-1}$, associated with coordinately held pyridine decreases rapidly as the temperature is raised implying that Lewis acidity is not that strong when compared to Bronsted acidity on these zeolites. There is a decrease in the B/L ratio at 673 K for the HZ-40 sample. This is probably because for samples with low Si/Al ratio, there must be large concentration of Bronsted sites with moderate to strong acidity and pyridine sorbed at these sites can be dislodged easily at lower temperatures. If we compare the parent sample, HZ-250 and the

modified samples, the B/L ratio increases, on modified samples with modification at lower evacuation temperatures and then decreases with higher temperatures. This is because surface aluminium species are active centers for initial silylation and hence the deposited silica can easily bridge them back to the lattice (15). This is how reinsertion of extra lattice alumina takes place. The reaction conditions of the CLD are sufficiently favourable for such structure healing process. This seems to be a plausible explanation for increase in Bronsted acidity and decrease in Lewis acidity on silylation of the parent sample (HZ-250 CLD). However the Bronsted acid sites so formed are not so strong and hence the B/L ratio decreases after 673 K. Another reason could be that the $SiO_2$ deposition at the pore mouth leads to a reduced diffusion rate of pyridine on to the intracrystalline Bronsted acid sites of the zeolite (16). In case of the HZ-250 CLD-LE even though the TPD shows decrease in total acidity, the pyridine FTIR shows increase in Bronsted acidity. This may be due to the creation of new Bronsted acid sites by the coordination of water with the lanthanum ion (17). Lanthanum also may be responsible for Lewis acidity in case of HZ-250 CLD-LE for the decrease in the B/L ratio.

**Table 3.4 Bronsted to Lewis acidity (B/L) ratios of the catalysts used in this study**

| Temp (K) | B/L ratio | | | | |
|---|---|---|---|---|---|
| | **HZ-40** | **HZ-100** | **HZ-250** | **HZ-250 CLD** | **HZ-250 CLD-LE** |
| **373** | 0.54 | 0.43 | 0.45 | 0.48 | 0.60 |
| **473** | 0.76 | 0.93 | 0.64 | 1.01 | 0.95 |
| **573** | 0.81 | 1.30 | 0.94 | 0.92 | 0.94 |
| **673** | 0.70 | 1.49 | 1.35 | 0.58 | 0.58 |

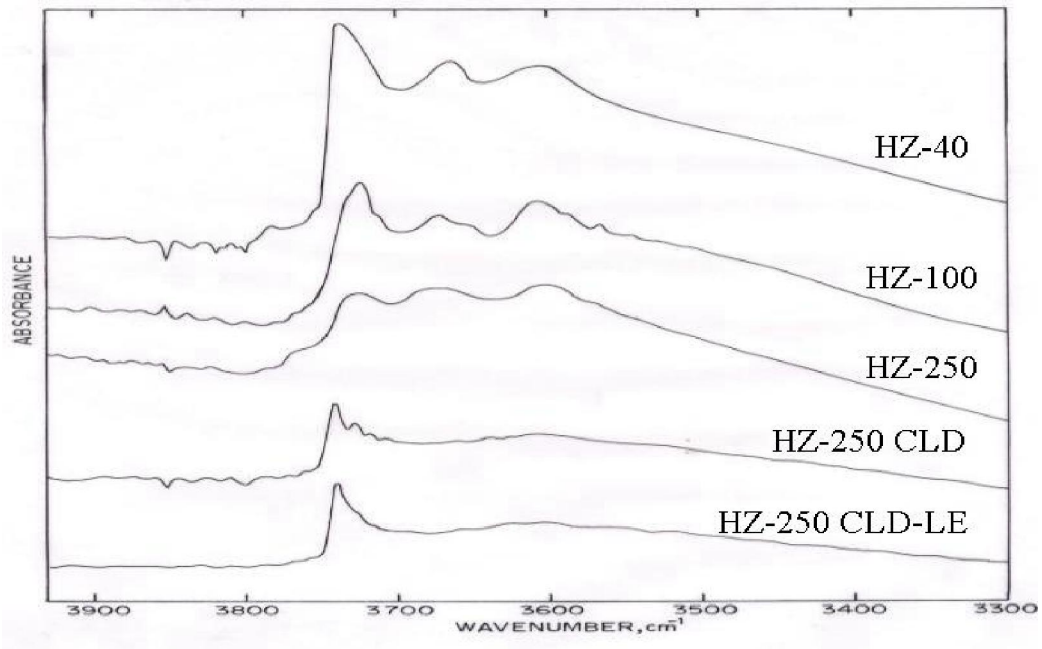


**A**

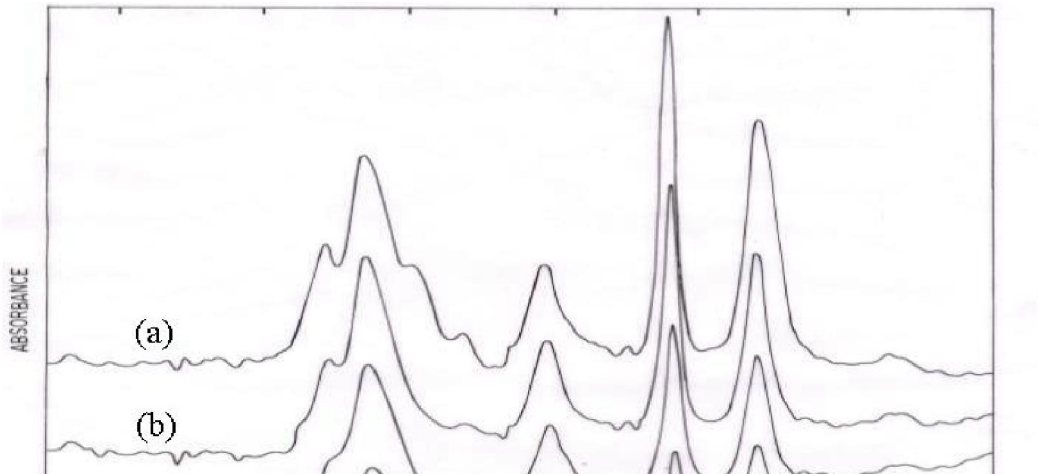

**Figure 3.3:**
(A) Hydroxyl spectra of the catalyst samples (B) Pyridine FT-IR spectra of HZ-40 after desorption (a) 373 K (b) 473 K (c) 573 K (d) 673 K

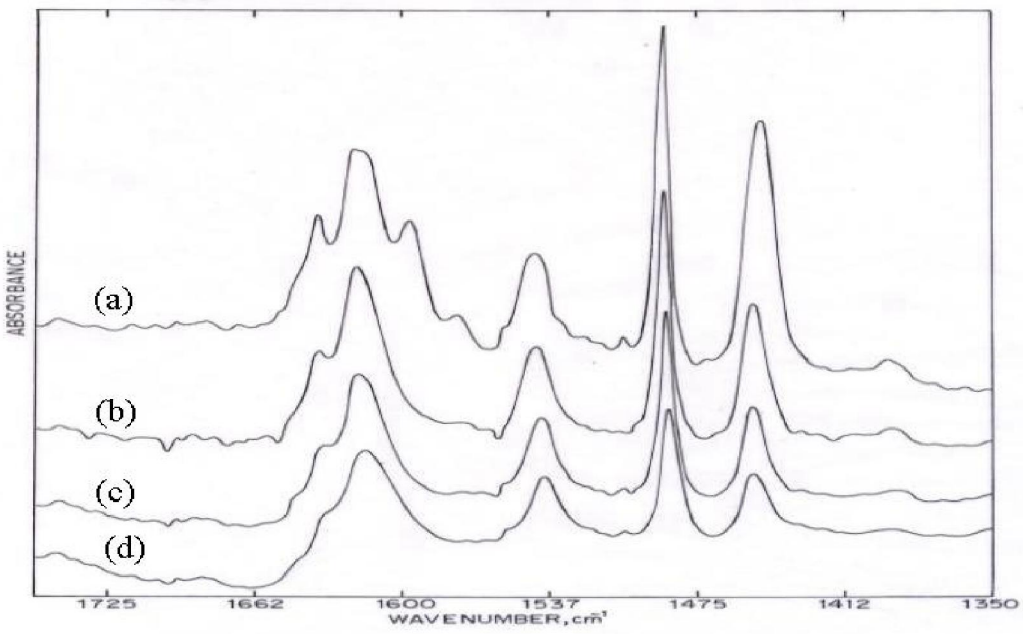


C

**Figure 3.3:**

(C) Pyridine FT-IR spectra of HZ-100 (a) 373 K (b) 473 K (c) 573 K (d) 673 K
(D) Pyridine FT-IR spectra of HZ-250 (a) 373 K (b) 473 K (c) 573 K (d) 673 K

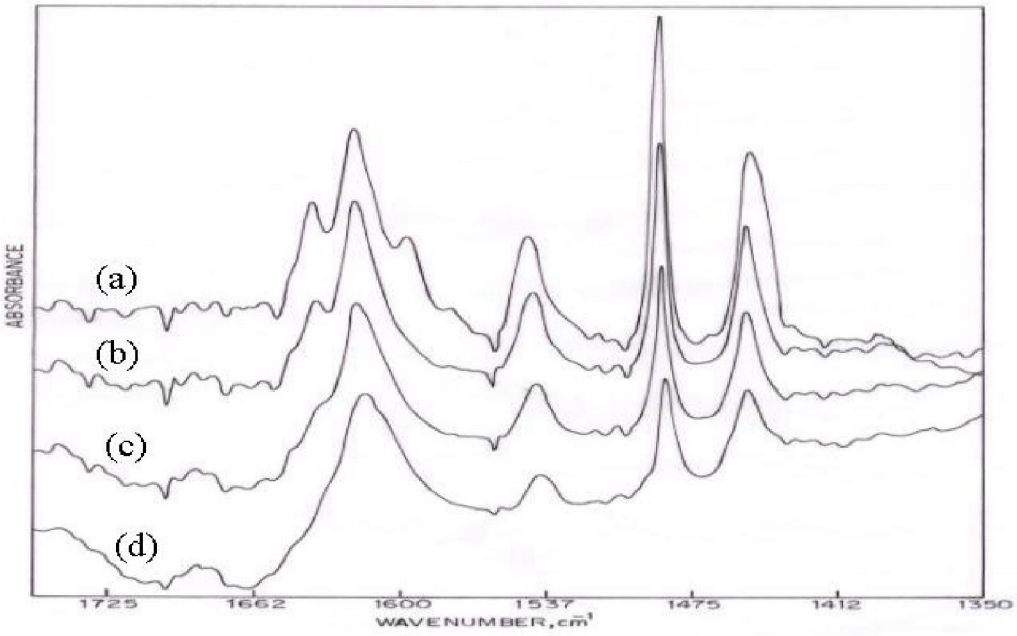


**E**

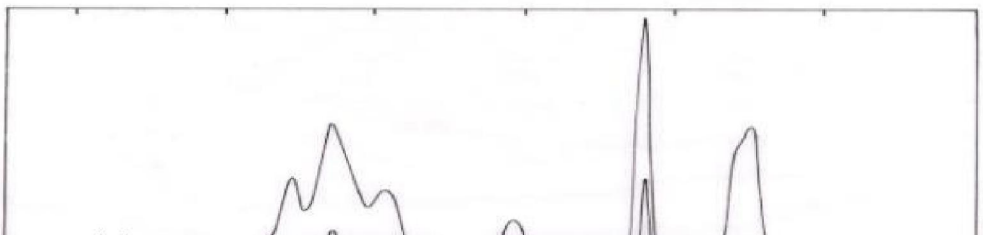

**Figure 3.3:**
(E) Pyridine FT-IR spectra of HZ-250 CLD (a) 373 K (b) 473 K (c) 573 K (d) 673 K
(F) Pyridine FT-IR spectra of HZ-250 CLD-LE (a) 373 K (b) 473 K (c) 573 K (d) 673 K

### 3.4.2 Evaluation of catalysts

The above described catalysts were tested for their activity in the EB ethylation using pure and mixed $C_8$ aromatic feeds (containing EB in high concentration) and also in the methylation of toluene.

#### 3.4.2.1 Preparation of p-DEB by alkylation

Preparation of p-DEB was carried out by direct alkylation of ethylbenzene with ethanol as an alkylating agent. The ethylation of ethylbenzene with ethanol is an electrophilic substitution reaction on the aromatic ring. It is activated at the ortho- and para- positions by the presence of ethyl group, by inductive and mesomeric effect. But rapid secondary isomerisation reactions usually generate mixtures of all three isomers. The meta isomer which is the major component among the other isomers is formed by isomerisation on external surface acid sites (non shape selective). The amount of meta-isomer formed through direct ethylation is negligible. For mechanistic reasons as mentioned, by far the

most important route is isomerisation. In addition to the pure EB feed, ethylation reaction has also been conducted on the $C_8$ aromatic cut, that is enriched in EB after removal of xylenes. This makes this feed useful for feeding into xylene isomerisation unit by reducing the concentration of EB, preventing its build up in the isomerisation loop. The $C_8$ aromatics consisting of ethylbenzene (EB) and various isomers of xylenes have very close boiling points, making their separation difficult through distillation. Since, the boiling point of o-xylene (OX) is slightly higher than other isomers, it is separated by distillation, while p-xylene (PX) is recovered by passing through an adsorption column. The remaining feed rich in meta-xylene (MX) and EB is sent through a catalytic isomeriser, to restore the equilibrium concentrations of the xylenes. During this process, EB is either dealkylated to benzene or isomerised to xylenes (18, 19). However, there are certain $C_8$ feeds, very rich in EB content (up to 80%), rest being xylenes. They cannot be fed to a xylene isomerisation unit due to the high concentration of EB and they do not find any other applications, except as fuel. In principle, it is possible to convert EB from this type of mix $C_8$ aromatic streams to some valulable high boiling products such as diethylbenzene (DEB), which can be separated easily. The only requirement for this type of process is that it should not lead to any loss of xylenes through dealkylation.

**Table 3.5 Effect of silica to alumina ratio on ethylation of EB**

| **Product (wt %)** | **Silica to Alumina ratio** | | |
|---|---|---|---|
| | **HZ-40** | **HZ-100** | **HZ-250** |
| **NA** | 1.8 | 1.3 | 0 |
| **Benzene** | 23.2 | 16.6 | 11.9 |
| **Toluene** | 7.0 | 3.6 | 2.0 |
| **EB** | 43.9 | 52.5 | 56.1 |
| **Xylenes** | 0.8 | 0.9 | 0.4 |
| **$C_9$ aromatics** | 5.5 | 3.5 | 2.4 |
| **p-DEB** | 4.5 | 6.6 | 9.8 |
| **m-DEB** | 10.9 | 12.9 | 16.4 |
| **o-DEB** | 0.3 | 0.2 | 0 |
| **HB** | 1.9 | 1.9 | 1.0 |
| **EB conv.** | 55.2 | 46.8 | 43.9 |
| **B/DEB (mole)** | 2.5 | 1.4 | 0.8 |

| | | | |
|---|---|---|---|
| **p-DEB Sel.** | 28.5 | 33.4 | 37.3 |
| **DEB Sel** | 29.2 | 42.8 | 59.7 |

Temp. 623 K, WHSV =2 $h^{-1}$, EB:Ethanol=4:1
particulate catalysts (100%)

### *Effect of silica/alumina ratio*

The silica: alumina ratio of the zeolite has a profound influence on the surface and catalytic properties. The effect of silica:alumina ratio on EB alkylation is presented in Table 3.5. It may be noted that at high silica:alumina ratio ethylbenzne conversion decreases as expected due to fewer number of acid sites that are associated with Al substitution in the framework. Conversion of ethylbenzene increases as the silca/alumina ratio decreases. One of the reason may be aluminium gradient in the crystal (the surface shows much higher aluminium content as compared to the bulk), the other reason may be the presence of octahedral species present. Both these favour different secondary reactions. It is known that dealkylation takes place on strong acid sites and hence benzene was produced in higher amounts on samples having high acid site density. Another indicator for determining the quality of a catalyst in this type of reactions is B/DEB ratio, which is very high for samples with low $SiO_2/Al_2O_3$ ratio. Also the amount of HBFs and $C_9$ aromatics decrease with decreasing acid site densities (acidity) of the catalyst. Alongwith decrease in the B/DEB ratio the DEB selectivity increases i.e. the alkylation selectivity increases. At higher silica to alumina ratio, p-DEB selectivity is enhanced as a result of the supression of the secondary isomerisation reactions.

**Table 3.6 Effect of the binder content on ethylation of EB**

| **Product (wt%)** | **Binder $Al_2O_3$ content (wt %)** | | | |
|---|---|---|---|---|
| | **0** | **30** | **50** | **75** |
| **NA** | 0 | 0.3 | 0 | 0 |
| **Benzene** | 11.9 | 8.6 | 7.3 | 5.1 |
| **Toluene** | 2.0 | 0.9 | 0.9 | 0.7 |
| **EB** | 56.1 | 64.3 | 69.6 | 75.6 |
| **Xylenes** | 0.4 | 0.4 | 0 | 0.3 |
| **$C_9$ aromatics** | 2.4 | 1.4 | 1.1 | 0.7 |

| | | | | |
|---|---|---|---|---|
| **p-DEB** | 9.8 | 9.5 | 9.1 | 8.7 |
| **m-DEB** | 16.4 | 13.2 | 11.1 | 8.3 |
| **o-DEB** | 0 | 0.2 | 0 | 0 |
| **HB** | 1.0 | 1.0 | 0.9 | 0.6 |
| **EB conv.** | 43.9 | 35.4 | 30.4 | 24.4 |
| **B/DEB (mole)** | 0.8 | 0.6 | 0.6 | 0.5 |
| **p-DEB Sel.** | 37.3 | 41.6 | 45.1 | 51.1 |
| **DEB Sel** | 59.8 | 64.9 | 66.4 | 70.1 |

Temp. 623 K, WHSV =$2h^{-1}$, EB:Ethanol=4:1, HZ-250

### *Effect of the binder content*

In the laboratory, only a few grams of zeolite is used for catalytic evaluation in granular form. In an industrial context, MFI has to be used in the form of extrudates of 1-5 mm in diameter or as tablets, to improve the crush strength and also to reduce the pressure drop across the reactor (20). The extrudates are formed by mixing the zeolite with inorganic binders such as alumina, silica or clay. It may be expected that extrusion would reduce the effectiveness factor and thus affect the catalyst activity. The increased diffusional path lengths due to binders may also influence selectivity (21). Hoelderich et al. (22) prepared a catalyst by extruding a mixture of 60% MFI zeolite and 40% binder consisting of boehmite, amorphous aluminium silicate and silica. They observed that aluminium oxide was unfavourable for methanol conversion since it catalyzed side reactions. An attempt to improve the activity of MFI by extruding with alumina has been reported (23). It has been shown that the activity of MFI with a Si/Al ratio of 1600 and above for n-hexane cracking, high pressure propene oligomerization and lube dewaxing was significantly enhanced when the catalyst was extruded with alumina. A comparison of the performance of MFI ($SiO_2/A1_2O_3$=250) extrudates containing different contents of binder (alumina) is shown in Table 3.6. The extrudates of alumina (not included in Table) showed only negligible catalytic activity for ethylation of ethylbenzene under the reaction conditions. With increase in zeolite content in the extrudate, ethylbenzene conversion increases due to the increased contact of the zeolite with the reactant. But the diethylbenzene selectivity is higher for samples with lower zeolite content.

**Table 3.7 Comparison of silylated extrudates and particulate catalysts**

| Product wt% | HZ-250 catalyst | |
|---|---|---|
| | Granules | Extrudates |
| **NA** | 0 | 0.5 |
| **Benzene** | 6.9 | 6.6 |
| **Toluene** | 1.4 | 0.8 |
| **EB** | 71.3 | 71.6 |
| **Xylenes** | 0.4 | 0.3 |
| **$C_9$ aromatics** | 1.1 | 1.2 |
| **p-DEB** | 17.7 | 14.4 |
| **m-DEB** | 0.5 | 3.7 |
| **o-DEB** | 0 | 0 |
| **HB** | 0.5 | 0.8 |
| **EB conv.** | 28.7 | 27.9 |
| **B/DEB** | 0.7 | 0.6 |
| **p-DEB Sel.** | 96.9 | 79.5 |
| **DEB Sel** | 63.8 | 65.0 |

Temp. 623 K, WHSV =$2h^{-1}$

EB:Ethanol=4:1

***Influence of physical form of zeolite used for silylation***

**It is seen that silica deposited on the pure granulated zeolite gives higher p-DEB selectivity than that for the extrudates under similar reaction conditions. Probably, silica deposition is taking place uniformly on granulated zeolite, whereas diffusion affects may**

**be hindering uniform deposition on extrudates. As in the case of the pure zeolite, ethylbenzene conversion was lower on the silylated zeolite. Preliminary experiments were conducted to investigate the concentration of TEOS required for optimum loading of silica through CLD technique. It was found that 20-25 wt% of TEOS gives optimum loading. Similarly, we have loaded silica on pure zeolite granules as well as on 70 % extrudates. The performance of these catalysts with the same amount of silica deposition is given in Table 3.7.**

***Ethylation of EB and mixed $C_8$ aromatic feeds on extruded catalysts: Influence of $SiO_2/Al_2O_3$ ratio***

We have also investigated the effect of silica/alumina ratio on ethylation of EB and $C_8$ mixed feed using 70% zeolite containing extrudates (Tables 3.8 and 3.9). As was the case with 100% zeolite, ethylbenzene conversion increased, para-diethylbenzene selectivity decreased for samples having low silica/alumina ratios. The trend for EB conversion in case of mixed feeds is the same as that for pure EB feed. In this case there is a loss of xylenes on catalyst samples with lower silica to alumina ratio. This may be due to the

dealkylation of xylenes that gives toluene. Followed by this, ethylation of toluene may take place to give ethyl toluenes. In case of mixed feeds, the concentration of $C_9$ aromatics is higher particularly on catalyst with low silica/alumina ratio. There is an increase in the DEB selectivity with increase in the silica to alumina ratio for both the feeds. But the p-DEB selectivity is slightly better in case of mixed feed, whereas DEB yields are low due to the presence of xylenes in the mixed feed.

**Table 3.8 Effect of silica to alumina ratio on pure EB ethylation**

| **Product (wt) %** | **Silica to alumina ratio** | | |
|---|---|---|---|
| | **HZ-40** | **HZ-100** | **HZ-250** |
| **NA** | 2.2 | 1.6 | 0.1 |
| **Benzene** | 16.3 | 12.2 | 7.4 |
| **Toluene** | 2.6 | 2.6 | 0.3 |
| **EB** | 56.9 | 58.3 | 67.9 |
| **Xylenes** | 0.6 | 0.7 | 0.2 |
| **$C_9$ aromatics** | 2.4 | 1.8 | 0.5 |
| **p-DEB** | 5.6 | 6.4 | 9.3 |
| **m-DEB** | 11.6 | 13.9 | 13.6 |
| **o-DEB** | 0.7 | 0.6 | 0.2 |
| **HB** | 1.2 | 1.8 | 0.5 |
| **EB conv.** | 41.9 | 40.7 | 32.1 |
| **B/DEB (moles)** | 1.6 | 1.0 | 0.6 |
| **p-DEB Sel.** | 31.5 | 30.7 | 40.2 |
| **DEB Sel** | 43.8 | 52.3 | 72.2 |

Temp. 623 K, WHSV =3$h^{-1}$, EB:Ethanol=5:1, Extrudates

**Table 3.9 Effect of silica to alumina ratio on mixed $C_8$ aromatics ethylation**

| **Product (wt%)** | **Silica to Alumina ratio** | | |
|---|---|---|---|
| | **HZ-40** | **HZ-100** | **HZ-250** |

| | | | |
|---|---|---|---|
| **NA** | 0.9 | 0.8 | 0.2 |
| **Benzene** | 10.0 | 8.8 | 5.0 |
| **Toluene** | 4.5 | 2.9 | 1.1 |
| **EB** | 38.3 | 37.6 | 44.7 |
| **Xylenes** | 29.7 | 30.7 | 32.2 |
| **$C_9$ aromatics** | 3.6 | 2.9 | 1.1 |
| **p-DEB** | 3.3 | 4.6 | 5.9 |
| **m-DEB** | 6.1 | 8.7 | 8.4 |
| **o-DEB** | 0.3 | 0.2 | 0.1 |
| **HB** | 3.1 | 2.5 | 1.3 |
| **EB conv.** | 44.7 | 45.0 | 33.8 |
| **B/DEB** | 1.8 | 1.1 | 0.6 |
| **p-DEB Sel.** | 34.1 | 34.2 | 41.1 |
| **DEB Sel** | 31.5 | 44.1 | 62.8 |

Temp. 623 K, WHSV=3$h^{-1}$, EB:Ethanol=5:1, extruded catalysts, Feed content (65 % EB + 35 % Xylenes)

***Ethylation on silylated and La exchanged HZ-250 zeolite***

Tables 3.10 and 3.11 shows the comparison of HZ-250, HZ-250 CLD (twice silylated), and HZ-250 CLD-LE (twice silylated-La exchanged) for ethylation using pure and mixed $C_8$ feeds. For both the feeds the results show that there is increase in p-DEB selectivity as a result of lanthanum exchange, while there is a drop in EB conversion on CLD-LE catalysts. The TPD of the CLD-LE catalyst also shows decrease in the amount of strong acid sites. In case of mixed feeds, the p-DEB selectivity is marginally higher than that in case of pure EB, probably because of the dilution effect of xylenes. Benzene content in the product decreases on silylated as well as lanthanum exchanged samples. However, the $C_9$ aromatics and toluene contents are higher on silylated and silylated-La exchanged catalysts.

## Table 3.10 Effect of silylation and lanthanum exchange on the pure EB ethylation

| **Product (wt %)** | **HZ-250** | **HZ-250 CLD** | **HZ-250 CLD-LE** |
|---|---|---|---|

| | | | |
|---|---|---|---|
| **NA** | 0.1 | 0.4 | 0.6 |
| **Benzene** | 7.4 | 6.7 | 6.3 |
| **Toluene** | 0.3 | 0.5 | 0.7 |
| **EB** | 67.9 | 73.3 | 73.6 |
| **Xylenes** | 0.2 | 0.3 | 0.3 |
| **$C_9$ aromatics** | 0.5 | 0.8 | 0.9 |
| **p-DEB** | 9.3 | 14.7 | 15.4 |
| **m-DEB** | 13.6 | 2.6 | 1.8 |
| **o-DEB** | 0.2 | 0.1 | 0 |
| **HB** | 0.5 | 0.7 | 0.4 |
| **EB conv.** | 32.1 | 26.4 | 25.9 |
| **B/DEB** | 0.6 | 0.7 | 0.6 |
| **p-DEB Sel.** | 40.2 | 84.5 | 89.4 |
| **DEB Sel** | 72.2 | 65.9 | 66.9 |

Temp. 623 K, WHSV=3$h^{-1}$, EB:Ethanol=5:1, extruded catalysts

**Table 3.11 Effect of silylation and lanthanum exchange on mixed $C_8$ feed ethylation**

| **Product (wt%)** | **HZ-250** | **HZ-250 CLD** | **HZ-250 CLD-LE** |
|---|---|---|---|
| **NA** | 0.2 | 0.4 | 0.3 |
| **Benzene** | 5.4 | 4.1 | 3.0 |
| **Toluene** | 1.1 | 1.4 | 1.7 |
| **EB** | 45.3 | 49.1 | 51.7 |
| **Xylenes** | 32.4 | 33.0 | 34.7 |
| **$C_9$ aromatics** | 0.9 | 1.3 | 1.2 |
| **p-DEB** | 5.5 | 8.8 | 6.5 |
| **m-DEB** | 7.9 | 1.5 | 0.6 |
| **o-DEB** | 0.1 | 0 | 0 |
| **HB** | 1.2 | 0.5 | 0.3 |
| **EB conv.** | 32.8 | 26.3 | 20.5 |
| **B/DEB** | 0.7 | 0.7 | 0.7 |
| **p-DEB Sel.** | 40.8 | 85.1 | 91.6 |

| | | | |
|---|---|---|---|
| **DEB Sel** | 60.8 | 58.8 | 53.1 |

Temp. 623 K, WHSV=3h$^{-1}$, EB:Ethanol=5:1, Extruded catalysts, Feed content (65 % EB + 35 % Xylenes)

### *Effect of temperature on the ethylation of pure EB and EB from mixed $C_8$ feed*

In case of pure EB ethylation (Figure 3.4) the activity is low at lower temperature. As the temperature is increased the EB conversion increased with a simultaneous increase in other side products. Higher reaction temperatures led to dealkylation of ethylbenzene to benzene and ethylene. As a result, B/DEB ratio increased and ethylation selectivity dropped considerably. In case of mixed feed EB ethylation, (Figure 3.5) too, the ethylbenzene conversion increases monotonously with increasing reaction temperature. The concentration of by products like benzene, toluene and $C_9$ aromatics also increase along with temperature. B/DEB ratio which is an indication of the dealkylation activity increases with temperature on these catalysts. However, the DEB selectivity was always high when pure EB feeds are used. Since, mixed $C_8$ feed contains only 65% of EB, the yield of DEB isomers as well as p-DEB contents were low when mixed $C_8$ feeds are used for alkylation.

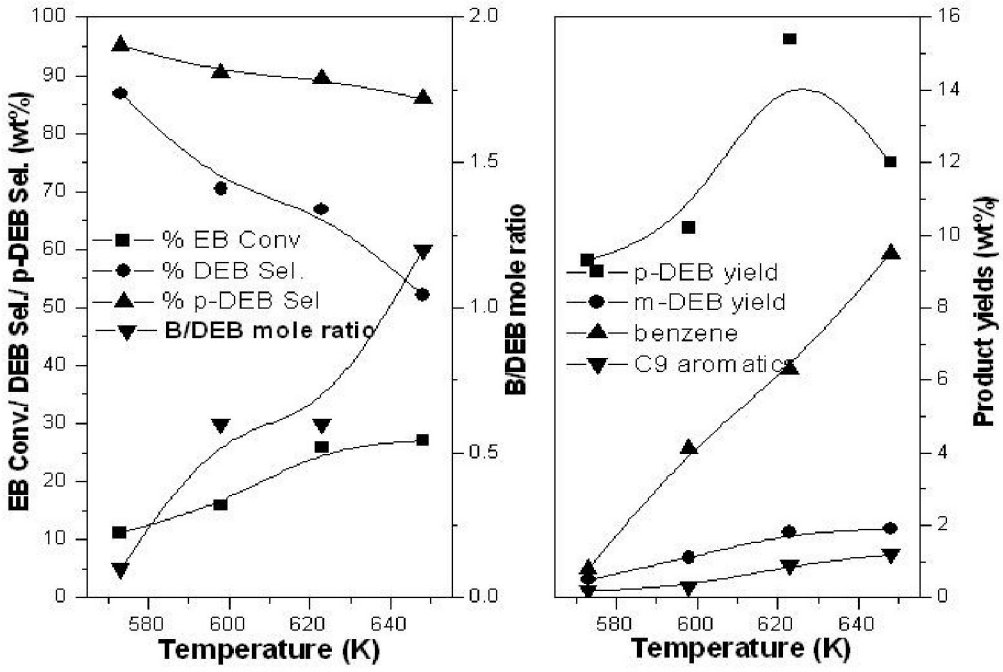

**Figure 3.4: Effect of temperature on pure EB ethylation**

WHSV=3h$^{-1}$, EB:Ethanol=5:1, Catalyst: HZ-250 CLD-LE

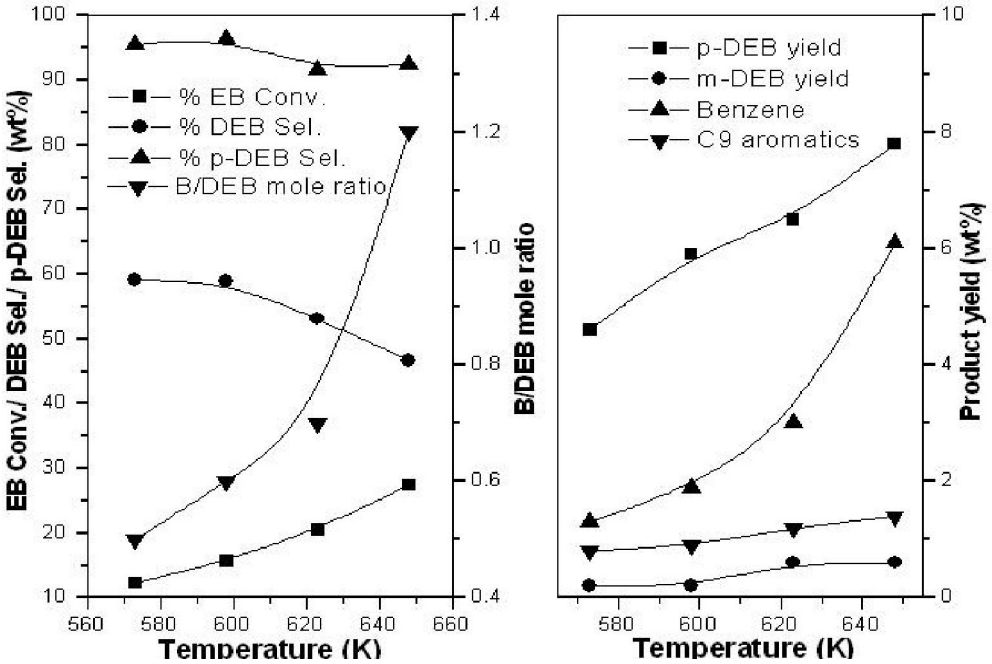


**Figure 3.5: Effect of temperature on ethylation of mixed C8 aromatics**

WHSV=3h$^{-1}$, EB:Ethanol=5:1, Catalyst: HZ-250 CLD-LE

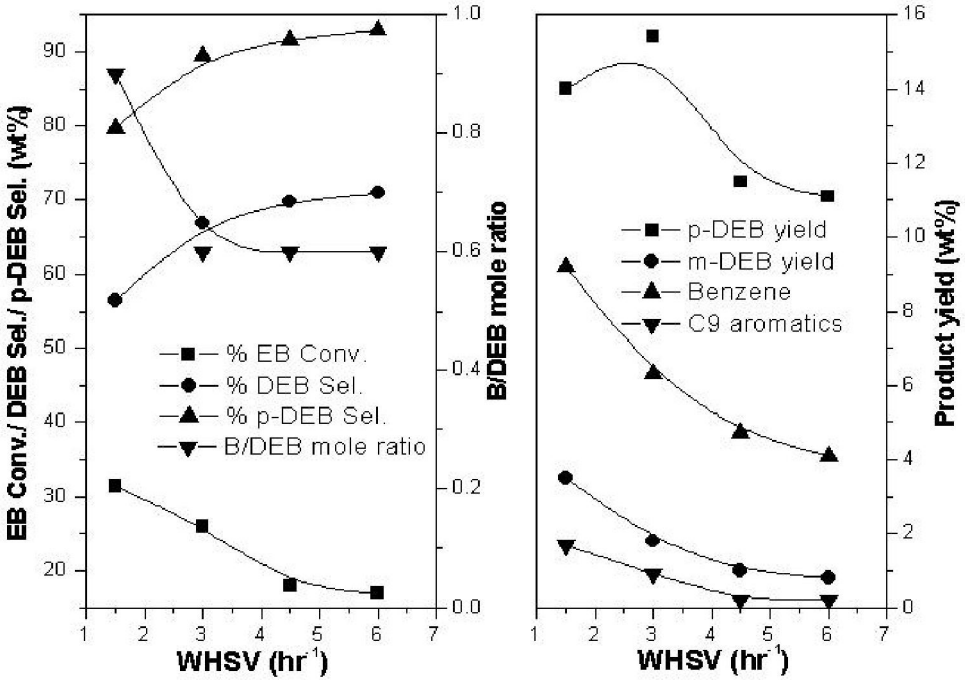

**Figure 3.6: Effect of space velocity on pure EB ethylation**

Temp 623 K, EB:Ethanol=5:1, Catalyst: HZ-250 CLD-LE

### *Effect of space velocity on pure EB and mixed $C_8$ feed ethylation*

Space velocity has a profound effect on EB conversion as well as on various selectivities. For pure EB ethylation (Fig. 3.6), the conversion decreased with increasing space velocity. However, this led to increase in para selactivity. This confirms that p-DEB is a primary product. At high space velocities, the secondary isomerization and dealkylation are suppressed and hence there is a drop in unwanted byproducts. At lower space velocities, diethylbenzene formation is higher as result of better contact time, but it also led to higher dealkylation activity. In case of mixed $C_8$ aromatics ethylation (Fig. 3.7), there is a continuous decrease in EB conversion with increasing space velocity. Better p-DEB selectivities could be achieved with increasing space velocity when mixed $C_8$ feed was used. At high space velocity, isomerization and the dealkylation reactions are supressed which gives a much cleaner product with lower concentration of by products. Though the p-DEB content was low with mixed $C_8$ feed, it was more steady even at higher space velocities. Surprisingly, the yield of $C_9$ products was relatively low when $C_8$ mixed feed is used, though one would expect it to be higher as a result of transalkylation reaction. However the narrow pores of MFI do not facilitate transalkylation among the $C_8$ isomers. These studies show that higher space velocities yield better results except for lower EB conversion.

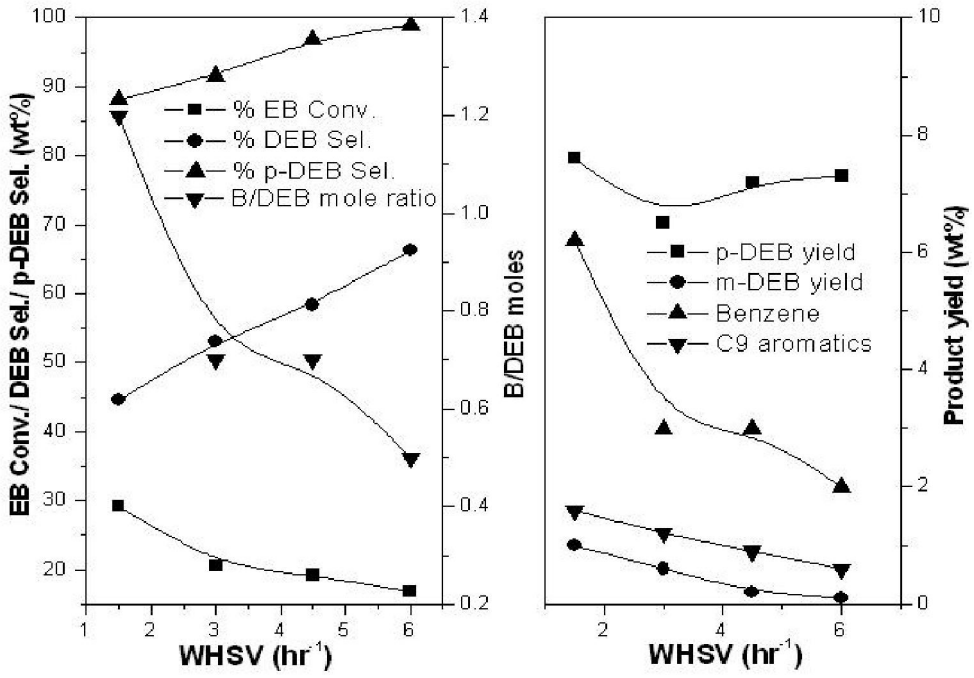

**Figure 3.7: Effect of space velocity on ethylation of mixed $C_8$ aromatics feed**

Temp 623 K, EB:Ethanol=5:1, Catalyst: HZ-250 CLD-LE

### *Effect of EB/EtOH mole ratio on ethylation of EB and mixed $C_8$ aromatics*

The effect of EB/EtOH mole ratio on ethylation of pure EB and EB from mixed $C_8$ is shown in Figures 3.8 and 3.9. For pure EB alkylation at low mole ratios of EB/EtOH, ethylbenzene conversion is higher because of the availability of alkylating agent in high proportion. The concentration of byproducts like xylenes, $C_9$ aromatics and high boilers is low when feed is rich in EB (high mole ratio). The differences in the product pattern have been observed only till EB to ethanol molar ratio of 5-6. Beyond that, the conversion reaches a steady state value. There is not much change in the p-DEB selectivity with variation in the EB/EtOH molar ratio. However, some drop in the DEB selectivity was observed when EB/EtOH molar ratio increases from 2.5 to 10. In case of mixed feeds, the EB conversion follows a similar trend as with pure EB, though the fall in EB conversion was more pronounced. The p-DEB selectivity during mixed $C_8$ aromatics alkylation was marginally higher than that obtained during pure EB alkylation. However, fall in the DEB selectivity was much higher with mixed $C_8$ aromatics feed compared to pure EB. The B/DEB ratio though initially increases during ethylation of pure EB, it remains a steady with further increase in EB/EtOH ratio. Whereas, during ethylation of mixed $C_8$ aromatics, the B/DEB steadily increases with higher EB content in the feed.

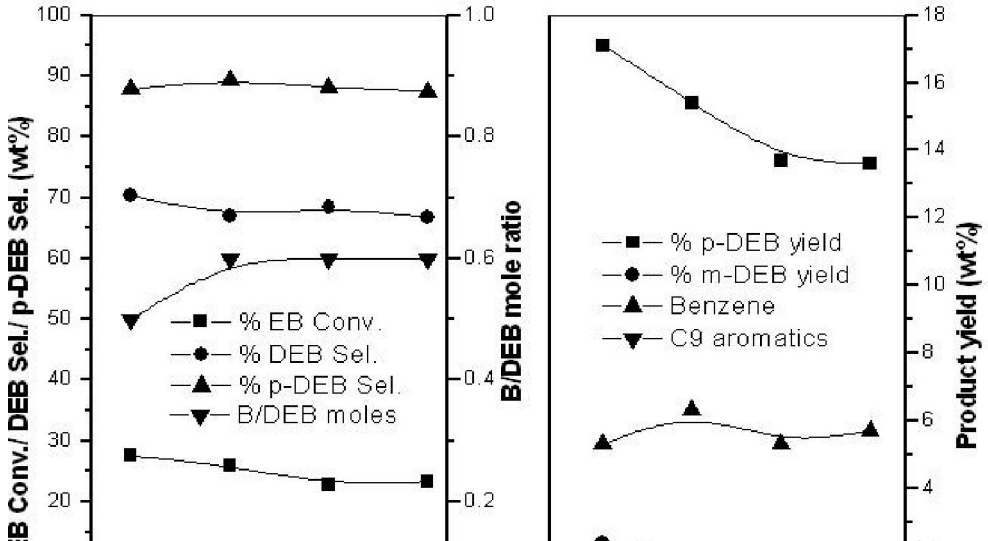

**Figure 3.8: Effect of EB/EtOH mole ratio on ethylation of pure EB**
Temp 623 K, WHSV=3$h^{-1}$, Catalyst:HZ-250 CLD-LE

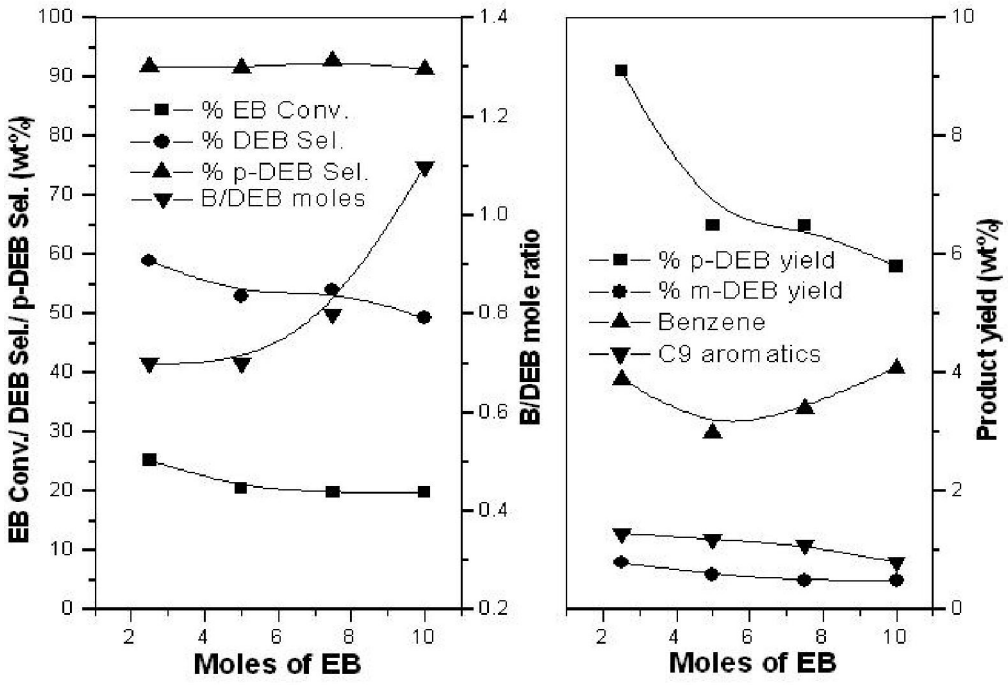

**Figure 3.9: Effect of EB/EtOH mole ratio on mixed $C_8$ feed ethylation**

Temp 623 K, WHSV=$3h^{-1}$, Catalyst: HZ-250 CLD-LE

### *Effect of EB content in the ethylation of mixed $C_8$ feed*

Bhat et al. (24) have performed ethylbenzene alkylation with ethanol in the presence of other aromatics particularly individual isomers of xylenes, 1,3,5-trimethylbenzene, p-DEB etc. They have concluded that the presence of products in recycled ethylbenzene has varied influence depending on their kinetic diameters. Bulky molecules like 1,3,5 trimethyl benzene and meta-xylene, which cannot diffuse inside the pores of modified MFI zeolite mainly act as a diluent. Molecules like benzene and toluene which have a kinetic diameter nearly the same as ethylbenzene cause hindrance inside the pore and also get alkylated resulting in decreased yield of desired product. para-Xylene and para-diethylbenzene create more hindrance than benzene or toluene inside the pore and cannot participate in the alkylation due to the constraint of space. In our case also we have used the $C_8$ aromatic cut for the alkylation reaction. The feed consisted of mainly equilibrium composition of xylenes, in addition to EB. The ethylation was performed using feeds consisting of various concentrations of xylenes in ethylbenzene.

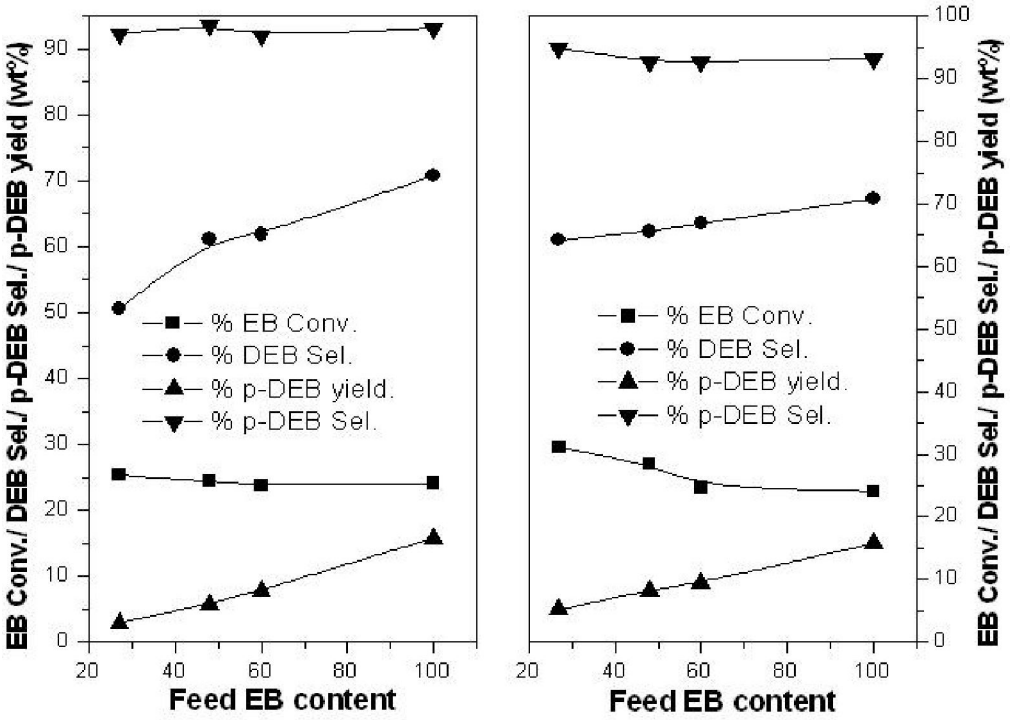

**A** **B**

**Figure 3.10 Effect of EB content in the ethylation of mixed $C_8$ feed**

Temp 623 K, WHSV=2$h^{-1}$, EB/EtOH=4:1 (A), $C_8$ / EtOH = 4:1(B),

Catalyst: HZ-250 CLD-LE

The results are shown in Figures 3.10. Two cases were considered one in which the EB/EtOH mole ratio was 4 and the other in which aromatics/EtOH mole ratio was 4. In the first case with increase in the EB concentration there is an increase in the yield of DEB's as one would expect. There is not much variation in EB conversion and p-DEB selectivity with change of composition. In the second case when the aromatics to ethanol ratio was maintained at 4 the conversion of ethylbenzene as well as the p-DEB yield were more than that in the first case because the amount of ethanol available for EB alkylation was more. Dimethyl ethylbenzenes are not found in the product, as even if they are formed inside the zeolite channels, cannot diffuse through the narrow pores, particularly after silylation.

### 3.4.2.2 p-DEB preparation by EB Disproportionation-Introduction

**The disproportionation of ethylbenzene was introduced as a test reaction by Karge et al. to characterize the Bronsted acidity of large pore zeolites, e.g., mordenites (25) and faujasites (26). After sufficiently long time on stream, the rate of this acid catalysed reaction is virtually constant and can**

**be correlated with the number of strong Bronsted acid sites. Interestingly, before this (quasi-) stationary stage is reached, the reaction shows an induction period, i.e., the rate increases with time-on-stream. Whereas this phenomena has been repeatedly observed with large pore zeolites (24-27), it has never been observed with medium pore molecular sieve catalysts, such as H-MFI and H-MEL (27, 28). In addition, the medium pore zeolites exhibit considerably lower transalkylation activity. These differences between medium and large pore zeolites can be rationalized if one assumes that transalkylation in large pore materials proceeds via a Streitwieser-Rief-type mechanism (29) involving diaryl ethane-type intermediates, whereas in medium pore**

**zeolites, the formation of these relatively bulky intermediates is hindered due to steric constraints. Hence, the reaction takes place through another transalkylation mechanism, viz. dealkylation / realkylation, which requires higher reaction temperatures (30).**

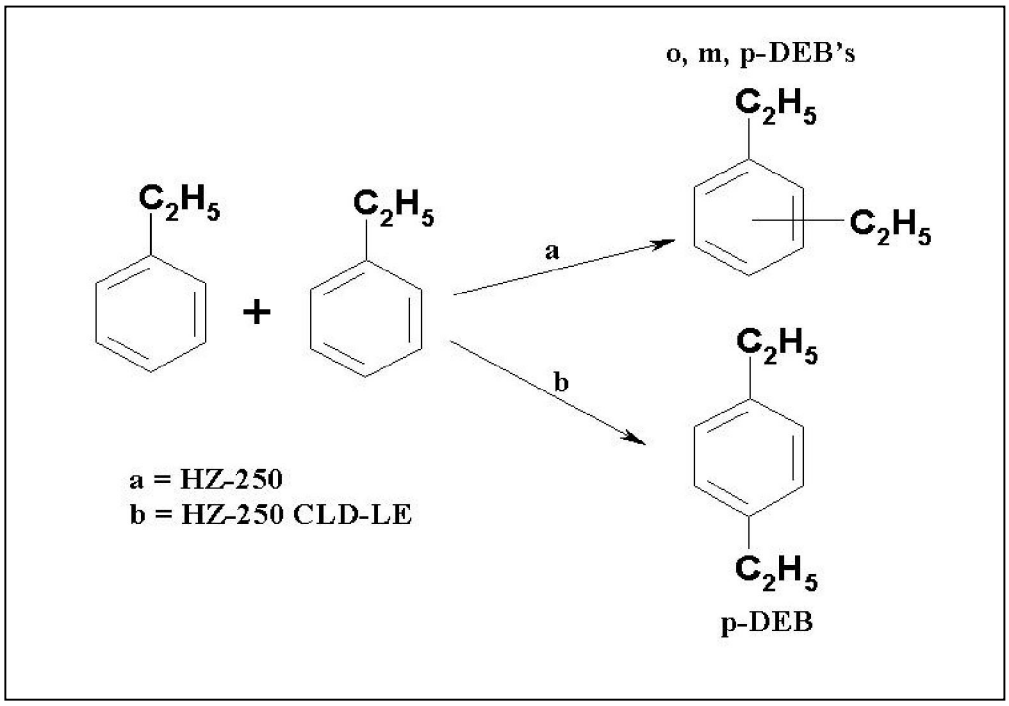


**Figure 3.11: Scheme for EB disproportionation on parent and modified catalysts**

The conversion of ethylbenzene over MFI zeolite takes place mainly by dealkylation and realkylation (31). Amelse (32) has reported that biphenyl-alkane intermediate cannot form within the pores of MFI zeolite and that the disproportionation occurs by dealkylation and realkylation. This has been confirmed by an isotope tracer technique. Tsai et.al. (33) have studied disproportionation of n-propylbenzene as a method to explore the relationship

between intrinsic reaction mechanism and internal pore systems of zeolites. They concluded that with MFI zeolites, disproportionation reaction proceeds through a monomolecular $S_N1$ mechanism (dealkylation/realkylation). Hence disproportionation of ethylbenzene is also expected to take place via dealkylation/realkylation over MFI zeolites.

p-DEB is important as it finds application in the recovery of p-xylene from a $C_8$-raffinate mixture by the adsorption process. Apart from the pure EB ethylation process, the selective disproportionation of ethylbenzene in the presence of xylenes is an important process for the purification of xylenes (1). For EB dispropotionation variety of zeolite catalysts, such as MFI, mordenite, faujasite and zeolite beta, etc. have been studied (34, 35). Compared to other monoalkylbenzene processes, EB disproportionation has a much more stable activity (36). Most catalysts show acceptable stability in EB disproportionation. The products obtained in the disproportionation reaction normally give the thermodynamic equilibrium composition that requires energy intensive separation process for p-DEB recovery. Thus, the technical challenge in producing p-DEB by EB disproportionation is development of a process to enhance para selectivity. In line with the developments in para selective processes, described earlier, many of the previous approaches are applied for p-DEB process development. Wang et al. (36, 37, 38) applied an in situ surface silylation by chemical vapor deposition (CVD) method to modify ZSM-5, by which they were able to obtain p-DEB with product selectivity up to 99% directly from EB disproportionation. They used orthosilicate mixture as the modification agent; typical composition of the selectivation mixtures was 45% methanol, 50% EB and 5% TEOS. Selectivation procedure was conducted at various temperatures until orthosilicate breakthrough was observed. The authors disclosed that orthosilicate first adsorbed on the external sites of the zeolite and then hydrolyzed into silica on the substrate. The hydrolysis temperatures vary with the type of substrate, as shown in Table 3.12. For example, ZSM-5 requires a lower hydrolysis temperature, ca. < 453 K, compared to the other substrates which are less acidic (for example, kieselghur). The authors also concluded that, among the various types of orthosilicates investigated, silylation by tetraethyl-orthosilicate (TEOS) yielded the best p-DEB selectivity. Moreover, the crystallite size of the zeolite and the extent of $SiO_2$ deposition are also found to play an important role on selectivation

performance. For a sample containing large crystallites of 10 mm, only 1.1 wt% of silica deposition is required to achieve p-DEB with 99.4% purity and the composition so-produced maintained 80% of initial activity. In contrast, for crystallite size of 1 mm, a silica content of 6.4 wt% is required to achieve the same p-DEB selectivity and the

**Table 3.12 Temperature requirement of Si-CVD deposition for various substrates**

| Substrates | Deposition Temp (K) |
|---|---|
| H-ZSM-5 | < 453 |
| $SiO_2$-$Al_2O_3$ | < 453 |
| $Al_2O_3$ | ~ 503 |
| Kieselguhr | > 593 |

composition retains initial activity down to 30%. Zeolite catalysts with larger crystallite size therefore require a small amount of deposited $SiO_2$ to achieve high p-DEB selectivity and more importantly, to retain a better activity. These observations are consistent with results of p-xylene selectivity in toluene disproportionation reported by Haag and Olson (31). The above p-DEB selectivation process using modified ZSM-5 by Si-CVD surface silylation method was successfully commercialized by Taiwan styrene monomer company (TSMC) in 1988. The commercial plant that produced p-DEB with 96% purity began its operation in 1990 with an annual production capacity of ca. 4000 tons/year. A schematic flow diagram of the process is depicted in Fig. 3.12. Recently, TSMC further upgraded their p-DEB production purity to 99%; representative analysis of the two commercial grade products is shown in Table 3.13. The TSMC process has a cycle length of over six months and its catalyst is fully regenerable. The para selectivity of various alkylbenzenes over modified catalysts by Si-CVD deposition has also been investigated by Wang et al. (39). Based on the results, it was found that the para selectivities are the same for p-DEB products obtained from either disproportionation or ethylation of EB, However, the observed p-xylene selectivity by methylation (ca. 70%) is much higher than that of toluene disproportionation (ca. 55%). Thus, the demand for modification to achieve same para selectivity enhancement for alkylbenzenes follows the trend: p-xylene > p-DEB > p-ET. Kaeding et al. (40) reported that MgO can enhance p-DEB selectivity up to 99.9% simultaneously suppressing formation of other heavy aromatics, such as ET, in the ethylation of EB.

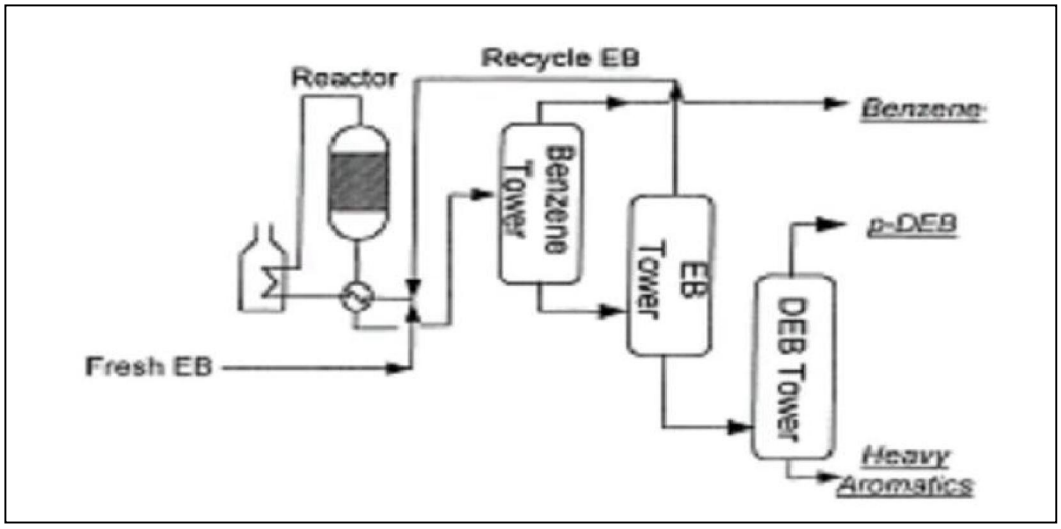


**Figure 3.12: Schematic of the Taiwan Styrene Monomer EB disproportionation plant**

**Table 3.13 Representative properties of p-DEB products by Taiwan Styrene Monomer**

| **Trade name** | **TSD-980** | **TSD-990** |
|---|---|---|
| Purity (wt %) | 98.4 | 99.1 |
| $C_9$ aromatics and lighter (wt%) | 0.07 | 0.05 |
| Other $C_{10}$ aromatics (wt%) | 1.17 | 0.75 |
| $C_{11}$ aromatics (wt%) | 0.40 | 0.10 |
| Total S (wppm) | Nil | Nil |
| Total nitrogen (wppm) | 0.35 | 0.22 |
| Total chloride (wppm) | Nil | Nil |
| Carbonyl number (mg/l) | 1.5 | 0.14 |
| Bromine index (mg/100 g) | 0.89 | 0.56 |
| Color, APHA | 5 | 3 |
| Specific gravity (g/cc at 4 $^{O}$C) | 0.863 | 0.863 |

### 3.4.2.2 p-DEB preparation by EB Disproportionation- Results

The disproportionation of ethylbenzene was carried out using EB as well as EB containing mixed $C_8$ aromatic feeds on the same catalysts that were used for EB ethylation above.

Parameters like effect of silica to alumina ratio, space velocity, mole ratio etc. have been studied.

### *Effect of $SiO_2/Al_2O_3$ ratio on disproportionation of pure EB and EB from $C_8$ aromatics*

Tables 3.14 and 3.15 show the effect of $SiO_2/Al_2O_3$ on the disproportionation of pure EB and EB from $C_8$ aromatics. The reaction has been carried out on extrudates (70% MFI extrudates). The mechanism of disproportionation is different from that of alkylation. The benzene concentration in products is higher in case of disproportionation because stoichiometric amounts of benzene is always formed during the reaction. With increasing silica/alumina ratio (decreasing acidity) the EB conversion decreases. Simultaneously the DEB yield as well as the p-DEB selectivity increase. Lower ratios yield higher fraction of benzene due to domination of dealkylation of EB. The B/DEB ratio decreases with increasing silica to alumina ratio. The concentration of $C_9$ aromatics and xylenes also decrease on catalysts with lower acidity. In case of EB disproportionation with mixed $C_8$ aromatics feed, the EB conversion decreases with increasing silica to alumina ratio. Similarly, the DEB selectivity increases alongwith decreasing B/DEB ratio. EB dealkylation is greater on samples with low $SiO_2/Al_2O_3$. Another important observation is that for $C_8$ aromatic feeds, there is loss of xylenes when lower silica to alumina ratio catalysts are used. The xylene loss may be because of dealkylation that occurs on catalysts with higher acid site densities. This is clearly reflected in the increased yields of $C_9$ aromatics.

**Table 3.14 Effect of silica to alumina ratio on pure EB disproportionation**

| **Product (wt %)** | **Silica to Alumina Ratio** | | |
|---|---|---|---|
| | **HZ-40** | **HZ-100** | **HZ-250** |

| | | | |
|---|---|---|---|
| **NA** | 1.6 | 0.8 | 0 |
| **Benzene** | 18.9 | 16.6 | 10.7 |
| **Toluene** | 2.4 | 1.6 | 0.2 |
| **EB** | 58.1 | 59.9 | 72.1 |
| **Xylenes** | 0.8 | 0.7 | 0.2 |
| **$C_9$ aromatics** | 2.3 | 1.8 | 0.3 |
| **p-DEB** | 4.6 | 5.9 | 6.5 |
| **m-DEB** | 9.4 | 11.2 | 9.5 |
| **o-DEB** | 0.6 | 0.4 | 0.2 |
| **HB** | 1.5 | 0.9 | 0.2 |
| **EB conv.** | 40.9 | 39.6 | 27.8 |
| **B/DEB** | 2.2 | 1.6 | 1.1 |
| **p-DEB Sel.** | 31.3 | 33.7 | 40.1 |
| **DEB Sel** | 36.2 | 44.8 | 58.1 |

Temp. 623 K, WHSV =3 $h^{-1}$ extruded catalysts

**Table 3.15 Effect of silica to alumina ratio on mixed $C_8$ feed disproportionation**

| **Product (wt%)** | **Silica to Alumina ratio** | | |
|---|---|---|---|
| | **HZ-40** | **HZ-100** | **HZ-250** |
| **NA** | 0.9 | 0.8 | 0.1 |
| **Benzene** | 13.1 | 13.2 | 6.8 |
| **Toluene** | 4.9 | 3.5 | 1.1 |
| **EB** | 37.6 | 35.5 | 48.3 |
| **Xylenes** | 30.5 | 31.7 | 34.2 |
| **$C_9$ aromatics** | 3.3 | 2.7 | 0.7 |
| **p-DEB** | 2.4 | 3.4 | 3.5 |
| **m-DEB** | 4.6 | 6.8 | 4.7 |
| **o-DEB** | 0.3 | 0.3 | 0.05 |
| **HB** | 2.4 | 2.0 | 0.5 |
| **EB conv.** | 45.2 | 47.3 | 26.5 |
| **B/DEB** | 3.1 | 2.2 | 1.4 |
| **p-DEB Sel.** | 32.9 | 32.7 | 42.1 |
| **DEB Sel** | 23.6 | 32.9 | 47.5 |

Temp. 623 K, WHSV =3 $h^{-1}$ extruded catalysts
Feed content (65 % EB + 35 % Xylenes)

**Table 3.16 Effect of silylation and lanthanum exchange on the pure EB disproportionation**

| Product (wt%) | HZ-250 | HZ-250 CLD | HZ-250 CLD-LE |
|---|---|---|---|
| **NA** | 0 | 0.2 | 0 |
| **Benzene** | 10.7 | 9.0 | 5.9 |
| **Toluene** | 0.2 | 0.3 | 0.2 |
| **EB** | 72.2 | 77.6 | 86.1 |
| **Xylenes** | 0.2 | 0.9 | 0.1 |
| **$C_9$ aromatics** | 0.3 | 0.4 | 0.1 |
| **p-DEB** | 6.5 | 8.1 | 6.9 |
| **m-DEB** | 9.5 | 3.1 | 0.5 |
| **o-DEB** | 0.2 | 0.2 | 0 |
| **HB** | 0.2 | 0.2 | 0.1 |
| **EB conv.** | 27.8 | 22.3 | 13.9 |
| **B/DEB** | 1.1 | 1.4 | 1.4 |
| **p-DEB Sel.** | 40.1 | 71.1 | 92.9 |
| **DEB Sel** | 58.1 | 51.3 | 53.9 |

Temp. 623 K, WHSV=3 $h^{-1}$, extruded catalysts

### *Effect of silylation and lanthanum exchange on pure EB and $C_8$ aromatics feed disproportionation*

Tables 3.16 and 3.17 show the comparison of parent, twice silylated (CLD) and twice silylated-lanthanum exchanged catalyst (CLD-LE) in EB disproportionation for pure and $C_8$ aromatic feeds. In both the cases, there is a reduction in the EB conversion and improvement in p-DEB selectivity with silylation. There is further improvement in p-DEB selectivity with lanthanum exchange while there is a sharp drop in EB conversion. The B/DEB ratio increases for modified samples as the DEB yield decreases while, benzene is produced from stoichiometric disproportionation reaction amounts as well as by dealkylation. As observed earlier with silylation the B/DEB ratios are consistently high when mixed $C_8$ aromatic feeds are used, when compared to pure EB. Though there was some xylenes loss, when mixed $C_8$ aromatic feed is used, it is not substantial. However, as one would anticipate the DEB yield is low when mixed $C_8$ aromatics feed is used.

**Table 3.17 Effect of silylation and lanthanum exchange on aromatics $C_8$ feed disproportionation**

| Product (wt%) | HZ-250 | HZ-250 CLD | HZ-250 CLD-LE |
|---|---|---|---|
| **NA** | 0.1 | 0.1 | 0 |
| **Benzene** | 6.8 | 5.9 | 2.5 |
| **Toluene** | 1.1 | 1.2 | 0.9 |
| **EB** | 48.3 | 50.8 | 58.7 |
| **Xylenes** | 34.2 | 34.5 | 34.6 |
| **$C_9$ aromatics** | 0.7 | 0.8 | 0.5 |
| **p-DEB** | 3.5 | 5.3 | 2.6 |
| **m-DEB** | 4.7 | 1.2 | 0.2 |
| **o-DEB** | 0.05 | 0 | 0 |
| **HB** | 0.5 | 0.2 | 0 |
| **EB conv.** | 26.5 | 22.3 | 10.3 |
| **B/DEB** | 1.4 | 1.6 | 1.6 |
| **p-DEB Sel.** | 42.1 | 81.9 | 94.3 |
| **DEB Sel** | 47.5 | 44.3 | 41.1 |

Temp. 623 K, WHSV =3$h^{-1}$ extruded catalysts
Feed content (65 % EB + 35 % Xylenes)

### *Effect of temperature on pure EB and mixed $C_8$ aromatics feed disproportionation*

Effect of temperature on the conversion and product distribution is presented in Fig 3.13 and 3.14. For pure EB disproportionation, with increase in the temperature from 573 K to 648 K the conversion of EB increases continuously. At lower temperatures the activity is not substantial because the activation energy for EB disproportionation is higher than that for required alkylation reaction. The yields of benzene and toluene increase significantly while there is a marginal increase in xylene and $C_9$ yields with temperature. The increase in the B/DEB ratio is linear with temperature. There is a decrease in the p-DEB selectivity with increasing temperature. In case of mixed EB disproportionation also the EB conversion increases with increasing temperature. However, the EB conversion is lower than that obtained with pure EB feeds. The concentration of side products like benzene, toluene and $C_9$ increase with increasing temperature. The B/DEB ratio increases and the p-DEB selectivity decreases with increasing temperature.

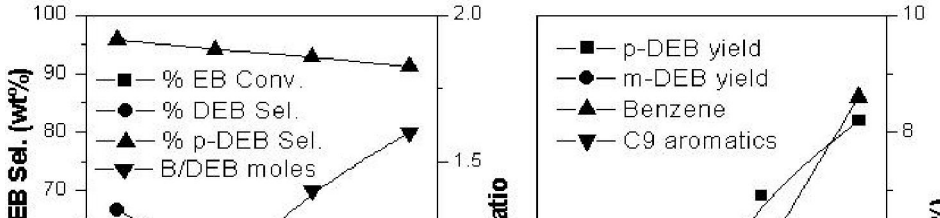

**Figure 3.13: Effect of temperature on pure EB disproportionation**

WHSV=3 $h^{-1}$, Catalyst: HZ-250 CLD-LE

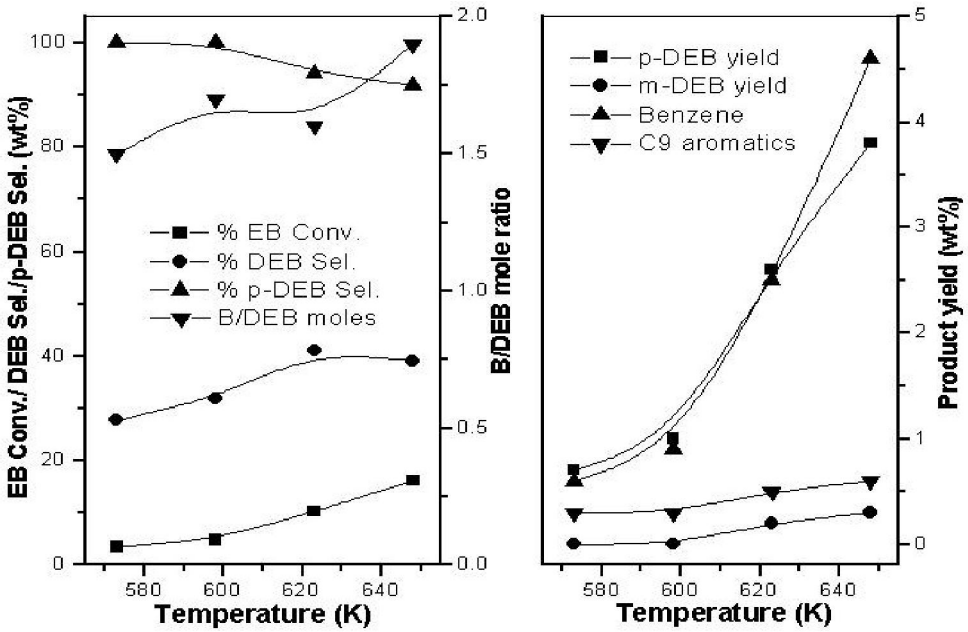


**Figure 3.14: Effect of temperature on mixed $C_8$ feed disproportionation**

WHSV=3 $hr^{-1}$, Catalyst: HZ-250 CLD-LE

***Effect of space velocity on disproportionation of EB and $C_8$ aromatics feed***

The results of influence of space velocity on EB disproportionation of pure EB and $C_8$ aromatics is shown in Figures 3.15 and 3.16. As one may expect, the EB conversion decreases at higher space velocities. This is because the contact time decreases at higher space velocity. Selectivity for p-isomer increases with increasing space velocity. At higher space velocity, the secondary isomerization is suppressed. Dealkylation is expected to be reduced at higher space velocities, hence there is a drop in the concentration of by products. At higher space velocities, diethylbenzene selectivity is better, though the EB conversion starts falling rapidly.

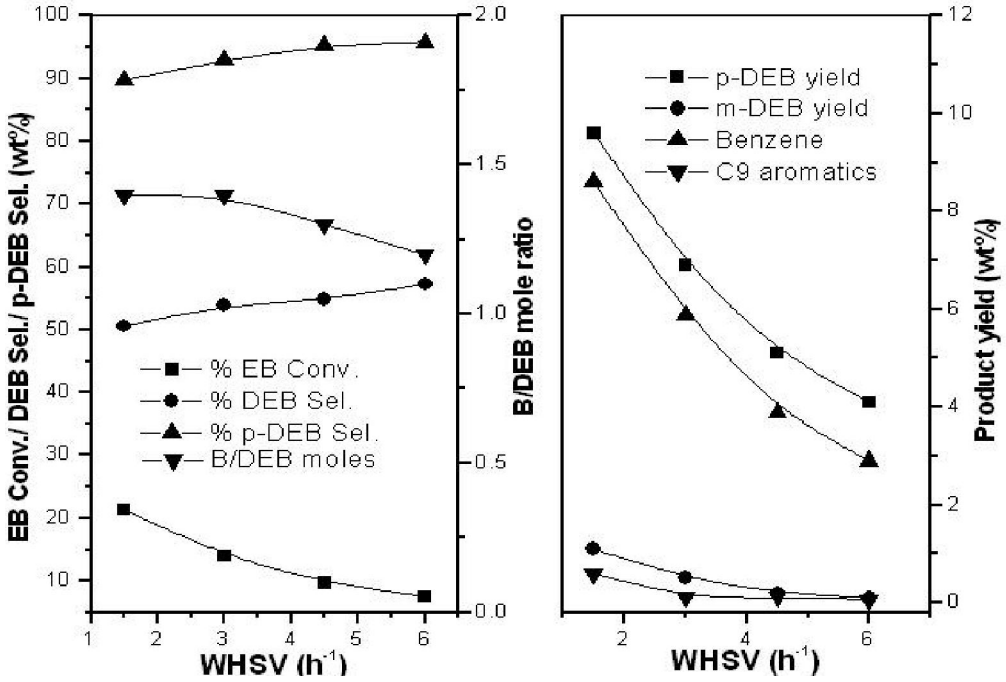


**Figure 3.15: Effect of space velocity on pure EB disproportionation**

Temp 623 K, Catalyst: HZ-250 CLD-LE

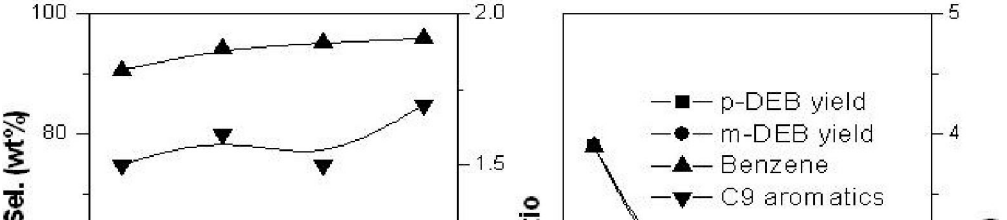

**Figure 3.16: Effect of space velocity on mixed $C_8$ feed disproportionation**

Temp 623 K, Catalyst: HZ-250 CLD-LE

***Mechanistic aspects of mixed EB disproportionation***

**The selective disproportionation of ethylbenzene in the presence of xylenes is an important process for the removal of EB as it produces valuable p-DEB (41). Two processes take place during this reaction. First, the initial step of the reaction over MFI, the dissociation of EB to give benzene and an ethyl moiety and in the second step, the**

# preferential migration of ethyl group to react with another EB molecule rather than react with the equally abundant xylene components.

***The dissociation Step***: Two mechanisms (Figure 3.17) have been proposed for the transalkylation reaction (42). In one mechanism, the alkyl group (R) on the benzene ring cleaves by acid catalysis. Then $R^+$ adds to another benzene ring (eq. 1). In the second mechanism, a dimeric intermediate is formed in which the aromatic rings are bridged by an R group. Subsequent cleavage effects R group transfer from one ring to the other (eq 2). If R is a simple alkyl group, Equation 2 would be a lower energy process due to resonance stabilization of the carbonium ion intermediate. However an intermediate such as **1** is very large relative to the reactants, and its formation may be hindered in small catalyst pores such as the 6 Å pores in MFI (42). In Y zeolite with 18 Å supercages or in amorphous silics alumina with >50 Å pores, the steric constraints to the formation of intermediates **1** would be minimized. Therefore, over these catalysts, the reaction can proceed via (eq(2)) (42). The rates of formation of 1-4 (the disproportionation intermediates from a mixture of xylene and EB) are expected to be similar for a variety of reasons. Due to these reasons, the rates of xylene and EB disproportionation over Y zeolite and amorphous silica alumina are almost similar. But over MFI zeolite, EB disappears 10 times faster than the xylenes. Although **1** may be larger than **2,** it is not likely that the selective disproportionation of ethylbenzene by MFI is due to the greator steric hindrance in forming **1 relative to 2**. This is based on the fact that during disproportionations of toluene and EB over MFI and H-Y the ratio of the rate of toluene disproportionation /rate of EB disproportionation over MFI was 0.07 which is one third of that of H-Y. Since, the dimeric intermediate for toluene disproportionation is smaller than **1** or **2,** toluene should have reacted faster if the mechanism described in eq(2) is important. Therefore it was concluded that the mechanism shown in eq (2) does not occur in MFI type zeolites. If the disproportionation reaction in MFI proceeds via eq (1), then the rate of reaction will be dependent on the stability of the

carbonium ion, R+. For toluene and the xylenes, $R^+$ is $CH_3^+$; while for EB, $R^+$ is $CH_3CH_2^+$, which is ca. 5 Kcal/mole stable than the methyl containing carbonium ion (43). For this reason EB is predicted to dissociate much faster than xylene or toluene in MFI.

***The Addition Step*** : If the predominant mechanism for the disproportionation in MFI is as shown in eq (1), there still remains the important question concerning why the ethyl carbonium ion preferentially adds to EB to give DEB's rather than to the equally abundant xylenes to give dimethyl ethylbenzenes. The importance of this selectivity can be gauged by the fact that during disproportionation of a 50/50 mix of xylenes and EB over MFI, the ratio of DEB/DMEB=7. Were it not for this selectivity, substantial amounts of xylene would be consumed and the economic value of the process would be significantly low. In the pores of MFI, formation of trisubstituted benzene products is less favoured than the production of the disubstituted products. It could be either due to transition state steric hindrance in the pores or due to diffusional restrictions that would lead to the initially formed dimethyl ethylbenzene to dealkylate and form xylene before it could exit the narrow pores of MFI zeolite. (the diffusitivity of trisubstituted benzenes is similar to or lower than that of o-substituted benzene which is many times lower than the diffusivity of m- and p-xylene in MFI).

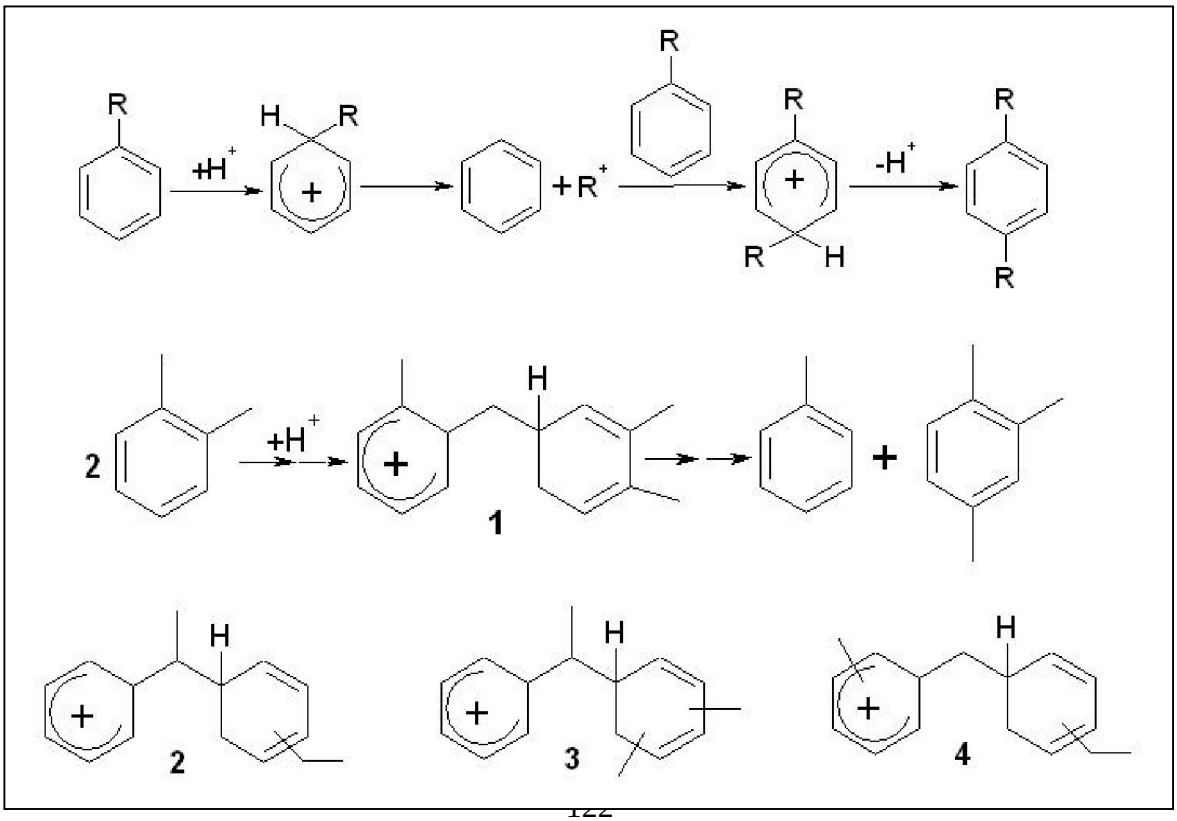

**Figure 3.17: Possible intermediated in mixed $C_8$ feed disproportionation on MFI**

### 3.4.2.3 Time on stream behaviour during alkylation and disproportionation

With time on stream, the alkylation activity, measured in terms of EB conversion decreased for pure and $C_8$ aromatic feeds. As the pore opening is narrowed, the reactant molecules are retained inside the porous structure of zeolite for a longer duration, thus leading to coke deposition, affecting mostly strong acid sites. This coke grows faster and covers most of the active sites, leading to a fall in catalytic activity. In the present case the coke formation seems to be due to ethanol that is used as an alkylating agent. Ethanol being a smaller molecule, can diffuse faster inside the narrow channels of H-MFI, dehydrated and forms corresponding olefin. If EB is not in the vicinity of this olefin, it may oligomerise and lead to formation of coke. The internal coke formation by the polymerisation of small olefins on MFI zeolite is well known. An XPS study of the coke on the Al-MFI zeolite provide strong evidence that the coke fills the MFI pore system initially before any significant amount of coke is formed on the external surface. It has been reported by Derouane et al. that on ZSM-5 zeolites, deactivation increasingly occurs, initially through limitation of the access to the active sites and then followed by the blockage of pore entrance. This blockage also cuts off the access to the active acid sites located at the channel intersections. It may be seen form Fig 3.18 A and B, that the catalyst HZ-250 CLD-LE is stable to both types of feeds during disproportionation when compared to alkylation with EtOH. In case of alkylation deactivation of the catalyst is much faster during alkylation of $C_8$ aromatic feed. However the p-DEB selectivity is higher for mixed $C_8$ aromatic feeds during alkylation as well as disproportionation reactions.

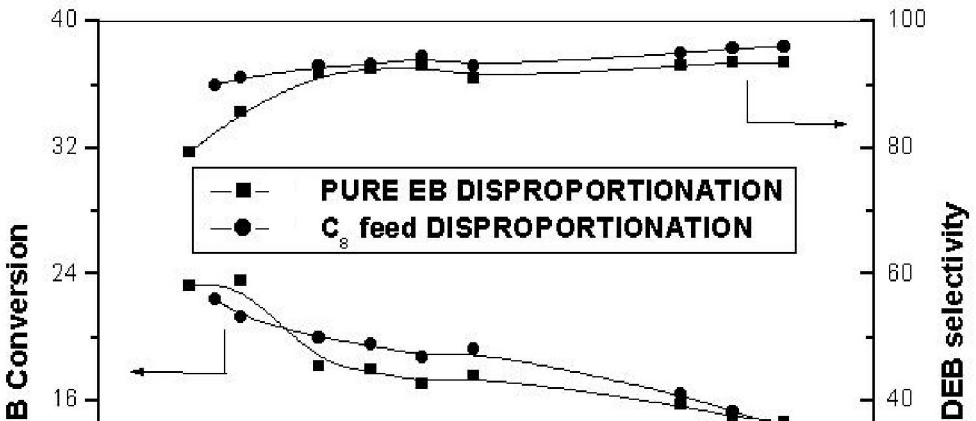

**Figure 3.18: (A) Time on stream studies of pure and mixed $C_8$ feed Disproportionation** Temp 623 K, WHSV=2.5 $h^{-1}$,Catalyst: HZ-250 CLD-LE

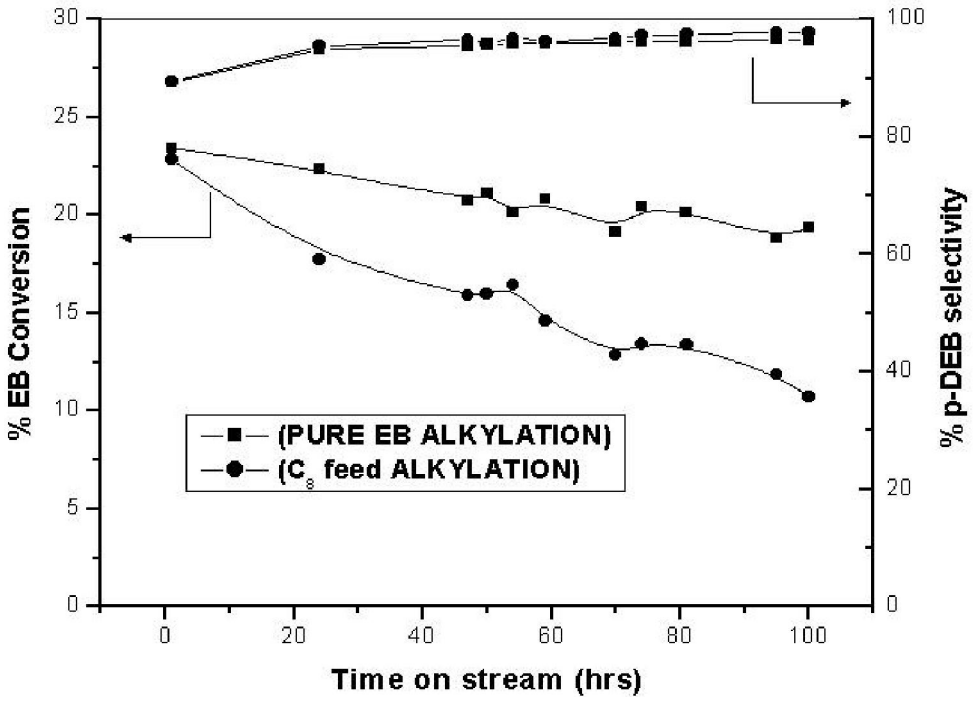


**Figure 3.18: (B) Time on stream studies of pure and mixed $C_8$ feed ethylation** Temp 623 K, EB: Ethanol 5:1, WHSV=2.5 $h^{-1}$, Catalyst: HZ-250 CLD-LE

### 3.4.2.4 Preparation of xylenes by methylation of toluene

#### *Recovery of p-xylene and o-xylene*

By convention, the so-called $C_8$ aromatics include four isomers, namely o-, m- and p-xylene and ethylbenzene (EB). As shown in Table 3.18, these four isomers have similar physical properties. In comparing its vast demand to the other $C_8$ isomers, p-xylene recovery plays the key role in determining the $C_8$ separation scheme.

#### a) o-Xylene recovery

o-Xylene has the highest boiling point among the $C_8$ aromatic isomers, which is 5.38 K higher than that of m-xylene (Table 3.18). o-Xylene plus $C_9$ aromatics are first separated out from the other three isomers in the xylene column. A typical xylene column design normally has 80-160 trays with a reflux ratio of 2 to 6. Moreover, the system usually maintains a low (30 to 50%) o-xylene recovery rate to prevent contamination of o-xylene product and to minimize energy consumption of the xylene splitter (46). High purity o-xylene can then be obtained with a purity up to 98.5% by separating out $A_9^+$ in the bottom of o-xylene distillation column.

**Table 3.18 Physical properties of dialkylbenzne aromatics (44, 45)**

| **Isomer** ($C_8$ aromatics) | **BP (K)** | **MP (K)** | **$d^{20}$** |
|---|---|---|---|
| Ethylbenzene | 411.45 | 178.15 | 0.8670 |
| p-Xylene | 409.35 | 286.45 | 0.8611 |
| m-Xylene | 412.25 | 225.25 | 0.8642 |
| o-Xylene | 417.55 | 247.95 | 0.8802 |

#### b) p-Xylene recovery

The mixture of EB, p- and m-xylene, and some residual o-xylene, which is collected from the top of xylene splitter, is subjected for p-xylene recovery. The separation of p-xylene from a $C_8$ mixture can be achieved either by crystallization or through adsorption separation. The conventional crystallization method takes the advantage of the fact that p-

xylene has the highest melting point among the $C_8$ isomers (Table 3.18). Several practical technologies are known, for example, Isofining SM (Esso), AntarSM (HRI, Hydrocarbon Research) and the proprietary processes developed by Krupp Koppers, Maruzen and ARCO (Atlantic Richfield). Conventionally, the crystallization process operates at low temperatures and utilizes a two-stage crystallization scheme (47). The first stage of the crystallizer, which is maintained in the temperature range from 203 K to 213 K, yields only a wet cake with relatively low p-xylene purity. In the second stage, the crystallizer is operated in the temperature range from 255-277 K. This further purifies the wet cake generated in the first stage. The wet cake from the second stage is then further washed with p-xylene or toluene to obtain p-xylene with 99.5% purity. The two-stage crystallizer scheme described above is operated at a high recycle rate of mother liquid. For typical thermodynamic equilibrium xylene compositions, the p-xylene recovery rate obtained by crystallization is ca. 65%, as compared to the value of 90-95% obtained through adsorption. The low recovery rate and low crystallization temperatures of the former results in an operating cost 2-6 times higher than the latter process (48). Hence, worldwide unit capacity that utilize crystallization technology is much lower than that using adsorption technology, accounting for 35% and 65% global p-xylene capacities, respectively (49). The adsorption method mostly utilizes modified faujasite (X-type zeolite) as the adsorbent over which p-xylene has the greatest adsorption affinity among the species in the isomer mixture (48, 5). Several industrial technologies are known, for example, Parex$^{SM}$ (UOP), Aromax$^{SM}$ (Toray) and Eluxyl$^{SM}$ (IFP). There has been a growing demand from the downstream PTA (pure terephthalic acid) industries to upgrade the p-xylene purity specification. For example, high purity p-xylene is indispensable for the production of PET bottle resins and microfiber polyester. As a result, the purity specification of p-xylene has increased from 99.2% in the 1970s to 99.8% in the 1990s (50). These days ultra-high purity p-xylene occupies about 20% of the worldwide xylene market and hence there is a need to use selective toluene methylation and disproportionation processes in combination with the conventional adsorption and crystallization processes to achieve ultra high purity. In this section we have made an

attempt at selective synthesis of p-xylene by toluene methylation using liquid phase surface inactivated H-MFI.

### *Effect of silylation and lanthanum exchange on toluene methylation*

Table 3.19 shows the comparison of HZ-250, HZ-250 CLD, and HZ-250 CLD-LE for the methylation of toluene. The results show that there is an increase in the p- xylene selectivity as a result of silylation and thereafter a further improvement after lanthanum exchange. As may be seen from the TPD pattern (Fig. 3.2), there is a decrease in the acidity, particularly reduction in acid sites with higher strength on the CLD-LE catalyst and hence the p-xylene selectivity increases as a result of lowering of isomerisation activity. But the conversion remains mostly similar for CLD and CLD-LE catalysts.

**Table 3.19 Effect of silylation and lanthanum exchange on toluene methylation**

| Product (wt%) | HZ-250 | HZ-250 CLD | HZ-250 CLD-LE |
|---|---|---|---|
| **NA** | 0.2 | 0.1 | 0.2 |
| **Benzene** | 0.3 | 0.3 | 0.3 |
| **Toluene** | 80.7 | 83.8 | 84.7 |
| **EB** | 0 | 0 | 0.3 |
| **P-Xylene** | 4.9 | 8.6 | 10.5 |
| **M-Xylene** | 6.6 | 3.1 | 0.6 |
| **O-Xylene** | 2.9 | 0.8 | 0.2 |
| **P-ET** | 1.1 | 2.1 | 2.7 |
| **M-ET** | 1.8 | 0.8 | 0.2 |
| **TMB** | 1.4 | 0.4 | 0.2 |
| **% Tol. Conv.** | 19.1 | 16.2 | 15 |
| **% Xyl. sel.** | 75.9 | 77.6 | 75.6 |
| **B/Xy** | 0.03 | 0.03 | 0.03 |
| **% p- Xylene sel.** | 33.7 | 68.8 | 91.9 |

Temp 673 K, WHSV=4$h^{-1}$, Tol:MeOH=2:1

### *Effect of temperature on methylation of toluene*

During toluene methylation (Fig. 3.19) the conversion increases with increasing temperature. However, at lower temperatures, though the conversion is low, selectivity for para-isomer is high. This lowering of the p-xylene selectivity with increasing temperature is not advantageous as the high p-xylene selectivity leads to a better process economics. With increase in temperature there is a decrease in the level of $C_9$ aromatics. This is due to the cracking of ethyl toluenes at higher temperatures. As a result, xylene selectivity increases with increasing temperature. The B/X (X-Xylenes) increases almost linearly with temperature leading to a loss of valuable aromatics. Based on these results, temperatures in the range of 648-673 K appear to be optimum for this process.

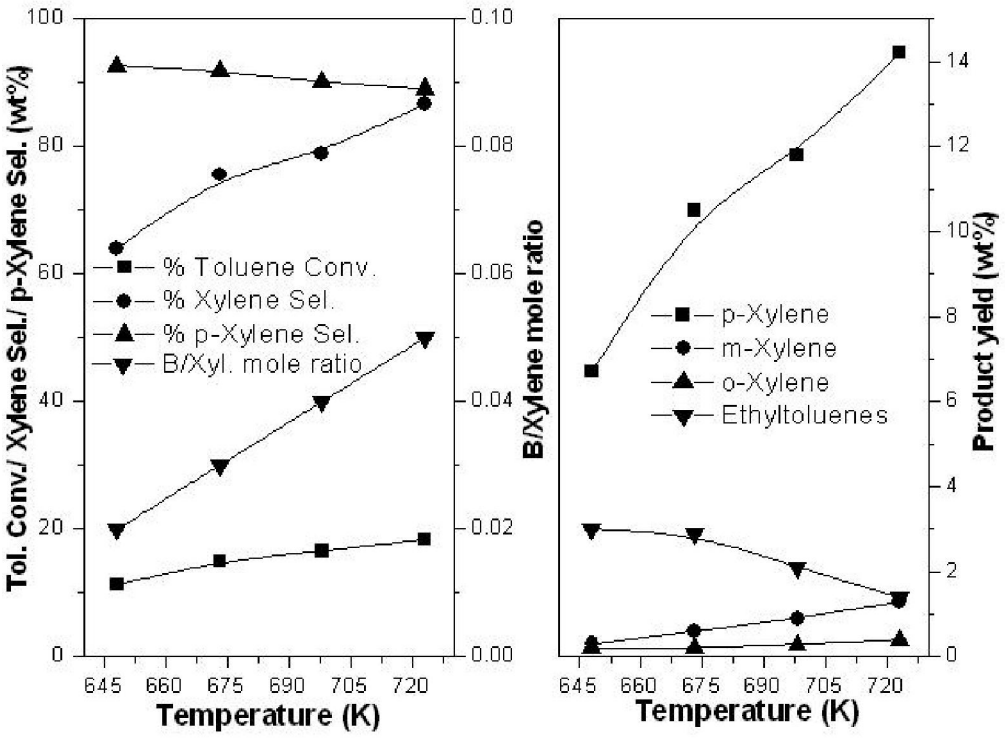

**Figure 3.19: Effect of temperature on toluene methylation**

WHSV=4 $h^{-1}$, Tol:MeOH=2:1, Catalyst: HZ-250 CLD-LE

### *Effect of space velocity*

For toluene methylation at lower space velocities (Figure 3.20), there is an increase in dealkylation activity which can be seen from the higher concentration of benzene and B/X ratio. At higher space velocity, though toluene conversion decreases, the selectivity for p-xylene is enhanced. This increase in para selectivity may be due to the fact that at higher WHSV, the contact time is low and as a result, the primary product formed, i.e. p-xylene, can diffuse out without undergoing secondary isomerization. The xylene selectivity remains more or less same throughout the WHSV range studied. The concentration of ethyltoluenes in the product remained in a similar in the range of space velocity studied.

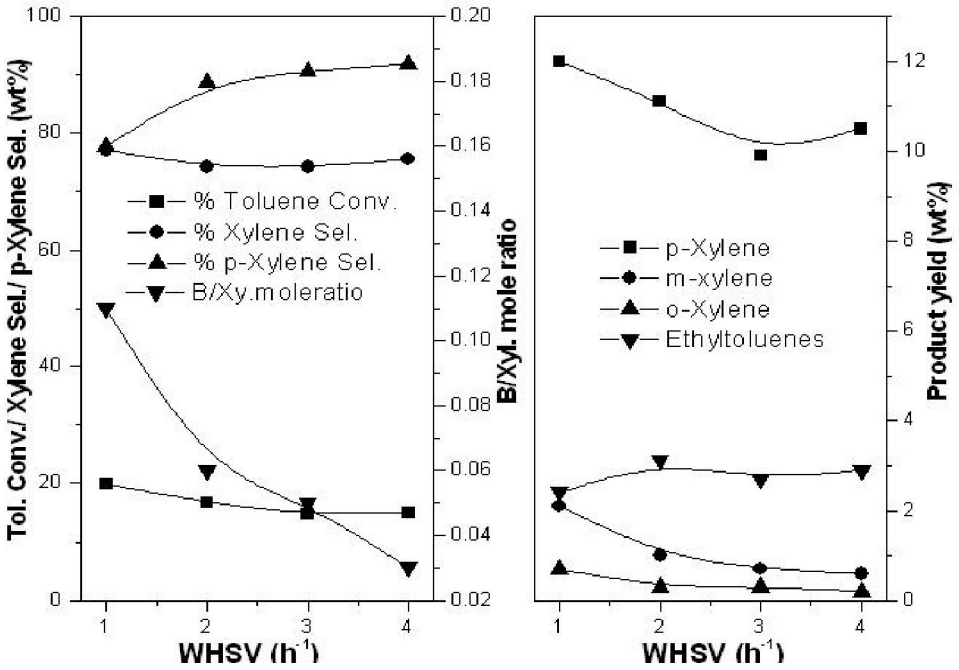


**Figure 3.20: Effect of space velocity on toluene methylation**

Tol:MeOH=2:1, Temp 673 K, Catalyst: HZ-250 CLD-LE

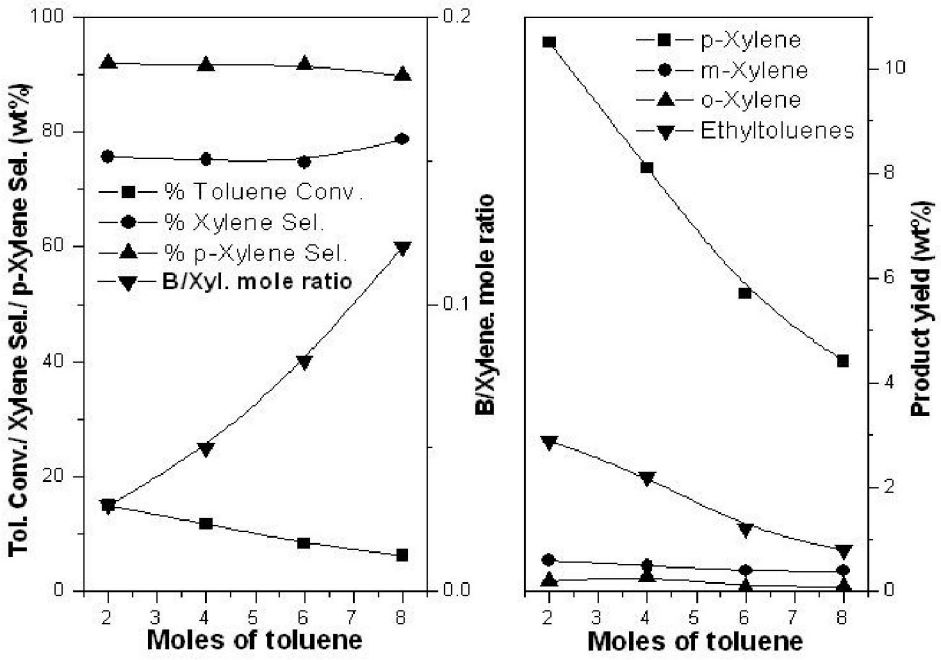


**Figure 3.21: Effect of mole ratio on toluene methylation**
WHSV=4h$^{-1}$, Temp 673 K, Catalyst: HZ-250 CLD-LE

### *Influence of Tol : MeOH*

At low mole ratio of Tol/MeOH, toluene conversion is high and the amount of benzene in the product is less which shows that dealkylation activity is low under these conditions. The toluene conversion as shown in Figure 3.21 decreases with increasing toluene concentration in the feed, as the amount of alkylating agent is relatively low. Dealkylation activity is high at higher toluene to methanol mole ratios, which is clearly reflected in the higher B/X ratios. Xylene selectivity increases, though marginally, with increasing mole ratio as there is a decrease in the concentration of side products. At higher Tol/MeOH ratios, the formation of $C_9$ is supressed as the concentration of MeOH is low. However, not much variation is observed in p-xylene selctivity.

All the above results show that it is better to conduct methylation of toluene in the temperature range of 648-673 K, at reasonably high space velocity ≥ 4h$^{-1}$ using toluene to methanol ratio in the range of 2 to 4.

## 3.5 References

1 Lewis, P.J., Hagopian, C., and Koch, P., Kirk-Othmer Encyclopedia of Chem. Tech.Vol.21, (1983) p.796.

2 Derosset, A.J., Neuzil, R.W., Tajbl, D.G., Braband, J.M., Sep.Sci.Technol. 15 (1980) 637.

3 Jasra, R.V.,and Bhat, S.G.T., Sep.Sci.Tech. 23 (1988) 945.

4 Swift, J.D., Moser, M.D. 20th Dewitt Petrochemical Review, 21-23 March 1995.

5 Mank, L., Hennico, A., Gendler, J.L. 20th 1995 Dewitt Petrochemical Review, 21-23 March 1995.

6 Hotier, G., Mank, L., Renard, P., Bourg, E.Y. Ref. LNG and Petrochem Asia 94, Singapore, 1994.

7 Kojima, M., Rautenbach, M.W. and O'Connor, C.T. J.Catal.112 (1984) 505

8 Topsoe, N-Y., Pederson, K. and Derouane, E.G. J.Catal. 70 (1981) 41.

9 Vedrine, J.C., Auroux, A., Bolis, V., Dejiafve, P., Naccache, C., Weirzchowski, P., Derouane, E.G., Nagy, J.B., Gilson, J.P., Van Hooff, J.H.C., Van Den Berg, J.P. and Worthuizen, J. J.Catal. 59 (1979) 248.

10 Qin, G., Zheng, L, Xie., Y. and Chang, C. J. Catal. 95 (1985) 609.

11 Datka, J. and Tuznik, E. Zeolites 5 (1985) 230.

12 Sayed, M.B., Kydd, R.A. and Cooney, R.P. J.Catal. 88 (1984) 137.

13 Hunger, M., Freude, D., Frohlich, T., Pfeifer, H. and Schweiger, W. Zeolites 7 (1987) 108.
14 Shrinivasan, S., Datye, A.K., Smith, M.H. and Peden, C.H.F., J. Catal. 145, (199) 565
15 Shaikh, R. A.; Hegde, S. G.; Behlekar, A. A.; Rao, B. S. Catal. Today, 49 (1999) 201.
16 Tynjdii, P., Pakkanen, T. T., J. Mol. Catal. A: Chemical 122 (1997) 159
17 Tynjdii, P., Pakkanen, T. T., J. Mol. Catal. A: Chemical 110 (1996) 153
19 Hancock, E.G. Toluene and Xylene and their Industrial Derivatives, Elsevier, Amsterdam, 1982.
19 Olson, D.H. and Haag, W.O. ACS Symp.Ser. No.248 (1984) p.244.
20 Miller, S.J. US Patent 4 608 450 (1986).
21 Smith, J.M. Chemical Engineering Kinetics, McGraw-Hill, New York, 1981, Ch.11.
22 Hoeldrich, W., Eichhorn, H., Lehnert, R., Marosi, L., Mross, W., Ranke, R., Ruppel, W. and Schlimper, H. in D.Olson and A. Bisio (Editors), Proceedings of 6th Int. Zeolite Conf., Reno, USA, Butterworths, New York (1984) p. 545.
23 Shihabi, D.S., Garwood, W.E., Chu, P., Miale, J.N., Chu, C.T.-W. and Chang, C.D. J. Catal. 93 (1985) 471.
24 Bhat, Y.S., Das,J., Halgeri, A.B. Applied Catalysis A: General 115 (1994) 257.
25 Karge, H.G., Ladebeck, J., Sarbak, Z. and Hatada, K. Zeolites 2 (1982) 94.
26 Karge, H.G., Hatada, K., Zhang Y. and Fiedorow, R. Zeolites 3 (1983) 13.
27 Karge, H.G., Wada, Y., Weitkamp, J., Ernst, S., Girrbach U., and Beyer, H.K. in "Catalysis on the Energy Scene", S.kaliaguine and a.mahay (ed.s), Studies in Surface Science and Catalysis, Vol.19, Elsevier, Amsterdam, (1984) p.101.
28 Weitkamp, J., Ernst, S., Jacobs, P.A. and Karge, H.G. Erdöl, Kohle-Erdgas Petrochem. 39 (1986) 13.
29 Streitwieser ,A. Jr., and Rief, L. J.Am.Chem.Soc. 82 (1960) 5003-5005.
30 Santilli, D.S. J.Catal. 99 (1986) 327.
31 Olson, D.H. and Hagg, W.O. Structure Selectivity Relationship in xylene Isomerisation and Toluene Disproportionation. ACS Symp.Ser. 248 (1984) 275.
32 Amelse, J.A. A shape selective shift in the mechanism of transethylation and its effect on the ability to hydroethylate ethylbenzene. Stud.Surf.Sci.Catal, 38 (1988) 165.
33 Tsai, T.C., Wang, I. Disproportionation Mechanism Study of Probing by n-propylbenzene. J.Catal. 133 (1992) 136.
34 Wang, I., Tsai, T.C., Aye, C.L. Stud. Surf. Sci. Catal. 75 (1993) 1673.
35 Tsai, T.C. Ph.D. Dissertation, National Tsing Hua University, Hsinchu, Taiwan, 1991.
36 Haag, W.O. in: D.H. Olson, A. Bisio (Eds.), Proceedings of the Sixth International

Zeol. Conference, Butterworths, Surrey, 1984, p. 466.

37 Wang, I., Aye, C.L., Lee, B.J., Chen, M.H. Proceedings of the Ninth International Congress on Catalysis, Calgary (1988) p.324.

38 Wang, I., Lee, B.J., Chen, M.H. US Patent 4 950 835 (1990).

39 Wang, I., Aye, C.L., Lee, B.J., Chen, M.H. Appl. Catal. 54 (1989) 257.

40 Kaeding, W. W. J. Catal. 95 (1985) 512.

41 U.S. Patent 3,856,871 Dec.24 (1974).

42 Jacobs, P.A. "Carboniogenic Activity of Zeolites", NewYork, 1977. Elsevier, p. 119.

43 Benson, S.W. " Thermochemical Kinetics", 2nd ed. Wiley, NewYork, 1976

44 Wang, S.L. Simulation results using PROII package (Sim Science), personal communication.

45 Mitsutani, A., Maruyama, K. Chem. Eco. Eng. Rev. V6 (9) N77 (1974) 36.

46 Ko, J.W. Personal communication.

47 Machell, E.F., Wylie, J.E., Thompson, R.B. US Patent 3 662 013 (1972).

48 Johnson, J.A., Kabza, R.G., I. Chem.E. Symp. Ser. 118, p. 35.

49 Johnson, J.A., Roeseler, C.A., Stoodt, T.J. 22nd Annual DeWitt Petrochemical Review, Houston, TX, 18-20 March 1997.

50 Swift, J., Adams, D.C., Craglione, A.J., Maise, P.B. Hydroc. Asia, (1998) 42.

## 4.1 Introduction

The alkylation of aromatic hydrocarbons to mono- and dialkylated aromatics has great industrial importance (1). Among para-dialkylated aromatics, p-xylene, p-di-isopropylbenzene, p-ethyltoluene, p-diethylbenzene, p- and m-cymenes and 4-*ter*t-butyltoluene are very important (2, 3). 4-*ter*t-Butyltoluene is an intermediate product for 4-*ter*t-butylbenzoic acid and 4-*ter*t-butylbenzaldehyde, especially used in perfumery and also for manufacture of plastics and resins (4, 5). 4-*ter*t-Butyltoluene is produced by alkylation of toluene with isobutylene, diisobutylene, methyl tertiary butyl ether (MTBE) and *ter*t-butanol (TBA) in the liquid phase and in the presence of activated clay or silica-alumina catalysts at 423–503 K (5). Ioffe et al. (6) studied different catalytic systems such as $AlCl_3$, $AlCl_3$– $CH_3NO_2$, sulphuric acid and polyphosphoric acid in the liquid phase for alkylation of toluene by $C_4$ alcohols. By *ter*t-butylation of toluene with TBA and $AlCl_3$ as catalyst, at 298 K, after 30 min, a mixture of *ter*t-butyltoluenes (67.5% meta- and 32.5% para-isomer) was obtained with 64% yield and with distribution of isomers very near to the equilibrium composition (64% meta- and 36% para-isomer). The formation of ortho-isomer was not observed (6). Butylation of toluene with tert-butylchloride, catalysed by calcined iron sulphate treated with hydrogen chloride at room temperature led to 86% conversion of toluene and a product distribution of 5% meta- and 95% para-isomer (7). Up till now, the use of zeolites as catalysts in *ter*t-butylation of toluene has not been extensively reported. The use of NiY has just been published, but catalytic activity and selectivity to the desired 4-*ter*t-butyltoluene were very low (8). Whereas, isopropylation of toluene has been carried out over a number of zeolites by different groups. The isopropylation of toluene is commercially carried out for the production of industrially important m- and p-cymenes. These cymenes are intermediates for production of cresols. The older technology for production of cymenes in the liquid phase at 333–353 K is based on $AlCl_3$–HCl as catalyst that leads to a mixture of 3% o-cymene, 64% m-cymene, and 33% p-cymene (1). The isopropylation of toluene has been largely studied using different zeolite catalysts, e.g. ZSM-5 (9–11), beta, mordenite and ZSM-12 (12–14), mesoporous materials MSA and MCM-41 (3). Zeolite beta is probably the best candidate to replace $AlCl_3$–HCl system as

catalyst for the liquid-phase alkylation of toluene with propylene (1). The present work deals with the extensive investigation of toluene *ter*t-butylation over large-pore zeolites (H-Y, H-Beta, H-MCM-22, and H-ZSM-12). The catalytic activity and para-selectivity of these zeolites are compared and discussed.

## 4.2 Experimental

### 4.2.1 Preparation of catalysts

Various chemicals used and procedures adopted for preparation of MCM-22 and ZSM-12 zeolites are given in the following sections, whereas HY and H-beta zeolites were obtained from Zeolyst International either in the ammonium or proton form.

#### 4.2.1.1 Synthesis of ZSM-12

ZSM-12 was synthesized using silica sol (30% $SiO_2$) and sodium aluminate as the silica and aluminium source. A solution of required amount of sodium aluminate was slowly added to 53.75 g of silica sol. The above solution was stirred vigorously for 1 hour and 0.9 g of NaOH solution was added to it. After stirring for 15 mins, 26.25 g of TEABr was added to the above mixture and the mixture was stirred for another 30 mins. Lastly 15 ml of aqueous ammonia (25%) was added to the solution and the gel was stirred for 2 h. The gel was finally transferred to a teflon lined stainless steel autoclave and maintained at 413 K for 10 days. The solid material formed was filtered and washed with distilled water and dried in oven at 383 K. After drying, the material was calcined at 823 K and exchanged thrice with 1 molar ammonium nitrate solution. The ammonium ZSM-12 was calcined at 773 K to obtain the proton (acidic) form of the zeolite.

#### 4.2.1.2 Synthesis of MCM-22

Zeolite MCM-22 was synthesized according to a method published by Corma et al. (15) using hexamethyleneimine as organic template. In a typical procedure, required amount of sodium aluminate (0.6–1.0 g, Riedel-de Haen, ≈55% of $Al_2O_3$, 45% of $Na_2O$) is added to a

solution of 0.6 g of sodium hydroxide diluted in 125 g of distilled water and stirred until dissolved. Then, 8.6 g of hexamethyleneimine (Fluka) is added to it and the resulting mixture is thoroughly mixed for at least 15 min. Finally, 9.2 g of fumed silica (Cab-O-Sil M5) is added and the resulting mixture is homogenized for another 60 min. The crystallization was conducted in a teflon-lined stainless steel autoclave under autogenous pressure at 438 K for 8 days under agitation.

### 4.2.2 Characterisation of Catalysts

The crystallinity and phase purity of the samples were evaluated by powder XRD (Rigaku Miniflex) using monochromatized Cu-$K_\alpha$ (30 KVA, 15 amp) radiation. The acidity was determined by temperature programmed desorption of ammonia on Micromeritrics 2910 instrument. The details of the TPD experiment are given in section 2.2.4. Surface area measurements were carried out on Nova 1200 by nitrogen sorption.

### 4.2.3 Reaction procedure and Analysis of products

The setup for catalyst evaluation has been described in section 2.2.3. The products were analysed by GC (HP-6890) equipped with FID and capillary column (BP-5, 50m x 0.32 μm). The products of the reaction were identified on GC-MS (QP5000, Shimadzu), GC-IR and also by comparing with Aldrich standards.

## 4.3 Results and discussion

### 4.3.1 Characterisation of catalysts

Various characterization results of zeolites and the butylation results are described in the subsequent sections.

#### 4.3.1.1 Structural characteristics and surface area

As may be seen from Table 4.1, ZSM-12 has only one dimensional channel network, others have 2D/ 3D network of channels and as a consequence have high surface areas. Zeolite beta has a three-dimensional interconnecting pore system with pores of 0.55 x 0.55

and 0.76 x 0.64 nm, whereas Y zeolite has a three-dimensional interconnecting pore system with supercages of 1.18 nm connected by circular 12-ring 0.74-nm windows. The structure of zeolite MCM-22 consists of two independent pore systems. One of them is defined by two-dimensional sinusoidal 10-membered ring channels (0.40 x 0.59 nm). The second pore system consists of large supercages with a free inner diameter of 0.71 nm which is circumscribed by 12-membered rings. The height of the large supercages amounts to 1.82 nm. ZSM-12 is a unidimensional zeolite consisting of non-interconnecting channels of dimensions 0.55 x 0.59 nm.

**Table 4.1 Physico-chemical characteristics of the zeolites used in toluene butylation**

| Catalyst | Silica Alumina ratio | Pore system and size ($A^o$) | SA $g/m^2$ | TPD $T_{max}$ (K) | (mmoles) of $NH_3$ | |
|---|---|---|---|---|---|---|
| **Y-5.2** | 5.2 | 7.4x7.4x7.4 | 750 | 464, 602 | 0.86 | 1.34 |
| **Y-30** | 30 | 7.4x7.4x7.4 | 780 | 440, 576 | 0.15 | 0.45 |
| **Y-80** | 80 | 7.4x7.4x7.4 | 780 | 431, 588 | 0.08 | 0.11 |
| **H-beta** | 25 | 5.5 ×5.5<br>7.6 ×6.4 | 685 | 476, 614 | 0.65 | 0.55 |
| **H-MCM-22** | 52 | 4.1 x 5.1<br>7.1x 7.1x 18 | 544 | 476, 620 | 0.32 | 0.28 |
| **H-ZSM-12** | 117 | 5.5 x 5.9 | 482 | 456, 637 | 0.09 | 0.08 |

### 4.3.1.2 X-ray Diffraction

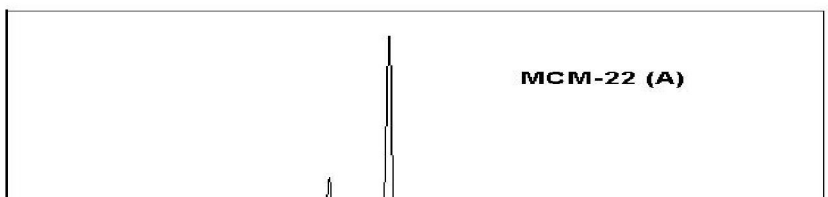

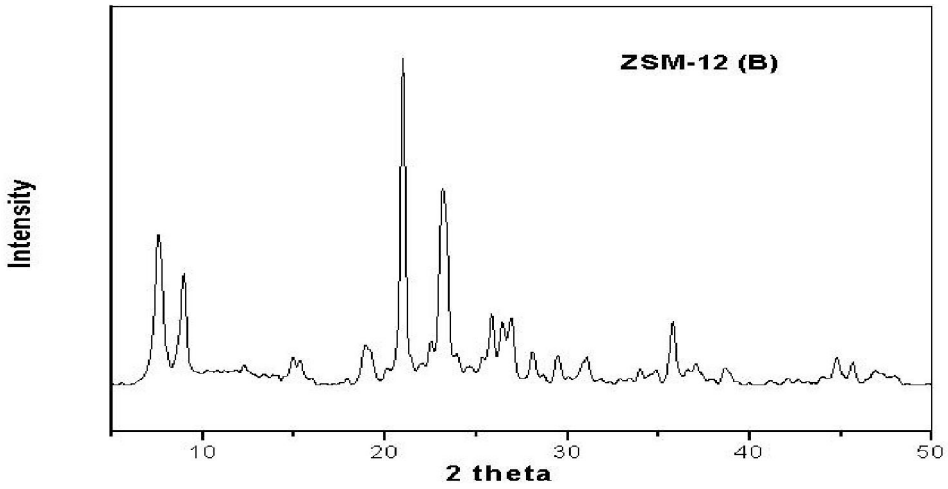


**Fig. 4.1: Powder XRD spectra of MCM-22 and ZSM-12 catalysts used for toluene butylation reaction**

The X-ray powder patterns of calcined samples of zeolite MCM-22 and ZSM-12 are depicted in Figure 4.1 A and B respectively. Comparison of the XRD patterns of both the zeolites with the patterns in the literature (16, 17) showed that the synthesized materials were highly crystalline containing no impurity phases.

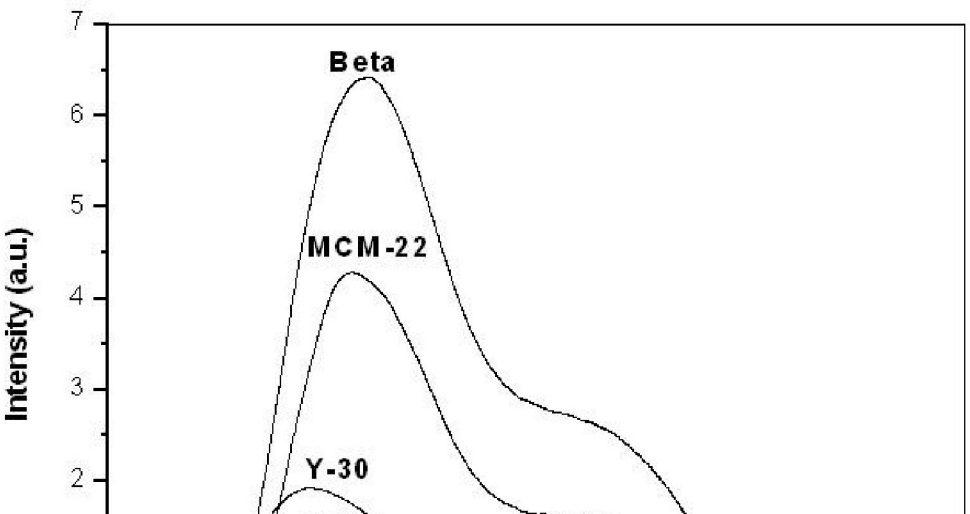

**Fig 4.2: Comparison of the TPD patterns of catalysts with varying acidity and Structure**

#### 4.3.1.3 TPD of Ammonia

Fig. 4.2 shows the TPD-ammonia patterns of zeolite samples with different structural characteristics and acidities. The TPD-ammonia technique provides valuable information about the number and distribution of the acid strength of the active sites. Two desorption peaks, characterized by two temperature maxima (Table 4.1), were observed in the $NH_3$-TPD spectra of all the samples. From the figure it can be seen that that zeolite ZSM-12 and MCM-22 have higher acid strength than zeolites beta and Y. Even though zeolites Y and beta have similar silica to alumina ratio, beta shows much higher acidity in terms of ammonia chemisorption. This difference in acid strength may be attributed to structural characteristics. Fig. 4.3 shows the TPD profiles of Y zeolites having different silica to alumina ratios. As the silica to alumina ratio increases the acidity of the zeolites clearly decrease, the decrease being more prominent for low temperature peak that is assigned to silanols and other adsorption centers.

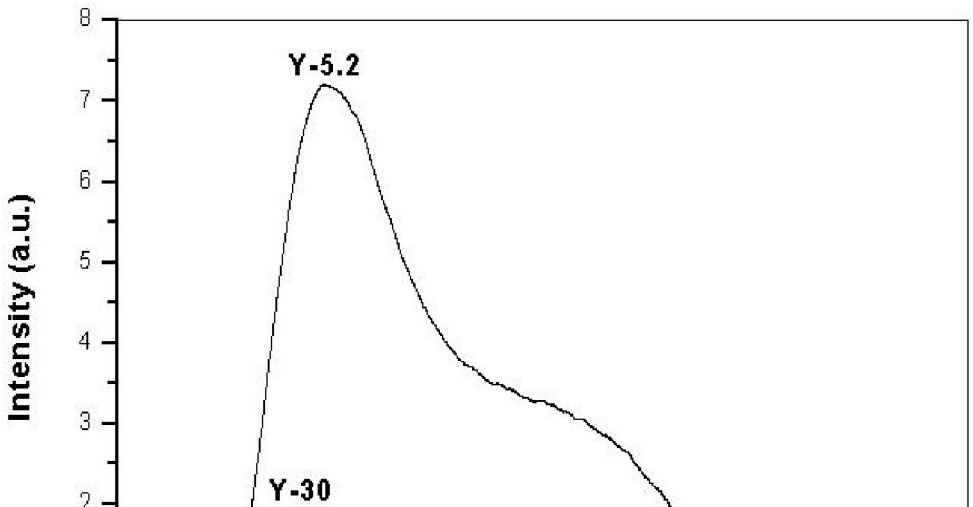

**Fig 4.3: TPD patterns of Y zeolite with different silica to alumina ratio**

### 4.3.2 Butylation of toluene on various zeolite catalysts

*ter*t-Butylation of toluene with *ter*t-butanol has been carried out over four zeolites with different structures and acidities viz., Hbeta, HY, HZSM-12 and HMCM-22 in the temperature range from 393 K to 453 K in a down flow fixed bed reactor. In all cases, the main reaction products were 4-*ter*t-butyltoluene (PTBT) and 3-*ter*t-butyltoluene (MTBT), 2-*ter*t-butyltoluene (OTBT) was completely absent in the product. The main product is expected to be 4-*ter*t-butyltoluene as it is kinetically favoured and also because of steric hindrance of the methyl group on one side and voluminous *ter*t-butyl group on the other side. Shape-selectivity also plays a role based on zeolite structure. In the higher boiling fraction 3,5-di-*ter*t-butyltoluene, where all alkyl groups are in the meta-position to each other is present in trace amounts over HY and Hbeta zeolites. This 3,5-di-*ter*t-butyltoluene was probably formed mainly on the outer surface of zeolite, because its diffusion from the inner channels of zeolites is hindered because of its bulkiness. The selectivity for the PTBT is higher than the thermodynamic equilibrium value of 64%.

#### 4.3.2.1 Tertiary butylation of toluene on zeolite beta

# Alkylation of toluene on zeolite beta was investigated by varying

# parameters like temperature, space velocity etc.

### *Effect of temperature*

Zeolite beta has been used by many groups for toluene isopropylation and has been shown to have very good activity for the reaction. Hence, this zeolite was used for the tertiary butylation of toluene. Figure 4.4 shows the effect of temperature on tertiary butylation of toluene. The temperature was varied from 393 to 453 K. The conversion of toluene (22%) was highest at 393 K, and with increasing temperature, the activity dropped to 16% at 453 K. However, the conversion of t-BuOH was complete at all temperatures. The drop in the toluene conversion may be because of two reasons, (i) the olefin formed on dehydration of t-butanol may not be available for alkylation as result of dominant secondary reactions involving oligomerisation and cracking or, (ii) the dealkylation of the product (TBT) may be predominant at higher temperatures than butylation reaction. There was slight increase in PTBT selectivity with increasing reaction temperatures. This increase in selectivity with temperature is due to the coking of the zeolite pores by the secondary reaction products such as 3,5-di-*tert*- butyltoluene, long chain alkylated products of toluene and oligomers of isobutylene. There was a slight drop in the yields of MTBT and PTBT with increasing reaction temperature, probably as a result of drop in the toluene alkylation activity. This is natural, due to the drop in the toluene alkylation activity.

## *Effect of time on stream*

The time on stream data for tertiary butylation of toluene is given in the Figure 4.5. The conversion of toluene increases with reaction time till four hours and then there is a slight decrease from 23 to 20 % after 4 hours. The drop in conversion after 4 hours may be due to the non-availability of some acid sites as a result of coke deposition. There is a continuous decrease in the MTBT yield with time on stream while the concentration of PTBT increases up to 4 hrs and then starts to drop. The selectivity to PTBT increases with time though in the initial stages the rise is steep but the increase tails off with time. The enhanced PTBT selectivity may be attributed to coke deposition on non- selective sites (outside pores).

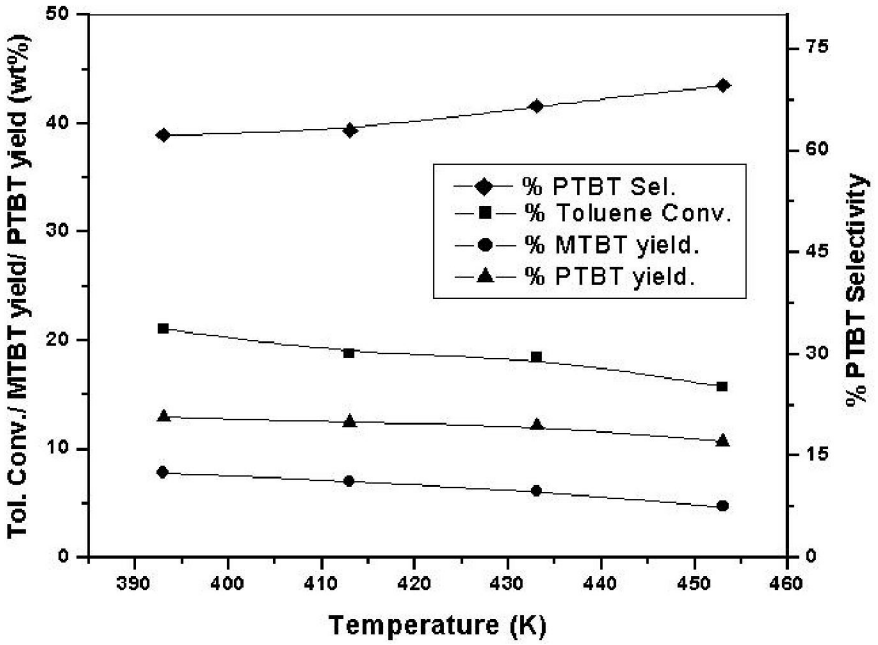


Fig 4.4: Effect of temperature on tert-butylation of toluene on beta zeolite

**WHSV=2h$^{-1}$ Tol:TBA=4:1**

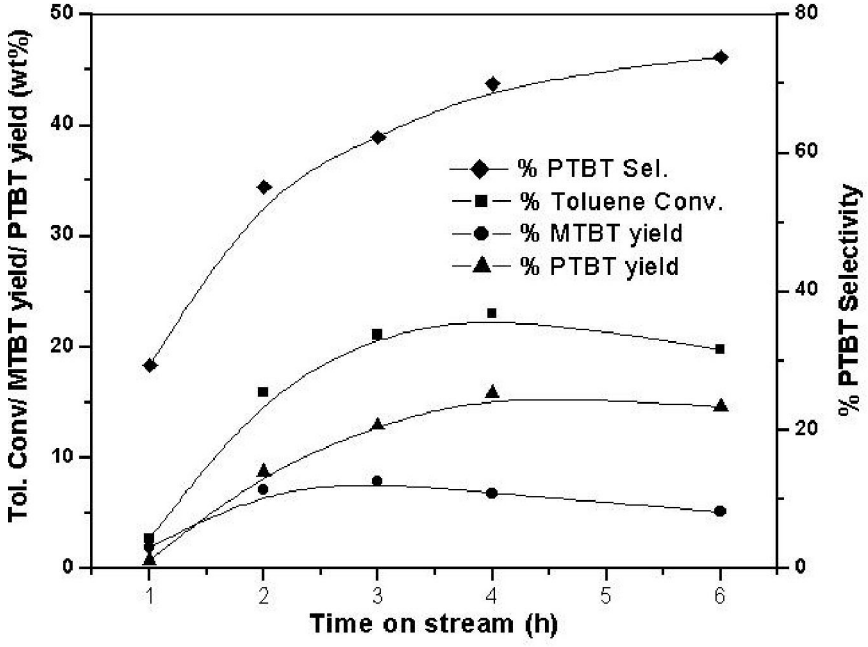

**Fig 4.5: Effect of time on stream tert-butylation of toluene on beta zeolite**

WHSV=2$h^{-1}$, Tol:TBA=4:1, Temperature 393 K

#### 4.3.2.2 Tertiary butylation of toluene on zeolite Y

# Tertiary butylation of toluene has been carried out on Y zeolite. The influence of various reaction parameters like silica to alumina ratio, temperature, space velocity and toluene to tertiary butanol mole ratio on conversion and selectivity to various products has been investigated.

***Effect of Silica to Alumina ratio***

Acidity has two variables, the number and strength of acid sites. It is well known that number of acid sites is linearly related to the amount of aluminium in the tetrahedral framework, hence, it is expected to fall with increasing $SiO_2/Al_2O_3$. Effect of $SiO_2/Al_2O_3$ variation on *tert*-butylation of toluene is shown in Table 4.2. Conversion of tert-butyl alcohol (TBA), the alkylating agent, which is used in dilute (TBA:toluene = 1:4) concentration, is complete on all catalysts. Only two isomers of butyltoluene, i.e., PTBT and MTBT were found in the product mixture, whereas OTBT is completely absent in the product. PTBT selectivity was greater on all catalysts when compared to equilibrium value (36%), whereas substantial increase was observed on high silica containing catalysts. On an acid catalyst that has strong acidity, consecutive reactions of isomerization and de-alkylation are expected to take place, followed by alkylation. However, these consecutive

reactions are likely to be suppressed if the acid site density of the catalyst is reduced as a result of increased $SiO_2/Al_2O_3$ of the sample. This is clearly reflected in our results, as the PTBT selectivity is high on catalysts that have high $SiO_2/Al_2O_3$ ratio (18, 19). The butylation selectivity on the Y zeolite catalysts is quite high as the yield of side products is very low. The conversion of toluene goes through a maximum at $SiO_2/Al_2O_3$ = 32. The conversion of toluene decreases on the sample with the highest $SiO_2/Al_2O_3$ ratio used. The above results show that Y catalysts with higher $SiO_2/Al_2O_3$ are better equipped for butylation of toluene than the low $SiO_2/Al_2O_3$ samples, though the acidity is expected to be higher on the later samples. The Y-80 catalyst, with $SiO_2/Al_2O_3$ = 80 seems to be optimum and is best among the Y catalysts used in this study for the *tert*-butylation of toluene with TBA. Hence, this catalyst has been studied further by varying different reaction parameters in order to find the optimum conditions for this reaction.

**Table 4.2 Influence of $SiO_2/Al_2O_3$ on tert-butylation of toluene**

| **Product(wt%)** | **$SiO_2/Al_2O_3$ ratio** | | |
|---|---|---|---|
| | **5.3** | **32** | **80** |
| **NA** | 0.2 | 0.3 | 0.3 |
| **Toluene** | 74.4 | 70.9 | 77.2 |
| **MTBT** | 8.0 | 7.1 | 2.8 |
| **PTBT** | 15.6 | 19.5 | 17.7 |
| **HB** | 1.8 | 2.2 | 1.9 |
| **Tol.Conv.** | 25.4 | 28.9 | 22.2 |
| **% PTBT Sel.** | 66.1 | 73.4 | 85.9 |

NA=non aromatics

WHSV=$2h^{-1}$, Tol:TBA=4:1, Temperature 393 K

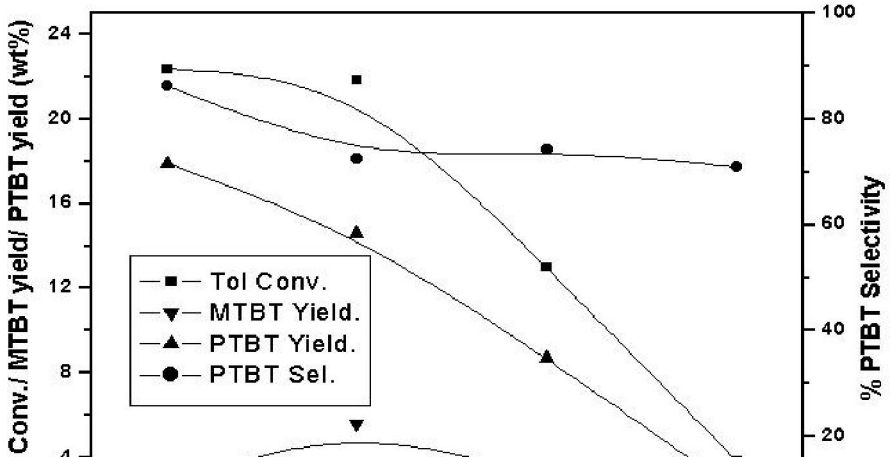

**Fig 4.6: Effect of temperature on tert-butylation of toluene on Y-80 zeolite**

WHSV=2$h^{-1}$, Tol:TBA=4:1

### *Effect of Temperature*

Effect of reaction temperature on the *tert*-butylation of toluene using high silica zeolite catalyst (Y-80) is shown in Figure 4.6 The toluene butylation reaction with TBA was performed in the temperature range 393 K to 453 K on this high silica H-Y (80) zeolite. Compared to alkylation of toluene with lower (C1–C3) alcohols, alkylation with TBA takes place at much lower (393–453 K) temperatures. It is seen that with increasing reaction temperature, there is a continuous fall in the conversion of toluene, though the decrease is steep after 420 K. The PTBT as well as MTBT yields fell at increasing temperatures as a result of fall in conversion. The PTBT selectivity shows a plateau (72%) at high temperatures (433–453 K). It is known that butene formed through dehydration of TBA on acidic catalysts can oligomerise to $C_8$ and $C_{12}$ olefins and then crack to low boilers. Since these reactions are dominant at higher reaction temperatures, a fall in the toluene conversion as well as butylation selectivity is on expected lines.

### *Influence of toluene to tert-butanol mole ratio*

Influence of toluene/TBA ratio on activity and selectivity to PTBT is shown in Table 4.3 for Y-80 catalyst. Conversion of TBA is complete at all toluene to TBA mole ratios. The effect of excess tertiary butanol is observed at Tol:TBA molar ratios of 1 and 2. Unlike mordenite zeolite (20) catalysts, where toluene conversion increased with higher alcohol content in the feed, there was a decrease in the toluene conversion on Y zeolites at higher

alcohol contents. From the Table it is seen that as the concentration of TBA in the feed increases the quantity of non-aromatics in the product increases. This is because at higher TBA concentration the oligomerisation of isobutylene formed by the dehydration of TBA is in competition with the main alkylation reaction. This lower utilization of alkylating agent led to a steep fall in alkylation selectivity with higher TBA contents in the feed. In addition, at high mole ratios, PTBT selectivity increases, though not to an appreciable extent. These results suggest that feeds rich in toluene (low TBA content) are desirable for butylation, particularly the mole ratios in 4:1 to 6:1 region being the most appropriate. Similar observations were reported for propylation of benzene to cumene and propylation of toluene to cymene on various zeolite catalysts (12). In fact, industrial processes based on beta zeolite for preparation of cumene use low propylene concentration (8:1 benzene to propylene) in the feed, to achieve high alkylation selectivity. Among the Y zeolites used, Y-80 gave the best alkylation selectivity, as catalysts with low acid site density promote selective alkylation through suppression of undesirable oligomerisation, cracking and disproportionation reactions. High boilers are also quite high when high TBA containing feeds are used as a result of consecutive alkylations.

**Table 4.3 Effect of toluene to TBA mole ratio on toluene tert-butylation on Y-80**

| **Product (wt % )** | **Mole Ratio of toluene : tert butanol** | | | | |
|---|---|---|---|---|---|
| | **1:1** | **2:1** | **4:1** | **6:1** | **8:1** |
| | 17.5 | 11.4 | 1.4 | 0.4 | 0.2 |
| **Toluene** | 71.3 | 75.4 | 76.6 | 80.2 | 84.9 |
| **MTBT** | 0.7 | 1.3 | 2.9 | 2.9 | 3.3 |
| **PTBT** | 3.4 | 8.3 | 17.9 | 15.4 | 11.1 |
| **HB** | 7.0 | 3.6 | 1.2 | 0.9 | 0.6 |
| **Tol.Conv.** | 13.5 | 14.9 | 22.4 | 19.4 | 14.9 |
| **%PTBT Sel.** | 83.8 | 86.2 | 86.2 | 83.9 | 77.3 |

WHSV=$2h^{-1}$, Temperature 393 K

### *Effect of space velocity*

Space velocity or contact time is an important parameter as it not only influences the conversion of a reactant, it also leads to changes in selectivity of various products. Diffusion constraints have a bearing on product shape selectivity, which in turn govern the product pattern, particularly in a zeolite driven catalytic process. Space velocity also influences the secondary and consecutive reactions. As a result, desired selectivity to a particular product can be achieved by choosing right space velocity. With decrease in contact time or with increasing space velocity, from WHSV=2 to WHSV=4 there is a drop in the conversion of toluene from 22.4 % to 11.8 %. The rate of deactivation of the catalyst is faster in case of higher space velocity. This may be due to the fact that lower contact time favours the oligomerisation of isobutylene than the toluene alkylation reaction. In many alkylation reactions, the selectivity to the desired product increases with space velocity, but in this case no change in the PTBT selectivity was observed with variation in space velocity. This could be due to the structure of zeolite Y which consists of supercages that do not hinder the formation of bulky transition state of MTBT, and also no diffusional constraints are in place facilitating easy diffusion of MTBT. The formation of higher boilers decreases with time in case of higher space velocity, probably due to catalyst deactivation (not shown in the Figure 4.7)

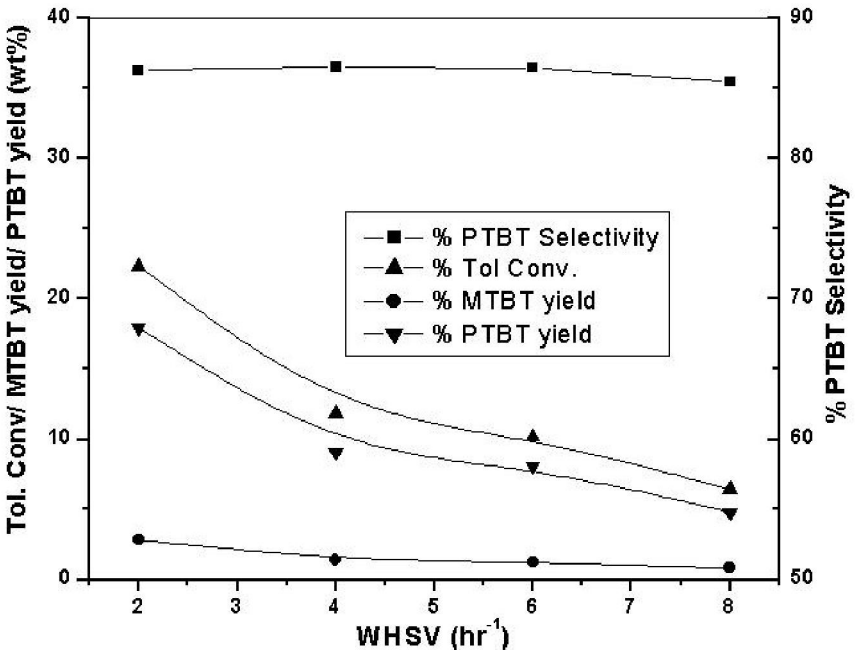

**Fig 4.7: Effect of space velocity on the activity and selectivity during butylation of toluene on Y-80 zeolite**

Tol:TBA=4:1, Temperature 393 K

### *Influence of Time on stream*

The influence of TOS was investigated on Y-80 zeolite as it was found to be a better catalyst for toluene *tert*-butylation reaction. The time on stream data for the butylation of toluene on this zeolite is given in the above Figure 4.8. PTBT selectivity reaches maximum level in the initial stages of the reaction and then it remains constant at 87 %. There was some surge in the conversion of toluene in the initial stages, while a marginal reduction in the conversion of toluene was observed with time on stream though it was to a much less extent compared to beta zeolite. This is probably because of the more open structure of zeolite Y as compared to beta, as the former does not trap the bulky multialkylated products in its channels. The MTBT and PTBT yield increase during first four hours on stream and then there is a slight decrease after that. This kind of initial increase in activity is typical of alkylation reactions on large pore zeolites. In the liquid phase tertiary butylation of toluene (21) the decrease in toluene conversion is accompanied by corresponding increase in the yield of MTBT and with simultaneous reduction in PTBT yields. But in our case, we have not found any decrease in PTBT selectivity with time. The selectivity reaches a steady level of 87% after 8 h at 393 K. This difference may be due to the effect of contact time in case of liquid and vapour phase reaction conditions.

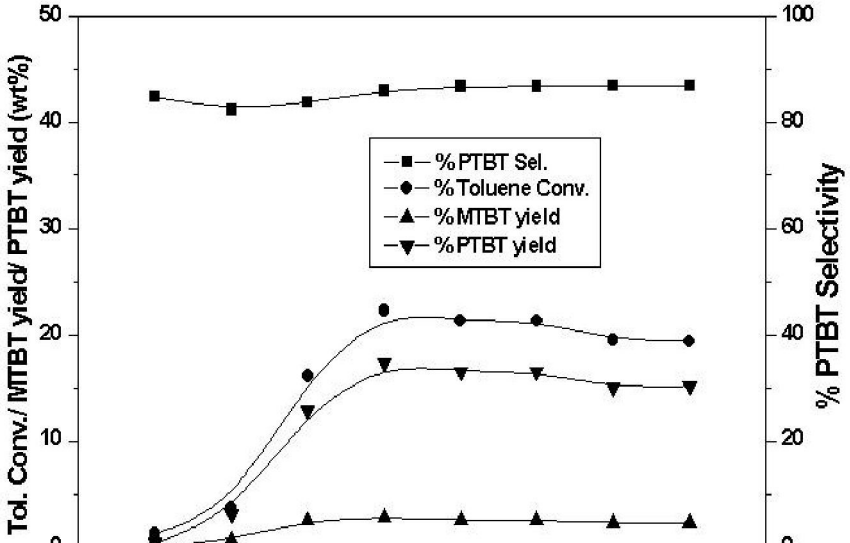

**Fig 4.8: Influence of time on stream on toluene butylation over Y-80 zeolite**

WHSV=2h$^{-1}$, Tol:TBA=4:1, Temperature 393 K

#### 4.3.2.3 Tertiary butylation of toluene on MCM-22 zeolite

Tertiary butylation of toluene has been carried out on H-MCM-22 zeolite. The influence of various reaction parameters on conversion and selectivity to various products has been investigated.

## *Effect of Temperature*

The conversion of toluene and various product selectivities on MCM-22 zeolite has been shown in the Figure 4.9. The toluene conversion on MCM-22 is much lower than that on zeolites Y and beta. The conversion increases from 393 K to 433 K and decreases beyond that temperature, though TBA conversion was 100 % even on this zeolite at all temperatures. Similarly, yield of PTBT increases till 433 K and then decreases. This is due to the fact that dealkylation must be dominant at higher reaction temperatures. The MTBT fraction in the product increases continuously even though there is a fall in the conversion. This may be due to the isomerization of PTBT to MTBT and as a result selectivity to PTBT decreases. The selectivity decreases from 90% at 393 K to 75% at 453 K. MCM-22 crystallite size is smaller than other zeolites, as a result there are less diffusional constraints for diffusion of MTBT. In addition, isomerization of PTBT is favoured outside the micropores.

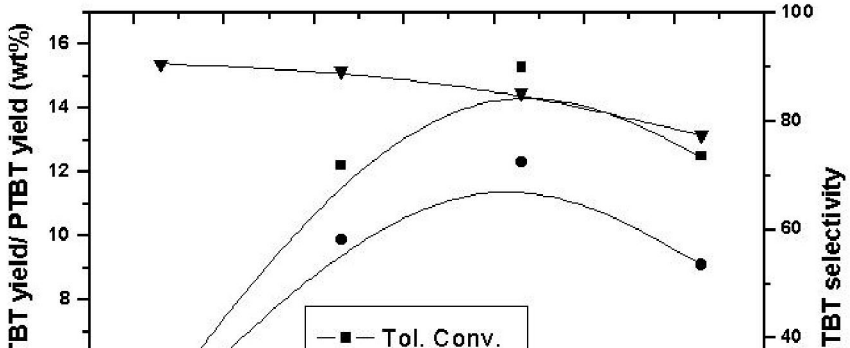

**Fig 4.9: Effect of temperature on tert-butylation of toluene on MCM-22 zeolite**

WHSV=2h$^{-1}$, Tol:TBA=4:1

Table 4.4 Effect of space velocity on toluene butylation on zeolite MCM-22

| Product (wt%) | WHSV h$^{-1}$ | | |
|---|---|---|---|
| | **2** | **3** | **4** |
| **NA** | 0.7 | 8.4 | 9.1 |
| **Toluene** | 93.7 | 87.0 | 87.8 |
| **MTBT** | 0.5 | 0.3 | 0.2 |
| **PTBT** | 5.1 | 4.2 | 2.8 |
| **HB** | 0 | 0 | 0 |
| **Tol.Conv.** | 5.6 | 4.9 | 3.3 |
| **% PTBT Sel.** | 90.7 | 92.7 | 93.0 |

Temp 393 K, Tol:TBA=4:1

## *Effect of space velocity*

Since the PTBT selectivity was found to be higher on MCM-22 than on zeolite Y, variation of space velocity was carried out at two temperatures to check for further improvements in the selectivity of PTBT. The results are shown in Tables 4.4 and 4.5. With increase in the space velocity there is an improvement in the PTBT selectivity at both temperatures. But there is a decrease in the toluene conversion with increase in the space

velocity, this is more apparent at higher reaction temperatures. TBA conversion was complete at all space velocities, as a result yield of NA has increased with space velocity.

Table 4.5 Effect of space velocity on toluene butylation over zeolite MCM-22

| Product (wt%) | WHSV $h^{-1}$ | | |
|---|---|---|---|
| | 2 | 3 | 4 |
| NA | 5.2 | 8.4 | 9.8 |
| Toluene | 85.9 | 86.2 | 86.8 |
| MTBT | 0.9 | 0.5 | 0.3 |
| PTBT | 7.6 | 4.8 | 3.1 |
| HB | 0.3 | 0.1 | 0 |
| Tol.Conv. | 9.3 | 5.8 | 3.7 |
| % PTBT Sel. | 89.2 | 91.1 | 90.8 |

Temp 413 K, Tol:TBA = 4:1

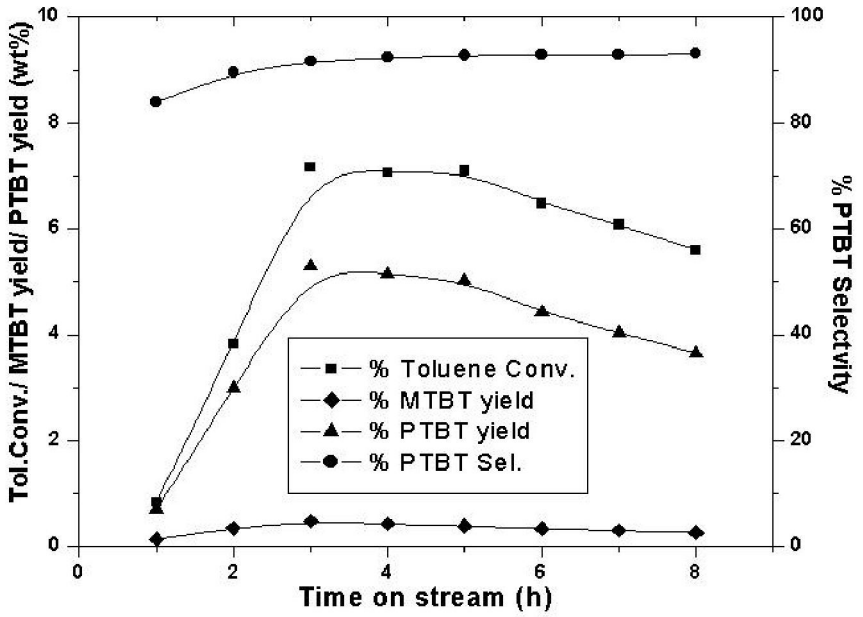


**Fig 4.10: Effect of time on stream on tert-butylation of toluene on MCM-22 zeolite**

Temp 393 K, WHSV=$2h^{-1}$, Tol:TBA = 4:1

## *Influence of time on stream*

In case of MCM-22 the conversion is much lower as compared to beta and Y. But the catalyst is stable to toluene alkylation up to 5 hrs without any fall in conversion (Fig. 4.10). There is a gradual decrease in the conversion after 5 hrs. But the selectivity for PTBT, which is very high at around 91%, is maintained. MCM-22 shows a promise for higher PTBT selectivity at a reasonably good conversion.

### 4.3.2.4 Tertiary butylation of toluene on zeolite ZSM-12

Butylation of toluene has been carried out using TBA as alkylating agent on ZSM-12 with $SiO_2/Al_2O_3$ =117. Influence of reaction parameters has been investigated for this reaction on this zeolite.

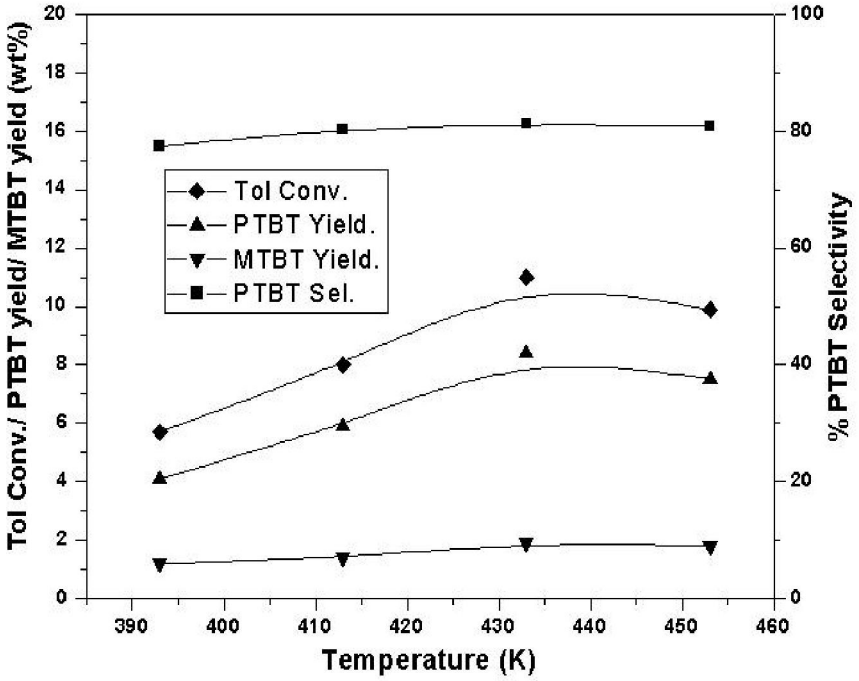


**Fig 4.11: Effect of temperature on tert-butylation of toluene on ZSM-12 zeolite**

WHSV=$2h^{-1}$, Tol:TBA = 4:1

***Effect of Temperature***

The toluene conversion on ZSM-12 is slightly less than that on MCM-22. This may be due to the lower acidity of ZSM-12 as compared to MCM-22. The temperature dependence profile (Figure 4.11) for the reaction is almost similar to that of MCM-22. The conversion

increases from 393 K to 433 K and decreases beyond that. There is a fall in the MTBT and PTBT concentrations after 433 K as a result of reduced toluene conversion. However, there is not much change in the PTBT selectivity over the entire range of temperatures studied. The PTBT selectivity on this catalyst is lower as compared to MCM-22 at similar conversion of toluene.

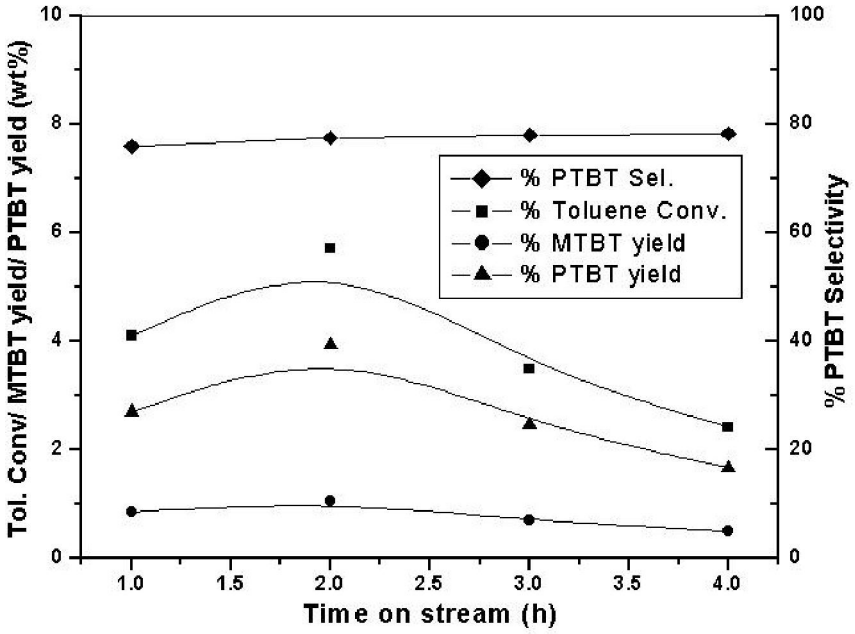


**Fig 4.12: Effect of time on stream on tert-butylation of toluene on ZSM-12 zeolite**

Temp 393 K, WHSV=2$h^{-1}$, Tol:TBA = 4:1

***Influence of time on stream***

In case of ZSM-12 the conversion is comparable to MCM-22 in the initial stages. But the deactivation of the catalyst is rapid, just after 2h (as shown in the figure 4.12) on stream and the selectivity is also much lower than that of MCM-22. The PTBT selectivity remains same even after rapid deactivation of the catalyst. Yields of PTBT and MTBT decrease, particularly the former to a large extent with time on stream. These results may be attributed to the nature of pore structure (one dimensional), when compared to other zeolites (beta, Y and MCM-22).

### 4.3.2.5 Selectivity in butylation (alkylation)

# Several acid-catalysed equilibrium reactions take place during toluene alkylation by TBA. The first reaction to be considered is the dehydration of TBA (reaction 1).

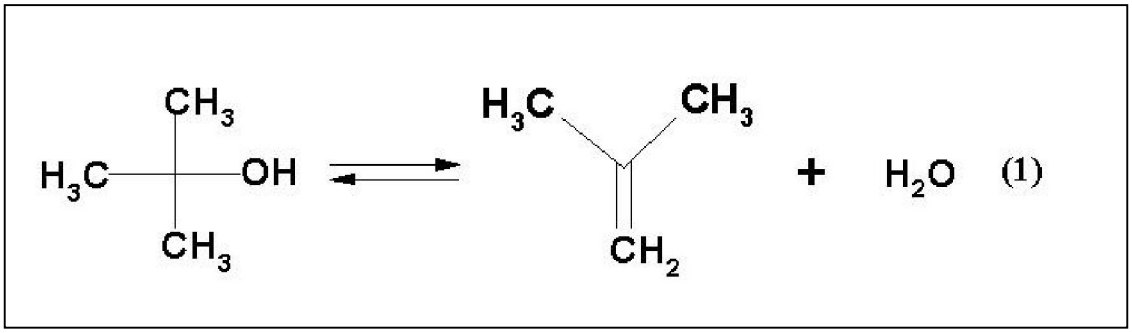


The reaction of interest is the alkylation of toluene by the isobutylene that is formed during dehydration of TBA (reaction 2).

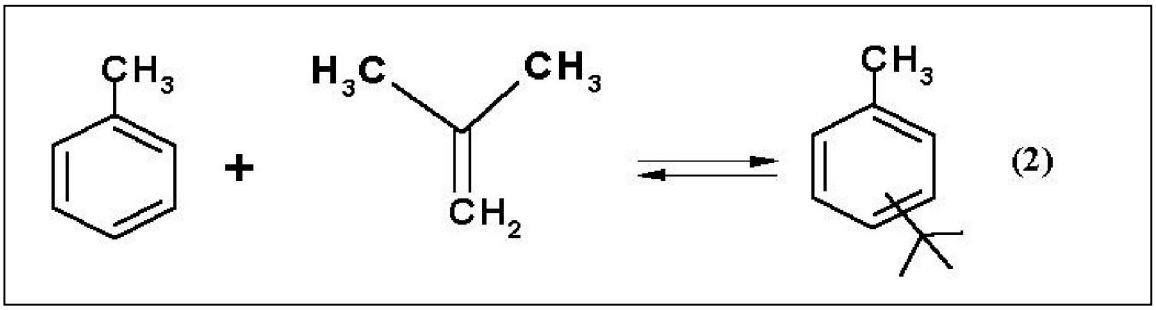


The unwanted side reactions are :

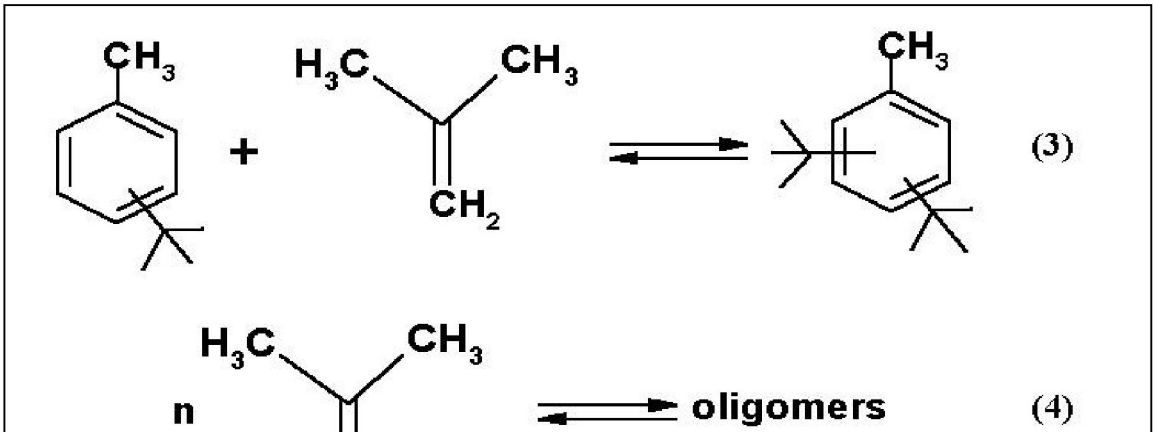

**R** – alkyl groups

The composition of reaction mixture is influenced by initial content of TBA in toluene. The rate of formation of products is influenced by the thermodynamic stability of different products and in the case of zeolites the diffusion rate of molecules in the pores. Since most of acid sites in zeolites are located in the internal surface of zeolite catalyst, mainly processes that take place within the pores of zeolites influence the composition of the reaction products. It is known, that the diffusion rate of compounds in zeolites is influenced by the ratio of the diameters of molecules to zeolite pores. PTBT is the narrowest of TBT isomers and has the highest diffusion rate in the zeolite channels and as a consequence has the highest chance of diffusion to outside the pore network, while MTBT because of larger diameter is expected to have lower diffusion rates. Since the MTBT is the thermodynamically most favoured mono-*tert*-butyltoluene, the kinetically favoured PTBT is transformed to MTBT. This isomerization takes place more easily on the external surface, where it is not sterically hindered compared to within pores of zeolite. The kinetically and thermodynamically favoured 3,5-di-*tert*-butyltoluene may not diffuse out of pores, as a result it is embedded in the channels of zeolite because of its larger size. The channels of zeolite may be clogged also by oligomers of isobutylene. Probably the formation of the last two products is the main reason for catalyst deactivation. The formation of classical coke at the temperatures below 473 K is less probable. Since the rate

of oligomerization of isobutylene is also significant, at longer reaction times and at higher temperatures, the equilibria (2) and (3) are gradually shifted to the left (TBT's are gradually dealkylated) with the decreasing concentration of isobutylene in the reaction mixture. The overall conversion of toluene versus the reaction time on all the catalysts investigated shows that the toluene conversion in the presence of the Y and beta zeolites is much higher than that obtained with the MCM-22 or ZSM-12 catalysts, though all the zeolites have the same large 12-membered ring pores. The experimental results indicate the following order of catalytic activity: beta-25 ≈ Y-30 > MCM-22 > ZSM-12. Zeolite beta has a three-dimensional interconnecting pore system with pores of 0.55 x 0.55 and 0.76 x 0.64 nm, whereas Y zeolite has a three-dimensional interconnecting pore system with supercages of 1.18 nm connected by circular 12-ring 0.74-nm windows. Zeolites beta and Y have open three-dimensional structures and hence even if their acidities are different they have similar activities. Due to open structures there is better interaction of the reactant molecules with the acid sites and the diffusivity of the product molecules is also higher. The structure of zeolite MCM-22 consists of two independent pore systems. One of them is defined by two-dimensional sinusoidal 10-membered ring channels (0.40 x 0.59 nm). The second pore system consists of large supercages with a free inner diameter of 0.71 nm which is circumscribed by 12-membered rings. The height of the large supercages amounts to 1.82 nm. These huge intracrystalline voids are accessible through 10-membered-ring apertures (0.40 x 0.59 nm) only. ZSM-12 is a unidimensional zeolite consisting of non-interconnecting channels of dimensions 0.55 x 0.59 nm. The catalytic activity on ZSM-12 as well as on MCM-22 is less than that on beta and Y zeolites. This is predictable from the structure of these zeolites. MCM-22 has one 10 membered ring system and hence even if it has a three dimensional structure the diffusion of reactants towards the internal acid sites is limited. Cejka et.al (22) have carried out toluene isopropylation on MCM-22 and they have found that it behaves as a large pore zeolite with no selectivity to p-cymene. But in case of toluene tertiary butylation we have found that MCM-22 gives good selectivity for p-tertiary butyl toluene even though the toluene conversion is low. The combination of supercages, 10 and 12 membered rings imposes a diffusiuonal barrier to MTBT thus allowing PTBT to come out faster than MTBT. The time on stream stability is also good

on this catalyst. The catalyst deactivates at a very slow rate. ZSM-12, even though has a 12 membered pore window shows very low activity for toluene butylation because of its one dimensional pore system. The stability is also not very good, mostly due to its lower acidity.

### 4.3.3 Tertiary butylation of toluene with methyl tertiary butyl ether (MTBE)

The tertiary butylation of toluene was carried out in the presence of MTBE as the alkylating agent on zeolite Y-80 to find out the effect of alkylating agent on the selectivity and stability of the catalyst. Due to the problems associated with unavailability, transportation and handling of isobutylene, particularly for usage in low-tonnage fine and speciality chemical industry, it is advantageous to generate isobutylene in situ, amongst them cracking of MTBE and dehydration of TBA are attractive (23–25). MTBE is a good source for the in situ generation of pure isobutylene and the co-product, methanol, can be recovered and reused as it is not expected to undergo any reactions under the toluene butylation conditions. The comparison of both alkylating agents is shown in the Figure 4.13. In case of TBA the conversion is low in the initial stages (up to 1.5 h) and then there is a steep rise in the toluene conversion up to 4 h and then the activity is stabilized thereafter. This is because in the initial stages of the reaction the isobutylene formed due to the dehydration of alcohol undergoes side reactions at a rate faster than that of the alkylation. With passage of time once the strong acid sites are blocked the alkylation reaction becomes dominant. In the case of MTBE the initial activity is higher than that with TBA, but the stable activity is less than that when TBA was used as the alkylating agent. Even though the mole ratio of the alkylating agent used was the same in both cases the amount of isobutylene generated in both cases was different (lesser in case of MTBE). This is because the mechanism of isobutylene generation is different from that using TBA. Isobutylene is directly formed by dehydration of TBA on zeolitic acid sites which is much more facile than the hydrolysis of MTBE. The catalyst has a better stability with MTBE due to the slow release of isobutylene in to the reaction medium thus decreasing the side reactions that lead to coke formation and deactivation. Whereas no influence of the alkylating agent on the PTBT selectivity was seen on this catalyst.

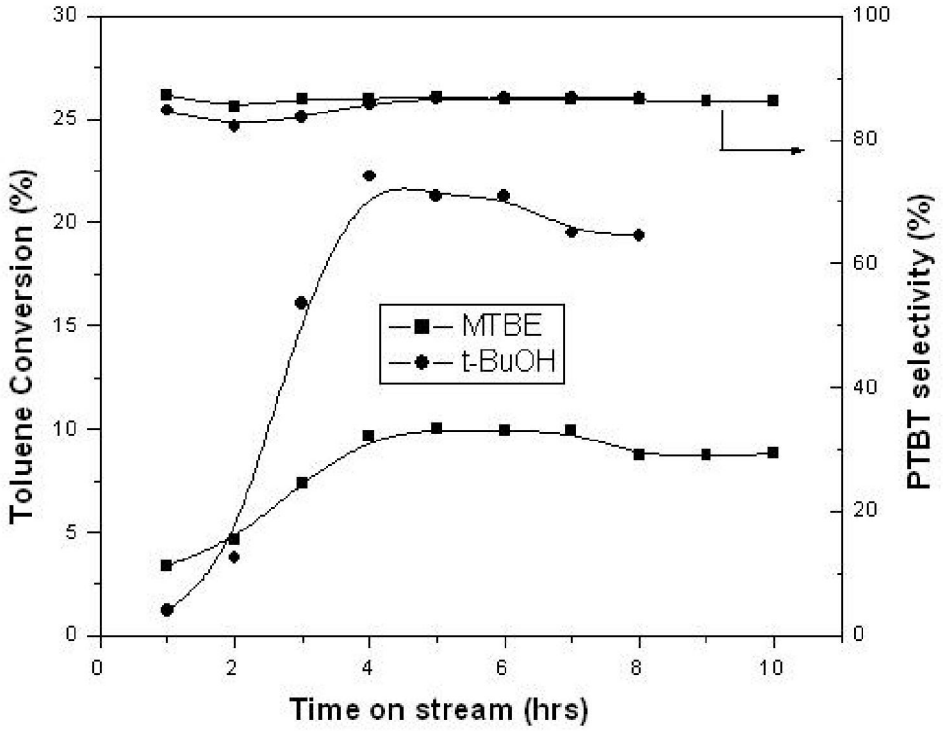


**Fig: 4.13 Comparison of TBA and MTBE as alkylating agents**

Temp 393 K, WHSV=2$h^{-1}$, Tol: Alkylating agent = 4:1

### 4.4 References

1 Perego, C., Ingallina, P. Catal. Today 73 (2002) 3.
2 Halgeri, A.B., Das, J. Catal. Today 73 (2002) 65.
3 Perego, C., Amarilli, S., Carati, A., Flego, C., Pazzuconi, G., Rizzo, C., Bellussi, G. Microporous Mater. 27 (1999) 345.
4 Hearne, G.W., Evans, T.W., Buls, V.W., Schwarzer, C.G. Ind. Eng. Chem. 47 (11) (1995) 2311.
5 Kusano, N., Kobayashi, T., Miyajima, H. JP 61145130 (1986).
6 Ioffe, B.V., Lemann, R. B., Stoljarov, V. Neftekhimija 9 (3) (1969)386.
7 Hino, M., Arata, K., Chem. Lett. (1977) 277.
8 Coughlan, B., Carroll, W.M., Nunan, J., J. Chem. Soc. Faraday Trans. 79 (1) (1983) 327.
9 Fraenkel, D., Levy, M. J. Catal. 118 (1989) 10.
10 Wichterlova, B., Cejka, J. J. Catal. 146 (1994) 523.
11 Parikh, P.A., Subrahmanyam, N. Appl. Catal. A Gen. 90 (1992) 1.

12 Reddy, K.S.N., Rao, B.S., Shiralkar, V. P. Appl. Catal. A Gen. 121(1995) 191.
13 Cejka, J., Žilková, N., Wichterlová, B. Coll. Czech. Chem. Commun. 61 (1996) 1115.
14 Parikh, P.A., Subrahmanyam, N., Bhat, Y.S., Halgeri, A.B. Chem.Eng. J. 54 (1994) 79.
15 Corma, A., Corell, C., Perez-Pariente, J. Zeolites 15 (1995) 2.
16 Ernst, S. in: H.G. Karge, J. Weitkamp (Eds.), Molecular Sieves—Science and Technology, vol. 1, Springer, Berlin, (1998) p. 65.
17 Szostak, R., Molecular sieves, Principles of synthesis and identification, Van NostrandRheinhold, New York, (1989) p. 285
18 Bhat, Y.S., Das, J., Halgeri, A.B. App. Catal. A: Gen. 122 (1995) 161.
19 Bezouhanova, C., Dimitrov, C., Nenova, V., Spassov, B., Lahert, H. Appl. Catal. 21 (1986) 149.
20 Sebastian, C.P., Pai, Shivanand, Sharanappa, N., Satyanarayana, C.V.V. Journal of Molecular Catalysis A: Chemical 223 (2004) 305–311
21 Mravec, D., Zavadan, P., Kaszonyi, A., Joffre, J., Moreau, P. Applied Catalysis A: General 257 (2004) 49–55
22 Cejka, J., Krejci, A., Zilkova, N., Kotrla, J., Ernst, S., Weber, A., Microporous and Mesoporous Materials 53 (2002) 121–133
23 Cunill, F., Tejero, J., Izquierdo, J.F. Appl. Catal. 34 (1987) 341.
24 Tajero, J., Cunill, F., Manzano, S. Appl. Catal. 38 (1988) 327.
25 Yadav, G.D. Bull. Catal. Soc. India 15 (1998) 21.

## 5.1 Introduction

The alkylation of phenol with olefins in the presence of an acid catalyst to produce alkylphenols has been the subject of investigation by many researchers. Both homogenous and heterogenous catalysts have been used for the alkylation of phenols. Solid acid catalysts such as zeolites, ion–exchange resins, amorphous silica alumina are preferred to homogenous acid catalysts since they can be easily separated from the reactant-product mixture. Other disadvantages of solid acid catalysts are that they eliminate corrosive environment that is often encountered with homogenous catalysts. The thermodynamic sorption or distribution characteristics of the reactant/product between the bulk liquid and solid acid framework may also play an important role and could possibly lead to results that are not achievable with homogenous acid catalysts.

The alkylation of phenol with a variety of olefins such as alpha-methylstyrene (AMS) and diisobutylene (DIB) and lower olefins such as propylene, 1-butene, isobutylene and isoamylene are of industrial relevance and also of academic interest. p-tert-Butylphenol is used as raw material for the production of a variety of resins by condensation with formaldehyde, which have outstanding properties in the manufacture of durable surface coatings, varnishes, wire enamels, printing inks, etc. p-tert-Amylphenol is used in the manufacture of surface-active agents, rubber chemicals, and petroleum additives. p-tert-octylphenol is used in the manufacture of oil-soluble phenol-formaldehyde resin. p-Cumylphenol [4-(1-phenylethyl)phenol, 4-CP] is used for the production of resins, antioxidants, fungicides, printing inks, chemical modifiers for polycarbonates, etc.

Published literature on the alkylation of phenol with α-methyl styrene (AMS) is very scanty. Zieborak and co-workers (1) have reported the synthesis of 4-CP in the presence of cation-exchange resin Amberlyst 15. Macho et al. (2) studied the reaction of phenol with a mixture of AMS and AMS dimers in the presence of active earth, polyphosphates and zeolites in the temperature range 333-513 K. These authors have claimed that the phenol aralkylation selectivity with AMS and its unsaturated dimers to o- and p-cumylphenols is

increased if AMS and AMS dimers are continuously or semi continuously added to an excess of phenol, the mole ratio of AMS to phenol being 1:2-10. Oberholtzer et.al (3) have performed the alkylation of phenol with AMS in the presence of cumene on ion-exchanged resins and have found that there is an increase in the 4-CP selectivity with increase in cumene concentration. It appears that a detailed study of this reaction has not been carried out over zeolites. Hence, we intend to examine the performance of large pore zeolites in the alkylation of phenol with AMS and to map the best operating conditions for producing predominantly 4-CP with reduced concentration of dimeric products.

## 5.2 Experimental

### 5.2.1 Characterization of catalysts

Zeolite beta and mordenite were obtained from PQ corporation and Y zeolites of different Si/Al ratios were obtained from Zeolyst International. The acidity of the zeolites was evaluated by temperature programmed desorption of ammonia on Micromeritrics 2910 model. Surface area measurements were carried out on Quantachrome by nitrogen sorption.

### 5.2.2 Alkylation of Phenol

The catalytic experiments were carried out in a 50-ml glass batch reactor, equipped with a magnetic stirrer, a thermometer, and a condenser. The catalyst was calcined at 723 K prior to the reaction. A typical batch consisted of 40 mmol of phenol (PhOH), 10 mmol of $\alpha$-methyl styrene (AMS) and 200 mg of catalyst. In all cases the reactant to catalyst ratio (w/w) was kept at 25. In addition, effect of dilution with cumene was studied. In this case the amount of cumene was increased keeping the total weight of the reaction mixture constant. Samples were withdrawn periodically and were analyzed by a GC (HP 6890) equipped with FID and a capillary column (BP-5, 50m x 0.32µm). Products were identified by means of GC-MS and GC-IR and by comparison with authentic compounds from Sigma-Aldrich.

### 5.3 Reaction scheme

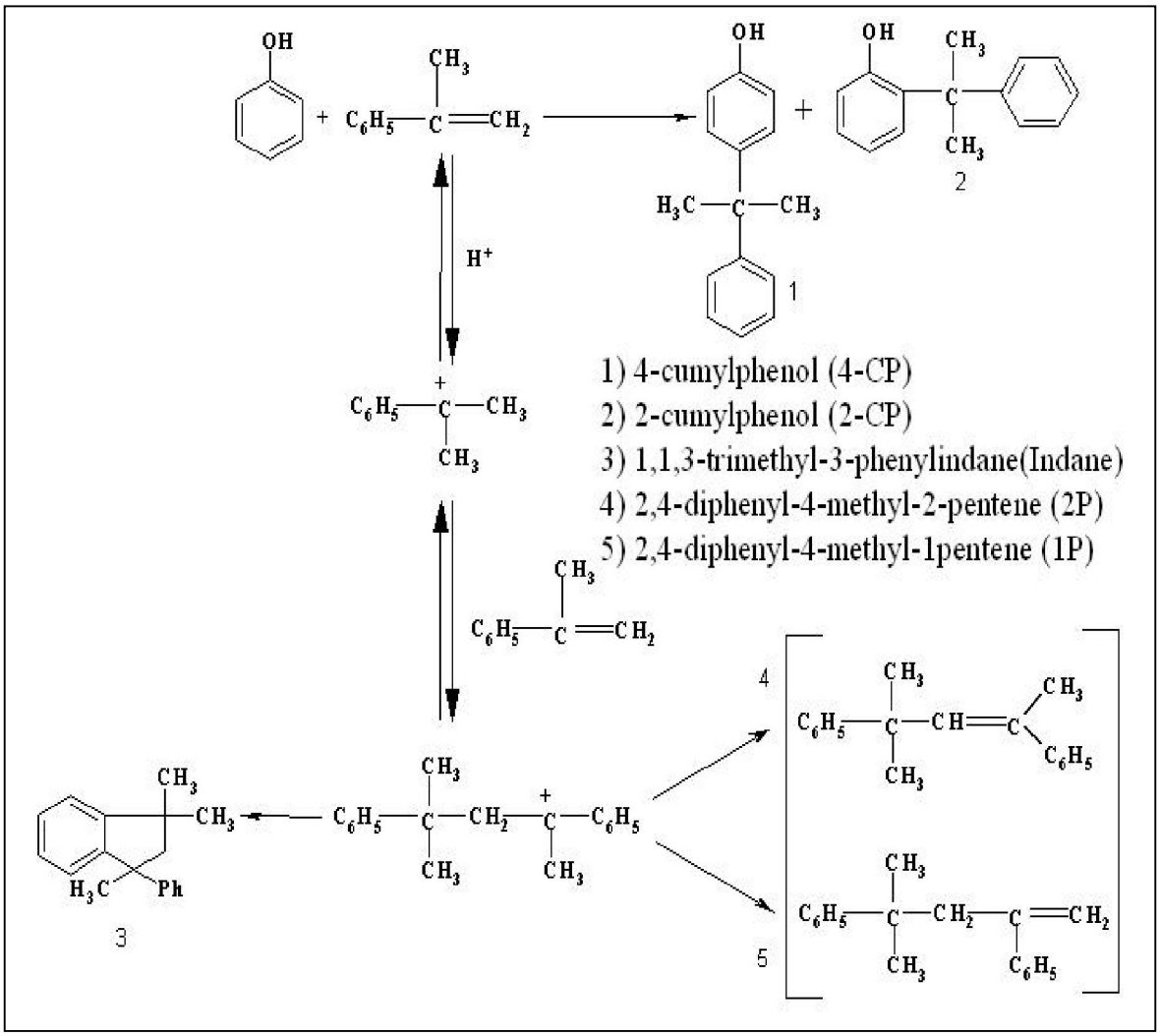


Fig. 5.1: Simultaneous series-parallel reactions occurring in the phenol + AMS system in the presence of acid catalyst

The reaction scheme for alkylation of phenol with AMS is presented in Fig. 5.1. From the scheme it can be seen that the reaction can proceed in two paths, one is the desired alkylation reaction in which AMS is utilized for the alkylation of phenol and the other is that AMS itself undergoes dimerisation to form saturated and unsaturated dimers which can lead to reduced selectivity for 4-CP

## 5.4 Results and Discussion

**5.4.1 Characterization:** The catalysts used for the alkylation reaction were characterized by $N_2$ sorption measurements and TPD of ammonia.

**5.4.1.1 Structural characteristics**

Table 5.1 shows the physico-chemical characteristics of the catalysts used for the reaction of phenol alkylation with AMS. Zeolites beta, USY, and MOR are defined as having a 12-membered ring pore system, but they differ in dimensionality. Zeolite beta has a three-dimensional interconnecting pore system with pores of 0.55 x 0.55 and 0.76 x 0.64 nm, whereas zeolite-Y has a three-dimensional interconnecting pore system with supercages of 1.18 nm connected by circular 12-ring 0.74-nm windows. Mordenite has a bidimensional pore system, with parallel circular 12-ring channels (0.65 x 0.70 nm) and elliptical 8-ring

**Table 5.1: Physico-Chemical characteristics of the zeolite catalysts used for the reaction of phenol alkylation with AMS**

| Catalyst | $SiO_2/Al_2O_3$ | Pore size (nm) | SA $m^2/g$ | $T_{max}$ (K) TPD | Acidity (mmoles) |
|---|---|---|---|---|---|
| **HY-5.2** | 5.2 | 0.74<br>Supercages 1.18 | 750 | 462, 628 | 2.2 |
| **HY-12** | 12 | -do- | 730 | 452, 619 | 1.3 |
| **HY-30** | 30 | -do- | 780 | 440, 615 | 0.6 |
| **HY-80** | 80 | -do- | 780 | 422, 604 | 0.2 |
| **Hbeta-25** | 25 | 0.55 ×0.55<br>0.76 ×0.64 | 685 | 480, 629 | 1.2 |
| **HMor-20** | 20 | 0.65 ×0.70<br>0.26 ×0.57 | 490 | 472, 813 | 1.8 |

channels (0.26×0.57 nm), but practically it functions as a monodimensional pore system since the 8-ring channels do not have access to most of organic molecules.

### 5.4.1.2 Surface area

The surface area measurements show that surface areas are in the expected range and increase in the order Y > beta > MOR. This is because Y has a pore window of 0.74 nm which opens in to supercages of 1.18 nm, while beta has slightly smaller pore window than Y without any supercages. Mordenite has lower surface area as it has only two pore systems consisting of 12 and 8 membered rings.

### 5.4.1.3 Acidity Measurements

The temperature programmed desorption results of the catalysts used for phenol alkylation with AMS are shown in Table 5.1. The acidities of the samples were estimated through the desorption of chemisorbed ammonia ($NH_3$-TPD). This technique provides general information about the number and distribution of the acid sites. Two peaks, characterized by the maximal temperature *T*max, were observed in the $NH_3$-TPD spectra of all the samples.

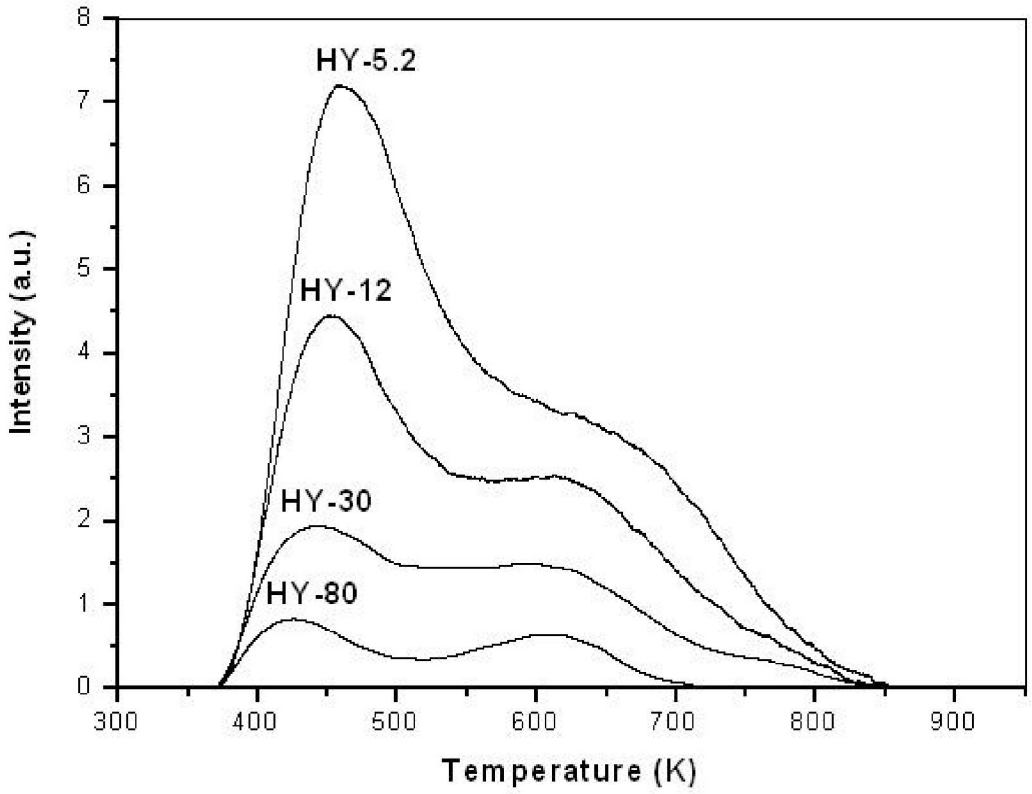


**Fi**

Tl of the

ac umina

ra of the

peaks decrease with different silica to alumina ratios. It was observed that ammonia

desorption from the acid sites occurred mainly at the relatively low temperatures for Y zeolites, at the intermediate temperatures for the Beta samples, and in the high temperature zone for the mordenite zeolite. These data and the maximal temperatures (*T*max) show that the acid strength of the samples decreases in the order MOR > Beta > USY. These results agree with previously reported enthalpy measurements (4–6). However, it is to be cautioned that the $T_{max}$ also depends upon the concentration of acid sites.

### 5.4.2 Catalytic activity in Phenol alkylation

The catalytic activities of various zeolite catalysts has been evaluated in phenol alkylation with AMS to obtain 4-CP with high selectivity.

#### 5.4.2.1 Influence of zeolite structure type

The main C-alkylated product of phenol alkylation with AMS is 4-cumylphenol, though some amount of 2-CP (2-cumyl phenol) is also found in the product mixture. Other side products that are formed through the dimerisation of AMS are also found in the products. They are unsaturated dimers of AMS, 2,4-diphenyl-4-methyl-1-pentene (1P), 2,4-diphenyl-4-methyl-2-pentene (2P) and saturated dimer 1,1,3-trimethyl-3-phenylindan (Indane). Fig. 5.3 shows the evolution of product selectivity for the reaction between phenol and AMS carried out over MOR, Y and beta zeolite catalysts. On Y and beta zeolites, in the early stages of the reaction (up to 0.5 h), when the concentration of the alkylating agent is high, the main product is 1P, which is formed by the dimerisation of AMS. The formation of C-alkylated products is minimal. Also, small amounts of 2P and indane are formed. Thereafter the decomposition of 1P takes place to give alkylated products. With increasing time the rate of isomerisation and the cyclisation increases thus leading to more of 2P and indane. From Fig. 5.3 it is observed that in case of Y and beta zeolites the concentration of 2P goes through a maximum. This is because the concentration of 2P increases initially due to the isomerisation of 1P and with time it slowly decreases due to is cyclisation to indane, the concentration of later being increased continuously. The mordenite-based catalysts behave differently compared to the zeolites beta and Y. The conversion obtained on mordenite is lower than when compared to other zeolites. The evolution of reactions in the presence of this catalyst is close to that observed for the beta and zeolites, but the

reaction rates for the chemical transformations are lower. Initially formed 1P decomposes very slowly to give alkylated products. Even the rates of isomerisation and cyclisation are not prominent as may be seen from the figure.

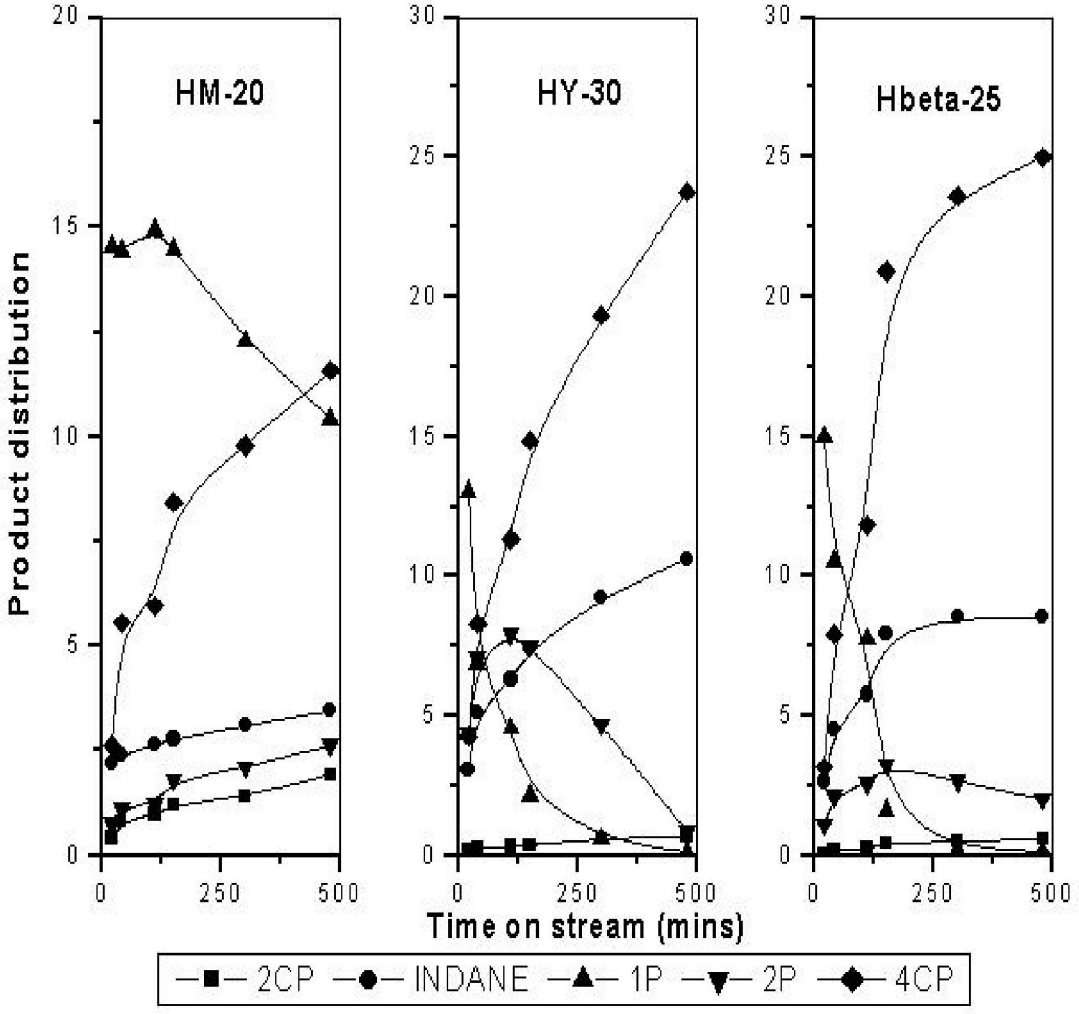


stream. Our results, on the liquid-phase alkylation of phenol with AMS on three different types of zeolites, showed very good catalytic activity for the beta and Y zeolites but low activity for the mordenite samples, though they have the same large pore 12-membered rings and similar silica/alumina ratios. The experimental results indicate that the catalytic activity follow the order : beta-25 > Y-30 > MOR-20. To explain these differences, two properties of these zeolites are taken into consideration (a) acid properties (the concentration of acid sites and the acid strength of the sites), (b) diffusional properties that

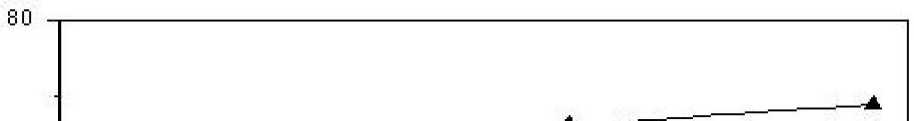

are determined by the pore architecture. These properties also influence the selectivity to the required product, i.e. 4-CP.

**Fig. 5.4: Phenol conversion and 4-CP selectivity over various zeolites**

Temp. 353 K, Phenol : AMS= 4:1 (moles), Reactants/catalyst (w/w)= 25

The reactions involved in this alkylation process are acid catalyzed. As given above (Table 5.1), the mordenite-based catalysts are characterized by higher acidity in terms of concentration as well as strength compared to Y or beta zeolites. So, it is expected that MOR-based catalysts will have a high catalytic activity at least in the initial stage of the reaction compared to other zeolite catalysts (e.g., Beta or Y). The differences in activity between the mordenite catalyst and other zeolite catalysts could be attributed mostly to their differences in pore structure that may lead to different diffusion rates for the reactants, the intermediates and the products. It is known that the problems of mass transfer as a result of the diffusional limitations is more important in the liquid-phase reactions than the gas-phase reactions. Though zeolites beta, Y, and MOR have a 12-membered ring pore system, their dimensionality differs. Zeolite beta has a three-dimensional interconnecting pore system with pores of 0.55 x 0.55 and 0.76 x 0.64 nm, whereas Y has a three-dimensional interconnecting pore system with supercages of 1.18 nm connected by circular 12-ring 0.74-nm windows. Mordenite has a bidimensional pore

system, with parallel circular 12-ring channels (0.65 x 0.70 nm) and elliptical 8-ring channels (0.26×0.57 nm), but practically it functions as a monodimensional pore system since the 8-ring channels do not allow access to most of organic molecules. It is known, that the spaciousness index (SI) is an important criterion for the characterization of 12 MR pore systems (8). SI is defined as the ratio of the yields of isobutene and *n*-butane in the cracking reaction of $C_{10}$ naphthenes (9) and it is based particularly on restricted transition state shape selectivity. SI values estimated for Y, beta, and MOR are 21, 18, and 7.5, respectively (7). Thus, it could be inferred that the mass transfer in mordenites is more limited when compared to Y and beta zeolites and this supposition can explain the differences in reaction rates observed above. In addition to the above effects, higher acidity in mordenite may be leading to non-selective reactions involving AMS, thus bringing down the alkylation selectivity.

### 5.4.2.2 Dimerisation of α-methyl styrene

The dimerisation of AMS on zeolites and ion exchange resins is very well reported (10-15). The scheme for the reaction of phenol with AMS (Figure 5.1) is reported by Basab et.al (11). The dimerisation of AMS was carried out over Y, MOR and beta catalysts to follow the product pattern in case of the alkylation reaction. The results are shown in Fig. 5.5. All the catalysts show very high activity for the reaction. The product pattern in this case also follows the same pattern as in the case of alkylation reaction. The main product in the initial stages is 1P, which isomerises to 2P and then further cyclises to indane with time. The isomerisation and cyclisation reactions take place to a lesser extent on mordenite catalysts. This may be due to the fact that the transition states for the isomerisation and the cyclisation reaction cannot fit in the one-dimensional channels of mordenite catalysts.

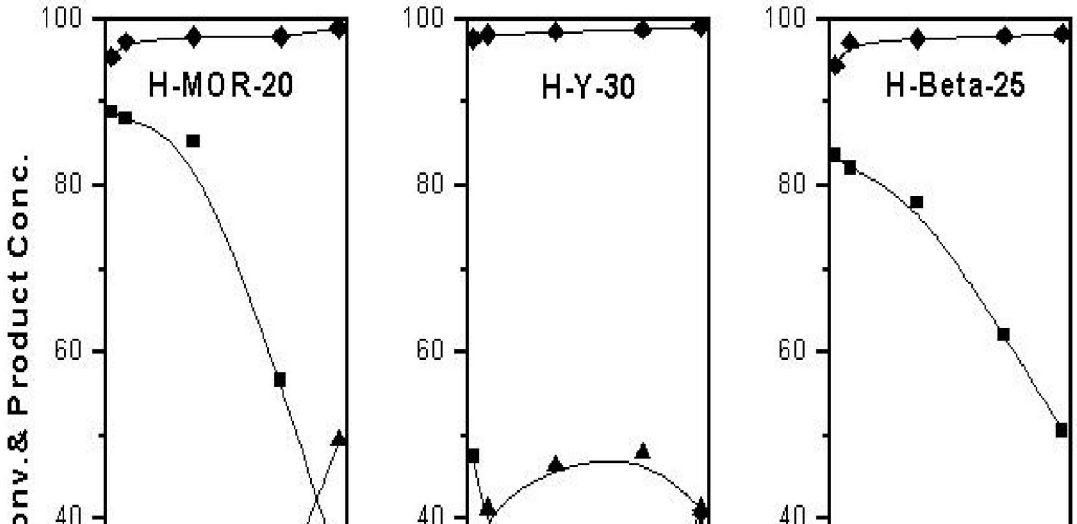

**Fig. 5.5: Dimerisation of AMS over different large pore zeolites**

Temp. 353 K , Reactants/catalyst (w/w)= 25

This is not the case with Y and beta zeolites. In case of HY zeolite, the selectivity for 1P is very less in the initial stages, which shows that the large space available inside the supercages allows easy isomerisation and cyclisation of 1P and 2P. The same must be true for the product pattern observed in alkylation of phenol with AMS.

### 5.4.2.3 Effect of silica to alumina ratio of Y zeolites

The temperature programmed desorption of ammonia results show that the total acidity of the samples decreases with increasing silica to alumina ratio. The effect of silica to alumina ratio of Y zeolites on phenol alkylation with AMS is shown in Table 5.2 and Fig. 5.6. Dimerisation of AMS is predominant at lower ratios and hence the alkylation as well as selectivity to 4-CP is lower. There is an increase in the phenol alkylation activity with increasing silica to alumina ratio, alongwith improved selectivity to 4-CP. It is known that increasing the framework Si/Al ratio has an effect not only on the acidity but also on the adsorption properties of the zeolite. On samples with higher acid site density the non selective dimerisation of AMS is predominant and hence it is not available for the

alkylation reaction. As the silica to alumina ratio increases, the dimerisation activity decreases and so more AMS is available for phenol alkylation. Hence the phenol conversion as well as selectivity to 4-CP increase with silica to alumina ratio.

**Table 5.2 Effect of silica to alumina ratio of Y zeolite on the alkylation of phenol with AMS**

| Catalyst | Conv. of Phenol (wt %) | Product distribution (wt %) | | | | | Sel.of 4-CP (wt %) |
|---|---|---|---|---|---|---|---|
| | | 2cp | ind | 1p | 2p | 4cp | |
| **Y-5.2** | 7.4 | 0.2 | 4.9 | 12.9 | 2.7 | 7.2 | 25.6 |
| **Y-12** | 12.4 | 0.3 | 6.1 | 5.9 | 7.9 | 12.1 | 37.4 |
| **Y-30** | 26.9 | 0.4 | 7.5 | 0.4 | 2.1 | 26.5 | 72.6 |
| **Y-80** | 34.5 | 0.5 | 8.4 | 0 | 0 | 34 | 79.1 |

Temp. 353 K, Phenol : AMS= 4:1(moles), Reactants/catalyst (w/w)= 25

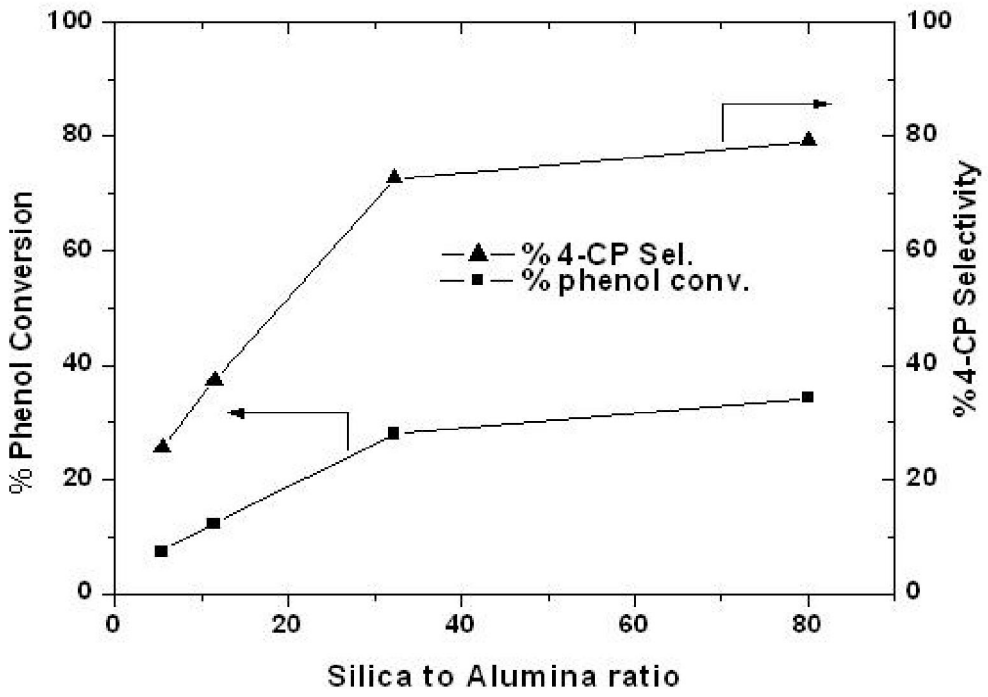

**Figure 5.6: Variation in the phenol conversion and 4-CP selectivity with changes in silica to alumina ratio**

Temp. 353 K, Phenol : AMS= 4:1(moles), Reactants/catalyst (w/w)= 25

### 5.4.2.4 Effect of Bronsted and Lewis acidity

When Na-Y or silica-alumina are used, they did not show significant activity either for the alkylation of phenol with AMS or AMS dimerisation. Kurokawa et al. (13) performed the dimerisation of AMS over H-Y zeolite in the presence of a small amount of pyridine. They found that the activity was lost completely by the addition of pyridine. These results show that Bronsted acid sites of zeolites promote the dimerisation of AMS. Our results in Table 5.3 also point to the same conclusion. Bronsted sites are required for the formation of the cumyl cation , which takes part in dimerisation or the alkylation reactions.

**Table 5.3 Effect of Bronsted and Lewis acidity on the synthesis of 4-CP**

| **Catalyst** | % Conv. of Phenol | **Product distribution (wt%)** | | | | | **Sel.of 4-CP** |
|---|---|---|---|---|---|---|---|
| | | **2cp** | **ind** | **1p** | **2p** | **4cp** | |
| HY-80 | 34.5 | 0.5 | 8.4 | 0 | 0 | 34 | 79.1 |
| NaY-5 | ------No Reaction------ | | | | | | |
| Amorphous $SiO_2$ –$Al_2O_3$ | 3.2 | 1.3 | 0 | 0 | 1.3 | 1.9 | 43.4 |

Temp. 353 K, Phenol : AMS= 4:1(moles), Reactants/catalyst (w/w)= 25

**Table 5.4 Effect of temperature on the synthesis of 4-CP**

| **Temp (K)** | Conv. of **Phenol (wt%)** | **Product distribution (wt%)** | | | | | **Sel.of 4-CP (wt%)** |
|---|---|---|---|---|---|---|---|
| | | **2cp** | **ind** | **1p** | **2p** | **4cp** | |

| | | | | | | | |
|---|---|---|---|---|---|---|---|
| 333 | 27.2 | 0.4 | 8.2 | 0 | 0 | 26.8 | 75.7 |
| 353 | 34.5 | 0.5 | 8.1 | 0 | 0 | 34.0 | 79.1 |
| 373 | 31.5 | 0.7 | 8.4 | 0 | 0 | 30.8 | 77.2 |
| 393 | 28.8 | 1.7 | 8.5 | 0 | 0 | 27.1 | 72.6 |

Zeolite H-Y (80), Phenol: AMS= 4:1(moles), Reactants/catalyst (w/w)= 25
Time on stream-5hr

### 5.4.2.5 Effect of temperature

The alkylation of phenol with AMS was studied on Y-80 zeolite, in the temperature range 333-393 K. The data is shown for 5$^{th}$ hour TOS in Table 5.4. At all temperatures, in the initial stages (approximately 1.5 h) of the reaction considerable formation of saturated dimers has been observed. But with time, i.e. after 2h the saturated dimers are either converted to unsaturated dimers or decompose to give phenol alkylation products. But as the temperature increases, there is slight increase in the concentration of the saturated dimers. This is because the activation energy for the cyclisation of 1p or 2p to the unsaturated dimer is higher than that required for the simple dimerisation of AMS. This increased activity for formation of unsaturated dimer leads to lesser phenol alkylation activity. Also, with increase in temperature the concentration of 2-CP increases. All these factors lead to decrease in the selectivity for 4-CP.

### 5.4.2.6 Effect of Phenol to AMS feed ratio

The amount of phenol taken for the reaction is always higher than that of the amount of AMS. The phenol to AMS mole ratio was altered in the range from 2.0-8.0. The results are shown in Table 5.5. The higher concentration of AMS leads to higher amounts of dimers (as seen in case of phenol: AMS 2:1), which lead to slightly lower selectivity for 4-CP. At lower mole ratios the formation of 2-CP and the saturated dimer is higher. As the mole ratio of phenol to AMS is increased, the formation of dimer decreases and the selectivity to 4-CP increases. The conversion of phenol also decreases at higher mole ratios.

**Table 5.5**: **Effect of mole ratio on the synthesis of 4-CP**

| **Mol ratio Phenol:AMS** | Conversion of **Phenol (wt%)** | **Product distribution (wt%)** | | | | | **Sel.of 4-CP (wt%)** |
|---|---|---|---|---|---|---|---|
| | | **2cp** | **ind** | **1p** | **2p** | **4cp** | |
| 2:1 | 37.9 | 1.0 | 9.3 | 0 | 0 | 36.9 | 78.1 |
| 4:1 | 34.5 | 0.5 | 8.1 | 0 | 0 | 34.0 | 78.7 |
| 6:1 | 23.7 | 0.4 | 5.2 | 0 | 0 | 23.3 | 80.5 |
| 8:1 | 20.8 | 0.3 | 5.0 | 0 | 0 | 20.5 | 79.4 |

Temp 353 K, Reactants/catalyst (w/w)= 25

### 5.4.2.7 Effect of cumene in the feed

AMS is prepared through dehydrogenation of cumene. Hence an expected impurity in AMS may be cumene. This led us to investigate the influence of cumeme as diluent. An advantage of dilution with cumene could be, if performance is not affected, crude AMS containing product can be used for reaction, avoiding purification step. The cumene concentration was varied from 20-80 wt% based on the total weight of the reaction mixture. The selectivity for 4-CP was higher than that observed when the reaction was

**Table 5.6: Effect of cumene concentration on the synthesis of 4-CP**

| **Cumene (%)** | **TOS hrs** | Conv.of Phenol (wt%) | **Product distribution (wt %)** | | | | | **Sel.of 4-CP (wt%)** |
|---|---|---|---|---|---|---|---|---|
| | | | **2cp** | **ind** | **1p** | **2p** | **4cp** | |

| | | | | | | | | |
|---|---|---|---|---|---|---|---|---|
| 0 | 5 | 34.5 | 0.5 | 8.1 | 0 | 0 | 34.0 | 79.1 |
| 20 | 5 | 31.4 | 0.4 | 7.9 | 0 | 0 | 31.0 | 78.9 |
| 40 | 5 | 32.4 | 0.5 | 6.2 | 0 | 0 | 31.9 | 82.6 |
| 60 | 5 | 28.3 | 0.3 | 3.6 | 0 | 0.2 | 28.0 | 87.1 |
| 60 | 8 | 30.6 | 0.3 | 3.9 | 0 | 0 | 30.3 | 87.6 |
| 80 | 8 | 31.6 | 0.4 | 3.3 | 0.2 | 1.2 | 31.2 | 86.0 |
| 80 | 10 | 32.0 | 0.4 | 3.4 | 0 | 0 | 31.6 | 89.34 |
| 80 [a] | 5 | 27.9 | 0.3 | 2.3 | 0 | 0 | 27.6 | 91.2 |

Phenol:AMS=4:1 (moles), Temp=353 K , Reactants/catalyst (w/w)= 25

[a] phenol :AMS = 6:1

carried out without cumene. This improved selectivity is in addition to the benefit obtained from not having to purify the AMS before utilizing it to produce cumyl phenols. This is useful from the point of view of the process since the output of the cumene dehydrogenation can be directly sent to the phenol alkylation reactor without distilling it. There was a continuous increase in the selectivity of 4-CP with increase in the concentration of cumene. However, there was no change in the conversion of phenol, while there was a decrease in the formation of side products. This is because cumene helps in uniformly dispersing the AMS in the system without causing localized concentration zones of AMS. Hence, more of phenol alkylation takes place thus reducing the dimerisation reactions. But with increase in the concentration of cumene the reaction rate is lowered (Table 5.6). The reason behind this might be that of competitive adsorption. Due to its dimensional and structural similarity to AMS, cumene may be physisorbed on the acid sites of the zeolite thus making them temporarily unavailable for AMS activation or for decomposition of 1P and 2P formed in the initial stages of the reaction. In due course, because of the reversible nature of physisorption the sites become available to AMS or its dimers and the reaction goes for completion. Also, cumene can be used as a solvent in the reaction because it helps in reducing the viscosity of the reactant mixture in addition to the above mentioned advantages.

### 5.4.2.8 Reusability of the catalyst

Recycling studies of the catalyst H-Y (80) used in the alkylation of phenol with AMS was carried out in order to check the activity, stability and reusability of the catalyst. The results are shown in Table 5.7. After completion of the reaction using fresh catalyst, the catalyst was separated from the reaction mixture via sedimentation or filtration, washed with acetone and oven dried at 393 K for 3 h. There was no change in the activity of H-Y-80 after each successive cycle. Similarly no change in the selectivity of 4-CP was observed. In the recycle study carried out with ion-exchange resins Chaudhari et.al (16) observed that the tendency of AMS to dimerise decreased markedly with repeatedly used ion exchange resin. But in our case we did not find any such change in the dimerisation activity with repeated use of the catalyst.

**Table 5.7: Effect of catalyst recycle on the synthesis of 4CP**

| **Cycle no** | **TOS hrs** | Conv.of Phenol (wt%) | **Product distribution (wt %)** | | | | | **Sel.of 4-CP (wt%)** |
|---|---|---|---|---|---|---|---|---|
| | | | **2cp** | **ind** | **1p** | **2p** | **4cp** | |
| 1 | 8 | 31.8 | 0.5 | 8.3 | 0 | 0 | 28.5 | 76.2 |
| 2 | 8 | 31.6 | 0.6 | 8.1 | 0 | 0 | 28.4 | 76.4 |
| 3 | 8 | 32.6 | 0.6 | 8.7 | 0 | 0 | 29.1 | 75.6 |

Catalyst wt. 1gm, Phenol:AMS =4:1(moles) ,Temp=353 K Reactants/catalysts(w/w)=25

### 5.4.2.9 Effect of semi-continuous addition of AMS

The effect of semi continuous addition of AMS to the reaction medium is shown in Table 5.8. The tendency of AMS to dimerise decreases with this type of addition. This may be due to the dilution effect of phenol on AMS. Also the concentration of AMS near the catalyst surface is lower. The selectivity to 4-CP is higher than that in which all the AMS is added at one time. The presence of cumene further helps to enhance the selectivity.

**Table 5.8: Effect of semi-continuous addition of AMS during the reaction**

| Cumene Wt% | TOS hrs | Conv.of Phenol (wt%) | Product distribution (wt %) | | | | | Sel.of 4-CP (wt%) |
|---|---|---|---|---|---|---|---|---|
| | | | 2cp | ind | 1p | 2p | 4cp | |
| 0 | 5 | 34.5 | 0.5 | 8.1 | 0 | 0 | 34.0 | 79.1 |
| 0 | 3.5* | 34 | 0.5 | 4.3 | 0 | 0 | 33.5 | 86.9 |
| 20 | 3.5* | 36.2 | 0.4 | 3.5 | 0 | 0 | 34.5 | 89.7 |

Phenol: AMS=4:1 (moles), Temp=353 K Reactants/catalysts (w/w)=25

* semi-continuous addition

### 5.4.2.10 Alkylation Selectivity (Alkylation Vs Dimerisation)

The most important problem area with respect to catalytic alkylation of phenol with AMS is the competition of alkylation and dimerisation reactions. The catalytic alkylation of phenol with AMS mainly leads to 4-CP. The alkyl phenyl ether that is formed in the alkylation reactions involving smaller alcohols and olefins does not form in this case .It is known that as the hydrocarbon chain increases the O-alkyl product is difficult to form, mainly due to high reactivity or the instability of the resulting ether. But depending on the reaction conditions, silica to alumina ratio, the dimerisation of AMS also takes place. Temperature is an important factor, which affects the dimerisation reaction. The activation energies for the isomerisation and cyclisation reactions are higher than that required for the formation of 1P product, which is kinetically favoured. Hence, increase in temperature will favour isomerisation and cyclisation reactions. Another critical factor is the time on stream. With increasing time, as shown in Figure 5.4 along with the alkylation reaction, conversion of 1P to 2P and indane takes place. The indane dimer is very stable and it cannot be decomposed back to the monomer. Hence available AMS for phenol alkylation decreases. Also the phenol to AMS mole ratio affects the dimerisation reaction. An excess of phenol is always preferred because this avoids the formation of large amounts of secondary products. As seen from the table, larger concentration of AMS in the feed leads to higher dimerisation activity

**5.5 References**

1) Zieborak, Z.; Rutajezak, W.; Kowalska H. Chem Stosowana, 3-4 (1987) 341-349.

2) Macho, V.; Jurecek, L.; Adam, V.; Kavala, M.; Jurecekova, E.; Hlinstak, K.; Mikula, O.; Storecko, J.; Schwaraz,F.; Varga, M. Czech. CS 245,895,1987, Chem.Abstr. 109 (1988) 112426

3) Oberholtzer, J., Kumbhar, P., Dave, S., and Badani, M. V. U.S.Patent 6,448,453 B1, (2002)

4) Miyamoto, Y., Katada, N., Niwa, M. Micropor. Mesopor. Mater. 40 (2000) 271.

5) Niwa, M., Katada, N., Catal. Surv. Jpn. 1 (1997) 215.

6) Niwa, M., Katada, N., Sawa, M., Murakami, Y. J. Phys. Chem. 99 (1995) 8812

7) Namba, S., Yashima, T., Itaba, Y., Hara, N. Stud. Surf. Sci. Catal. 5 (1980) 105.

8) Wang, B., Lee, C.W., Cai, T.-X., Park, S.-E. Stud. Surf. Sci. Catal. 135 (2001) 281.

9) Weitkamp, J., Ernst, S., Kumar, R. Appl. Catal. 27 (1986) 207.

10) Fujiwara, M., Kuraoka, K., Yazawa, T., Xu, Q., Tanaka M., and Souma Y. Chem. Commun., (2000) 1523.

11) Chaudhari, B., and Sharma, M. M. ; Ind.Eng.Chem.Res. 28 (1989) 1757.

12) Heidekum, A., Harmer, M., and Hölderich, W. F. Catalysis Letters,47 (1997) 243.

13) Kurokawa, H., Ohta, M., Sugiyama K., and Miura, H. Appl.Catal.A: General 202 (2000) 147.

14) Issakov, J., Litvin, E., Minachev, Ch., Öhlmann, G., Scharf, V., Thome, R., Tißler, A. and Unger, B. Studies in Surface Science and Catalysis, 84 (1994) 2005.

15) Sun, Q., Farneth, W. E. and Harmer, M. A. J.Catal. 164 (1996) 62.

16) Chaudhari, B., and Sharma, M. M. ; Ind.Eng.Chem.Res. 30 (1991) 227.

**Summary and conclusions**

This thesis reports the para-selective synthesis of various dialkylbenzenes, e.g. p-diethylbenzene, p-xylene, p-tert-butyltoluene and p-cumylphenol on various zeolite catalysts and characterization of these catalytic materials by x-ray diffraction (XRD), surface area, scanning electron microscopy (SEM), temperature programmed desorption (TPD) of ammonia and FTIR of adsorbed base. The thesis is divided in to six chapters.

Chapter 1 is a general introduction to zeolites, their classification based on morphology, secondary building units, chemical composition, and effective pore diameter. The special features of zeolites like acidity and shape selectivity are discussed in great detail with examples. A brief summary of various modification methods involved in the preparation of selective catalysts is described. The importance of zeolites and their advantages over homogenous catalysts has also been discussed. Some of the reported literature pertaining to the reactions that are described in the succeeding chapters has also been cited. In the last section, the aim and objectives of the present work has been proposed. From the introduction, it can be seen how some of the driving forces such as market demand, feedstock availability, operating cost, legislative aspects such as environmental laws and new reformulated gasoline specifications, has led to the development of new processes using solid acid catalysts. In response to the worldwide environmental awareness, there are active programs in search of clean processes for manufacturing of fine chemicals and petrochemicals. Solid acid catalysts have been found to be key drivers in the efforts.

Chapter 2

Isomophous substitution offers a strong potential to design zeolites for novel applications. It was found that incorporation of heteroatoms led to changes in acidity and pore structure of zeolites and such zeolites have altered catalytic activity, selectivity and stability. The acid strength of isomorphously substituted zeolites follows the order Al-(OH)-Si > Ga-(OH)-Si > Fe-(OH)-Si >> B-(OH)-Si. This was confirmed from the ammonia TPD spectra where in the temperature maximum shifts to lower temperatures in the above order. The

SEM pictures show that the crystal sizes of Al-MFI are larger than that of Ga-MFI, but the activity of Ga-MFI is less than that of Al-MFI, which is due to lower acid strength of the gallium substituted samples. The above catalysts were evaluated and compared for EB ethylation. The activity was higher for Al- and Ga-substituted MFI zeolites, while it was low for Fe and B substituted samples. Due to the higher acidity, EB dealkylation activity was highest on Al-MFI. This is seen from the higher benzene concentration in the product. The Ga-MFI zeolite showed appreciable EB conversion and higher DEB yield. The silylation was performed on Ga-MFI zeolite. EB ethylation was performed on unmodified and modified samples with one or two successive CLD treatments. The catalytic activity of the samples decreased in the order Ga-MFI > Ga-MFI-CLD1 > Ga-MFI-CLD2, while the p-DEB selectivity increased in the order Ga-MFI < Ga-MFI-CLD1 < Ga-MFI-CLD2. This is due to the passivation of surface acidity brought about by the deposition of $SiO_2$. Because of the inactivation of external surface sites, the secondary isomerisation activity is reduced and the concentration of p-DEB increases. Second CLD treatment led to some pore narrowing which further increased the selectivity to 99%. The time on stream studies of Ga-MFI-CLD2 and Al-MFI-CLD2 show that though conversion is low on Ga-MFI it shows but better stability. Al-MFI-CLD2 shows higher activity in the initial stages and then deactivates relatively rapidly.

During toluene methylation on modified and unmodified Ga-MFI and Al-MFI zeolites, Al-MFI shows higher toluene conversion than Ga-MFI. This may be due to the stronger acidity required for toluene methylation than that for EB ethylation. The dealkylation activity is also higher on Al-MFI. The ethyltoluene concentration is higher on Ga-MFI, than Al-MFI, probably as a result of dealkylation of ethyltoluenes on Al-MFI. The time on stream studies on modified Al- and Ga-MFI shows that in the initial stages of the reaction the p-xylene selectivity is slightly lower for the aluminium substituted catalyst, but with time both give almost similar selectivity for p-xylene.

Chapter 3

This chapter describes the importance of p-DEB and the traditional routes used for its preparation in the introduction. The performance of pure granulated and extrudated (with

alumina) forms of zeolites were compared for p-DEB and p-xylene synthesis. The zeolites were modified by chemical liquid deposition with two successive treatments and the extrudates were also exchanged with lanthanum after the silylation treatment. The XRD pattern shows that there is no change in the relative intensities of the peaks for modified and unmodified zeolites. Ammonia TPD shows that as the silica to alumina ratio increases the concentration of strong acid sites increases in relation to weak acid sites. The TPD of ammonia also shows decrease in the total acidity after silylation treatment and lanthanum exchange. This is due to the inactivation of surface acid sites that are out side the pore structure by $SiO_2$ deposition. The lanthanum exchange leads to further reduction of acidity on the silylated catalyst. This may be due to the exchange of lanthanum at some of the Bronsted acid sites. The FTIR hydroxyl spectra shows decrease in the intensity of the band centered around 3600 $cm^{-1}$ assigned to the bridging hydroxyl groups, with increasing silica to alumina ratio. This is because the concentration of bridging hydroxyl groups varies with the tetrahedral aluminium content in the framework. The FTIR spectra of pyridine shows three peaks at 1450-1455 $cm^{-1}$, 1490 and 1545-1547 $cm^{-1}$. The band near 1450 $cm^{-1}$ is due to pyidine adsorbed at Lewis site and the one at 1545 $cm^{-1}$ is due to pyridine chemisorbed at Bronsted site. Intensity of the infrared band at 1450 $cm^{-1}$ associated with co-ordinatively held pyridine decreases rapidly as the temperature is raised showing that the Lewis acidity is not relatively strong compared to Bronsted acidity. Catalytic activity results show that there is a decrease in the EB ethylation activity as the silica to alumina ratio increases. There is an increase in p-DEB selectivity with increase in the silica to alumina ratio. In case of extrudates the EB conversion increases with increase in the zeolite content. The p-DEB selectivity is higher for extrudate catalysts with lower zeolite content. The optimum concentration of TEOS in the solution was found to be between 20 to 25% to get better selectivity for p-DEB. Also extrudated catalysts require higher amounts of silica loading to achieve the same selectivity as that of granulated catalyst. This is due to the better dispersion of acid sites on extrudates. When the reaction was performed with 70 % zeolitic extrudates of different silica to alumina ratios, the trend in the EB conversion was the same as that for pure zeolites. When the parent, twice silylated and twice silylated lanthanum exchanged catalyst were used for EB ethylation, the EB conversion decreases and p-DEB

selectivity increased in the above mentioned order. This is because of the decrease in the surface acidity by silica deposition and also from the decrease in internal acidity by lanthanum exchange. Same catalysts were used for ethylation of $C_8$ aromatics as well as pure EB. Similarlaly EB disproportionation was carried out on all these catalyst. The trend in the EB conversion and p-DEB selectivity was found to be the same as that for pure EB ethylation. The $C_8$ cut showed higher p-DEB selectivity for ethylation as well as disproportionation. The time on stream study shows that the catalyst stability is not that high for $C_8$ ethylation and disproportionation.

Toluene methylation was also carried out over the same catalysts for selective p-xylene synthsis. The performance is the same as that for EB ethylation and disproportionation reactions.

Chapter 4

4-*ter*t-Butyltoluene is an intermediate product for 4-*ter*t-butylbenzoic acid and 4-*ter*t-butylbenzaldehyde that are used in perfumery, manufacture of plastics and resins. For this purpose, ZSM-12 and MCM-22 zeolites were synthesized and characterized. The ammonia TPD spectra show that zeolite ZSM-12 and MCM-22 have higher acid strength than zeolites beta and Y. The main product of the reaction, 4-*ter*t-butyltoluene is kinetically favoured. The steric hindrance of the methyl group on one side and voluminous *ter*t-butyl group on the other side also favours its formation. Shape-selectivity also plays a role depending on the zeolite structure. The formation of 2-*ter*t-butyltoluene is hindered by ortho-position of methyl to the voluminous *ter*t-butyl group. The selectivity for the 4-tert butyl toluene is higher than that of thermodynamic equilibrium value of 64%. When the reaction was carried out on zeolite beta at different temperatures, the highest toluene conversion was obtained at lowest temperature i.e. at 393 K and with increase in temperature, there was drop in the conversion. This may be due to the oligomerisation of isobutylene formed on dehydration of tert-butanol that is predominant at higher temperatures or due to the dealkylation of tert-butyl toluenes at higher temperatures. The stability of zeolite beta was found to be very good because there was only 3% drop in toluene conversion after 6 h. The reaction was carried out in detail on zeolite Y. When the

reaction was carried out on Y zeolites of different Si/Al ratios, the toluene conversion was low on samples with higher ratios, but it helped in obtaining better PTBT selectivity. Though the conversion of toluene increases with increasing temperatures, it fell at higher (413 K) temperatures. However the PTBT selectivity continuously falls with increasing temperature. There was a reduction in the toluene conversion, when feeds containing higher alcohol contents are used. From the Table 4.3 it is seen that as the concentration of TBA in the feed increases the quantity of non-aromatics in the product increases. This is because at higher TBA concentration the oligomerisation of isobutylene that is formed from the dehydration of tertiary butanol is in competition with the main alkylation reaction. This lower utilization of alkylating agent led to a steep fall in alkylation selectivity with higher TBA contents in the feed. With time on stream, on zeolite Y, there was some surge in the conversion of toluene in the initial stages, while a marginal reduction was observed with time on stream though, it was to a much less extent compared to beta zeolite. This is probably because of the more open structure of zeolite Y as compared to beta, which does not trap the bulky multialkylated products. PTBT selectivity reaches maximum level in the initial stages of the reaction and then it remains constant at 87 %. The toluene conversion on MCM-22 is much lower than that on zeolites Y and beta. The MTBT fraction in the product increases continuously even though there is a fall in the conversion. This may be due to the isomerisation of PTBT to MTBT resulting in lower selectivity to PTBT. With increasing space velocity, there is an improvement in the PTBT selectivity, though there is a decrease in the toluene conversion. A gradual decrease in the conversion was observed after 5 hrs. MCM-22 shows a promising value for higher PTBT selectivity with a reasonably good conversion. In case of ZSM-12 the conversion is comparable to MCM-22 in the initial stages, but the deactivation is rapid after 2hrs on stream. The para-selectivity is also much lower on ZSM-12 compared to MCM-22. Our results, of the vapour-phase alkylation of toluene with TBA on four different types of zeolites, showed very good catalytic activity for the beta and USY zeolites but low activity for the MCM-22 and ZSM-12 zeolites, though both of them have the same 12-membered ring large pores. The experimental results indicate the following order of total catalytic activity: Beta 25 ≈ Y-30 > MCM-22 > ZSM-12. This may be due to better interaction of

the reactant molecules with the acid sites and the higher product diffusivity possible as a result of more open structures in case of beta and Y. It is to be noted that ZSM-12 is one dimensional zeolite and MCM-22 has one 10 membered ring system. Though the later has a three dimensional structure the diffusion of reactants towards the internal acid sites is limited because of 10-membered ring pores. When MTBE was used as the alkylating agent, the catalyst had a better stability due to the slow release of isobutylene in to the reaction medium, thus reducing the side reactions that lead to coke formation and deactivation. In case of tert-butanol the generation of butylene is rapid and hence coke formation is higher, leading to catalyst deactivation. There was no influence of the alkylating agent on the PTBT selectivity.

Chapter 5

The alkylation of phenol with olefins in the presence of an acid catalyst to produce alkylphenols is a reaction of academic as well as of industrial importance. Alkylphenols are chemical intermediates for a variety of important fine chemicals. Phenol alkylation with α-methyl styrene (AMS) was performed in the liquid phase, using on large pore zeolites like beta, Y and mordenite. The reaction takes place in two pathways, the desired alkylation pathway and the competitive AMS dimerisation. The surface areas of catalysts used for the reaction show the following trend viz., Y > beta > mordenite. The TPD spectra show that ammonia desorbs at higher temperature for mordenite, at intermediate temperatures for beta and at lower temperatures for Y zeolites. The reaction of phenol with AMS leads to 4-CP, 2-CP and the dimerisation products of AMS which are 1P, 2P and indane. The phenol conversion is higher on zeolites beta and Y, but lower on mordenite catalyst. This may be attributed to the differences in the structure of these zeolites. In the initial stage of the reaction, kinetically favourable 1P predominates, which slowly isomerises to 2P or decomposes to give alkylated phenol products. The saturated dimer indane is more stable than the unsaturated dimers and hence once formed does not decompose. The dimerisation of AMS performed in the absence of phenol, shows the above trend and hence we conclude that the reaction takes place as per the above mechanism. When the reaction was performed on Y zeolite with different silica to alumina

ratios, the phenol conversion as well as 4-CP selectivity improved on samples with higher Si/Al ratio. This is because, at lower silica to alumina ratios, the AMS undergoes dimerisation due to higher acid site density and is unavailable for phenol alkylation. It is found that Bronsted acid sites are essential for this reaction as neither silica-alumina nor Na-Y showed any significant activity. The phenol conversion as well as the 4-CP selectivity decreased at higher temperatures. Higher fraction of phenol in the feed led to better selectivity for 4-CP because of the decrease in the dimerisation activity of AMS. When cumene was used as a diluent it led to much higher 4-CP selectivity. Cumene helps to disperse the AMS in such a way that the probability of its reaction with phenol increases. But as the cumene concentration increases the rate of the reaction decreases. This may be due to the competitive adsorption of cumene on the acid sites. The catalyst was found to have very good activity even after 3 cycles of reaction with good reproducibility. When AMS was added semi-continuously to the reaction medium, the dimerisation decreases with fall in the concentration of saturated dimer in the product. This helps to increase the 4-CP selectivity.